0026-895X/88/050605-09$02.00/0

MOLECULAR PHARMACOLOGY, 34:605-613

ACCELERATED COMMUNICATION

Determination and Characterization of a Cannabinoid Receptor in Rat Brain

WILLIAM A. DEVANE, FRANCIS A. DYSARZ III, M. ROSS JOHNSON,[1] LAWRENCE S. MELVIN, and ALLYN C. HOWLETT

Department of Pharmacology, St. Louis University Medical School, St. Louis, Missouri 63104 (W.A.D., F.A.D. and A.C.H.) and Pfizer Central Research, Groton, Connecticut 06340 (M.R.J. and L.S.M.)

Received August 4, 1988; Accepted August 30, 1988

SUMMARY

The determination and characterization of a cannabinoid receptor from brain are reported. A biologically active bicyclic cannabinoid analgetic CP-55,940 was tritium-labeled to high specific activity. Conditions for binding to rat brain P_2 membranes and synaptosomes were established. The pH optimum was between 7 and 8, and specific binding could be eliminated by heating the membranes to 60°. Binding to the P_2 membranes was linear within the range of 10 to 50 μg of protein/ml. Specific binding (defined as total binding displaced by 1 μM Δ^9-tetrahydrocannabinol (Δ^9-THC) or 100 nM desacetyllevonantradol) was saturable. The K_d determined from Scatchard analysis was 133 pM, and the B_{max} for rat cortical P_2 membranes was 1.85 pmol/mg of protein. The Hill coefficient for [^{3}H]CP-55,940 approximated 1, indicating that, under the conditions of assay, a single class of binding sites was determined that did not exhibit cooperativity. The binding was rapid ($k_{on} \approx 2.6 \times 10^{-4}$ pM^{-1} min^{-1}) and reversible ($\kappa_{off} \approx 0.016$ min^{-1}) and ($k_{off}' > 0.06$ min^{-1}). The two K_d values estimated from the kinetic constants approximately 55 pM and exceeded 200 pM, respectively. The binding of the agonist ligand [^{3}H]CP-55,940 was decreased by the nonhydrolyzable GTP analog guanylylimidodiphosphate. The guanine nucleotide induced a more rapid dissociation of the ligand from the binding site, consistent with an allosteric regulation of the putative receptor by a G protein. The binding was also sensitive to $MgCl_2$ and $CaCl_2$. Binding of [^{3}H]CP-55,940 was displaced by cannabinoid drugs in the following order of potency: CP-55,940 ≥ desacetyllevonantradol > 11-OH-Δ^9-THC = Δ^9-THC > cannabinol. Cannabidiol and cannabigerol displaced [^{3}H]CP-55,940 by less than 50% at 1 μM concentrations. The (−)-isomer of CP-55,940 displaced with 50-fold greater potency than the (+)-isomer. This pharmacology is comparable to both the inhibition of adenylate cyclase *in vitro* and the analgetic activity of these compounds *in vivo*. The criteria for a high affinity, stereoselective, pharmacologically distinct cannabinoid receptor in brain tissue have been fulfilled.

Various preparations of *Cannabis sativa* (marihuana) have traditionally been used therapeutically and for their psychological manifestations [see reviews by Hollister (1) and Dewey (2)]. Δ^9-THC is the major compound in extracts of cannabis to have effects on the CNS (3). The predominant CNS responses to Δ^9-THC include analgesia and antiemesis, as well as a "psychological high," drowsiness, alterations in cognition and memory, and a decrement in psychomotor performance in humans (1, 2). Animal behavioral patterns associated with cannabinoid drug actions include altered behavior in monkeys, a characteristic static ataxia in dogs, and hypothermia, analgesia, a typical cannabinoid immobility, and a biphasic change in spontaneous locomotor activity in rodents (3). Although extensive structure-activity relationships have been studied in humans and in these animal models (3), the actions of cannabinoid drugs in the brain remain poorly understood. At the present time, very little is known concerning the neuroanatomical location of cells responsive to cannabinoid drugs, the classical neurotransmitter pathways that may interact with cannabinoceptive cells, or the effects that cannabinoid drugs have on neurons in the CNS.

One reason for our lack of insight concerning the actions of cannabinoid drugs in the CNS is that a clearly defined cellular mechanism(s) for this class of drugs has remained elusive [see Ref. 4 for a thorough evaluation). Our recent studies have overcome this obstacle by demonstrating that the centrally active cannabinoid drugs inhibit adenylate cyclase activity in a model neuronal system (5, 6). The ability of cannabinoid drugs

This work was supported in part by National Institutes of Health Grant R01-DA03690 and Research Career Development Award K04-NS00868 to A.C.H. W.A D. was supported by a Neuropharmacology Training Grant T32-NS07254. F.A.D. was supported by a Medical Student Summer Fellowship from St. Louis University Medical School.

[1] Present Address: Glaxo, Inc., 5 Moore Drive, Research Triangle Park, NC 27709.

ABBREVIATIONS: THC, tetrahydrocannabinol; DALN, desacetyllevonantradol; Gpp(NH)p, guanyl (β,γ)-imidodiphosphate; CNS, central nervous system; HEPES, 4-(2-hydroxyethyl)-1-piperazineethanesulfonic acid.

to regulate adenylate cyclase was determined to be related to the ability of these compounds to produce CNS effects in humans and animal models (7, 8). The response could be produced at submicromolar concentrations (7, 8) and thus would be consistent with drug levels that might be expected to be present in the brain during peak activity (9–11). Using a series of cannabinoid compounds, developed at Pfizer Central Research for their analgetic activity (12), enantioselectivity was demonstrated for the inhibition of adenylate cyclase that paralleled the isomeric selectivity exhibited in analgetic tests in animals (8). The inhibition of adenylate cyclase occurred only in certain cell types (13, 14), arguing that the effect on adenylate cyclase was not a universal phenomenon such as would be expected of cannabinoid-induced membrane fluidity changes. Further studies clearly demonstrated the requirement for G_i (6, 13), a guanine nucleotide regulatory protein that mediates the responses of hormone receptors to ultimately decrease adenylate cyclase activity. The evidence accrued from these studies strongly suggested the presence of pharmacologically unique cannabinoid receptors on the cultured neuronal cells. Logically, neurons in the CNS should also possess cannabinoid receptors.

The tools to search for a cannabinoid receptor in the brain were not available until recently. The relatively low potency and tendency to partition into biological membranes suggest that Δ^9-THC is a poor candidate for a radiolabeled ligand for the detection and characterization of cannabinoid receptors. Δ^9-THC was able to inhibit adenylate cyclase with a K_{inh} of 430 nM (7). It might be expected that radioactively labeled Δ^9-THC would have an affinity for cannabinoid receptors in the nanomolar range and would bind to receptors estimated to be present in the brain in the range of fmoles per milligram of tissue. Reports of the membrane/buffer partition coefficient for Δ^9-THC have ranged from 400 (15) to 12,500 (16). It can be calculated that the amount of labeled Δ^9-THC binding to receptors could potentially be 5 or 6 orders of magnitude smaller than the amount that would be expected to partition into membranes.

A collaborative interaction between our laboratories has allowed the investigation of cannabinoid receptors in the brain using a highly potent analgetic bicyclic cannabinoid compound, CP-55,940 (8, 12). This structure is one of a series of compounds that conform to a postulated three-point agonist-receptor interaction model proposed for the cannabinoid association with the CNS receptor that mediates analgesia (12). The important functional groups for agonist-receptor interaction were proposed to be 1) the C-ring hydroxyl, 2) the phenolic A-ring hydroxyl, and 3) the A-ring alkyl side chain. These same functional groups were found to be required for the inhibition of adenylate cyclase *in vitro* (8). The regulation of adenylate cyclase by CP-55,940 was found to exhibit a K_{inh} of 25 nM, and the (−)-isomer was found to be 200-fold more potent than the poorly analgetic (+)-isomer (8). The high affinity and enantioselectivity exhibited by CP-55,940 made it a potentially useful radioligand for binding studies to characterize the cannabinoid receptor. The studies reported here describe the binding site for [^{3}H]CP-55,940 and provide convincing evidence that this binding site is the elusive cannabinoid receptor.

Experimental Procedures

Materials. The natural cannabinoid drugs were provided by the National Institute on Drug Abuse. DALN and the isomers of CP-55,940 were synthesized at Pfizer Central Research. Cannabinoid drugs were stored as 10 mM stock solutions in absolute ethanol at −20°. Drugs were initially diluted to 20 μM in 9.4 mg/ml fatty acid-deficient bovine serum albumin using Regisil-treated glassware. All subsequent dilutions were made into a vehicle containing 5 mg/ml bovine serum albumin.

[^{3}H]CP-55,940 was radiolabeled at DuPont NEN by tritium reduction, in the presence of a Pd catalyst, of a double bond between carbons 2 and 3 of the A-ring alkyl side chain (Fig. 1). Labile tritium was removed by several washes with methanol. Product was purified by high performance liquid chromatography on a 25-cm Zorbax ODS column using the solvent system CH_3CN/25 mM NaH_2PO_4, pH 4.3 (65:35). Purified material was judged by high performance liquid chromatography to be greater than 97% chemically pure. The specific activity was determined to be 93.4 Ci/mmol, using the UV absorbance to quantitate the yield of product. Tritium exchange with labile hydrogens probably accounts for the labeling in excess of the theoretical specific activity. [^{3}H]CP-55,940 was stored at 1 mCi/ml in ethanol at −80° for long term storage and at −20° for routine usage. Purity of the stored material was monitored by thin layer chromatography on silica gel GHLF plates using the solvent system ether/isopropanol (98:2). Biological activity of the radioligand was also monitored. [^{3}H]CP-55,940 was able to inhibit the adenylate cyclase activity of N18TG2 membranes in a dose-dependent manner, using the protocol previously described (6) (data not shown).

Membrane preparations. Male Sprague-Dawley rats weighing 250 to 370 g were decapitated, and the brains were rapidly removed and dissected on ice. Unless indicated, all results reported were obtained with a washed P_2 preparation prepared as follows. The entire cortices of two or three rats were homogenized with a Dounce glass homogenizer in 45 ml of a solution consisting of 320 mM sucrose, 2 mM Tris·EDTA, and 5 mM $MgCl_2$. The homogenate was centrifuged at 1600 × *g* for 10 min. The supernatant was saved, and the pellets were washed twice as above. The combined supernatant fractions were then centrifuged at 39,000 × *g* for 15 min. The pellet was resuspended in 90 ml of buffer A (50 mM Tris·HCl, pH 7.0 at 30°, 2 mM Tris·EDTA, 5 mM $MgCl_2$), incubated at 37° for 10 min, and centrifuged at 23,000 × *g* for 10 min. The membranes were resuspended in buffer A, incubated at 30° for 40 min, and centrifuged at 11,000 × *g* for 15 min. These two washing steps were found to be important for observing a single homogeneous binding site in equilibrium studies (see Results). The final pellet was resuspended in buffer B (50 mM Tris·HCl, pH 7.4 at 30°, 1 mM Tris·EDTA, 3 mM $MgCl_2$) at a protein concentration of 4 to 5 mg/ml and stored at −80°. Storage for up to 6 weeks had no noticeable effect on binding. Protein values were determined by the method of Bradford (17) using bovine γ-globulin as the standard. Some of the studies were also performed using a synaptosomal preparation derived from the hippocampus plus prefrontal cortex of the rat. The synaptosomal preparation was made following the protocol of Dodd *et al.* (18) with several modifications. The initial homogenization was performed using a 50-ml Dounce glass homogenizer and the homogenate was centrifuged in 50-ml tubes at 1600 × *g* for 10 min. The differential sedimentations over 1.2M and 0.8M sucrose were performed at 50,000 rpm in a Beckman Ti50 rotor for 12 min. The final synaptosomal pellet was resuspended to 5 mg/ml protein in a buffer containing 25 mM Tris·HCl, pH 7.4, 1 mM Tris·EDTA, and 16.6 mM sucrose and was stored at −80°.

Ligand binding assays. Ligand binding assays were performed in Regisil-treated test tubes in a volume of 1 ml containing buffer B, radioligand, and cannabinoid drugs as specified. The incubation was started by the addition of 20 to 50 μg of membrane protein. With the exception of the kinetic experiments, all reactions were carried out at 30° for 50 min. After incubation, the samples were transferred to 1.5-ml polypropylene microfuge tubes and immediately centrifuged for 9 min at 13,000 × *g*. After centrifugation, the supernatant was aspirated and counted to determine the concentration of free [^{3}H]CP-55,940. The microfuge tubes were drained on drying pins for 30 min, after

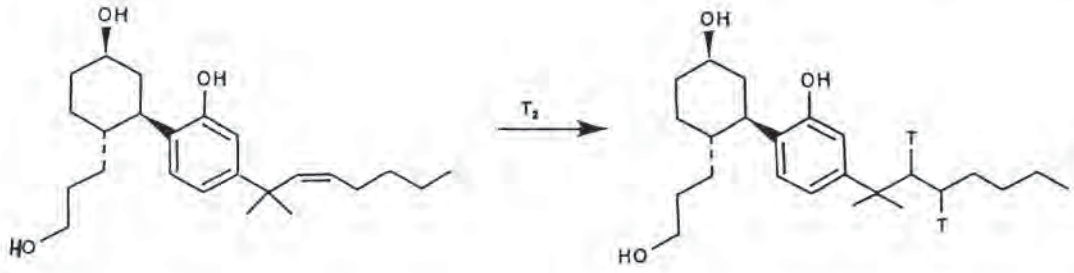

1

$^3H_2$ -CP-55,940

Fig. 1. The synthesis of [^{3}H]CP-55,940 by the tritium reduction of compound 1.

which the tips of the tubes were sliced, using a heated spatula and a cutting block designed to ensure that the cut tips were of identical size. The tips were then placed in scintillation vials and submersed in 2 ml of a solubilizing solution (5% ethanol, 5% Triton X100, 0.2 N NaOH). The vials were then shaken for at least 4 hr in order to dissolve the pelleted membranes. Scintillation cocktail (10 ml) was added to each vial and the radioactivity was determined using a Beckman LS1800 with an efficiency for tritium of 30%. Nonspecific binding to the microfuge tip was assessed in control tubes having radioligand but no protein (typically 2% to 3% of the total radioactivity available in the incubation medium). Subtracting this value from total binding gave the total binding in the pelleted membranes. Specific binding was defined as the difference between total binding to the membranes in the absence and presence of either 100 nM DALN or 1 μM Δ^9-THC. Nonspecific binding to the membranes was typically 15% to 30% of the total binding to the membranes, dependent upon the membrane and ligand concentrations (see Fig. 2). Assays were carried out in triplicate with an average coefficient of variation for the samples of 2.5%, and experiments were repeated at least three times.

Metabolism of [^{3}H]CP-55,940. To determine whether [^{3}H]CP-55,940 was metabolized during the binding assay, 40 μg of membrane protein were incubated with 70 pM [^{3}H]CP-55,940 for 90 min at 30° in the standard assay buffer described above. After centrifugation, the supernatant and the pellet were separated and the radioactivity was extracted from each using ether. After drying with N_2 gas, the samples and an unincubated [^{3}H]CP-55,940 control were resuspended in absolute ethanol, and thin layer chromatography was performed using the procedure described above. The plate was sprayed with EN^{3}HANCE (NEN, Boston, MA), placed against Kodak X-Omat film and stored at −80° for 6 days. Upon developing, a single band was observed for the samples which comigrated with the control. These studies demonstrated that neither the free nor bound [^{3}H]CP-55,940 was metabolized or chemically modified during the assay procedure.

Results

Conditions for cannabinoid receptor binding. Initial studies addressed the separation of unbound ligand from bound radiolabeled ligand. In agreement with the experience of Roth and Williams (16) and Harris *et al.* (19) using THC as the labeled ligand, separation of free [^{3}H]CP-55,940 using a filtration technique met with little success. The binding of ligand to glass fiber and cellulose nitrate or cellulose acetate filters was excessive and varied with the concentration of radioligand added. Treatment of the filters with various organic solvents, detergents, polyethyleneimine, or bovine serum albumin did not provide acceptable conditions for separation. Separating the free [^{3}H]CP-55,940 by adsorption onto dextran-coated charcoal was also unsuccessful (see also Ref. 19). Optimal conditions were achieved using the sedimentation procedure described above. The incubations were performed in Regisil-treated glass tubes in an effort to minimize the adsorption of cannabinoid compounds to the surface (20). Similarly, the presence of bovine serum albumin in the incubation mixture would also effectively decrease the amount of cannabinoid drug bound to the glassware (16). Any alterations in the free concentration of [^{3}H]CP-55,940 resulting from adherence to the glassware during the incubation were accounted for by determining the exact amount of radiolabeled ligand in the supernatant and adhering to the microfuge tube after the sedimentation for each assay.

To determine the optimal incubation conditions for binding, several different buffers were tried at various concentrations and pH values. Of the buffers tested, including K^+ HEPES, *K^+N-tris[Hydroxymethyl]methyl-2-aminoethanesulfonate, K^+ phosphate, and imidazole Cl^-, none performed any better than 50 mM Tris Cl^-. Optimal binding was observed between pH 7 and 8, with specific binding of only 60% of optimal at pH 6 or 9 (data not shown). The phenolic moiety of [^{3}H]CP-55,940 might be expected to have a pK in the vicinity of pH 10. The 40% loss of specific binding observed between pH 8 and 9 cannot be entirely accounted for by a modification of the ligand. The pH requirement can be postulated to also reflect the optimal pH for amino acids that would interact with the ligand or be required to maintain the optimal protein conformation.*

Under the experimental conditions used, linear binding extended from 10 to 50 μg/ml of protein for the P_2 membrane preparation (data not shown). Experiments were routinely conducted using 20 to 40 μg/ml P_2 protein, and in this range specific binding typically represented 85% of the total binding. Specific binding was linear through 120 to 150 μg/ml of protein for the synaptosomal preparation (data not shown). As the concentration of membranes was increased, there was a decline in the percentage of the total binding that could be described as specific.

Thermolability of the specific binding was demonstrated. Membrane preparations that were incubated at 60° for 12 min before assay failed to show significant specific binding (data not shown). These findings would be consistent with the binding of [^{3}H]CP-55,940 to a protein component of the membranes that is subject to thermal denaturation.

Characterization of the [^{3}H]CP-55,940 binding site. [^{3}H]CP-55,940 binding to cortical membranes was saturable, whereas nonspecific binding continued to increase with increasing concentrations of [^{3}H]CP-55,940 (Fig. 2A, *inset*). An example of a saturation binding isotherm and the Scatchard plot obtained therefrom are depicted in Fig. 2. A K_d of 133 ± 11 pM was obtained by Scatchard transformation (21) of the data from four experiments (mean ± standard error). The density of binding sites for the P_2 cortical preparation was 1.85 ± 0.26 pmol/mg of protein (four experiments). The data were analyzed by the Hill transformation (21), yielding a straight line (Fig.

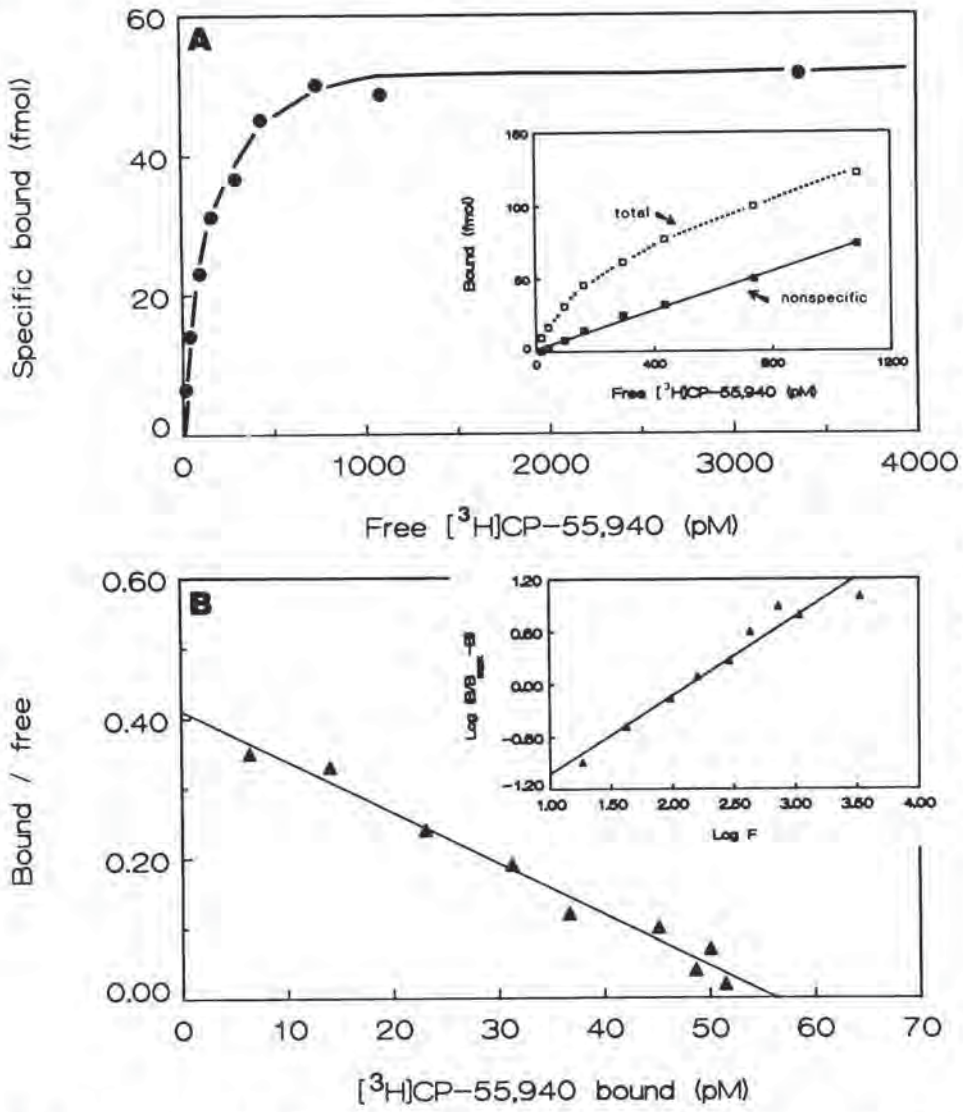

Fig. 2. Equilibrium binding of [^{3}H]CP-55,940. Membranes (43 μg of protein) were incubated with various concentrations of [^{3}H]CP-55,940. A, The saturation isotherm of specific binding. *Inset;* binding of [^{3}H]CP-55,940 in the absence (□) or presence (■) of 1 μM DALN. B, Scatchard transformation of [^{3}H]CP-55,940 binding data from A with the bound ligand being expressed in terms of concentration (pM). This experiment exhibited K_d and B_{max} values of 139 pM and 1.3 pmol/mg of protein, respectively. *Inset;* The Hill transformation of data from A. *F*; free drug concentration; *B*; specifically bound drug. The Hill coefficient (n_H) was calculated to be 0.90 for this experiment. The *lines* drawn represent the best fit as determined by least squares linear regression analysis.

2B, *inset*). The K_d derived from such analysis was 116 ± 12 pM and the n_H was 0.88 ± 0.08 (four experiments). The observation that the n_H approaches one suggests that a single class of binding sites is being labeled by [^{3}H]CP-55,940 under the assay conditions described and that no significant cooperativity exists among binding sites.

Kinetic analysis of the binding of [^{3}H]CP-55,940 to P_2 membranes indicates a rapid association of the ligand with the receptor (Fig. 3A). Equilibrium was reached rapidly, with greater than 90% of maximal specific binding attained within 50 min at 30°. The binding plateau remained stable for at least 2 hr. This is consistent with the determination that the radioligand is not being metabolized or chemically altered during the incubation (see Experimental Procedures). The nonspecific binding component reached steady state at the earliest time point measurable and underwent no further change through 3 hr.

The dissociation of the [^{3}H]CP-55,940-receptor complex initiated by the addition of 100 nM DALN is depicted in Fig. 3B. These studies were performed by establishing equilibrium directly in the microfuge tubes rather than by transferring the reaction mixture before sedimentation. Semilog plots suggest that dissociation was not monophasic (Fig. 3B). When the microfuge tubes were centrifuged immediately upon addition of 100 nM DALN, 20% of the specific binding at equilibrium was already displaced. It should be noted that the time for complete sedimentation is 10 min. However, one would expect that the major fraction of membranes would have sedimented within the first 3 min of centrifugation. Thus, the data obtained for the earliest time points depicted may represent the displacement occurring during the period of manipulation. Assuming first-order dissociation (21), the k_{-1} for the slower component was 0.016 ± 0.001 min^{-1} (three experiments) ($t_{1/2}$ = 45 min). A more rapid dissociation could also be discerned, having at $t_{1/2} \leq$ 11 min ($K_{-1} \geq 0.06$ min^{-1}). It is possible that these two kinetic states may represent interchangeable forms of the receptor. One mechanism for this may be the transient interaction of the receptor with G proteins either possessing tightly bound GDP or free of guanine nucleotides. Evidence for such an interaction is described below. It is of interest that two binding affinities were not discernible in the equilibrium binding studies. In preliminary studies using unwashed P_2 membranes, it was observed that multiple affinity states could be discerned in equilibrium binding studies (data not shown). An explanation

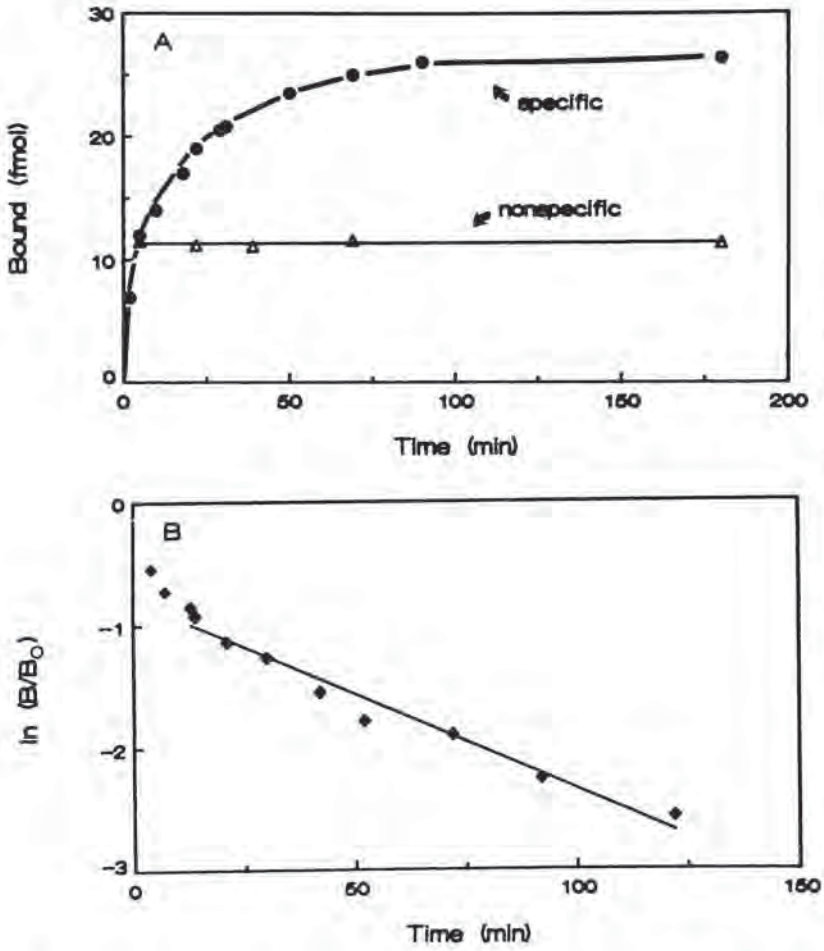

Fig. 3. Time course of association (A) and dissociation (B) of [^{3}H]CP-55,940. [^{3}H]CP-55,940 (81 pM) was incubated with 28 μg of P_2 membranes at 30°. A, The times indicated are those that elapsed between the addition of protein (start of the reaction) and the start of centrifugation of the microfuge tubes. Specific and nonspecific binding were determined with 100 nM DALN as described in Experimental Procedures. B, After equilibrium binding of [^{3}H]CP-55,940 had been reached (70 min), 100 nM DALN was added (t = 0) and dissociation was monitored. Data presented are a first-order representation with B/B_0 denoting the specific binding at the time indicated/specific binding at t = 0. The results are means of triplicate determinations from a single representative experiment, which was performed three times.

for these results might be that the population of G proteins possessing tightly bound GDP could be greater in unwashed membranes.

The K_d for binding may be calculated from the association and dissociation rates. The initial rate of association was estimated by assuming that pelleting of the membranes required 3 min and that the dissociation would not contribute appreciably to the reaction until after 5 min of incubation. The k_{+1} estimated from the initial rate of binding (22) was 3.4 ± 0.76 × 10^{-4} pM^{-1} min^{-1} (three experiments). Using this value, the K_d calculated for the slowly displacing site was 47 pM. The K_d for the rapidly dissociating site would have to exceed 180 pM. An alternative treatment of the data would be to estimate a k_{obs} as the reaction proceeds to equilibrium using a pseudo-first-order method (21, 22). Using the slower dissociation rate, the k_{+1} may be calculated to be 2.6 ± 0.2 × 10^{-4} pM^{-1} min^{-1} and the K_d would be 62 pM. Although both of these methods for estimating the k_{+1} (and thus the K_d values) have theoretical and methodological limitations, the kinetic estimates of the K_d are similar to the values calculated using linear transformation of the equilibrium binding data. Thus, an internal consistency for the methodology has been demonstrated.

Allosteric regulation of binding. One would hypothesize that a receptor that transmits its signal to the adenylate cyclase system via a G protein would be regulated by allosteric mechanisms similar to those that have been demonstrated for other functionally homologous receptors. Our current understanding of the influence of G proteins on agonist-receptor interactions has been reviewed by Birnbaumer and colleagues (23) and Casey and Gilman (24). To summarize briefly, G proteins are believed to exist in a heterotrimer form ($\alpha\beta\gamma$) possessing tightly bound GDP in the presence of Mg^{2+}. Upon interaction with a receptor-agonist complex, a conformational change confers sufficient energy to the system such that the GDP dissociates. In the absence of guanine nucleotides, the receptor-hormone-G protein intermediate complex exhibits a relatively high affinity for the agonist. Upon binding of GTP or a nonhydrolyzable analog to this complex, the affinity of the agonist ligand for the receptor is decreased, and the G protein dissociates from the receptor and separates into α and $\beta\gamma$ subunits. The effector (e.g., adenylate cyclase) interacts with the GTP-bound α subunit. Dissociation of the hormone from the receptor and hydrolysis of the GTP on the α subunit allow the system to perpetually respond to altered concentrations of hormone.

For the cannabinoid receptor, equilibrium binding studies indicated that the presence of 100 μM Gpp(NH)p resulted in a 40% decrease in specific binding of [^{3}H]CP-55,940 (data not shown). The kinetics of dissociation were analyzed in the presence or absence of guanine nucleotide (Fig. 4). The addition of Gpp(NH)p reduced the $t_{1/2}$ from 45 min to 12 min. The k_{-1} calculated for dissociation in the presence of Gpp(NH)p was 0.059 ± 0.009 min^{-1} (three experiments) and the K_d was 176 pM. This value is similar to the K_d estimated for the rapidly dissociating component described above. An in-depth analysis

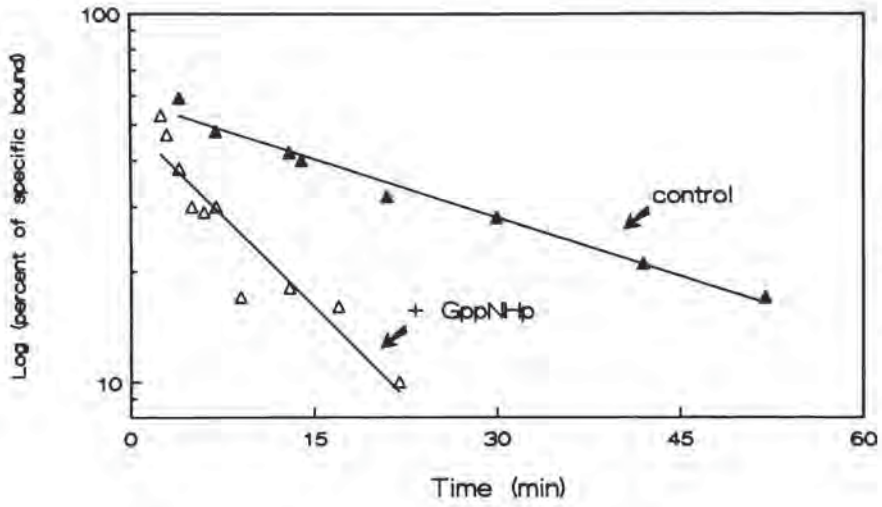

Fig. 4. Effect of Gpp(NH)p on the dissociation rate of [^{3}H]CP-55,940. [^{3}H]CP-55,940 (81 pM) was incubated with 28 μg of P_2 preparation membranes for 70 min at 30° and dissociation was monitored after addition of 100 nM DALN (t = 0). *Control*, addition of 100 nM DALN; *+Gpp(NH)p*, simultaneous addition of 100 nM DALN plus 100 μM Gpp(NH)p. The x axis indicates the time that elapsed between the addition of the above compounds and 2 min after the start of centrifugation. The y axis is a log-scale presentation of the percentage of specific binding at the indicated time/specific binding at t = 0. The data are the means of triplicate determinations from a single representative experiment, which was repeated three times.

of the interaction of the [^{3}H]CP-55,940 binding site with G proteins in various states is beyond the scope of this study. The most facile interpretation of the results presented here is that the [^{3}H]CP-55,940 binding site can be influenced by guanine nucleotides in a manner consistent with the interaction of a receptor with a G protein.

Divalent cations have been reported to influence the affinity of agonists for their receptors. It is believed that the G protein possesses at least one site for Mg^{2+} (23, 24). A role for this divalent cation has been shown for the dissociation of GDP in the presence of the receptor-hormone complex, in addition to other functions associated with a site having a much higher affinity for Mg^{2+} (23, 24). The effects of Mg^{2+} to increase the affinity of agonist ligands for receptors associated with adenylate cyclase have been discussed by Maguire (25). In the present investigation, concentrations of $MgCl_2$ as low as 1 mM stimulated specific binding of the agonist ligand [^{3}H]CP-55,940 by greater than 50% (Fig. 5). Qualitatively similar effects were observed with $CaCl_2$. $MnCl_2$ also stimulated specific binding in a manner similar to $MgCl_2$ (data not shown).

Studies of the opioid receptor, which is coupled to adenylate cyclase in an inhibitory manner, indicated that Na^+ may act as an allosteric regulator (26, 27). Na^+ has been demonstrated to decrease the affinity of agonist ligands for the opioid receptor (see Ref. 26 and references therein). In an effort to determine whether regulation of the binding of [^{3}H]CP-55,940 by monovalent cations could be observed, the effects of various chloride salts were determined (Fig. 5). Monovalent cations were tested at concentrations that might be expected to be present intracellularly or extracellularly. At 20 mM, Na^+ reduced specific binding by about 40%. Low concentrations of K^+ had minimal effects. Concentrations of 120 mM NaCl and 100 mM KCl inhibited specific binding by about 80%. The selectivity of this response to Na^+ does not appear to be great, suggesting that this inhibition may not be the result of a specific interaction with a Na^+ site. It is possible that a chaotropic effect of higher salt concentrations is altering the ability of the ligand to bind to the receptor.

Pharmacology of the cannabinoid receptor. The specificity of [^{3}H]CP-55,940 binding was established by determining the ability of related synthetic compounds and several natural cannabinoid compounds to compete with [^{3}H]CP-55,940 for occupancy of the specific binding sites in the cortical membranes (Fig. 6). Unlabeled CP-55,940 had a K_i of 68 ± 6.2 pM and B_{max} of 1.75 ± 0.20 pmol/mg protein (three experiments) as determined by computer analysis of homologous displacement data using the LIGAND program (version 2.3.11; May, 1987) (28). A one-site model fit the data better than a two-site model for both CP-55,940 and other cannabinoid drugs tested using an F test criterion on the residual variances at the level

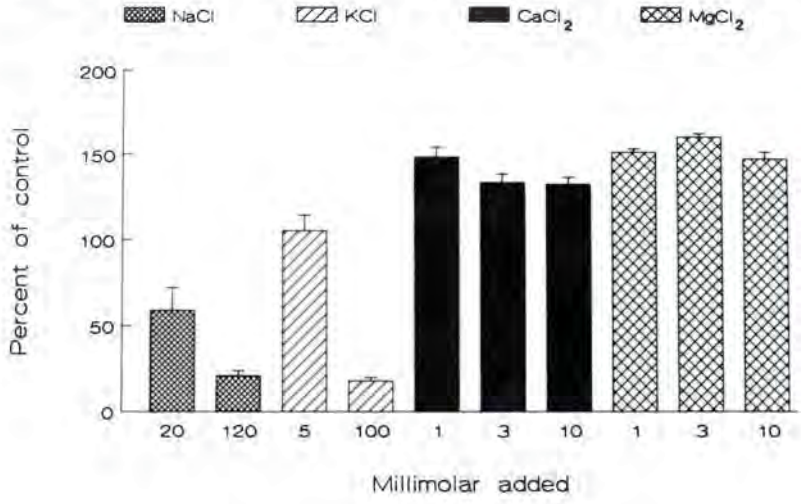

Fig. 5. The influence of cations on specific binding of [^{3}H]CP-55,940. Control samples contained 50 mM Tris·HCl, 1 mM Tris·EDTA, and 0.1 mM $MgCl_2$. Experimental samples contained the same buffer plus the indicated concentrations of salts. The data are the means ± standard error of triplicate determinations from a single representative experiment. All values were different from control at $p < 0.05$ except 20 mM NaCl and 5 mM KCl. Similar results were observed in two other experiments.

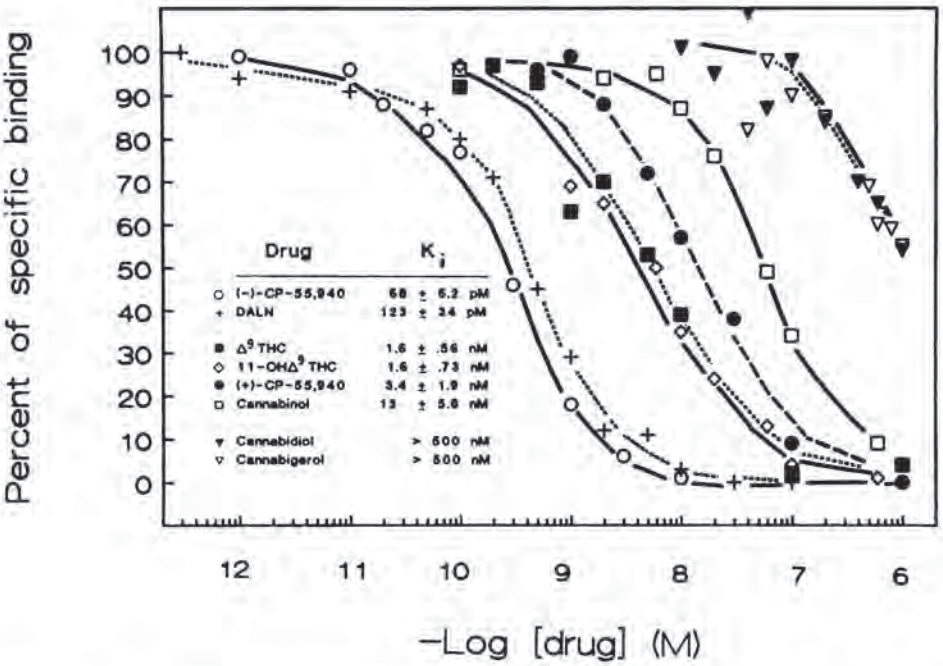

Fig. 6. Competitive inhibition of [^{3}H]CP-55,940 binding by various synthetic and natural cannabinoid drugs. [^{3}H]CP-55,940 (50–70 pM) was incubated with P_2 membranes (16–30 μg) for 50 min at 30° with either the indicated concentrations of drug or vehicle alone. The results were normalized to 100% of specific binding, which was determined with 100 nM DALN as described in Experimental Procedures. Data points represent the averages of triplicate determinations from single representative experiments. The K_i values listed in the *inset table* were determined using the LIGAND program and represent the mean ± standard error of three independent experiments for each drug.

of $p = 0.05$. Using 68 pM as the K_d for [^{3}H]CP-55,940, the K_i values of the various compounds were determined by LIGAND analysis of heterologous displacement data. The (+)-isomer of CP-55,940 was 50-fold less potent than the (−)-isomer, having a K_i of 3.4 nM. DALN was nearly equipotent with CP-55,940, having a K_i of 123 pM. Δ^9-THC and 11-OH-Δ^9-THC both exhibited high affinity binding with K_i values of 1.6 nM. Cannabinol was 8-fold less potent than Δ^9-THC, having a K_i of 13 nM. This order of potency generally parallels the order of potency for both CNS activity *in vivo* (1, 3, 12, 29) and inhibition of adenylate cyclase *in vitro* (7, 8).

Cannabidiol and cannabigerol were much less potent, binding the [^{3}H]CP-55,940 site with K_i values estimated to be greater than 500 nM. Cannabidiol and cannabigerol were unable to fully displace the specifically bound [^{3}H]CP-55,940 at the highest concentrations tested (1 μM). Concentrations greater than this were not tested due to the limited solubility of cannabinoid drugs above 1 μM and the confounding aspects of increasing the solvent or bovine serum albumin concentration, which would be necessary to maintain higher concentrations of cannabinoid compounds in solution. These latter two compounds fail to exhibit cannabinoid activity in humans or animal models (1–3). One of several explanations for the binding results could apply. 1) The two compounds could bind to the receptor with low affinity, but the concentrations required to observe a biological response may not be possible to achieve *in vivo*. 2) The cannabinoid response to these two compounds may be masked by drug effects at high concentrations, such as membrane perturbation in *in vitro* studies and CNS depression in *in vivo* studies. 3) The observed binding displacement may be the result of a contaminant in the drug preparation. The latter explanation is a possible artifact that must be dealt with in future investigations. These drugs were isolated from organic extracts of cannabis that originally contained a variety of cannabinoid compounds, including Δ^9-THC.

Discussion

Studies suggestive of a cannabinoid receptor were based on the ability of centrally active cannabinoid drugs to interact with a well characterized, cellular second messenger system. The ability of cannabinoid compounds to inhibit adenylate cyclase in a reversible, cell type-specific, potent, and enantioselective manner (5–8) would support the hypothesis that these compounds interact with a biological membrane-bound receptor. Additional arguments in favor of a receptor mediating the interaction of cannabinoid drugs with adenylate cyclase are the characteristic guanine nucleotide and divalent cation requirements for this interaction and the demonstrated pertussis toxin sensitivity characteristic of G_i-linked receptors (6, 13).

The findings presented in this study provide the strongest argument currently available for a cannabinoid receptor. The binding site described here is entirely consistent with a receptor that would be associated with a second messenger system via a G protein. The pH sensitivity and thermolability are consistent with a protein structure for this binding site. The rapid and reversible binding are properties expected of a neuromodulator receptor. The binding saturability and the B_{max} determined in the rat cortex are consistent with values reported for CNS neuromodulator receptors (30). The K_d for binding of [^{3}H]CP-55,940 derived from the kinetic constants agrees remarkably with the K_d obtained from equilibrium binding studies. The affinity determined for this agonist ligand is consistent with what would be expected for a neuromodulatory receptor in the CNS (30).

It may be hypothesized that the binding site for [^{3}H]CP-55,940 is linked to adenylate cyclase in the brain. Previous investigations of the inhibition of adenylate cyclase by cannabinoid drugs have utilized a cloned neuroblastoma cell model system. To strengthen the putative association of the cannabinoid receptor with adenylate cyclase in the CNS, we now have evidence using brain slice preparations. Cyclic AMP production in several rat brain regions is decreased in response to cannabinoid drugs (31, 32). The affinity of the agonist [^{3}H]CP-55,940 for its cortical binding site in the absence of guanine nucleotides was more than 2 orders of magnitude greater than its K_{inh} for regulation of adenylate cyclase in the neuronal cell

model (8). However, the affinity state promoted by the addition of Gpp(NH)p would be the prevalent state concurrent with adenylate cyclase regulation (23, 24). The order of potencies for ligand interaction and the enantioselectivity described for this binding site are consistent with previously reported data for the inhibition of adenylate cyclase (7, 8).

One of the responses that the [^{3}H]CP-55,940 receptor site may regulate *in vivo* is analgesia. This ligand was specifically designed to possess potent analgetic activity (12). The analgetic activity for CP-55,940 was demonstrated in the tail flick, hot plate, phenylbenzylquinone writhing, tail clamp, and flinch jump tests in rodents (8, 12). The ratio of the activities of the (−)- to the (+)-isomer in the analgetic tests was 200-fold. This agrees reasonably well with the 50-fold enantioselectivity demonstrated here for the [^{3}H]CP-55,940 binding site. The order of potency for analgetic activity is mimicked by the order of potency reported here for the binding to the receptor. Other functions typical of the cannabinoid class of drugs, including changes in spontaneous locomotor activity, hypothermia, and immobility, have also been demonstrated for CP-55,940 and have been shown to be enantioselective (29). Thus, this receptor site appears to be associated with certain of the typical cannabinoid responses observed in animals in addition to analgesia.

Previous attempts to find and characterize a cannabinoid receptor associated with *in vitro* or *in vivo* functions have not met with success. Harris and colleagues (19) and Roth and Williams (16) demonstrated binding of [^{3}H]Δ^8-THC and [^{3}H]Δ^9-THC, respectively, to crude or purified synaptosomal membranes from rat brains. The former group were able to displace up to 10% of the binding with 1 μM Δ^8-THC; however, the binding was not saturable and pharmacological displacement by other cannabinoid ligands was not performed (19). The latter investigators were unable to discern a high affinity component of binding other than membrane adsorption, which was not dependent upon the concentration of free Δ^9-THC (16).

A high affinity binding site in brain membranes was described by Nye and colleagues (33, 34) using the [^{3}H]5′-trimethylammonium analog of Δ^8-THC. The ligand used for binding to this site does not exhibit biological activity in typical animal behavioral models of cannabinoid action, with the exception of CNS depression (35). This poor biological activity is consistent with our previous demonstration of the importance of maintaining the hydrophobic nature of the alkyl side chain extending from the A-ring (8). The pharmacological profile for displacement of [^{3}H]5′-trimethylammonium Δ^8-THC indicated that cannabinoid compounds having greatest affinity in several brain regions (e.g., cannabigerol and cannabidiol) are neither agonists nor antagonists in *in vivo* animal models or in humans (33). Thus, the pharmacological relevance of this binding site to cannabinoid effects *in vivo* may be questioned. The selectivity of the [^{3}H]trimethylammonium Δ^8-THC binding site for stereoisomers of Δ^9-THC and Δ^8-THC was less than 2-fold, and no stereoselectivity was observed for levonantradol and dextronantradol (33). The kinetic constants derived for the binding of [^{3}H]trimethylammonium Δ^8-THC yielded a K_d that was 3 orders of magnitude lower than the K_d determined by Scatchard analysis of the equilibrium binding data (34). This unusual finding may in part be explained by the observation that, throughout these experiments, the aqueous solubility and adsorption to glass of the ligands were not considered (33). Evidence suggests that this binding site is not linked to a G protein inasmuch as binding of [^{3}H]trimethylammonium Δ^8-THC was enhanced rather than decreased by nonhydrolyzable analogs of guanine nucleotides (34). It is clear that the [^{3}H]trimethylammonium Δ^8-THC binding site is definitely different from the cannabinoid receptor described here using [^{3}H]CP-55,940 as the ligand.

Other laboratories have suggested that cannabinoid drugs alter the binding of other neuromodulators to their receptors. Hillard and Bloom (36) reported that concentrations in excess of 3 μM Δ^9-THC or 11-OH-Δ^9-THC in the presence of a detergent vehicle increased the specific binding of the β-adrenergic antagonist ligand [^{3}H]dihydroalprenolol in mouse cortical homogenates. The interpretation of this finding was that the cannabinoid drugs altered membrane properties such that the binding behavior was modified (36). This mechanism is supported by additional studies from that laboratory, which demonstrated that similarly high concentrations of cannabinoid drugs altered fluidity of synaptic plasma membranes as detected by fluorescence polarization (37). Vaysse and colleagues (38) reported a similar interference with certain binding assays for opioid receptors by addition of high concentrations of several cannabinoid drugs in the presence of 100 mM ethanol. We have previously demonstrated that the site of cannabinoid action in neuroblastoma cells is not related to the binding of agonists to the δ opioid receptor or to subsequent signal transduction (14). The studies reported in the present work clearly indicate the presence of a pharmacologically selective, high affinity binding site for cannabinoid drugs. However, membrane perturbation may be the mechanism by which high concentrations of cannabinoid drugs may interfere with binding determinations made for a variety of other receptor types.

The development of a ligand binding assay for the cannabinoid class of drugs will allow investigations of cannabinoid actions that have previously not been possible. Pathways in the brain that may be involved in cannabinoid action can be examined. The cellular regulation of the receptor can be more fully characterized and its interaction with alternative second messenger systems can be assessed. Perhaps an antagonist for the cannabinoid drugs can be developed now that a binding site has been found that correlates with a cellular function (inhibition of adenylate cyclase). Furthermore, efforts to search for a putative endogenous ligand can now proceed. Thus, the importance of the characterization of a cannabinoid receptor will make a major impact on research in this field.

Acknowledgments

The excellent clerical assistance of Maggie Klevorn is gratefully appreciated.

References

1. Hollister, L. E. Health aspects of cannabis. *Pharmacol. Rev.* **38**:1–20 (1986).
2. Dewey, W. L. Cannabinoid pharmacology. *Pharmacol. Rev.* **38**:151–178 (1986).
3. Razdan, R. K. Structure-activity relationships in cannabinoids. *Pharmacol. Rev.* **38**:75–149 (1986).
4. Martin, B. R. Cellular effects of cannabinoids. *Pharmacol. Rev.* **38**:45–74 (1986).
5. Howlett, A. C., and R. M. Fleming. Cannabinoid inhibition of adenylate cyclase: pharmacology of the response in neuroblastoma cell membranes. *Mol. Pharmacol.* **26**:532–538 (1984).
6. Howlett, A. C. Cannabinoid inhibition of adenylate cyclase: biochemistry of the response in neuroblastoma cell membranes. *Mol. Pharmacol.* **27**:429–436 (1985).
7. Howlett, A. C. Cannabinoid inhibition of adenylate cyclase: relative activity of constituents and metabolites of marihuana. *Neuropharmacology* **26**:507–512 (1987).
8. Howlett, A. C., M. R. Johnson, L. S. Melvin, and G. M. Milne. Nonclassical cannabinoid analgetics inhibit adenylate cyclase: development of a cannabinoid receptor model. *Mol. Pharmacol.* **33**:297–302 (1988).

9. Gill, E. W., and G. Jones. Brain levels of Δ^1-tetrahydrocannabinol and its metabolites in mice— Correlation with behaviour, and the effect of the metabolic inhibitors SKF 525A and piperonyl butoxide. *Biochem. Pharmacol.* **21**:2237–2248 (1972).
10. Ho, B. T., V. S. Estevez, and L. F. Englert. The uptake and metabolic fate of cannabinoids in rat brains. *J. Pharm. Pharmacol.* **25**:488–490 (1973).
11. Ohlsson, A., M. Widman, S. Carlsson, T. Ryman, and C. Strid. Plasma and brain levels of Δ^9-THC and seven monooxygenated metabolites correlated to the cataleptic effect in the mouse. *Acta Pharmacol. Toxicol.* **47**:308–317 (1980).
12. Johnson, M. R., and L. S. Melvin. The discovery of nonclassical cannabinoid analgetics, in *Cannabinoids as Therapeutic Agents* (R. Mechoulam, ed.). CRC Press, Boca Raton, FL, 121–145 (1986).
13. Howlett, A. C., J. M. Qualy, and L. K. Khachatrian. Involvement of G_i in the inhibition of adenylate cyclase by cannabimimetic drugs. *Mol. Pharmacol.* **29**:307–313 (1986).
14. Devane, W. A., J. W. Spain, C. J. Coscia, and A. C. Howlett. An assessment of the role of opioid receptors in the response to cannabimimetic drugs. *J. Neurochem.* **46**:1929–1935 (1986).
15. Seeman, P., M. Chau-Wong, and S. Moyyen. The membrane binding of morphine, diphenylhydantoin and tetrahydrocannabinol. *Can. J. Physiol. Pharmacol.* **50**:1193–1200 (1972).
16. Roth, S. H., and P. J. Williams. The non-specific membrane binding properties of Δ^9-tetrahydrocannabinol and the effects of various solubilizers. *J. Pharm. Pharmacol.* **31**:224–230 (1979).
17. Bradford, M. M. A rapid and sensitive method for the quantitation of microgram quantities of protein utilizing the principle of protein-dye binding. *Anal. Biochem.* **72**:248–254 (1976).
18. Dodd, P. R., J. A. Hardy, A. E. Oakley, J. A. Edwardson, E. K. Perry, and J.-P. Delaunoy. A rapid method for preparing synaptosomes: Comparison with alternative procedures. *Brain Res.* **226**:107–118 (1981).
19. Harris, L. S., R. A. Carchman, and B. R. Martin. Evidence for the existence of specific cannabinoid binding sites. *Life Sci.* **22**:1131–1138 (1978).
20. Garrett, E. R., and C. A. Hunt. Physicochemical properties, solubility, and protein binding of Δ^9-tetrahydrocannabinol. *J. Pharm. Sci.* **63**:1056–1064 (1974).
21. Limbird, L. E. *Cell Surface Receptors: A Short Course on Theory and Methods.* Martinus Nijhoff Publishing, Boston, 51–96 (1986).
22. Bennett, J. P., and H. I. Yamamura. Neurotransmitter, hormone, or drug receptor binding methods, in *Neurotransmitter Receptor Binding* (H. I. Yamamura, S. J. Enna, and M. J. Kuhar, eds.). Raven Press, New York 61–89 (1985).
23. Birnbaumer, L., J. Codina, R. Mattera, R. A. Cerione, J. D. Hildebrandt, T. Sunyer, F. J. Rojas, M. G. Caron, R. J. Lefkowitz, and R. Iyengar. Regulation of hormone receptors and adenylyl cyclases by guanine nucleotide binding N proteins. *Recent Prog. Horm. Res.* **41**:41–99 (1985).
24. Casey, P. J., and A. G. Gilman. G protein involvement in receptor-effector coupling. *J. Biol. Chem.* **263**:2577–2580 (1988).
25. Maguire, M. E. Hormone-sensitive magnesium transport and magnesium regulation of adenylate cyclase. *Trends Pharmacol. Sci.* **5**:73–77 (1984).
26. Blume, A. J., D. Lichtshtein, and G. Boone. Coupling of opiate receptors to adenylate cyclase: requirement for Na^+ and GTP. *Proc. Natl. Acad. Sci. USA* **76**:5626–5630 (1979).
27. Koski, G., R. A. Streaty, and W. A. Klee. Modulation of sodium-sensitive GTPase by partial opiate agonist. An explanation for the dual requirement for Na^+ and GTP in inhibitory regulation of adenylate cyclase. *J. Biol. Chem.* **257**:14035–14040 (1982).
28. Munson, P. J., and D. Rodbard. LIGAND: a versatile computerized approach for characterization of ligand-binding systems. *Anal. Biochem.* **107**:220–239 (1980).
29. Little, P. J., D. R. Compton, M. R. Johnson, L. S. Melvin, and B. R. Martin. Pharmacology and stereoselectivity of structurally novel cannabinoids in mice. *J. Pharmacol. Exp. Ther.*, in press.
30. Burt, D. R. Criteria for receptor identification, in *Neurotransmitter Receptor Binding* (H. I. Yamamura, S. J. Enna, and M. J. Kuhar, eds.). Raven Press, New York, 41–60 (1985).
31. Bidaut-Russell, M., and A. C. Howlett. Cannabinoid drugs regulate cyclic AMP metabolism in rat brain. *Trans. Am. Soc. Neurochem.* **19**:163 (1988).
32. Bidaut-Russell, M., and A. Howlett. Opioid and cannabinoid analgetics both inhibit cyclic AMP production in the rat striatum. *Adv. Biosci.* in press.
33. Nye, J. S., H. H. Seltzman, C. G. Pitt, and S. H. Snyder. High-affinity cannabinoid binding sites in brain membranes labeled with [^{3}H]-5′-trimethylammonium Δ^8-tetrahydrocannabinol. *J. Pharmacol. Exp. Ther.* **234**:784–791 (1985).
34. Nye, J. S., and S. H. Snyder. The high-affinity cannabinoid binding site in brain: regulation by guanine nucleotides and isolation of an endogenous inhibitor. *Natl. Inst. Drug Abuse Res. Monogr.* **79**:134–147 (1987).
35. Compton, D. R., P. J. Little, and B. R. Martin. Cannabinoid behavioral effects: specific versus non-specific actions, in *Marijuana '87: Proceedings of the Melbourne Symposium on Cannabis* (G. B. Cheshire, P. Consroe, and R. Musty, eds.). NCADA Monograph, Australian Government Publishing Service, Canberra, 213–218 (1988).
36. Hillard, C. J., and A. S. Bloom. Δ^9-Tetrahydrocannabinol-induced changes in β-adrenergic receptor binding in mouse cerebral cortex. *Brain Res.* **235**:370–377 (1982).
37. Hillard, C. J., R. A. Harris, and A. S. Bloom. Effects of the cannabinoids on physical properties of brain membranes and phospholipid vesicles: fluorescence studies. *J. Pharmacol. Exp. Ther.* **232**:579–588 (1985).
38. Vaysse, P. J.-J., E. L. Gardner, and R. S. Zukin. Modulation of rat brain opioid receptors by cannabinoids. *J. Pharmacol. Exp. Ther.* **241**:534–539 (1987).

Send reprint requests to: Dr. Allyn C. Howlett, Department of Pharmacology, St. Louis University School of Medicine, 1402 South Grand Boulevard, St. Louis, MO 63104.

Proc. Natl. Acad. Sci. USA
Vol. 87, pp. 1932–1936, March 1990
Neurobiology

Cannabinoid receptor localization in brain

(tetrahydrocannabinol/autoradiography/basal ganglia/hippocampus/cerebellum)

MILES HERKENHAM*†, ALLISON B. LYNN*, MARK D. LITTLE*, M. ROSS JOHNSON‡, LAWRENCE S. MELVIN§, BRIAN R. DE COSTA¶, AND KENNER C. RICE¶

*Unit on Functional Neuroanatomy, Building 36, Room 2D-15, National Institute of Mental Health, Bethesda, MD 20892; ‡Glaxo Inc., Research Triangle Park, NC 27709; §Central Research, Pfizer Inc., Groton, CT 06340; and ¶Laboratory of Medicinal Chemistry, National Institute of Diabetes and Digestive and Kidney Diseases, Bethesda, MD 20892

Communicated by Walle J. H. Nauta, December 7, 1989

ABSTRACT **[^{3}H]CP 55,940, a radiolabeled synthetic cannabinoid, which is 10–100 times more potent *in vivo* than Δ^9-tetrahydrocannabinol, was used to characterize and localize a specific cannabinoid receptor in brain sections. The potencies of a series of natural and synthetic cannabinoids as competitors of [^{3}H]CP 55,940 binding correlated closely with their relative potencies in several biological assays, suggesting that the receptor characterized in our *in vitro* assay is the same receptor that mediates behavioral and pharmacological effects of cannabinoids, including human subjective experience. Autoradiography of cannabinoid receptors in brain sections from several mammalian species, including human, reveals a unique and conserved distribution; binding is most dense in outflow nuclei of the basal ganglia—the substantia nigra pars reticulata and globus pallidus—and in the hippocampus and cerebellum. Generally high densities in forebrain and cerebellum implicate roles for cannabinoids in cognition and movement. Sparse densities in lower brainstem areas controlling cardiovascular and respiratory functions may explain why high doses of Δ^9-tetrahydrocannabinol are not lethal.**

Marihuana (*Cannabis sativa*) is one of the oldest and most widely used drugs in the world (1, 2). The major psychoactive ingredient of the marihuana plant is Δ^9-tetrahydrocannabinol (Δ^9-THC) (3). Δ^9-THC and other natural and synthetic cannabinoids produce characteristic motor, cognitive, and analgesic effects (4, 5). Early reports showing cannabinoid-like activity of 9β-hydroxyhexahydrocannabinol (β-HHC) (6–8) inspired the synthesis of several distinct cannabinoids for studies of their potential use as analgesics (9). The synthetic cannabinoids share physicochemical properties with the natural cannabinoids and produce many behavioral and physiological effects characteristic of Δ^9-THC but are 5–1000 times more potent and show high enantioselectivity. One of these, CP 55,940, was tritiated and used to identify and fully characterize a unique cannabinoid receptor in membranes from rat brain (10). In this study we characterize and validate the binding of [^{3}H]CP 55,940 in slide-mounted brain sections and use the same assay conditions to autoradiographically visualize the distribution of cannabinoid receptors.

METHODS

[^{3}H]CP 55,940 is a bicyclic molecule that is one of a series of synthetic cannabinoids whose structure and biological activity have been documented (9–12) (Fig. 1). It was custom radiolabeled at DuPont/NEN by tritium reduction of CP 60,106 (10). The product was purified by thin layer chromatography on silica gel, eluting with ethylacetate/hexane [1:9 (vol/vol)], and the band comigrating with unlabeled CP 55,940 was extracted, giving a radiochemical yield of 15% and a specific activity of 79 Ci/mmol (1 Ci = 37 GBq). Optimization and competition studies were carried out with slide-mounted sections cut from unfixed frozen rat brains. Incubations were in plastic cytomailers (CMS), each containing eight 30-μm-thick "sausage" sections on four gelatin-coated slides in 5 ml of solution (13). The sausage sections were prepared by combining and mincing three whole rat brains to achieve relative homogeneity of receptor and protein con-

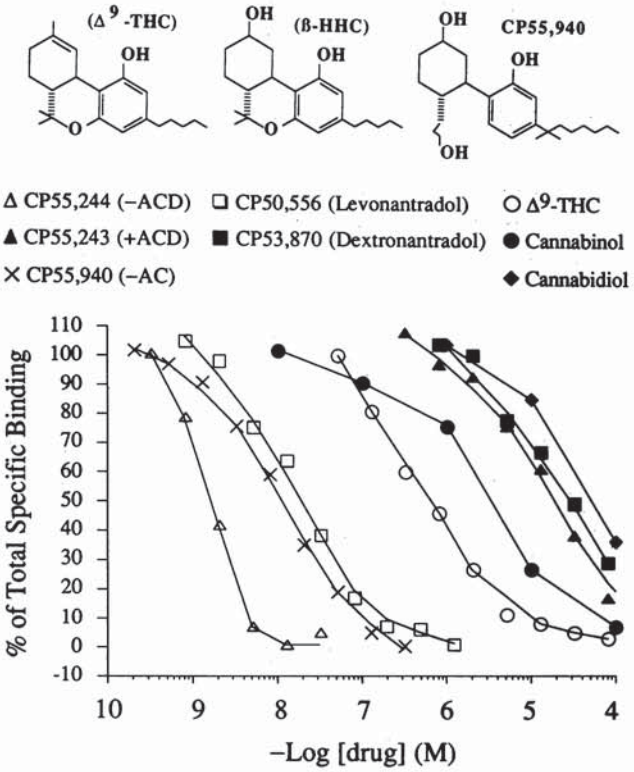

FIG. 1. (*Upper*) Structures of Δ^9-THC (the active ingredient of marihuana), β-HHC (the original synthetic cannabinoid from which the CP compounds were derived), and CP 55,940. (*Lower*) Competitive inhibition of 1 nM [^{3}H]CP 55,940 binding in whole rat brain sausage sections by various synthetic and natural cannabinoids at the concentrations indicated. The data are normalized to specific binding (total minus nonspecific binding) in the absence of competitors. Nonspecific binding was determined by addition of 10 μM CP 55,244 [the most potent cannabinoid in the CP series (9)] and typically represented 10–20% of total binding at both 1 and 10 nM [^{3}H]CP 55,940. Data points represent means of eight determinations. ACD, tricyclic; AC, bicyclic ring nomenclature of Johnson and Melvin (9).

The publication costs of this article were defrayed in part by page charge payment. This article must therefore be hereby marked "*advertisement*" in accordance with 18 U.S.C. §1734 solely to indicate this fact.

Abbreviations: Δ^8- and Δ^9-THC, Δ^8- and Δ^9-tetrahydrocannabinol, respectively; BSA, bovine serum albumin; HHC, hydroxyhexahydrocannabinol; SNr, substantia nigra pars reticulata.

†To whom reprint requests should be addressed.

tent, then placing the paste into a tube, and freezing it to produce a cylindrical sausage that can be cryostat-cut to make sections of uniform composition and size (14). Accuracy of dilutions was checked in mock-incubations in which either [^{3}H]CP 55,940 or [^{3}H]Δ^9-THC (provided by the National Institute on Drug Abuse) were substituted for unlabeled drug, and the solutions were assayed for radioactivity.

To determine binding kinetics, two concentrations of [^{3}H]CP 55,940 (1 and 10 nM) were each competitively inhibited by 6–12 concentrations of unlabeled drug. Competitive inhibition curves were subjected to binding surface analysis, which is a computerized iterative curve-fitting program for determining best-fit parameter estimates (K_d, K_i, and B_{max}) according to 1- or 2-site competitive binding models (15–17). Determination of fmol bound per section was by liquid scintillation counting of the section-laden slide fragments placed overnight in detergent fluor. Some sausage sections were analyzed for protein content by the method of Lowry *et al.* (18) and found to have 456 ± 26 μg of protein per section.

Autoradiography was performed on 25-μm-thick brain sections of rat (male Sprague–Dawley, n = 12), guinea pig (male Hartley, n = 4), dog (beagle, n = 2), rhesus monkey (n = 1), and human (dying of nonneurological disorders, n = 3). Sections were incubated in 10 nM [^{3}H]CP 55,940 by using optimized conditions, washed, dried, and exposed to tritium-sensitive film (LKB or Amersham) for 3–4 weeks before developing.

RESULTS

Assay conditions yielding 80–90% specific binding were as follows: incubation at 37°C for 2 hr in 50 mM Tris·HCl (pH 7.4) containing 5% (wt/vol) bovine serum albumin (BSA) and 1–10 nM [^{3}H]CP 55,940 and washing at 0°C for 4 hr in the same buffer with 1% BSA. By using these optimized conditions, the sausage studies showed that binding was saturable and that competitive inhibition curves were best-fit by a single-site kinetic model: the affinity (K_d) of [^{3}H]CP 55,940 was 15 ± 3 nM and the capacity (B_{max}) in whole brain was 0.9 pmol/mg of protein. Similar parameters were obtained if 1% BSA was used in the incubation, but variability was greater. Binding of 1 nM [^{3}H]CP 55,940 was completely blocked by 10 μM Δ^9-THC, which showed inhibition in a dose-dependent fashion (Fig. 1).

Table 1. Relative potencies of cannabinoid analogs in *in vitro* and *in vivo* animal and human experiments

Drug	K_i, nM	Dog ataxia, mg/kg	Mouse catalepsy, mg/kg	Mouse spontaneous activity, mg/kg	Mouse analgesia, mg/kg			Cyclase inhibition, nM	Inhibition of ileal contractions, nM	Human high	
					Tail flick	Hot plate	Writhing			% Δ^9-THC	mg
CP 55,940 (−AC)	15 ± 3 (K_d)		0.35	0.04	0.09	0.7	0.06	25			
CP 56,667 (+AC)	470 ± 57		>10	3	6		15	>5,000			
CP 55,244 (−ACD)	1.4 ± 0.3		0.085	0.004	0.01	0.09	0.02	5			
CP 55.243 (+ACD)	18,000 ± 1100		>10	8	>10		>100	>10,000			
CP 50,556	14 ± 2		1.5	0.1	0.3	0.4	0.07	100	10	400	0.5
CP 53,870	26,000 ± 3500		>10	>10	>10		6.5	>5,000			
CP 54,939	14 ± 2	0.05			0.7		0.06	7			
Nabilone	120 ± 13	0.03		2.5					100	500	1
β-HHC	124 ± 17	0.1		2.5		1.6					
α-HHC	2,590 ± 360	0.5		5.0		>50					
(−)-Δ^9-THC	420 ± 51	0.5	1.6	3.1	1.3	10	5.9	430	100	100	1
(+)-Δ^9-THC	7,700 ± 2100	>2.0	>75	14.6		>100			>2000		
Δ^8-THC	498 ± 52	0.5	0.5	10		8.8			100	75	2
11-OH-Δ^9-THC	210 ± 56	0.05		1.2		1.9			15	120	1
TMA-Δ^8-THC	2,300 ± 1000								1000		
8β-OH-Δ^9-THC	4,200 ± 700								1000	20	10
8α-OH-Δ^9-THC	8,700 ± 1800								3500	25	10
11-OH-Cannabinol	800 ± 150								<1000		
Cannabinol	3,200 ± 450			83					>2000	0	>15
Cannabidiol	53,000 ± 6700	Inactive	25	83		>100			>2000	0	>30
Cannabigerol	275,000	>7.0							>2000	0	
9-COOH-11-nor-Δ^9-THC	75,000		>40			10					
9-COOH-11-nor-Δ^8-zTHC	Inactive			>40			20				
Regression on K_i:R^2		0.96	0.40	0.34	0.78	0.69	0.26	0.54	0.44	0.90	
Significance (2-tailed)		$P < 0.0001$	$P < 0.03$	$P < 0.03$	$P < 0.005$	$P < 0.001$	$P > 0.05$	$P < 0.05$	$P < 0.03$	$P < 0.0001$	

CP analogs were synthesized at Pfizer Central Research; their structures are given in Johnson and Melvin (9). The first six analogs are enantiomeric pairs. Nabilone was a gift of Lilly Research Laboratories. β-HHC was provided by May's group (6–8). The remaining analogs were provided by the National Institute on Drug Abuse. The last two drugs are Δ^9-THC metabolites. The K_i values (mean ± SD) were derived from binding surface analysis of data from the sausage-section binding assay (13, 17). The potencies in other tests, given as 50% of the effective dose or maximum possible effect, are from the literature as follows: dog ataxia, mouse catalepsy, spontaneous activity, and analgesia (6–9, 12, 19); cyclase inhibition (11); inhibition of guinea pig ileal contractions (20); human high (subjective rating, not connoting either pleasantness or unpleasantness; values are: potencies relative to Δ^9-THC, and mg p.o. or i.v. per dose per subject) (3). R^2 values were determined by least squares linear regression analysis. Drugs that show no inhibition of [^{3}H]CP 55,940 binding at 10 μM concentration are as follows: amphetamine, β-estradiol, *cis*-flupenthixol, cocaine, corticosterone, cyclohexyl-adenosine, dexamethasone, etorphine, γ-aminobutyric acid, glutamate, leukotriene B_4 and D_4 (both at 1 μM), lysergic acid diethylamide (LSD), phencyclidine (PCP), prostaglandin E_2, and Ro 15-1788. The significance was determined relative to K_i values. ACD and AC, ring nomenclature (9). TMA, trimethylammonium. CP 50,556 is levonantradol; CP 53,870 is dextronantradol; CP 54,939 is desacetyl levonantradol.

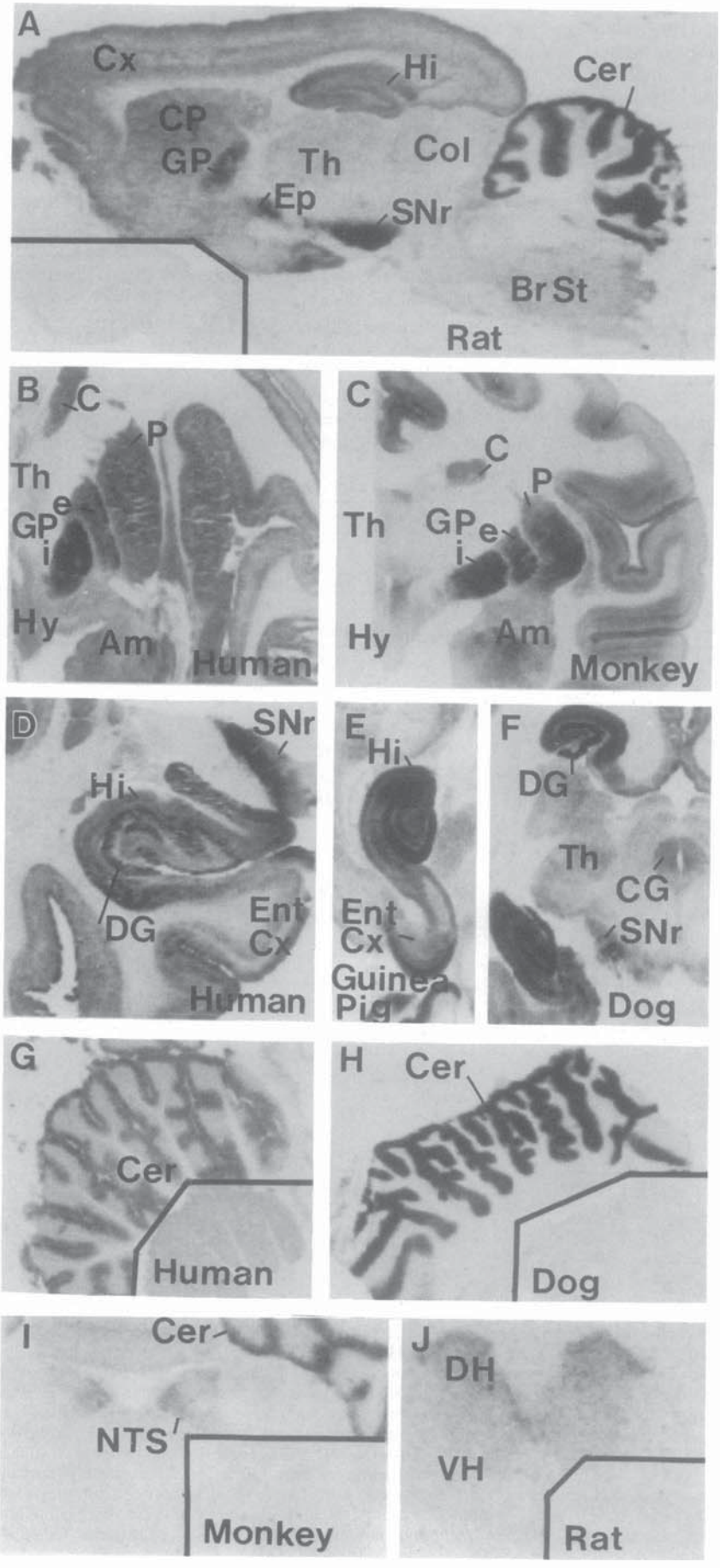

FIG. 2. Autoradiography of 10 nM [^{3}H]CP 55,940 binding in brain. Tritium-sensitive film was exposed for 4 weeks, developed, and computer digitized. Images were photographed directly from the computer monitor. Gray levels represent relative levels of receptor densities. Sagittal section of rat brain is in *A* (×4.7). Coronal brain sections of human are in *B* (×1.3), *D* (×1.7), and *G* (×2.6); rhesus monkey is in *C* (×1.8) and *I* (×4.8); dog is in *F* (×2.1) and *H* (×2.6); and rat is in *J* (×13). Horizontal section of guinea pig brain is in *E* (×4.1). *Insets* in *A* and *G–J* show nonspecific binding in adjacent sections. Miniaturized images are shown. Nonspecific binding accounted for 5% of the total binding in densely labeled structures and all of the binding in the most sparsely labeled structures. Am, amygdala; Br St, brainstem; Cer, cerebellum; CG, central gray; C, caudate; Col, colliculi; CP, caudate-putamen; Cx, cerebral cortex; DG, dentate gyrus; DH, dorsal horn of spinal cord; Ent Cx, entorhinal cortex; Ep, entopeduncular nucleus (homolog of GPi); GP, globus pallidus (e, external; i, internal); Hi, hippocampus; Hy, hypothalamus; NTS, nucleus of solitary tract; P, putamen; Th, thalamus; VH, ventral horn of spinal cord.

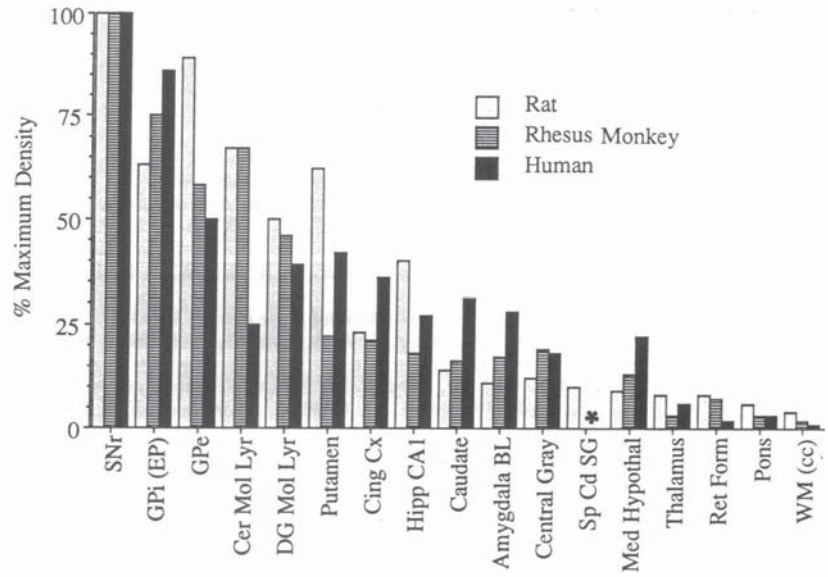

FIG. 3. Relative densities of cannabinoid receptors across brain structures in rat, rhesus monkey, and human. Autoradiographic images were digitized by a solid state video camera and Macintosh II computer-based system for quantitative densitometry using IMAGE software (Wayne Rasband, Research Services Branch, National Institute of Mental Health). Transmittance levels were converted to fmol/mg of tissue by using tritium standards (Amersham high-density microscales) and then normalized to the most dense structure in each animal (SNr for all three). For every section incubated for total binding, an adjacent section was incubated in the presence of CP 55,244 to permit subtraction of nonspecific binding on a regional basis. Structure abbreviations not given in Fig. 2 legend are as follows: Cing Cx, cingulate cortex; Hipp CA1, hippocampal field CA1; Med Hypothal, medial hypothalamus; Sp Cd SG, substantia gelatinosa of spinal cord (*only rat measured); Ret Form, reticular formation; WM (cc), white matter of corpus callosum.

Inhibition by other natural and synthetic cannabinoids was also shown (Fig. 1; for K_i values, see Table 1).

The data from the section-binding assay were in close agreement with data from a centrifugation assay using membranes from rat cortex (10). The B_{max} was similar in the two studies (though ours was derived from whole brain), but the K_d in our assay was about 100-fold higher. The low affinity in sections relative to that in membranes appears to reflect differences in the nature of the assays. In both assays the addition of guanine nucleotides converted the receptor to a low-affinity state. In sections the nonhydrolyzable GTP analog, guanosine 5′-[β,γ-imido]triphosphate, at 10 μM inhibited binding of 10 nM [^{3}H]CP 55,940 by 94%, and the GDP analog, guanosine 5′-[β-thio]diphosphate, at 10 μM inhibited binding by 79%. Finally, in both assays there was a similar rank order of drug potencies.

For several cannabinoids, inhibition constants (K_i values) and relative biological potencies are given in Table 1. Highly significant correlations exist between the K_i values and potencies of the drugs in tests of dog ataxia and human subjective experience, the two most reliable markers of cannabinoid activity (4, 5). Correlations with potencies in the other tests suggest that the measured effects were similarly receptor-mediated. Enantioselectivity was striking; the (−) and (+) forms of CP 55,244 differed by more than 10,000-fold *in vitro*, a separation predicted by the rigid structure of the molecule (9) and by potencies *in vivo*. Natural cannabinoids lacking psychoactive properties, such as cannabidiol, showed extremely low potency at the receptor, and all tested noncannabinoid drugs had no potency (Table 1).

Autoradiography showed that in all species very dense binding was found in the globus pallidus, substantia nigra pars reticulata (SNr), and the molecular layers of the cerebellum and hippocampal dentate gyrus (Figs. 2 and 3). Dense binding was also found in the cerebral cortex, other parts of the hippocampal formation, and striatum. In rat, rhesus monkey, and human, the SNr contained the highest level of binding (Fig. 3). In dog, the cerebellar molecular layer was most dense (Fig. 2*H*). In guinea pig and dog, the hippocampal formation had selectively dense binding (Fig. 2 *E* and *F*). Neocortex in all species had moderate binding across fields, with peaks in superficial and deep layers. Very low and homogeneous binding characterized the thalamus and most of the brainstem, including all of the monoamine-containing cell groups, reticular formation, primary sensory, visceromotor and cranial motor nuclei, and the area postrema. The exceptions—hypothalamus, basal amygdala, central gray, nucleus of the solitary tract, and laminae I–III and X of the spinal cord—showed slightly higher but still sparse binding (Figs. 2 and 3).

Quantitative autoradiography confirmed the very high numbers of receptors, exceeding 1 pmol/mg of protein in densely labeled areas (data not shown). Cannabinoid receptor density was far in excess of densities of neuropeptide receptors and was similar to levels of cortical benzodiazepine (21), striatal dopamine (22, 23), and whole-brain glutamate receptors (24).

DISCUSSION

Previous attempts to characterize the cannabinoid receptor were unsuccessful for several reasons (for discussion, see ref. 10). Cannabinoids are extremely hydrophobic and adhere to filters (see ref. 10) and other surfaces (25). The section assay circumvents some of these problems; in addition, BSA appears to act as a carrier to keep cannabinoids in solution without appreciably affecting binding kinetics. The low nonspecific binding and absence of binding in white matter indicates that the autoradiographic patterns are not affected by ligand lipophilia. Other obstacles were the use of Δ^8-[^{3}H]THC (26) or Δ^9-[^{3}H]THC (27), which bind with low affinity and have low specific activities, or the use of 5′-[^{3}H]trimethylammonium-Δ^8-THC (20), which does not act like a cannabinoid in most animal tests and which has low affinity for the presently described receptor (Table 1). In contrast, [^{3}H]CP 55,940 has high specific activity, high affinity, and biological activity similar to that of Δ^9-THC.

The structure–activity profile suggests that the receptor defined by the binding of [^{3}H]CP 55,940 is the same receptor that mediates all of the behavioral and pharmacological effects of cannabinoids listed in Table 1, including the subjective experience termed the human "high". All other tested psychoactive drugs, neurotransmitters, steroids, and eicosanoids at 10 μM concentrations failed to bind to this receptor (Table 1). There was no compelling evidence for receptor subtypes from the present analysis.

The overall central nervous system distribution, although not similar to any known drug or neurotransmitter receptor pattern, resembles autoradiographic distributions of second messengers (28, 29). These mapping similarities, the very high abundance of the cannabinoid receptor, and the profound inhibition of binding by guanine nucleotides suggest that the cannabinoid receptor is closely associated with second messenger systems. Total inhibition of binding by the GTP analog indicates that the receptor is functionally and

strongly coupled to a guanine nucleotide-binding regulatory (G) protein in our assay. It also indicates that the ligand is an agonist and that there are multiple affinity states of the receptor, as found with the other major receptor classes coupled to adenylate cyclase by G proteins (30).

Dense binding in the basal ganglia and cerebellum suggests cannabinoid involvement in movement control. Cannabinoids depress motor functions with a characteristic stimulatory component (4, 5). Dog shows a static ataxia (Table 1) and has high receptor levels in cerebellum and relatively low levels in SNr (Fig. 2 *F* and *H*). Human shows much less motor depression (3–5) and lower relative densities in cerebellum (Fig. 3), suggesting cerebellar mediation of the motor impairments in animals.

Accounts of cannabis use in humans stress the loosening of associations, fragmentation of thought, and confusion on attempting to remember recent occurrences (5, 31). The most consistent effect of Δ^9-THC on performance is disruption of selective aspects of short-term memory tasks, similar to that found in monkeys and patients with damage to limbic cortical areas (31–33). These cognitive effects may be mediated by receptors in the cerebral cortex. The hippocampal cortex "gates" information during memory consolidation and codes spatial and temporal relations among stimuli and responses (34, 35). Δ^9-THC causes memory "intrusions" (36), impairs temporal aspects of performance (37), and suppresses hippocampal electrical activity (38).

The presence of cannabinoid receptors in the ventromedial striatum suggests an association with dopamine circuits thought to mediate reward (39–41). However, reinforcing properties of cannabinoids have been difficult to demonstrate in animals (42, 43). Moreover, cannabinoid receptors in the basal ganglia are not localized on dopamine neurons (44).

There are virtually no reports of fatal cannabis overdose in humans (1, 4, 5). The safety reflects the paucity of receptors in medullary nuclei that mediate respiratory and cardiovascular functions.

Anticonvulsant and antiemetic effects of cannabinoids have therapeutic value (4, 5). The localization of cannabinoid receptors in motor areas suggests additional therapeutic applications. Cannabinoids exacerbate hypokinesia in Parkinson disease but are beneficial for some forms of dystonia, tremor, and spasticity (4, 5, 45–47). The development of an antagonist could provide additional therapeutic uses of value. The receptor binding assay will be helpful in this regard, and it can be used also to screen drugs that have greater potency or bind irreversibly to aid in the identification of the receptor gene and the putative endogenous ligand.

We thank Drs. J. Atack, J. Hill, and J. Johannessen for providing human and dog tissues, Dr. R. Rothman for pharmacokinetics advice, and Drs. A. Howlett and W. Devane for sharing unpublished data.

1. Harris, L. S., Dewey, W. L. & Razdan, R. K. (1977) in *Handbook of Experimental Pharmacology*, ed. Martin, W. R. (Springer, New York), pp. 371–429.
2. Mechoulam, R. (1986) in *Cannabinoids as Therapeutic Agents*, ed. Mechoulam, R. (CRC, Boca Raton, FL), pp. 1–19.
3. Razdan, R. K. (1986) *Pharmacol. Rev.* **38,** 75–149.
4. Dewey, W. L. (1986) *Pharmacol. Rev.* **38,** 151–178.
5. Hollister, L. E. (1986) *Pharmacol. Rev.* **38,** 1–20.
6. Wilson, R. S. & May, E. L. (1975) *J. Med. Chem.* **18,** 700–703.
7. Wilson, R. S., May, E. L., Martin, B. R. & Dewey, W. L. (1976) *J. Med. Chem.* **19,** 1165–1167.
8. Wilson, R. S., May, E. L. & Dewey, W. L. (1979) *J. Med. Chem.* **22,** 886–888.
9. Johnson, M. R. & Melvin, L. S. (1986) in *Cannabinoids as Therapeutic Agents*, ed. Mechoulam, R. (CRC, Boca Raton, FL), pp. 121–145.
10. Devane, W. A., Dysarz, F. A. I., Johnson, M. R., Melvin, L. S. & Howlett, A. C. (1988) *Mol. Pharmacol.* **34,** 605–613.
11. Howlett, A. C., Johnson, M. R., Melvin, L. S. & Milne, G. M. (1988) *Mol. Pharmacol.* **33,** 297–302.
12. Little, P. J., Compton, D. R., Johnson, M. R. & Martin, B. R. (1988) *J. Pharmacol. Exp. Ther.* **247,** 1046–1051.
13. Herkenham, M. (1988) in *Molecular Neuroanatomy*, eds. van Leeuwen, F., Buijs, R. M., Pool, C. W. & Pach, O. (Elsevier, Amsterdam), pp. 111–120.
14. Rothman, R. B., Schumacher, U. K. & Pert, C. B. (1983) *Neuropeptides* **3,** 493–499.
15. Rothman, R. B. (1986) *Alcohol Drug Res.* **6,** 309–325.
16. McGonigle, P., Neve, K. A. & Molinoff, P. B. (1986) *Mol. Pharmacol.* **30,** 329–337.
17. Rothman, R. B., Long, J. B., Bykov, V., Jacobson, A. E., Rice, K. C. & Holaday, J. W. (1988) *J. Pharmacol. Exp. Ther.* **247,** 405–416.
18. Lowry, O. H., Rosebrough, N. J., Farr, A. L. & Randall, R. J. (1951) *J. Biol. Chem.* **193,** 265–275.
19. Burstein, S. H., Hull, K., Hunter, S. A. & Latman, V. (1988) *FASEB J.* **2,** 3022–3026.
20. Nye, J. S., Seltzman, H. H., Pitt, C. G. & Snyder, S. H. (1985) *J. Pharmacol. Exp. Ther.* **234,** 784–791.
21. Zezula, J., Cortés, R., Probst, A. & Palacios, J. M. (1988) *Neuroscience* **25,** 771–795.
22. Boyson, S. J., McGonigle, P. & Molinoff, P. B. (1986) *J. Neurosci.* **6,** 3177–3188.
23. Richfield, E. K., Young, A. B. & Penney, J. B. (1986) *Brain Res.* **383,** 121–128.
24. Greenamyre, J. T., Young, A. B. & Penney, J. B. (1984) *J. Neurosci.* **4,** 2133–2144.
25. Garrett, E. R. & Hunt, C. A. (1974) *J. Pharm. Sci.* **63,** 1056–1064.
26. Harris, L. S., Carchman, R. A. & Martin, B. R. (1978) *Life Sci.* **22,** 1131–1138.
27. Roth, S. H. & Williams, P. J. (1979) *J. Pharm. Pharmacol.* **31,** 224–230.
28. Worley, P. F., Baraban, J. M., De Souza, E. B. & Snyder, S. H. (1986) *Proc. Natl. Acad. Sci. USA* **83,** 4053–4057.
29. Worley, P. F., Baraban, J. M. & Snyder, S. H. (1986) *J. Neurosci.* **6,** 199–207.
30. Dohlman, H. G., Caron, M. G. & Lefkowitz, R. J. (1987) *Biochemistry* **26,** 2257–2264.
31. Miller, L. L. (1984) in *The Cannabinoids: Chemical, Pharmacologic, and Therapeutic Aspects*, eds. Agurell, S., Dewey, W. L. & Willette, R. E. (Academic, New York), pp. 21–46.
32. Miller, L. L. & Braconnier, R. J. (1983) *Psychol. Bull.* **93,** 441–456.
33. Aigner, T. G. (1988) *Psychopharmacology* **95,** 507–511.
34. Douglas, R. J. (1967) *Psychol. Bull.* **67,** 416–442.
35. Eichenbaum, H. & Cohen, N. J. (1988) *Trends Neurosci.* **11,** 244–248.
36. Hooker, W. D. & Jones, R. T. (1987) *Psychopharmacology* **91,** 20–24.
37. Schulze, G. E., McMillan, D. E., Bailey, J. R., Scallet, A., Ali, S. F., Slikker, W. J. & Paule, M. G. (1988) *J. Pharmacol. Exp. Ther.* **245,** 178–186.
38. Campbell, K. A., Foster, T. C., Hampson, R. E. & Deadwyler, S. A. (1986) *J. Pharmacol. Exp. Ther.* **239,** 941–945.
39. Kornetsky, C. (1985) *NIDA Res. Monogr.* **62,** 30–50.
40. Di Chiara, G. & Imperato, A. (1988) *Proc. Natl. Acad. Sci. USA* **85,** 5274–5278.
41. Ng Cheong Ton, J. M., Gerhardt, G. A., Friedemann, M., Etgen, A. M., Rose, G. M., Sharpless, N. S. & Gardner, E. L. (1988) *Brain Res.* **451,** 59–68.
42. Stark, P. & Dews, P. B. (1980) *J. Pharmacol. Exp. Ther.* **214,** 124–130.
43. Gardner, E. L., Paredes, W., Smith, D., Donner, A., Milling, C., Cohen, D. & Morrison, D. (1988) *Psychopharmacology* **96,** 142–144.
44. Herkenham, M., Lynn, A. B., de Costa, B. & Richfield, E. K. (1989) *Soc. Neurosci. Abstr.* **15,** 905.
45. Marsden, C. D. (1981) in *Disorders of Movement, Current Status of Modern Therapy*, ed. Barbeau, A. (Lippincott, Philadelphia), Vol. 8, pp. 81–104.
46. Petro, D. J. & Ellenberger, C. E. (1981) *J. Clin. Pharmacol.* **21,** 413s–416s.
47. Clifford, D. B. (1983) *Ann. Neurol.* **13,** 669–671.

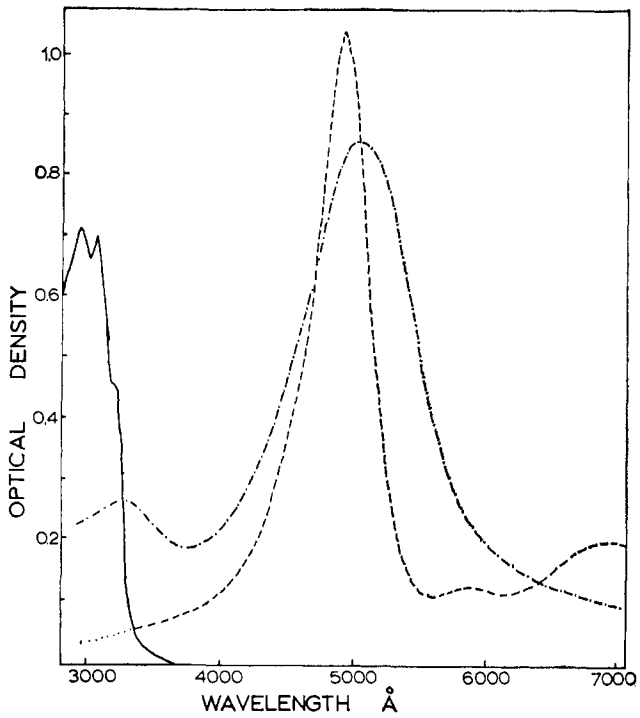

Fig. 1.—Visible and near-ultraviolet spectra of stilbene (———), stilbene$^-$ (- - - -), and stilbene^{-2} (-·-·-·-). Cation and solvent effects on the spectra were small. The ratios of the heights of the various peaks attributed to stilbene$^-$ were constant with changing temperature and exhibited only minor variations with solvent and metal ion. The following extinction coefficients were employed in the calculations: stilbene (3050 Å.), 2.95×10^4; stilbene$^-$ (4800 Å.), 6.21×10^4; stilbene$^-$ (5600 Å.), 0.80×10^4; stilbene^{-2} (4800 Å.), 3.28×10^4; stilbene^{-2} (5600 Å.), 1.49×10^4. These values were obtained directly in experiments involving careful mass balancing and were reproducible with a variation of about ±3%.

strongly solvated than triple ions,[1b,5] the difference being greater for cations of smaller radii, leading to a trend to smaller K with decreasing cationic radii. Both effects, in opposite directions, should operate in solution. The directions of the effects can be similarly rationalized if ionic association is incomplete, but the arguments are slightly more complex.

The quantitative measurements were spectrophotometric. Figure 1 gives the forms of the spectra of stilbene, stilbene$^-$, and stilbene^{-2} in tetrahydrofuran, 2-methyltetrahydrofuran, and 1,2-dimethoxyethane. By suitable choices of solvent, metal ion, and amount of metal allowed to react with the stilbene, extinction coefficients for all three species could be directly determined. These appeared to be rather insensitive to solvent variation. K was calculated directly from the equilibrium expression and was sensibly constant for a given solvent and metal ion. The concentrations of hydrocarbons and ions employed in these experiments ranged about 10^{-4} M. All experiments were done at room temperature.

Corresponding equilibria for triphenylethylene have been observed in 1,2-dimethoxyethane, tetrahydrofuran, and dioxane, with the disproportionation constants (sodium cation) being $<10^{-3}$, of the order of 10, and $>10^3$, respectively. In general the value of K for triphenylethylene appears to be intermediate between that for stilbene and that for tetraphenylethylene, a trend which is consistent with the operation of a steric effect favoring disproportionation of the monoalkali adducts. More explicit tests of the steric effect are in progress.

Acknowledgment.—This work was supported by funds provided through the Director of General Research of the University of Georgia.

DEPARTMENT OF CHEMISTRY
THE UNIVERSITY OF GEORGIA
ATHENS, GEORGIA
ERNEST R. ZABOLOTNY
JOHN F. GARST

RECEIVED FEBRUARY 20, 1964

Isolation, Structure, and Partial Synthesis of an Active Constituent of Hashish[1]

Sir:

Hashish (marihuana), the psychotomimetically active resin of the female flowering tops of *Cannabis sativa* L. is one of the most widely used illicit narcotic drugs. A number of groups have reported the isolation of active constituents.[2] Most of these substances are not fully characterized, and comparisons with or between them are difficult.

We now wish to report the isolation of an active constituent of hashish to which we assign structure I (Δ^1-3,4-*trans*-tetrahydrocannabinol).[3] This is the first active component whose constitution is fully elucidated.[4]

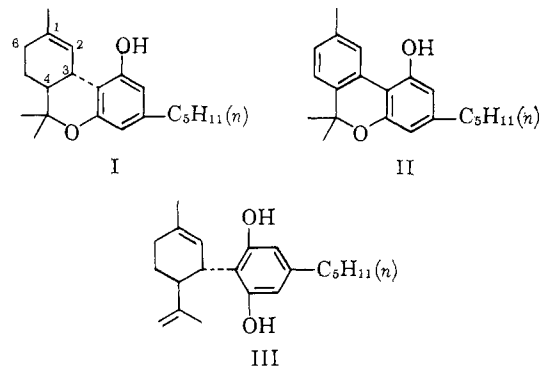

Chromatography of a hexane extract of hashish on Florisil yielded an active fraction, which on repeated chromatography on alumina could be separated into the inactive cannabinol (II)[2a] and the tetrahydrocannabinol (I). Further purification of the latter was achieved by the preparation of the crystalline[5] 3,5-dinitrophenylurethane of I [m.p. 115–116°, $[\alpha]^{CHCl_3}D$ −140°; *Anal.* ($C_{28}H_{33}O_7N_3$). Found: C, 64.17; H, 6.54], followed by mild basic hydrolysis to the pure tetrahydrocannabinol (I) [b.p. 155–157° (0.05 mm.); λ_{max}^{EtOH} 300 mμ (sh) (ε 840), 282 (ε 2075), 278 (ε 2040), $[\alpha]^{CHCl_3}D$ −150°; *Anal.* ($C_{21}H_{30}O_2$). Found: C, 80,20; H, 9.55.]. Purity was established by chromatoplate and by

(1) Hashish. Part III; for part II, see Y. Gaoni and R. Mechoulam, *Proc. Chem. Soc.*, in press.

(2) For a review of the early publications see: (a) A. R. Todd, *Experientia*, **2**, 55 (1946). For more recent work see: (b) F. Korte and H. Sieper, *Ann.*, **630**, 71 (1960); (c) R. S. de Ropp, *J. Am. Pharm. Assoc., Sci. Ed.*, **49**, 756 (1960).

(3) The hashish investigated by us contains a single tetrahydrocannabinol. Most previous reports suggest the presence of mixtures of isomers.

(4) It has been generally accepted that the active constituents are isomers of I, the position of the double bond and the stereochemistry of the asymmetric centers remaining undefined: *cf.* ref. 2a; also, E. C. Taylor and E. J. Strojny, *J. Am. Chem. Soc.*, **82**, 5198 (1960).

(5) G. Powel, M. Salmon, T. H. Bembry, and R. P. Walton [*Science*, **93**, 522 (1941)] have described the preparation of a crystalline 3,5-dinitrophenylurethane (m.p. 216°) of an active hashish constituent. This report has not been confirmed, and since then no other crystalline derivative seems to have been described. It is possible that Powel's compound was an impure sample of the 3,5-dinitrophenylurethane of cannabinol (m.p. 233–234°).

vapor phase chromatography. The tetrahydrocannabinol as obtained in the initial chromatography is not isomerized in the subsequent reactions. This was shown by the infrared and n.m.r. spectra, which remained unchanged during all purification steps, except for the disappearance of bands due to small impurities consisting mainly of cannabinol. Sulfur dehydrogenation of I gave cannabinol (II) in practically quantitative yield. This reaction defines the carbon skeleton of I.

The n.m.r. spectrum of I (see Table I) shows the presence of only one aliphatic methyl group and of

TABLE I[a]

N.M.R. SPECTRUM OF TETRAHYDROCANNABINOL (I)

Group	Chemical shift, p.p.m.
$-CH_3$	0.88 (t) (3)
$-CH_3$ (olefinic and α to O)	1.08 (s) 1.38 (s) 1.65 (s) (9)
C-3H	3.14 (br,d; J = 10 c.p.s.)
C-2H	6.35 (br,s) (1)
H (aromatic)	6.00 (d; J = 2 c.p.s.) (1)
	6.18 (d; J = 2 c.p.s.) (1)
$-OH$[b]	(1)[b]

[a] Determined on a Varian A-60 spectrometer in CCl_4; values are given in p.p.m. relative to $(CH_3)_4Si$ as internal standard; letters in parentheses denote singlet (s), doublet (d), triplet (t), broad (br), coupling constant (J); numbers in parentheses denote number of protons determined by integration of areas. [b] Peak disappears on addition of D_2O.

three methyl groups which are either α to an oxygen or are olefinic. This observation places the double bond in the Δ^1 or $\Delta^{1(6)}$ position. It is of interest to compare the chemical shifts of the C-2 and C-3 protons in tetrahydrocannabinol (I) and in cannabidiol[6] (III). The olefinic proton in I (δ 6.35) is unshielded as compared to that in III (δ 5.59), while the reverse relationship exists as regards the C-3 protons (I, δ 3.14; III, δ 3.85). This can be readily understood by examination of molecular models of these two compounds. In cannabidiol, the aromatic ring, which can rotate freely, is most probably in the same plane as the C-3 hydrogen, which is therefore unshielded.[7] In tetrahydrocannabinol the additional ring tilts the aromatic ring, so that the latter is now in (or nearly in) the same plane as the olefinic proton, which is therefore unshielded. Such an effect is possible only if the double bond occupies the Δ^1 position and the protons on the two asymmetric carbons are *trans*, *i.e.*, if tetrahydrocannabinol possesses structure I.

This structural determination is supported by a partial synthesis. A solution of cannabidiol (III) in absolute ethanol containing 0.05% hydrochloric acid on boiling for 2 hr. gives a mixture of the starting material and I. It can be assumed that these rather mild conditions cause no isomerization of the asymmetric centers or of the double bond.

Tetrahydrocannabinol (I) shows strong activity in the ataxia test[8] in dogs. A full report will be submitted elsewhere by Dr. H. Edery.

Acknowledgments.—We are indebted to Prof. F. Sondheimer for his kind interest and encouragement, to Dr. Y. Shvo for the n.m.r. spectra, to Dr. H. Edery of the Israel Institute for Biological Research for the biological tests, and to the Israeli Police for the supply of hashish.

THE DANIEL SIEFF RESEARCH INSTITUTE Y. GAONI
WEIZMANN INSTITUTE OF SCIENCE R. MECHOULAM
REHOVOTH, ISRAEL

RECEIVED FEBRUARY 14, 1964

(6) R. Mechoulam and Y. Shvo, *Tetrahedron*, **19**, 2073 (1963).
(7) L. M. Jackman, "N.M.R. Spectroscopy in Organic Chemistry," Pergamon Press, New York, N. Y., 1959, p. 125.
(8) S. Loewe, *Arch. Exptl. Pathol. Pharmakol.*, **211**, 175 (1950).

An Improved Method of Calculating Spin Properties from Spin-Polarized Wave Functions

Sir:

Amos and Hall[1] have given formulas for π-electron spin properties computed by the application of an annihilation operator to a single determinant wave function. They assumed that the annihilator could be taken as idempotent and that it commuted with the spin density operator. We would like to report π-electron spin properties, the spin density ρ, and the expectation value $\langle S^2 \rangle$, computed with new formulas which remove these assumptions and which correspond to integrations in which the annihilator operates upon the single determinant everywhere it appears in an integrand.

The single determinant we use is a spin-polarized open-shell (LCAO–MO–SCF)[2] function, *i.e.*, one having different molecular orbitals for electrons with different spins. Let p electrons have α-spin and q β-spin (with $p > q$). The major spin component of the determinant will have multiplicity $2s + 1$ where $s = {}^1/_2(p - q)$ but there will also be spin states of higher multiplicities included in the wave function. Because of their presence, spin properties deduced from the single determinant will only approximate those of its major components. Considerable improvement might be expected if the most important cause of this, the spin state with multiplicity $2s + 3$, were removed from the wave function by applying the annihilator $[S^2 - (s + 1)(s + 2)]$ since the remainder of the spin components usually have negligible effect.[1]

Spin densities and $\langle S^2 \rangle$ for a number of π-electron radicals when this is done accurately are shown in Tables I and II and subscripted (aa). The same properties computed using the approximate formulas of Amos and Hall are also given and subscripted (asa). For comparison we include the results deduced from the original determinant (sd) and from Hückel orbitals (h). The calculations were carried out on an I.B.M. 7090 computer with the Parr–Pariser[3] integral approximations; all C–C bond lengths were assumed equal. Full details of the calculations and the lengthy new formulas will be given later as will a large number of applications.

As can be seen from the tables, the errors involved in the approximate formulas are small but so are some of the quantities to be calculated. In particular we note that $\langle S^2 \rangle_{asa}$ can sometimes fall below $s(s + 1)$, which is certainly wrong, whereas $\langle S^2 \rangle_{aa} > s(s + 1)$ as must be true. The annihilated single determinant must be very nearly the pure major spin component since $\langle S^2 \rangle_{aa}$ is very close to $s(s + 1)$ for the radicals considered here. For the single determinant we find $\langle S^2 \rangle_{sd}$ much larger than $s(s + 1)$. From Table I we see that negative spin densities occur in ρ_{aa}, ρ_{asa}, and ρ_{sd} at carbon atoms for which $\rho_h = 0$. At these atoms $\rho_{aa} \simeq$

(1) A. T. Amos and G. G. Hall, *Proc. Roy. Soc.* (London), **A263**, 483 (1961).
(2) J. Pople and R. Nesbet, *J. Chem. Phys.*, **22**, 571 (1954).
(3) R. G. Parr and R. Pariser, *ibid.*, **23**, 711 (1955).

Structure of a cannabinoid receptor and functional expression of the cloned cDNA

Lisa A. Matsuda, Stephen J. Lolait, Michael J. Brownstein, Alice C. Young & Tom I. Bonner

Laboratory of Cell Biology, National Institutes of Mental Health, Bethesda, Maryland 20892, USA

MARIJUANA and many of its constituent cannabinoids influence the central nervous system (CNS) in a complex and dose-dependent manner[1,2]. Although CNS depression and analgesia are well documented effects of the cannabinoids, the mechanisms responsible for these and other cannabinoid-induced effects are not so far known[3]. The hydrophobic nature of these substances has suggested that cannabinoids resemble anaesthetic agents in their action, that is, they nonspecifically disrupt cellular membranes. Recent evidence, however, has supported a mechanism involving a G protein-coupled receptor found in brain and neural cell lines, and which inhibits adenylate cyclase activity in a dose-dependent, stereoselective and pertussis toxin-sensitive manner[4–7]. Also, the receptor is more responsive to psychoactive cannabinoids than to non-psychoactive cannabinoids[8]. Here we report the cloning and expression of a complementary DNA that encodes a G protein-coupled receptor with all of these properties. Its messenger RNA is found in cell lines and regions of the brain that have cannabinoid receptors. These findings suggest that this protein is involved in cannabinoid-induced CNS effects (including alterations in mood and cognition) experienced by users of marijuana.

In our attempts to clone novel receptors, we isolated a cDNA (SKR6) from a rat cerebral cortex cDNA library, using an oligonucleotide probe derived from the sequence of bovine substance-K receptor[9]. The translated sequence of this cDNA identified its 473-amino-acid protein product as a member of the G protein-coupled family of receptors (Fig. 1). Seven hydrophobic domains, numerous residues that are highly conserved among G protein-coupled receptors and several potential glycosylation sites were apparent (Fig. 1). If glycosylated, the relative molecular mass of this receptor would therefore exceed that of 52,823 predicted from its amino-acid constituents. Despite its general similarity to other receptors in this family, the resemblance of SKR6 to the amino-acid sequence of any other receptor was not close enough to allow us to predict either the identity of the receptor's ligand or the coupling system responsible for its signal transduction processes in the cell. Before the identification of SKR6 as a cannabinoid receptor, therefore, many candidate ligands were examined.

Identification of the ligand for SKR6 initially involved screening either SKR6-transfected mammalian cells or *Xenopus* oocytes injected with RNA transcribed from the cDNA *in vitro*. Ligands for receptors that exist on cell lines in which SKR6 mRNA was also found (N18TG-2 or NG108-15 cells; Fig. 2*a*) were considered strong candidates[5,10]. In addition, many substances were examined because their receptors and the distribution of SKR6 mRNA (L.A.M., T.I.B. and S.J.L., manuscript in preparation) displayed similar localization patterns in brain. In transfected cells, however, many substances failed to interact with the receptor in radiolabelled ligand binding assays (that is, bradykinin, angiotensin II, neurotensin, cholecystokinin, vasoactive intestinal peptide, adenosine analogues), as well as in assays designed to detect alterations in cyclic AMP production (that is, D-Ala-D-Leu enkephalin, somatostatin, secretin and others at 1 or 10 μM). In addition, electrophysiological effects in oocytes due to receptor-mediated changes (including those due to increased phosphatidylinositol turnover) were not detected when tested with angiotensin II, bradykinin, substance P, neuropeptide Y, neurotensin, vasopressin and other ligands at 1 or 10 μM. Although this strategy for selecting candidate ligands is beset with limitations, the critical findings, which prompted us to examine cannabinoids as ligands for SKR6, included the presence of both cannabinoid receptors[5,11] and SKR6 mRNA in the same cell lines (Fig. 2*a*) and the localization of both the receptor[12,13] and SKR6 mRNA in similar brain areas (Fig. 2*b*; data not shown).

In Chinese hamster ovary K1 cells stably transfected with SKR6, expression of a cannabinoid-responsive, G protein-coupled receptor was obtained. The major psychoactive cannabinoid found in marijuana (Δ^9-tetrahydrocannabinol, Δ^9-THC) and a synthetic analogue with potent analgesic properties (CP 55940) inhibited forskolin-stimulated accumulation of cAMP in a dose-dependent manner (Fig. 3*a*). In addition, the dose-response curves for the opposite (+) enantiomeric forms of these two cannabinoids indicated this effect was stereoselective. The effector concentration for half-maximum response (EC_{50}) of CP 55940 compared with that of its (+) enantiomer (CP 56667) revealed a >100-fold difference in potencies between these compounds. By contrast, the difference in EC_{50} observed between (+) and (−) Δ^9-THC was only 50-fold. These data are in general agreement with data for N18TG-2 cell membranes, that is, that the degree of stereoselectivity between various cannabinoid analogues is greater with more potent compounds (such as CP 55940 compared with CP 56667) (ref. 14). As observed in neuroblastomas[8,14], none of the cannabinoids inhibited cAMP accumulation by 100 per cent but CP 55940 inhibited the accumulation of cAMP more than Δ^9-THC. In addition, (−) Δ^8-THC was less potent than (−) Δ^9-THC yet affected cAMP to a similar extent (inhibition of 36 versus 39 per cent). Finally, in transfected cells, cannabinol produced only a slight effect on cAMP accumulation, whereas the non-psychoactive cannabinoid, cannabidiol, did not markedly alter cAMP (Fig. 3*b*).

In N18TG-2 neuroblastomas, the relative potencies of various cannabinoids that inhibit adenylate cyclase correlate well with those of the psychoactive cannabinoids in producing a 'high' in humans[8]. The rank order of potencies for several cannabinoid compounds in SKR6-transfected cells (Fig. 3*b*) was also similar to that for both the effects in N18TG-2 cell membranes and psychoactive effects in humans[8,15]: 11-OHΔ^9-THC > (−) Δ^9-THC > (−) Δ^8-THC > cannabinol > cannabidiol. In addition, nabilone, a synthetic cannabinoid analogue marketed for its anti-emetic effects also inhibited cAMP accumulation in SKR6-transfected cells. These cannabinoid-induced responses were probably mediated by the G protein, G_i (ref. 16), as the inhibition of cAMP accumulation was prevented by pretreatment with pertussis toxin (data not shown).

Clearly the dose-dependent, stereoselective and ligand-specific responses of SKR6-transfected cells were those that would be expected from a cannabinoid receptor. These data, along with the work of others, provide evidence for a receptor-mediated mechanism in the effects observed with cannabinoids. Nonetheless, given the substantial amount of research that has focused on the nonspecific actions of these compounds on cellular membranes[17,18], one might argue that cannabinoids could considerably compromise the ability of membrane-located receptors to respond correctly to their appropriate ligands. Cannabinoid-induced inhibition of adenylate cyclase activity might then seem to be receptor-mediated but would not be receptor-specific. The lack, however, of cannabinoid-induced inhibition of cAMP accumulation in nontransfected cells (data not shown) demonstrates that these compounds (Δ^9-THC, 11-OH Δ^9-THC, nabilone and CP 55940) failed to interact with the endogenous receptors present on CHO cells. Furthermore, when transfected into this same host (CHO cells), neither an α-adrenergic (M. Voigt and C. Felder, personal communication) nor muscarinic receptor[9] responded to (−) Δ^9-THC or CP 55940 (Table 1). Both these receptors, however, reduced cAMP

production in response to their respective agonists. As both the muscarinic and adrenergic receptors are G_i-coupled, the cannabinoid-induced inhibition of adenylate cyclase activity observed in SKR6-transfected cells was not due to the interaction of cannabinoids with this class of receptors and was clearly specific to SKR6.

Although the receptor-mediated actions of cannabinoids in N18TG-2 and SKR6-transfected cells help to define their biochemical and cellular effects, the physiological (increased heart rate, inhibition of vomiting, reduction of intraocular pressure), behavioural (appetite stimulation, CNS depression), and psychoactive (hallucinations, memory deficits, altered time and space perception) effects of these compounds have traditionally been examined in humans and various animal models[15]. Data linking receptor-mediated responses in cultured cells with effects in animals or humans, therefore, are critical. The presence of SKR6-hybridizing signals of similar size (~6 kilobases (kb)) in northern blots of rat brain (data not shown) and neural cell-line RNAs (Fig. 2*a*) indicate that the receptor found in these cells is also present in brain. In addition, the degree of overlap

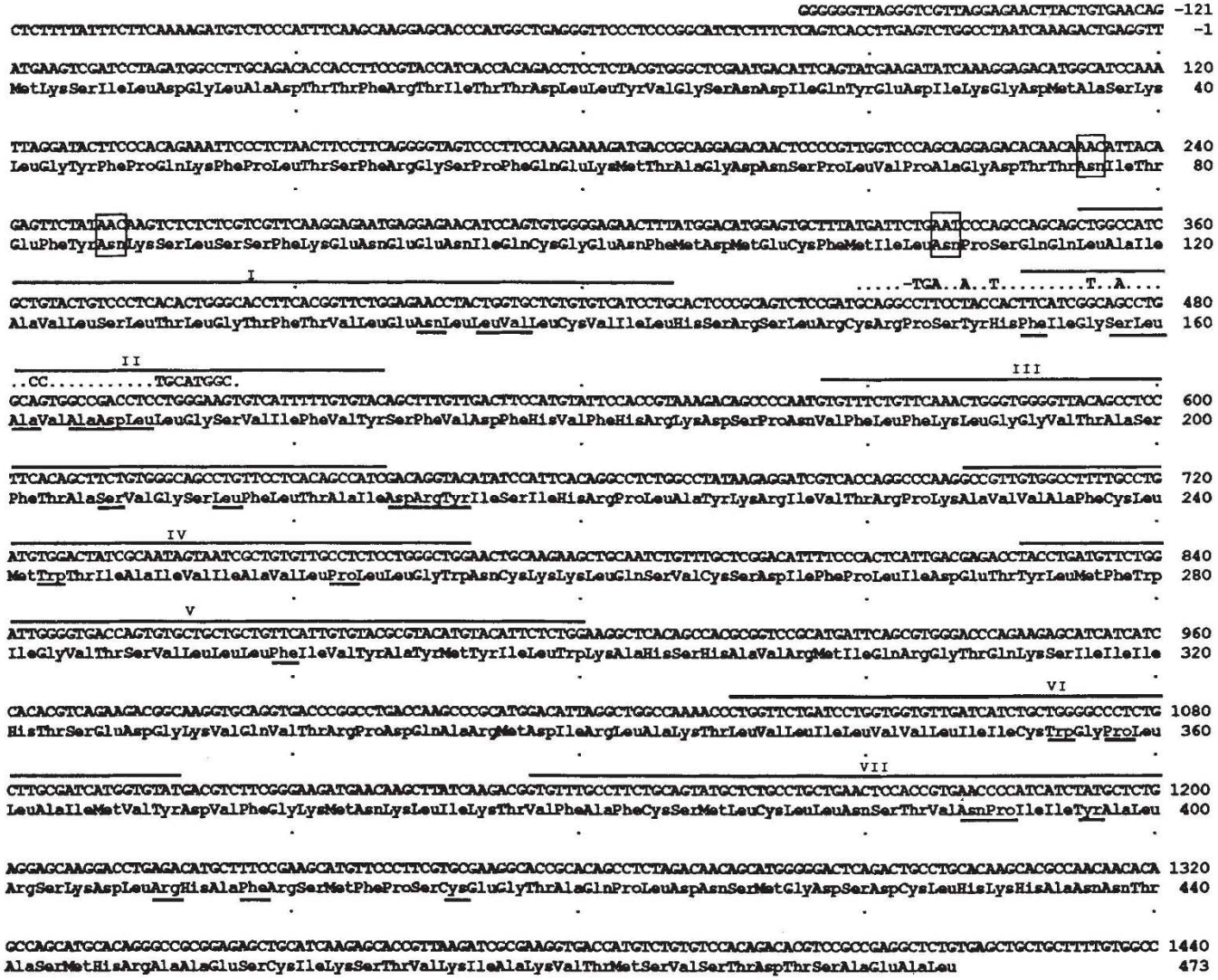

FIG. 1 Partial nucleotide sequence of SKR6 cDNA. Indicated above and below the sequence are the predicted hydrophobic domains (I–VII) and the translated primary structure of the receptor, respectively. The initial stretch of guanine nucleotides represent the G tail produced during cDNA synthesis. The 56-base probe sequence is indicated by dots (bases identical to SKR6) beginning at base number 449; nonidentical bases are provided above the cDNA sequence and a single nucleotide gap (hyphen) has been introduced to align the probe with the cDNA sequence. Although this oligonucleotide was derived from the nucleic acid sequence of the substance-K receptor[19], less than 25% homology overall exists between the amino-acid sequences of SKR6 and the substance-K receptor. Underlined amino acids are those that are highly conserved among other G protein-coupled receptors. Notably absent from SKR6 is a proline residue in the fifth hydrophobic domain and a cysteine just before hydrophobic domain III. In terms of structure, these substitutions may indicate interesting similarities between SKR6 and the LH-CG receptor (lacks the corresponding proline[20,21]) or the *mas* oncogene product (lacks the same cysteine residue[22]). Indeed, the homologous cysteine is essential in functional rhodopsin[23]. Potential *N*-linked glycosylation sites are enclosed within boxes. The entire SKR6 cDNA (5.7 kb) includes an additional ~4,100 bases 3′ of the given sequence. In addition to SKR6, a second clone (SKR14) was isolated whose coding region, although incomplete, was identical to SKR6. The 3′ untranslated sequence of SKR14, however, was ~2,900 bases shorter than that of SKR6. Comparison of the sequences of these clones indicates that SKR14 was the product of an alternatively polyadenylated mRNA.

METHODS. SKR6 was isolated from a rat cerebral cortex cDNA library constructed in the mammalian expression vector pCD (ref. 24). Screening was as described previously for cloning muscarinic receptor subtype cDNAs[9]. Nucleic acid sequence was determined by dideoxynucleotide chain termination of single-stranded DNA obtained from restriction fragments inserted into M13 mp 18 or 19.

TABLE 1 Cyclic AMP accumulation

Cell line	Receptor/cDNA	Forskolin	Δ9THC (100 nM)	CP 55940 (10 nM)	Carbachol/clonidine
CHO	SKR6	100 ± 4 (12.6 ± 0.5)	61 ± 5	—	—
CHO	SKR6	100 ± 5 (12.1 ± 1.4)	—	44 ± 11	—
CHO	muscarinic m2	100 ± 5 (18.0 ± 0.9)	104 ± 8	104 ± 10	8 ± 1
CHO	adrenergic α2d	100 ± 4 (13.9 ± 0.5)	100 ± 4	96 ± 7	73 ± 5
N18TG-2	—	100 ± 10 (44.4 ± 4.3)	61 ± 8	16 ± 2	—
NG108-15	—	100 ± 4 (320.5 ± 11.7)	91 ± 7	57 ± 3	—

Effect of Δ^9-THC and CP 55940 on forskolin-stimulated accumulation of cAMP in CHO-K1 cells transfected with SKR6, muscarinic and α-adrenergic receptor cDNAs. Values represent the average accumulation of cAMP ± s.e.m. as per cent of forskolin-stimulated controls. In each cell line, the effects of the various agonists were examined in three to five experiments (each performed in triplicate). Numbers in parentheses are the absolute values of cAMP as determined by radioimmunoassay (pmol cAMP per 10^6 cells per 5 min). Final concentrations of forskolin were 500 nM for all cell lines except NG 108-15; forskolin concentration for this cell line was 250 nM. The muscarinic and adrenergic receptor-transfected cells were assayed under conditions identical to those routinely used to test the SKR6-transfected cells (see Fig. 3). Final concentrations of carbachol (agonist for muscarinic receptors) and clonidine (agonist for α-adrenergic receptors) were 100 μM and 10 μM, respectively. Clearly, the extent to which a receptor can inhibit cAMP accumulation varies considerably across different cell lines. The moderate effect of clonidine to inhibit cAMP accumulation reported here is lower than normally observed in this transfected cell line (inhibits cAMP accumulation to 50–25% of forskolin-stimulated control). This difference is due to the bovine serum albumin included in our assay.

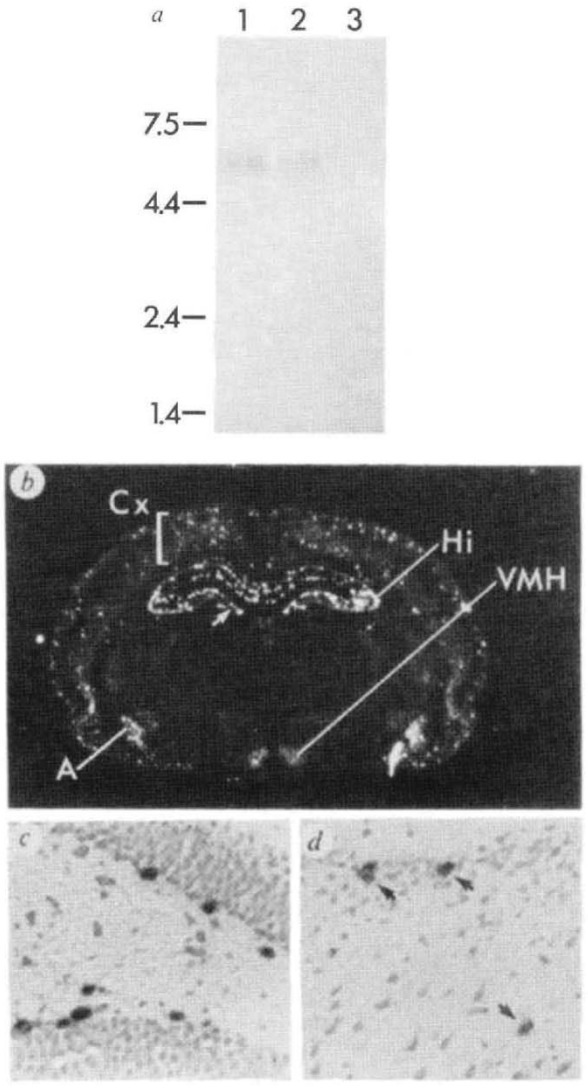

FIG. 2 Presence of SKR6 mRNA in cell lines and its localization in rat brain. *a*, Northern analysis of total RNA from N18TG-2 (lane 1), NG108-15 (lane 2) and C6BU-1 (lane 3) cell lines. N18TG-2 and C6BU-1 cells are the neuroblastoma and glioma parents of the NG108-15 hybrid cell line, respectively. The single hybridizing bands present in lanes 1 and 2 are ~6 kb. Size markers (kb), on the left. Northern analysis was also performed on both total (10 μg) and poly(A)$^+$ RNA (5 μg) prepared from several peripheral tissues (data not shown). But using conditions in which the SKR6 message is readily detected in rat brain RNAs, we saw no hybridizing signal in rat heart, liver, kidney, spleen, thymus, small intestine, testes and ovary RNAs. These data do not prove the absence of cannabinoid receptors in these tissues as they may be present at considerably lower abundance than in brain. *b*, Low-magnification photograph of an *in situ* hybridization histochemical autoradiogram. In this negative image of a coronal rat brain section, the silver grains appear white. Very high levels of SKR6 mRNA are expressed in isolated cells of the hippocampus and cerebral cortex. In the hippocampus, the strongly labelled cells include granule cells in the dentate gyrus (arrow) as well as cells in both the pyramidal and molecular layers of Ammon's horn. Similarly, in the cortex, layers II, V and VI contain a moderate number of cells expressing very high levels of SKR6 mRNA. These layers also appear to contain many cells that have a much lower message level. Control sections (hybridized under the same condition with a 48-base probe that corresponds to no known message and that gives no signal on northern blots) give a low level, uniform signal (not shown). Cx, cerebral cortex; Hi, hippocampal formation; VMH, ventromedial hypothalamic nucleus; A, amygdaloid nuclei. *c*, Bright-field photomicrograph of the hilar region (see arrow in *b*) of the dentate gyrus (×250). Three heavily labelled cells are shown lining the innermost edge of the granule cell layer of the external limb. An additional five cells with high levels of SKR6 mRNA are associated with the internal limb. *d*, Bright-field photomicrograph of the superficial layers of the cerebral cortex (×300) showing cells expressing high levels (arrows) of SKR6 mRNA. In this same brain region, cells that express less message are readily seen when a dark-field condenser is used (image similar to that seen in *b*); these less intensely labelled cells, however, are not easily discernible in bright-field photomicrographs.

METHODS. Northern analysis: RNAs were isolated from cultured cells using the guanidinium thiocyanate method as described previously[25] and loaded (10 μg per lane) into a 1% agarose–formaldehyde gel. After electrophoresis and electrotransfer the filter was hybridized to a nick-translated *Eco*RV–*Xba*I fragment (bases 97–1,271) of the SKR6 cDNA, washed (0.1 × SSPE buffer, 0.1% sodium dodecyl sulphate (SDS), 60 °C) and exposed to X-ray-sensitive film for 6 days (−80 °C). *In situ* hybridization histochemistry; the brain from a male, Sprague–Dawley rat (200–250 g) was sectioned and the 12-μm slices were thaw-mounted to gelatin-coated slides. *In situ* hybridization histochemistry was as described previously[26,27]. An ^{35}S-labelled 48-base oligonucleotide (SKR6-1, complimentary to bases 349–396) was used to probe the section. Under similar hybridization conditions, this oligonucleotide probe hybridized to a single ~6 kb band in preparations of rat cerebral cortex, hippocampal and cerebellar RNA (data not shown). Similar hybridization patterns were also observed in brain sections hybridized with another 48-base probe SKR6-2 (complementary to bases 4–51, data not shown); *b* was produced by placing this section against X-ray-sensitive film (25 °C) for 16 days. The hybridized sections were then dipped in NBT-2 emulsion (Kodak), exposed for 21 or 28 days (4 °C), developed, stained with 0.1% toluidine blue and a coverslip applied, to produce the images shown in *c* and *d*.

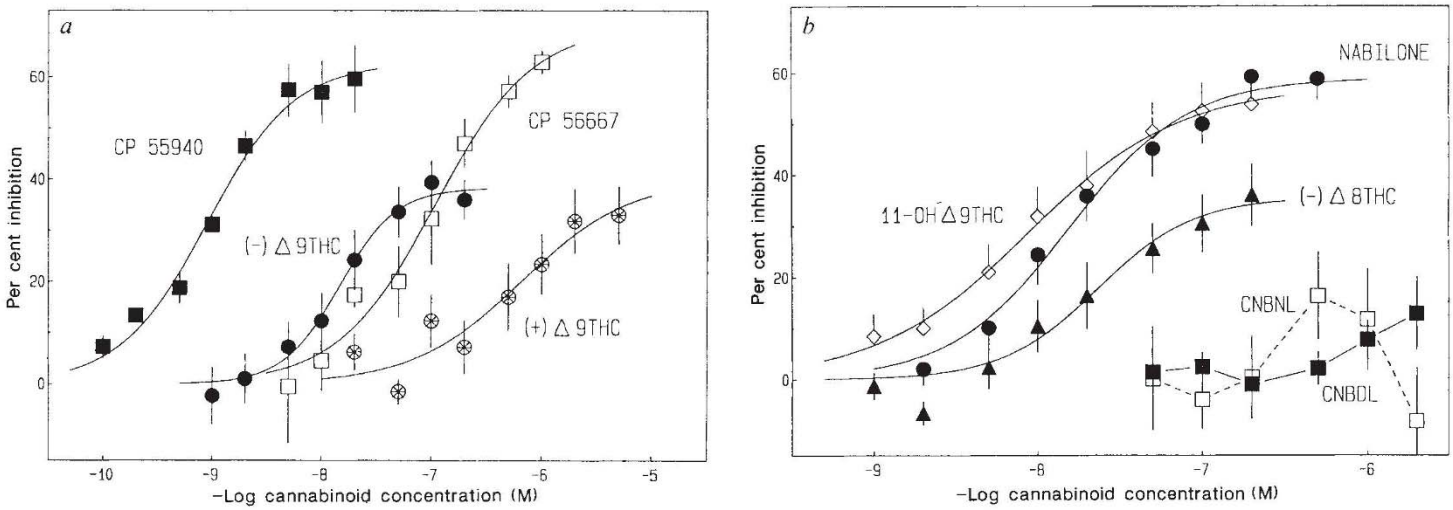

FIG. 3 Cannabinoid-induced inhibition of forskolin-stimulated cAMP production in SKR6-transfected CHO-K1 cells. *a*, Stereoselective inhibition by Δ^9-THC and CP 55940. *b*, Dose–response curves of various cannabinoids and cannabinoid analogues. Data represent the average per cent inhibition ±s.e.m. of cAMP accumulation for three to five experiments, each performed in triplicate. Curves were generated using the Graph-Pad InPlot nonlinear regression analysis programme. Cannabinoids did not significantly inhibit cAMP accumulation in nontransfected cells (data not shown). EC_{50} values (mean nM ± s.e.m.) for the inhibition of stimulated cAMP accumulation were: 13.5 ± 2.7, (−) Δ^9-THC; 773 ± 187, (+) Δ^9-THC; 0.87 ± 0.20, CP 55940; 96.3 ± 7.1, CP 56667; 8.9 ± 1.8, 11-OH Δ^9-THC; 16.6 ± 4.9, nabilone; 27.4 ± 8.4, Δ^8-THC. Cannabinoid-induced inhibition of cAMP accumulation was also observed in transfected cells in which cAMP production was stimulated by the peptide hormone, calcitonin gene-related peptide, instead of forskolin. CP 55940 and CP 56667 are synthesized by Pfizer. Nabilone is produced by Lilly Research laboratories. Other cannabinoids are distributed by the National Institute of Drug Abuse. CNBNL, cannabinol; CNBDL, cannabidiol.

METHODS. Transfection and selection of cells were performed as described previously[28]. A monoclonal line expressing the SKR6 cDNA was obtained by limiting-dilution cloning of cells expressing the corresponding mRNA as determined by northern blot analysis. Methods used for measurements of cAMP were similar to those of Howlett *et al.*[6]. Transfected cells were grown to confluence and released with 0.5 mM EDTA in PBS. Washed cells were resuspended (1.25×10^6 cells ml^{-1}) in culture media (37 °C) containing HEPES buffer (20 mM) and RO-20 1724 (0.25 mM). Cells were aliquoted (0.4 ml) into silanized glass tubes and the assay initiated with the addition (0.1 ml) of forskolin (0.1 ml, 0.5 μM, final) ± cannabinoids in media containing fatty acid-free BSA (0.25%). Final ethanol concentrations were less than or equal to 0.2%. Cells were incubated (37 °C) for 5 min and the reaction terminated with the addition of 0.1 N HCl, 0.1 mM $CaCl_2$. Samples were frozen at −20 °C and thawed just before determination of cAMP by radioimmunoassay (refs 29, 30). Forskolin increased cAMP ~20-fold above basal concentrations; absolute values in forskolin-stimulated controls ranged from 9.5 to 17.7 pmole cAMP per 10^6 cells per 5 min. In experiments involving pertussis toxin, subconfluent cultures of cells were grown in the presence of the holoenzyme (1 ng ml^{-1}) for 24 hours before treatment with forskolin ± cannabinoids.

between the relative amounts of SKR6 mRNA and cannabinoid receptors[12] in individual brain areas is substantial. High levels of both SKR6 message and cannabinoid receptors (localized by ^{3}H-labelled CP 55940 autoradiography; ref. 12) are found in the dentate gyrus, hippocampal formation and the cerebral cortex (Fig. 2*b*, and ref. 12). A striking feature of the SKR6 message, in these areas, is the presence of many isolated cells expressing very high levels of receptor message (Fig. 2*c*, *d*). Assuming that protein expression is proportional to message levels, these cells probably account for the very high density of cannabinoid receptor reported previously[12]. Although more diffuse, there were moderate to high amounts of message in the hypothalamus and amygdala. Although receptors in these regions are relatively sparsely distributed[12], these data support the notion that cannabinoid-induced effects in the brain are mediated by the same receptor as found in neural cell lines and in cell lines expressing the SKR6 cDNA.

Our data do not eliminate the possibility that other mechanisms also contribute to various cannabinoid-induced effects. Assuming there is an endogenous 'cannabinoid,' SKR6-transfected cell lines can be used to facilitate its identification and purification. These cell lines should prove particularly valuable, as an antagonist for this receptor is not so far available. Addressing the physiological significance of both this receptor and its endogenous ligand should increase our understanding of not only the actions of the cannabinoids but also the CNS. □

Received 24 April; accepted 8 June 1990.

1. Hollister, L. E. *Pharmac. Rev.* **38,** 1–20 (1986).
2. Martin, B. R. *Pharmac. Rev.* **38,** 45–74 (1986).
3. Dewey, W. L. *Pharmac. Rev.* **38,** 151–178 (1986).
4. Howlett, A. C. *Molec. Pharmacol.* **27,** 429–436 (1985).
5. Howlett, A. C. & Fleming, R. M. *Molec. Pharmacol.* **26,** 532–538 (1984).
6. Howlett, A. C., Qualy, J. M. & Khachatrian, L. L. *Molec. Pharmacol.* **29,** 307–313 (1986).
7. Devane, W. A., Dysarz, F. A., Johnson, M. R., Melvin, L. S. & Howlett, A. C. *Molec. Pharmacol.* **34,** 605–613 (1988).
8. Howlett, A. C. *Neuropharmacology* **26,** 507–512 (1987).
9. Bonner, T. I., Buckley, N. J., Young, A. C. & Brann, M. R. *Science* **237,** 527–532 (1987).
10. Nirenburg, M. *et al. Science* **222,** 794–799 (1983).
11. Devane, W. A., Spain, J. W., Coscia, C. J. & Howlett, A. C. *J. Neurochem.* **46,** 1925–1935 (1986).
12. Herkenham, M. *et al. Proc. natn. Acad. Sci. U.S.A.* **87,** 1932–1936 (1990).
13. Bidaut-Russell, M., Devane, W. A. & Howlett, A. C. *J. Neurochem.* **55,** 21–26 (1990).
14. Howlett, A. C., Johnson, M. R., Melvin, L. S. & Milne, G. M. *Molec. Pharmacol.* **33,** 297–302 (1988).
15. Razdan, R. K. *Pharmac. Rev.* **38,** 75–149 (1986).
16. Gilman, A. G. *Cell* **36,** 577–579 (1984).
17. Lawrence, D. K. & Gill, E. W. *Molec. Pharmacol.* **11,** 595–602 (1975).
18. Hillard, C. J., Harris, R. A. & Bloom, A. S. *J. Pharmac. exp. Ther.* **232,** 579–588 (1985).
19. Masu, Y. *et al. Nature* **329,** 836–838 (1987).
20. McFarland, K. C. *et al. Science* **245,** 494–499 (1989).
21. Loosfelt, H. *et al. Science* **245,** 525–528 (1989).
22. Young, D., Waitches, G., Birchmeier, C., Fasano, O. & Wigler, M. *Cell* **45,** 711–719 (1986).
23. Karnik, S. S., Sakmar, T. P., Chen, H.-B. & Khorana, H. G. *Proc. natn. Acad. Sci. U.S.A.* **85,** 8459–8463 (1988).
24. Okayama, H. & Berg, P. *Molec. cell. Biol.* **3,** 280–289 (1983).
25. Chomczynski, P. & Sacchi, N. *Analyt. Biochem.* **162,** 156–159 (1987).
26. Young, W. S. III, Bonner, T. I. & Brann, M. R. *Proc. natn. Acad. Sci. U.S.A.* **83,** 9827–9831 (1986).
27. Young, W. S. III, Warden, M. & Mezey, E. *Neuroendocrinology* **46,** 439–444 (1987).
28. Chen, C. & Okayama, H. *Molec. cell. Biol.* **7,** 2745–2752 (1987).
29. Brooker, G., Harper, J. F., Terasaki, W. L. & Moylan, R. D. *Adv. Cyclic Nucleotide Res.* **10,** 1–33 (1979).
30. Borst, S. & Conolly, M. *Life Sci.* **43,** 1021–1030 (1988).

ACKNOWLEDGEMENTS. We thank H. Okayama for the pCDneo plasmid and M. Nirenberg for cell lines N18TG-2 and C6BU-1. Special thanks to M. Herkenham for providing samples of various cannabinoids and for disclosing autoradiographic data before publication, K. Kusano for his assistance in screening ligands in the *Xenopus* oocyte expression studies and to C. Gerfen for production of photographs. We also thank F. Gusovsky, R. Karler and C. Felder for insightful discussions and technical guidance. L.A.M. was sponsored by the National Institutes of General Medical Sciences as a Pharmacological Research Associate Training follow. S.J.L. was supported by a C. J. Martin Fellowship from the National Health and Medical Research Council of Australia and awards from the McKnight and Stanley Foundations.

British Journal of Pharmacology

British Journal of Pharmacology (2017) **174** 3242–3256 3242

Themed Section: Pharmacology of Cognition: a Panacea for Neuropsychiatric Disease?

REVIEW ARTICLE

Cannabidiol regulation of emotion and emotional memory processing: relevance for treating anxiety-related and substance abuse disorders

Correspondence Carl Stevenson, School of Biosciences, University of Nottingham, Sutton Bonington Campus, Loughborough LE12 5RD, UK. E-mail: carl.stevenson@nottingham.ac.uk

Received 7 November 2016; **Revised** 31 December 2016; **Accepted** 18 January 2017

Jonathan L C Lee[1], Leandro J Bertoglio[2], Francisco S Guimarães[3] and Carl W Stevenson[4]

[1]School of Psychology, University of Birmingham, Birmingham, UK, [2]Department of Pharmacology, Federal University of Santa Catarina, Florianopolis, SC, Brazil, [3]Department of Pharmacology, University of São Paulo, Ribeirão Preto, SP, Brazil, and [4]School of Biosciences, University of Nottingham, Sutton Bonington Campus, Loughborough, UK

Learning to associate cues or contexts with potential threats or rewards is adaptive and enhances survival. Both aversive and appetitive memories are therefore powerful drivers of behaviour, but the inappropriate expression of conditioned responding to fear- and drug-related stimuli can develop into anxiety-related and substance abuse disorders respectively. These disorders are associated with abnormally persistent emotional memories and inadequate treatment, often leading to symptom relapse. Studies show that cannabidiol, the main non-psychotomimetic phytocannabinoid found in *Cannabis sativa*, reduces anxiety via 5-HT_{1A} and (indirect) cannabinoid receptor activation in paradigms assessing innate responses to threat. There is also accumulating evidence from animal studies investigating the effects of cannabidiol on fear memory processing indicating that it reduces learned fear in paradigms that are translationally relevant to phobias and post-traumatic stress disorder. Cannabidiol does so by reducing fear expression acutely and by disrupting fear memory reconsolidation and enhancing fear extinction, both of which can result in a lasting reduction of learned fear. Recent studies have also begun to elucidate the effects of cannabidiol on drug memory expression using paradigms with translational relevance to addiction. The findings suggest that cannabidiol reduces the expression of drug memories acutely and by disrupting their reconsolidation. Here, we review the literature demonstrating the anxiolytic effects of cannabidiol before focusing on studies investigating its effects on various fear and drug memory processes. Understanding how cannabidiol regulates emotion and emotional memory processing may eventually lead to its use as a treatment for anxiety-related and substance abuse disorders.

LINKED ARTICLES

This article is part of a themed section on Pharmacology of Cognition: a Panacea for Neuropsychiatric Disease? To view the other articles in this section visit http://onlinelibrary.wiley.com/doi/10.1111/bph.v174.19/issuetoc

Abbreviations

BNST, bed nucleus of the stria terminalis; CBD, cannabidiol; CS, conditioned stimulus; dlPAG, dorsolateral periaqueductal gray; EPM, elevated plus-maze; IL, infralimbic; PAG, periaqueductal gray; PL, prelimbic; PTSD, post-traumatic stress disorder; THC, Δ^9-tetrahydrocannabinol; US, unconditioned stimulus

DOI:10.1111/bph.13724

Tables of Links

TARGETS	
Other protein targets[a]	**Voltage-gated ion channels**[d]
Fatty acid binding proteins (FABPs)	TRPA1
GPCRs[b]	TRPM8
5-HT_{1A} receptor	TRPV1
A_1 receptor	TRPV2
CB_1 receptor	**Nuclear hormone receptors**[e]
CB_2 receptor	PPARγ
D_4 receptor	**Catalytic receptors**[f]
GPR55	TrkB
Ligand-gated ion channels[c]	**Enzymes**[g]
GluA1 receptor	Fatty acid amide hydrolase (FAAH)

LIGANDS
Adenosine
Anandamide
Cannabidiol
Cocaine
Morphine
THC

These Tables list key protein targets and ligands in this article which are hyperlinked to corresponding entries in http://www.guidetopharmacology.org, the common portal for data from the IUPHAR/BPS Guide to PHARMACOLOGY (Southan *et al.*, 2016), and are permanently archived in the Concise Guide to PHARMACOLOGY 2015/16 ([a,b,c,d,e,f,g]Alexander *et al.*, 2015a,b,c,d,e,f,g).

Introduction

Anxiety (e.g. generalized and social anxiety, panic and phobias), trauma-related [i.e. post-traumatic stress disorder (PTSD)] and substance abuse disorders are serious forms of mental illness associated with a significant lifetime prevalence. These disorders pose an enormous social and financial burden as they are often chronic in nature and inadequately treated (Di Luca *et al.*, 2011). Certain anxiety-related disorders (e.g. phobias and PTSD) and addiction are characterized by aberrant and persistent emotional memories of fear- and drug-related stimuli. These discrete or contextual cues can trigger the emergence of symptoms or even their re-emergence after treatment, highlighting the limited effectiveness of the psychological and pharmacological therapies currently available to curtail symptom relapse over the long-term (Tronson and Taylor, 2013; Everitt, 2014; Kindt, 2014; Singewald *et al.*, 2015). Moreover, there is also significant co-morbidity between substance abuse disorders and PTSD, which can further complicate how PTSD develops and is treated. For example, the learning and memory processes involved in the psychological therapies that are used for treating PTSD can be adversely affected by different drugs of abuse, which may also have complex drug–drug interactions with pharmacological treatments for PTSD (Tipps *et al.*, 2014). Thus, there is an urgent need to improve the treatment of these disorders.

An area of real promise in this field involves the use of existing or novel medications as adjuncts to psychological therapies to enhance the efficacy of treatment. Cannabidiol (CBD) is one such drug that shows therapeutic potential in a broad range of neurological and psychiatric diseases (Campos *et al.*, 2012b). This phytocannabinoid is the main non-psychotomimetic constituent of the *Cannabis sativa* plant, and mounting evidence indicates that CBD has anxiolytic properties (Blessing *et al.*, 2015). Emerging preclinical and clinical evidence also indicates that CBD regulates different aversive and appetitive memory processes (Prud'homme *et al.*, 2015; Jurkus *et al.*, 2016), in keeping with the findings of recent studies showing a role for CBD in modulating other types of memory, such as novel object and social recognition, in cognitively-impaired animals (Fagherazzi *et al.*, 2012; Cheng *et al.*, 2014). In this paper, we begin with a brief historical account of the discovery of CBD and touch on the first studies that investigated its behavioural effects in rodents and humans. We then review the literature on CBD regulation of anxiety and the pharmacological and brain mechanisms involved. The bulk of the paper focuses on discussing the findings from the growing number of studies, mostly preclinical, that have examined the regulation of learned fear and, more recently, addictive drug memory processing by CBD. Importantly, these studies have used experimental procedures with clinical relevance for understanding the psychological and neurobiological mechanisms involved in the pathophysiology and treatment of anxiety-related and substance abuse disorders.

CBD discovery and initial studies on its behavioural effects

The *C. sativa* plant contains more than 100 chemically related terpenephenol components called phytocannabinoids (Izzo *et al.*, 2009; Gould, 2015). Since the seminal work of Raphael Mechoulam's group in the 1960s, Δ^9-tetrahydrocannabinol (THC) is considered the main component responsible for the pharmacological effects of the plant (Gaoni and Mechoulam, 1964). The second major

component of most samples of *C. sativa* is CBD. Originally isolated by Adams and co-workers in 1940 (Adams *et al.*, 1940), its structure was elucidated by Mechoulam and Shvo (1963). Although the CBD molecule is similar to THC, it has a distinct spatial conformation that could help to explain their different pharmacological properties. Whereas THC has a planar conformation, CBD presents a 'bent' structure with two rings at a right angle to each other (Burstein, 2015).

Initial studies performed in the 1970s, mostly in Brazil, indicated that CBD could block some effects induced by THC in rodents (Karniol and Carlini, 1973; Russo and Guy, 2006). Following these initial studies, Zuardi and collaborators investigated if CBD could prevent the effects of high doses of THC in healthy human volunteers. They found that it attenuates the psychotomimetic and anxiogenic effects of THC (Zuardi *et al.*, 1982). Although the mechanisms of action of these two drugs were completely unknown at that time, the fact that not all effects of THC were blocked by CBD indicated that the latter was not simply an antagonist of a putative THC receptor. On the contrary, the study suggested that CBD possesses its own antipsychotic and anxiolytic properties (Zuardi *et al.*, 1982).

Laboratory animal tests used to assess the anxiolytic properties of CBD

The potential anxiolytic effect of CBD was initially investigated in preclinical studies. Several animal tests have been employed to explore the effects of putative anxiolytic drugs and the neurobiology of anxiety, which can be defined separately from fear as the emotional response to potential or anticipated (as opposed to actual and present) threat (Tovote *et al.*, 2015). These tests are based on the measurement of defensive behaviours (either active or inhibitory) expressed in response to a threatening or unpleasant stimulus (Campos *et al.*, 2013a). The initial preclinical studies investigating the possible anxiolytic-like effects of CBD were performed in learning-based models and produced mixed results. These apparently conflicting results were later explained by Guimarães *et al.* (1990) using the elevated plus-maze (EPM). This is a commonly used test to investigate anxiety-like behaviour in preclinical studies and is based on the natural aversion that rodents show to open spaces (Handley and Mithani, 1984; Pellow *et al.*, 1985; Treit *et al.*, 1993; Carobrez and Bertoglio, 2005).

Using the EPM and performing a full dose–response curve in rats, Guimarães and co-workers showed that acute systemic administration of CBD produces a typical 'bell-shaped' dose–response curve, being anxiolytic at low and intermediate doses but not at high doses. Although some contradictory results exist in the literature, most studies using unlearned or operant conditioning models of anxiety have confirmed these initial findings, and the studies investigating CBD effects in classical (Pavlovian) conditioning models also go in the same direction, which will be discussed separately below (summarized in Tables 1 and 2). Moreover, these anxiolytic effects of CBD in animals have been replicated in human studies using healthy subjects exposed to anxiety-provoking stimuli or situations (Zuardi *et al.*, 1982, 1993; Crippa *et al.*, 2004; Fusar-Poli *et al.*, 2009, 2010) and in patients with anxiety, and possibly also substance abuse, disorders (Bergamaschi *et al.*, 2011, Crippa *et al.*, 2011; Hurd *et al.*, 2015; Shannon and Opila-Lehman, 2016; summarized in Table 3).

Pharmacological mechanisms and brain sites involved in the anxiolytic effects of CBD

The potential therapeutic effects of CBD have been related to multiple pharmacological mechanisms, including the agonism of 5-HT_{1A} receptors, inhibition of reuptake and/or metabolism of the endocannabinoid anandamide (resulting indirectly in cannabinoid receptor activation), activation of transient receptor potential vanilloid 1 (TRPV1) channels, inhibition of adenosine reuptake, antagonism of GPR55, agonism of PPARγ receptors, intracellular Ca^{2+} increase, and anti-oxidative effects, among others (summarized in Figure 1). These pharmacological mechanisms have been discussed recently in several reviews (Izzo *et al.*, 2009; Campos *et al.*, 2012a; Ibeas Bih *et al.*, 2015; McPartland *et al.*, 2015), to which the reader is referred. So far, however, only two of these mechanisms – 5-HT_{1A} receptor activation and indirect potentiation of endocannabinoid transmission – have been implicated in the attenuation of defensive responses to threatening or stressful stimuli.

Two primary brain systems organize defensive responses to threatening stimuli: one responsive to innate threats and the other responsible for the association between neutral and aversive stimuli, although the neural circuit mechanisms underlying the regulation of anxiety and learned fear show considerable overlap (for reviews, see McNaughton and Corr, 2004; Canteras *et al.*, 2010; Gross & Canteras, 2012; Tovote *et al.*, 2015). The brain areas implicated in the anxiolytic effects of cannabidiol include certain medial prefrontal cortical subregions [e.g. prelimbic (PL) and infralimbic (IL) cortex], the bed nucleus of the stria terminalis (BNST), periaqueductal gray (PAG) and amygdala. This evidence comes from preclinical studies and functional imaging studies in humans, which have confirmed the involvement of some of these brain areas. For example, CBD reduced amygdala activation in both mice and humans (Todd and Arnold, 2016; Crippa *et al.*, 2004). Activity in and functional connectivity between the amygdala and anterior cingulate cortex, the homologous region to the rodent dorsomedial prefrontal cortex, were both also decreased by CBD when viewing fearful facial expressions (Fusar-Poli *et al.*, 2009; 2010).

In an initial preclinical study using the EPM test, Campos and Guimarães (2008) showed that the anxiolytic-like effects of CBD injected into the dorsolateral PAG (dlPAG) were prevented by local treatment with the 5-HT_{1A} receptor antagonist WAY100635. Even if this drug can also activate D_4 receptors (Chemel *et al.*, 2006), the anti-aversive effects of CBD were similar to other 5-HT_{1A} receptor agonists infused into the dlPAG (Graeff, 2002). The involvement of the 5-HT_{1A} receptor in the acute anxiolytic/anti-stress effect of

Table 1

CBD effects on anxiety-like behaviour in male animals

Reference	Test used	Strain, species, effective dose, and route/site of administration	Effect	Pharmacological mechanism
Guimarães *et al.* (1990)	EPM	Wistar rats, 2.5–10 mg·kg^{-1}, i.p.	Anxiolytic (bell-shaped dose–response curve)	Not tested
Onaivi *et al.* (1990)	EPM	ICR mice, 1 and 10 mg·kg^{-1}, i.p.	Anxiolytic (bell-shaped dose–response curve)	BZD (blocked by flumazenil)
Guimarães *et al.* (1994)	EPM	Wistar rats, 5 mg·kg^{-1}, i.p.	Anxiolytic	Not tested
Bitencourt *et al.* (2008)	Fear-potentiated EPM	Wistar rats, 6.4 nmol, i.c.v.	Anxiolytic	Not tested
Campos and Guimarães (2008)	EPM	Wistar rats, 30 nmol, intra-dlPAG	Anxiolytic (bell-shaped dose–response curve)	5-HT$_{1A}$ receptor activation
Campos and Guimarães (2009)	EPM	Wistar rats, 30 nmol, intra-dlPAG (60 nmol effective when combined with a TRPV1 channel antagonist)	Anxiolytic	Lack of anxiolytic effect of high doses associated with TRPV1 channel activation
Malone *et al.* (2009)	THC-induced decrease in social interaction	Sprague Dawley rats, 20 mg·kg^{-1}, i.p.	Anxiolytic	Not tested
Resstel *et al.* (2009)	Restraint stress, autonomic changes, delayed (24 h) anxiogenic effect in EPM	Wistar rats, 10 mg·kg^{-1}, i.p.	Anti-stress	5-HT$_{1A}$ receptor activation
Casarotto *et al.* (2010)	MBT	C57BL/6 mice, 15–60 mg·kg^{-1}, i.p.	Anti-compulsive	Indirect CB$_1$ receptor activation
Soares Vde *et al.* (2010)	ETM, electrical stimulation of dlPAG	Wistar rats, 15–60 nmol, intra- dlPAG	Anxiolytic/panicolytic	5-HT$_{1A}$ receptor activation
Long *et al.* (2010)	Open field and light–dark tests	C57BL/6 mice, 1 mg·kg^{-1} (light–dark test) and 50 mg·kg^{-1} (open-field), i.p., daily for 21 days	Anxiolytic	Not tested
Gomes *et al.* (2011)	EPM	Wistar rats, 30 nmol, intra-BNST	Anxiolytic	5-HT$_{1A}$ receptor activation
Granjeiro *et al.* (2011)	Restraint stress, autonomic reactivity, delayed (24 h) anxiogenic effect in EPM	Wistar rats, 30 nmol, intra-cisterna magna	Anti-stress	Not tested
Campos *et al.* (2012a)	EPM after predator (cat) exposure	Wistar rats, 5 mg·kg^{-1}, i.p., daily for 7 days	Anxiolytic	5-HT$_{1A}$ receptor activation
Deiana *et al.* (2012)	MBT	Swiss mice, 120 mg·kg^{-1}, orally or i.p.	Anticompulsive	Not tested
Long *et al.* (2012)	Open field and light–dark tests	C57BL/6 Arc mice, 1 and 100 mg·kg^{-1}, i.p. daily for 13 days	Anxiolytic (open-field only)	Not tested
Uribe-Mariño *et al.* (2012)	Snake exposure	Swiss mice, 0.3–30 mg·kg^{-1}, i.p.	Panicolytic	Not tested
Hsiao *et al.* (2012)	Repeated EPM and open-field	Wistar rats, 3.2 nmol, intra-central amygdaloid nucleus	Anxiolytic	Not tested

continues

Table 1 (Continued)

Reference	Test used	Strain, species, effective dose, and route/site of administration	Effect	Pharmacological mechanism
Campos *et al.* (2013a,b)	EPM and NSF	C57BL/6 mice, 30 mg·kg^{-1}, daily for 14 days (CUS-exposed animals)	Anti-stress	CB_1 receptor-mediated facilitation of hippocampal neurogenesis
O'Brien *et al.* (2013)	Light–dark test	Sprague Dawley rats, 2.5 mg·kg^{-1}, i.p. for 14 days	No effect	Not tested
Twardowschy *et al.* (2013)	Snake exposure	Swiss mice, 3.0 mg·kg^{-1}, i.p.	Panicolytic	5-HT_{1A} receptor activation
Almeida *et al.* (2013)	Social interaction test	Wistar and SHR rats, 1 mg·kg^{-1}, i.p.	Increased social interaction (Wistar rats only)	Not tested
Cheng *et al.* (2014)	EPM	C57BL/6 J mice, 20 mg·kg^{-1}, i.p. daily for 21 days	No effect	Not tested
Fogaça *et al.* (2014)	EPM	Wistar rats, 30 nmol, intra-PL cortex	Anxiogenic (bell-shaped dose-response curve), anxiolytic 24 h after restraint stress	5-HT_{1A} receptor activation
Nardo *et al.* (2014)	MBT	Swiss mice, 30 mg·kg^{-1}, i.p.	Attenuated mCPP-induced increase in marble-burying (bell-shaped dose response curve)	Indirect CB_1 receptor activation
Marinho *et al.* (2015)	EPM	Wistar rats, 15–30 nmol, intra-IL cortex	Anxiolytic (bell-shaped dose response curve), no effect 24 h after restraint stress	5-HT_{1A} receptor activation
Todd and Arnold (2016)	Open-field	C57BL/6 mice, 10 mg·kg^{-1}, i.p.	Prevented THC- induced anxiogenesis	Not tested
Schiavon *et al.* (2016)	EPM	Swiss mice, 3 mg·kg^{-1}, i.p.	Anxiolytic	Not tested

BZD, benzodiazepine; CUS, chronic unpredictable stress; ETM, elevated T-maze; ICR, Institute of Cancer; MBT, marble burying test; NSF, novelty suppressed feeding; SHR, spontaneously hypertensive rats.

CBD was further demonstrated in other relevant brain regions, including the BNST (Gomes *et al.*, 2011) and IL cortex (Marinho *et al.*, 2015). Moreover, systemic treatment with 5-HT_{1A} receptor antagonists was also able to prevent this CBD-induced anxiolysis (see Table 1).

In the marble-burying test and after repeated administration, however, CBD effects on anxiety seem to depend on CB_1 receptors rather than 5-HT_{1A} receptors (Casarotto *et al.*, 2010; Campos *et al.*, 2013a; Nardo *et al.*, 2014). Even if the (+)-CBD enantiomer shows affinity for CB_1 receptors, the naturally occurring (−) CBD does not bind to these receptors (Hanuš *et al.*, 2005), indicating that the CB_1 receptor-mediated anti-aversive effects of CBD are probably indirect. Bisogno *et al.* (2001) showed that CBD blocked the reuptake and metabolism of anandamide *in vitro*. Correspondingly, using embryonic hippocampal cells, Campos *et al.* (2013b) showed that the increase in cell proliferation induced by CBD is prevented by antagonism of either CB_1 or CB_2 receptors, as well as by overexpression of fatty acid amide hydrolase (FAAH), the enzyme responsible for anandamide metabolism. More recently, Dale Deutsch's group demonstrated that CBD binds to fatty acid-binding proteins (FABPs) necessary for the transport of anandamide from the plasma membrane to intracellular FAAH, which might be a primary mechanism by which CBD decreases anandamide uptake/metabolism (Elmes *et al.*, 2015). Consistent with these *in vitro* studies, the anti-stress (in mice) and antipsychotic (in humans) effects of repeated CBD administration were associated with increased hippocampal and serum levels, respectively, of anandamide (Leweke *et al.*, 2012, Campos *et al.*, 2013b).

Emotional learning and memory processing

We will first summarize the psychological mechanisms involved in classical conditioning, a type of associative learning whereby discrete cues or contexts come to predict the occurrence of threatening or rewarding stimuli, before reviewing the evidence demonstrating a role for CBD in regulating different fear and drug memory processes. During conditioning,

Table 2

CBD effects on learned fear processing in male animals

Reference	Test used	Strain, species, effective dose and route/site of administration	Effect	Pharmacological mechanism
Studies conducted in operant conditioning paradigms				
Silveira Filho and Tufik, 1981	Geller-Seifter conflict test	Wistar rats, 100 mg·kg^{-1}, i.p.	No effect	Not tested
Musty *et al.* (1985)	Vogel punished licking test	Sprague–Dawley rats, 5–10 mg·kg^{-1}, i.p.	Anxiolytic (bell-shaped dose–response curve)	Not tested
Moreira *et al.* (2006)	Vogel punished licking test	Wistar rats, 10 mg·kg^{-1}, i.p.	Anxiolytic	Not blocked by BZD antagonism (flumazenil)
Gomes *et al.* (2011)	Vogel punished licking test	Wistar rats, 30–60 nmol, intra-BNST	Anxiolytic	5-HT$_{1A}$ receptor activation
Studies conducted in classical (Pavlovian) conditioning paradigms				
Zuardi and Karniol, 1983	AFC	Wistar rats, 10 mg·kg^{-1}, i.p.	Anxiolytic (decreased fear expression)	Not tested
Resstel *et al.* (2006)	CFC	Wistar rats, 10 mg·kg^{-1}, i.p.	Anxiolytic (decreased fear expression)	Not tested
Bitencourt *et al.* (2008)	CFC	Wistar rats, 6.4 nmol, i.c.v.	Facilitated fear memory extinction	Indirect CB$_1$ receptor activation
Lemos *et al.* (2010)	CFC	Wistar rats, 10 mg·kg^{-1}, i.p.	Anxiolytic (decreased fear expression)	Not tested
Lemos *et al.* (2010)	CFC	Wistar rats, 30 nmol, intra-PL cortex	Anxiolytic (decreased fear expression)	Not tested
Lemos *et al.* (2010)	CFC	Wistar rats, 30 nmol, intra-IL cortex	Anxiogenic (increased fear expression)	Not tested
ElBatsh *et al.* (2012)	CFC	Lister-hooded rats, 10 mg·kg^{-1}, i.p. daily for 14 days	Anxiogenic (increased f ear expression)	Decreased hippocampal BDNF and TrkB, reduced frontal cortex phospho-ERK1/2 expression
Gomes *et al.* (2012)	CFC	Wistar rats, 30–60 nmol, intra-BNST	Anxiolytic (decreased f ear expression)	5-HT$_{1A}$ receptor activation
Levin *et al.* (2012)	CFC	Wistar and SHR rats, 1–15 mg·kg^{-1}, i.p.	Anxiolytic (decreased fear expression) and/or disrupted fear memory formation (Wistar rats only)	Not tested
Stern *et al.* (2012)	CFC	Wistar rats, 3–30 mg·kg^{-1}, i.p.	Disrupted fear memory reconsolidation (bell-shaped dose response curve)	Indirect CB$_1$ receptor activation
Do Monte *et al.* (2013)	CFC	Long–Evans hooded rats, 1.3 nmol, intra-IL cortex	Facilitated fear memory extinction	Indirect CB$_1$ receptor activation
Cheng *et al.* (2014)	AFC	C57BL/6 J mice, 20 mg·kg^{-1}, i.p. daily for 21 days	No effect	Not tested
Fogaça *et al.* (2014)	CFC	Wistar rats, 30 nmol, intra-PL cortex	Anxiolytic (decreased fear expression)	5-HT$_{1A}$ receptor activation
Gazarini *et al.* (2015)	CFC	Wistar rats, 10 mg·kg^{-1}, i.p.	Disrupted fear memory reconsolidation	Not tested
Stern *et al.* (2014)	CFC	Wistar rats, 10 mg·kg^{-1}, i.p.	Disrupted fear memory reconsolidation	Indirect CB$_1$ receptor activation in PL cortex
Marinho *et al.* (2015)	CFC	Wistar rats, 30 nmol, intra-IL cortex	Anxiogenic (increased fear expression)	5-HT$_{1A}$ receptor activation

continues

Table 2 (Continued)

Reference	Test used	Strain, species, effective dose and route/site of administration	Effect	Pharmacological mechanism
Stern *et al.* (2015)	CFC	Wistar rats, 1 mg·kg^{-1} + THC 0.1 mg·kg^{-1}, i.p.	Disrupted fear memory reconsolidation	Not tested
Norris *et al.* (2016)	OFC	Sprague Dawley rats, 0.03–0.32 nmol, intra-nucleus accumbens shell	Disrupted fear memory formation (acquisition)	5-HT$_{1A}$ receptor activation
Song *et al.* (2016)	CFC	Lister hooded rats, 10 mg·kg^{-1}, i.p., before extinction (after weak or strong conditioning)	Impaired or enhanced extinction after weak or strong conditioning, respectively	Not tested
Jurkus *et al.* (2016)	AFC	Lister hooded rats, 5–20 mg·kg^{-1}, i.p.	Anxiolytic (decreased fear expression) at highest dose, no effect on extinction	Not tested
Stern *et al.* (2016)	CFC	Wistar rats, 10–30 mg·kg^{-1}, i.p.	Disrupted fear memory consolidation	Indirect CB$_1$ or CB$_2$ receptor activation

AFC, auditory fear conditioning; BZD, benzodiazepine; CFC, contextual fear conditioning; OFC, olfactory fear conditioning.

Table 3

CBD effects on anxiety in humans

Reference	Subjects and test(s) used	Effective dose and route of administration	Effect	Possible pharmacological or neural mechanism
Zuardi *et al.* (1982)	Healthy subjects, THC-induced anxiety	~70 mg (1 mg·kg^{-1}) orally	Prevented the anxiogenic effects of THC	Not tested
Zuardi *et al.* (1993)	Healthy subjects, simulated public speaking-induced anxiety	300 mg orally	Prevented public speaking-induced increase in anxiety	Not tested (effects similar to the 5-HT$_{1A}$ receptor partial agonist ipsapirone)
Crippa *et al.* (2004)	Healthy subjects, SPECT	400 mg orally	Anxiolytic	Decreased blood flow in medial temporal structures and posterior cingulate gyrus
Fusar-Poli *et al.* (2009, 2010)	Healthy subjects, fearful faces, fMRI	600 mg orally	Anxiolytic (trend)	Decreased blood flow in amygdala and anterior cingulate cortex that correlated with a reduced SCR to fearful faces
Bergamaschi *et al.* (2011)	Social anxiety disorder patients, simulated public speaking-induced anxiety	600 mg orally	Anxiolytic	Not tested
Crippa *et al.* (2011)	Generalized anxiety disorders patients, SPECT	400 mg orally	Decreased subjective anxiety	Altered blood flow in limbic and paralimbic brain areas
Hurd *et al.* (2015)	Abstinent heroin abusers, heroin cue-induced anxiety	400 or 800 mg orally	Decreased subjective anxiety (preliminary data)	Not tested
Shannon and Opila-Lehman, 2016	A 10 year-old girl with PTSD (case report)	At least 25 mg daily for 5 months	Reduced anxiety and improved sleep	Not tested

fMRI, functional magnetic resonance imaging; SCR, skin conductance response; SPECT, single-photon emission computed tomography.

an innocuous conditioned stimulus (CS), which can be a discrete cue (e.g. sound, light or odour) or a context (e.g. testing chamber/arena), becomes associated with an aversive (e.g. footshock) or appetitive (e.g. drug reward availability) unconditioned stimulus (US). After conditioning, the CS–US association undergoes consolidation into long-term memory, and

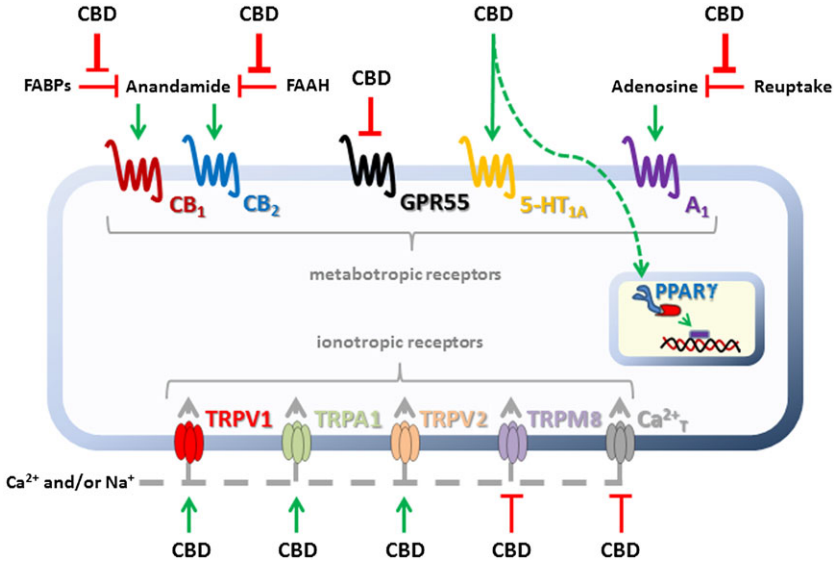

Figure 1

The main molecular targets and potential mechanisms of action of CBD. This drug inhibits both FAAH, the enzyme which metabolizes anandamide, and FABPs, which mediate the transport of anandamide to FAAH; both mechanisms ultimately result in the indirect activation of CB_1 and/or CB_2 receptors. CBD also activates the 5-HT_{1A} receptor, PPARγ and the transient receptor potential channels TRPV1, TRPA1 and TRPV2. Finally, CBD inhibits adenosine reuptake and antagonizes GPR55, TRPM8 and T-type Ca^{2+} channels. 5-HT_{1A} and (indirect) cannabinoid receptor activation are the mechanisms that have been implicated in the anxiolytic effects of CBD to date (see Ibeas Bih *et al.* (2015) and McPartland *et al.* (2015) for further details).

later presentation of or re-exposure to the CS alone initially elicits conditioned fear (e.g. freezing/avoidance) or drug-seeking (e.g. lever pressing/place preference) responses (Peters *et al.*, 2009). Retrieval of the CS can make emotional memories labile by destabilizing the memory trace, which allows for these memories to be maintained or updated through the process of reconsolidation (Lee, 2009). Repeated presentations of or prolonged exposure to the CS causes the extinction of emotional memories, resulting in the formation of a new CS–no US association which competes with the original emotional memory to suppress conditioned responding to the CS (Peters *et al.*, 2009). Understanding how behavioural and/or pharmacological interventions can attenuate conditioned responding, disrupt memory reconsolidation and/or enhance extinction has clinical relevance given that all of these mechanisms are potential therapeutic strategies for alleviating the symptoms of PTSD (i.e. pathological fear) and addiction (i.e. drug craving) (Tronson and Taylor, 2013; Everitt, 2014; Kindt, 2014; Singewald *et al.*, 2015).

CBD effects on fear memory processing

As alluded to above, there is growing evidence indicating that CBD also regulates learned fear (see Table 2). Systemic CBD administration has been shown to reduce the expression of fear memory when given acutely (Zuardi and Karniol, 1983; Resstel *et al.*, 2006; Lemos *et al.*, 2010; Jurkus *et al.*, 2016). CBD has also been reported to impair the acquisition of fear learning; acute systemic administration before fear conditioning resulted in attenuated fear expression during later memory retrieval testing (Levin *et al.*, 2012). In contrast, there are few reported effects of repeated CBD administration on fear memory expression and those that exist are conflicting. In one study, daily injections of CBD for 14 days prior to conditioning enhanced fear expression during retrieval testing, suggesting that chronic CBD facilitated fear learning (ElBatsh *et al.*, 2012), whereas another study showed no effect of CBD on fear conditioning when it was administered for 21 days (Cheng *et al.*, 2014).

The results of several studies indicate that CBD also modulates the extinction and reconsolidation of conditioned fear, leading to lasting effects on learned fear expression. I.c.v. infusions of CBD given before three extinction sessions resulted in enhanced contextual fear extinction (Bitencourt *et al.*, 2008). Systemic administration of CBD given acutely before extinction has been shown to affect contextual fear extinction depending on the strength of fear conditioning beforehand. CBD impaired extinction after weak conditioning but enhanced extinction after strong conditioning (Song *et al.*, 2016). However, CBD given systemically before auditory fear extinction reduced fear expression acutely without affecting extinction memory (Jurkus *et al.*, 2016). Interestingly, a study in humans also showed that CBD had no effect on the extinction of visual fear memory when given before extinction, but it did enhance extinction memory when given immediately after extinction (Das *et al.*, 2013).

Contrary to the reported facilitatory effects of CBD on fear extinction, this drug has been shown to disrupt the reconsolidation of contextual fear memory after its brief retrieval (Stern *et al.*, 2012; 2015; Gazarini *et al.*, 2015), although these contrasting effects of CBD on fear extinction and memory reconsolidation both result in a lasting reduction of learned fear expression. The disruptive effect of

systemic CBD administration on reconsolidation required that it was given immediately after memory retrieval as CBD had no effect if it was given without, or 6 h after, retrieval. CBD was also able to disrupt the reconsolidation of both newer and older fear memories. Moreover, the subsequent reduction of learned fear expression lasted for over 21 days and was not reinstated by later shock presentation, indicating that the effects of CBD were due to disrupted memory reconsolidation and not enhanced extinction (Stern *et al.*, 2012).

In another study, CBD given immediately after retrieval disrupted the reconsolidation of an abnormally persistent fear memory when the partial NMDA receptor agonist D-cycloserine was first administered before retrieval to facilitate memory destabilization. Fear memory was strengthened pharmacologically by enhancing adrenergic transmission immediately after conditioning, resulting in generalized fear expression and impaired fear suppression by extinction (Gazarini *et al.*, 2015). Understanding the mechanisms underlying reconsolidation disruption of such fear memories is important because there is evidence indicating that strong fear memories can show resistance to pharmacological disruption of reconsolidation (Lee, 2009), which has implications for using this potential therapeutic approach to weaken traumatic memories in the treatment of PTSD.

Pharmacological mechanisms and brain sites involved in the effects of CBD on learned fear

Just as the anxiolytic effects of CBD involve a direct effect on 5-HT_{1A} receptors and an indirect effect on cannabinoid receptors via elevated endocannabinoid levels, so too do its effects on different fear memory processes. Similarly, there is overlap in the neural circuitry involved in mediating the effects of CBD on anxiety and learned fear. The reduction in conditioned fear expression induced by CBD was accompanied by attenuated c-Fos expression in the PL and IL cortices and the BSNT. Moreover, CBD infusion into the BNST or PL cortex reduced fear memory expression, although infusing CBD into the IL cortex enhanced the expression of learned fear (Lemos *et al.*, 2010). This discrepancy between the effects of CBD infused into the PL or IL cortex is probably due to these medial prefrontal cortical subregions exerting opposing influences on learned fear, with the former facilitating its expression and the latter being involved in its suppression and/or extinction (Fenton *et al.*, 2014; Giustino and Maren, 2015). The regulation of conditioned fear expression by CBD in these brain areas was shown to be dependent on 5-HT_{1A} receptors (Gomes *et al.*, 2012; Fogaça *et al.*, 2014; Marinho *et al.*, 2015). The inhibitory effect of CBD on the acquisition of fear conditioning has also been shown to depend on 5-HT_{1A} receptor activation in the nucleus accumbens shell (Norris *et al.*, 2016).

In contrast to the acquisition and expression of fear memory, the reconsolidation and extinction of learned fear involve (indirect) cannabinoid receptor activation. The facilitatory effect of i.c.v. CBD infusion on fear extinction was inhibited by prior CB_1 receptor antagonism but not TRPV1 channel blockade (Bitencourt *et al.*, 2008). CBD was shown to act in the IL cortex to facilitate fear extinction as infusing CBD into this region enhanced extinction, an effect which also depended on CB_1 receptors (Do Monte *et al.*, 2013). The disruptive effect of CBD on fear memory reconsolidation was blocked by pretreatment with a CB_1 receptor antagonist given systemically or infused into the PL cortex, whereas prior 5-HT_{1A} receptor antagonism had no effect on the disruption of reconsolidation by CBD (Stern *et al.*, 2012; 2014).

CBD effects on addictive drug memory processing

In contrast to the study of fear memories, to date there has been a much more limited exploration of the effects of CBD on addictive drug-related memories. This necessitates a narrative review of the relevant literature, which follows below. Moreover, the small number of studies has been conducted across a variety of experimental paradigms and with different drugs of abuse. These drugs can elicit sensitized responses with intermittent repeated administration, which is context-dependent and thereby reliant upon context-drug associations. Similarly, the acquisition and expression of conditioned place preference behaviour depends upon the integrity of context-drug and/or cue-drug associations. Finally, cue-drug associations can precipitate cue-induced relapse of drug seeking in rodents previously trained to self-administer a drug (Aguilar *et al.*, 2009; Steketee and Kalivas, 2011). Each of these paradigms can be studied using stimulants (e.g. cocaine and amphetamine), opiates (e.g. heroin and morphine), and other drugs (e.g. alcohol and nicotine).

Unlike THC, studies have shown that CBD lacks any rewarding effects of its own given that it fails to induce conditioned place preference or enhance the reinforcing effects of electrical brain self-stimulation (Parker *et al.*, 2004; Vann *et al.*, 2008; Katsidoni *et al.*, 2013). In a study of amphetamine-induced locomotor sensitization, infusions of CBD (100 ng) into the shell subregion of the nucleus accumbens attenuated the development of locomotor sensitization (Renard *et al.*, 2016). While this might suggest that CBD impaired the formation of an amphetamine memory that supports locomotor sensitization, these findings were within the context of mesolimbic mechanisms involved in the potential antipsychotic action of CBD. Moreover, even though the attenuation of locomotor sensitization was paralleled by modulation of cellular mechanisms of synaptic plasticity, it remains a challenge to distinguish learning-related behavioural effects from modulation of drug reward (cf. Katsidoni *et al.*, 2013; Prud'homme *et al.*, 2015), which would impact upon reward-dependent learning. The non-mnemonic interpretation is supported by a failure of CBD to prevent the acquisition of amphetamine place preference (Parker *et al.*, 2004). However, while it appears that CBD does not disrupt the formation of amphetamine-related memories, this does not rule out potential effects on memories formed in relation to other drugs of abuse.

Subsequent to their acquisition, CBD might affect the expression of drug memories. Here there appears to be a disparity depending upon the drug reward under study. Acute administration of CBD (5 and 10 $mg \cdot kg^{-1}$) did not alter cocaine self-administration or cue-induced relapse to cocaine

seeking (Mahmud *et al.*, 2016) and so failed to replicate an earlier study of heroin self-administration (Ren *et al.*, 2009). While CBD (5 and 20 mg·kg^{-1}) similarly did not alter heroin self-administration, it did have an effect on cue-induced relapse to heroin seeking (Ren *et al.*, 2009), a measure of cue-heroin memory expression. CBD (5 mg·kg^{-1}) reduced responding in a cue-induced relapse test but only when given 24 h, and not 30 min, prior to the test. This long-lasting effect on the expression of the cue-heroin memory was even more persistent (up to 14 days) when three consecutive daily injections of 5 mg·kg^{-1} CBD were given. This ability of CBD to have such long-lasting effects may be mediated by an up-regulation of AMPA GluA1 receptors in the nucleus accumbens (Ren *et al.*, 2009).

The impaired expression of cue-heroin relapse in response to CBD administration in animals suggests that this drug might have anti-relapse properties in opiate addiction in humans. This has been explored in a preliminary study of heroin addicts, in which participants were given daily doses of CBD (400 or 800 mg) or placebo for 3 days (Hurd *et al.*, 2015). CBD reduced craving both 24 h and 7 days later, mirroring the preclinical rodent study (Ren *et al.*, 2009). This beneficial effect of CBD may not be limited to opiate addiction as a conceptually similar, albeit more modest, effect has also been observed in tobacco smokers (Morgan *et al.*, 2013). In this small week-long study, smokers were instructed to inhale a metered dose of CBD (400 μg) or placebo when they felt like smoking. CBD acutely reduced the number of cigarettes smoked, but this effect was not maintained after the cessation of CBD administration. Interestingly, and in contrast to the heroin study, CBD did not alter craving, either acutely or persistently. Therefore, it is not clear whether CBD has generalized effects on the expression of cue-drug memory to elicit craving and precipitate relapse, or whether its effects are specific to certain classes of addictive drugs.

For the maintenance (i.e. reconsolidation) of drug-related memories, there is a single study on morphine and cocaine conditioned place preference. When the place preference memory was briefly reactivated in order to trigger reconsolidation, CBD administration (10 mg·kg^{-1}) immediately thereafter led to an impairment in the subsequent maintenance of both cocaine and morphine memories to reduce place preference at test (de Carvalho and Takahashi, 2016). This was a long-lasting effect, which is usually evidence for reconsolidation impairments. However, the study lacked a true non-reactivation control, and so the long-lasting impairment, especially for morphine place preference, is not dissimilar to the aforementioned persistent reduction in the expression of cue-heroin memories in the self-administration setting (Ren *et al.*, 2009). Therefore, it is still unclear whether CBD indeed impairs the reconsolidation of drug memories. Nevertheless, there are indications from the comparison between the place preference and self-administration studies to suggest that their results might be underpinned by qualitatively different processes. For example, while the CBD-induced impairment failed to ameliorate heroin-primed reinstatement of drug seeking (Ren *et al.*, 2009), post-reactivation CBD did prevent morphine-primed reinstatement of place preference (de Carvalho and Takahashi, 2016). Moreover, the contrasting effects of post-reactivation CBD and acute CBD treatment on the subsequent expression of cocaine memories (de Carvalho and Takahashi, 2016) suggest that the impairment in cocaine place preference is not simply explained by long-lasting modulation of drug memory expression.

Similarly, there is a single study on the effect of CBD on drug memory extinction. Injection of CBD (5 mg·kg^{-1}) prior to an extinction trial enhanced the subsequent reduction in cocaine and amphetamine place preference (Parker *et al.*, 2004). Despite the lack of a no-extinction control, the observation that CBD reduces the expression of stimulant-induced place preference again suggests that such a reduction was, at least in part, due to the concomitant extinction trial. Interestingly, the ability of CBD to reduce cocaine and amphetamine place preference in this extinction study (Parker *et al.*, 2004) is similar to the previous observation that CBD impairs the reconsolidation of morphine and cocaine memories in the same place preference setting (de Carvalho and Takahashi, 2016). Indeed, while there was a difference in the timing of CBD administration between the two studies, the single behavioural trial that served to extinguish (Parker *et al.*, 2004) or destabilize (de Carvalho and Takahashi, 2016) the drug memory did not differ greatly. The extinction trial was 15 min in duration, compared with a 10 min reactivation trial, although the former was confined to the drug-paired chamber, whereas the latter was a test. Moreover, the conditioning parameters were similar across the two studies, and also to previous studies of reconsolidation that have used 30 min confined reactivation trials for amphetamine place preference (Sakurai *et al.*, 2007), 20 min confined reactivation trials for cocaine place preference (Valjent *et al.*, 2006) and 10 min confined reactivation trials for morphine and nicotine place preference (Wang *et al.*, 2008; Fang *et al.*, 2011). Also, given that the parameters of appetitive memory reconsolidation and extinction are usually well distinguished, such that they are each typically defined by very different durations of context re-exposure or numbers of cue presentations (Flavell and Lee, 2013), it is unclear if CBD both enhances extinction and impairs reconsolidation of drug memories. It is perhaps more likely that the ability of CBD to reduce later drug place preference observed in these two studies (Parker *et al.*, 2004; de Carvalho and Takahashi, 2016) instead reflects qualitatively similar processes. By simply considering the parametric comparisons presented above, we conclude that there is stronger evidence for CBD impairing drug memory reconsolidation than there is for it enhancing drug memory extinction. Furthermore, given that pharmacological enhancement of extinction is usually dependent upon appreciable extinction-mediated memory reduction (Weber *et al.*, 2007; Bouton *et al.*, 2008), and there was no evidence for any such reduction in the CBD study (Parker *et al.*, 2004), it remains unclear if CBD actually enhances drug memory extinction.

Concluding remarks and future directions

Converging lines of evidence have established that acute CBD treatment is anxiolytic in both animals and humans. A growing number of preclinical studies also indicate that this drug reduces fear memory expression when given acutely. Importantly, CBD produces an enduring reduction in learned

fear expression when given in conjunction with fear memory reconsolidation or extinction by disrupting the former and facilitating the latter. This makes CBD a potential candidate for testing as a pharmacological adjunct to psychological therapies or behavioural interventions used in treating PTSD and phobias. These effects of CBD are mediated at least in part by 5-HT_{1A} receptors and indirectly via endocannabinoid-mediated action on cannabinoid receptors, although the involvement of other possible pharmacological mechanisms has not yet been investigated. Studies have begun to elucidate the neural circuit mechanisms underlying the effects of CBD on anxiety and learned fear. The recent functional imaging studies in humans, which examined the alterations in brain activity that accompany the anxiolytic effects of CBD, may inform future preclinical and clinical studies investigating the wider neural circuitry involved in mediating its effects on learned fear. In contrast to anxiety and learned fear, research into the effects of CBD on addictive drug memory processing is still in its infancy. Therefore, further studies are needed to determine the psychological, pharmacological, and brain mechanisms involved in the attenuation of drug memory expression by CBD in relation to different classes of abused drugs. Given the significant co-morbidity between anxiety-related and substance abuse disorders, CBD should also be investigated as a common treatment for such disorders. One outstanding issue that needs to be addressed is determining the effects of chronic CBD treatment on different emotional memory processes. For example, one potential therapeutic strategy is to use CBD chronically to reduce symptoms by dampening fear and/or drug memory expression. However, CBD given acutely during the psychological therapy session aimed at impairing memory reconsolidation or enhancing extinction might be sufficient to facilitate this effect. Another important consideration is how CBD would be delivered for treating these disorders. Most of the recreationally used cannabis available today contains low levels of CBD and high levels of THC, which can exacerbate symptoms; however, cannabis strains containing a more favourable CBD : THC ratio might be an option (Hurd *et al.*, 2015). Similarly, novel formulations of CBD containing only trace amounts of other phytocannabinoids have recently become available for the putative treatment of childhood epileptic disorders (e.g. Epidiolex, GW Pharmaceuticals; Gofshteyn *et al.*, 2016). In summary, this line of research may lead to the development of a formulation of CBD for use as a treatment for anxiety-related and substance abuse disorders in the future.

Acknowledgements

F.S.G., J.L.C.L. and C.W.S. were funded jointly by a FAPESP-University of Birmingham-University of Nottingham pump-priming award (2012/50896-8). L.J.B. was funded by a Brazilian CNPq research fellowship (307895/2013-0). The funders had no other involvement in any aspect of this work.

Conflict of interest

F.S.G. is co-inventor of the patent 'Fluorinated CBD compounds, compositions and uses thereof. Pub. No.: WO/2014/108899. International Application No.: PCT/IL2014/050023'; Def. US no. Reg. 62193296; 29/07/2015; INPI in 19/08/2015 (BR1120150164927).

References

Adams R, Hunt M, Clark JH (1940). Structure of cannabidiol, a product isolated from the marihuana extract of minnesota wild hemp. J Am Chem Soc 62: 196–200.

Aguilar MA, Rodríguez-Arias M, Miñarro J (2009). Neurobiological mechanisms of the reinstatement of drug-conditioned place preference. Brain Res Rev 59: 253–277.

Alexander SPH, Kelly E, Marrion N, Peters JA, Benson HE, Faccenda E *et al.* (2015a). The Concise Guide to PHARMACOLOGY 2015/16: Overview. Br J Pharmacol 172: 5729–5143.

Alexander SPH, Davenport AP, Kelly E, Marrion N, Peters JA, Benson HE *et al.* (2015b). The Concise Guide to PHARMACOLOGY 2015/16: G protein-coupled receptors. Br J Pharmacol 172: 5744–5869.

Alexander SPH, Peters JA, Kelly E, Marrion N, Benson HE, Faccenda E *et al.* (2015c). The Concise Guide to PHARMACOLOGY 2015/16: Ligand-gated ion channels. Br J Pharmacol 172: 5870–5903.

Alexander SPH, Catterall WA, Kelly E, Marrion N, Peters JA, Benson HE *et al.* (2015d). The Concise Guide to PHARMACOLOGY 2015/16: Voltage-gated ion channels. Br J Pharmacol 172: 5904–5941.

Alexander SPH, Cidlowski JA, Kelly E, Marrion N, Peters JA, Benson HE *et al.* (2015e). The Concise Guide to PHARMACOLOGY 2015/16: Nuclear hormone receptors. Br J Pharmacol 172: 5956–5978.

Alexander SPH, Fabbro D, Kelly E, Marrion N, Peters JA, Benson HE *et al.* (2015f). The Concise Guide to PHARMACOLOGY 2015/16: Catalytic receptors. Br J Pharmacol 172: 5979–6023.

Alexander SPH, Fabbro D, Kelly E, Marrion N, Peters JA, Benson HE *et al.* (2015g). The Concise Guide to PHARMACOLOGY 2015/16: Enzymes. Br J Pharmacol 172: 6024–6109.

Almeida V, Levin R, Peres FF, Niigaki ST, Calzavara MB, Zuardi AW *et al.* (2013). Cannabidiol exhibits anxiolytic but not antipsychotic property evaluated in the social interaction test. Prog Neuropsychopharmacol Biol Psychiatry 41: 30–35.

Bergamaschi MM, Queiroz RH, Chagas MH, de Oliveira DC, De Martinis BS, Kapczinski F *et al.* (2011). Cannabidiol reduces the anxiety induced by simulated public speaking in treatment-naïve social phobia patients. Neuropsychopharmacology 36: 1219–1226.

Bisogno T, Hanus L, De Petrocellis L, Tchilibon S, Ponde DE, Brandi I *et al.* (2001). Molecular targets for cannabidiol and its synthetic analogues: effect on vanilloid VR1 receptors and on the cellular uptake and enzymatic hydrolysis of anandamide. Br J Pharmacol 134: 845–852.

Bitencourt RM, Pamplona FA, Takahashi RN (2008). Facilitation of contextual fear memory extinction and anti-anxiogenic effects of AM404 and cannabidiol in conditioned rats. Eur Neuropsychopharmacol 18: 849–859.

Blessing EM, Steenkamp MM, Manzanares J, Marmar CR (2015). Cannabidiol as a potential treatment for anxiety disorders. Neurotherapeutics 12: 825–836.

Bouton ME, Vurbic D, Woods AM (2008). D-cycloserine facilitates context-specific fear extinction learning. Neurobiol Learn Mem 90: 504–510.

Burstein S (2015). Cannabidiol (CBD) and its analogs: a review of their effects on inflammation. Bioorg Med Chem 23: 1377–1385.

Campos AC, de Paula SV, Carvalho MC, Ferreira FR, Vicente MA, Brandão ML *et al.* (2013a). Involvement of serotonin-mediated neurotransmission in the dorsal periaqueductal gray matter on cannabidiol chronic effects in panic-like responses in rats. Psychopharmacology (Berl) 226: 13–24.

Campos AC, Ferreira FR, Guimarães FS (2012a). Cannabidiol blocks long-lasting behavioral consequences of predator threat stress: possible involvement of 5HT1A receptors. J Psychiatr Res 46: 1501–1510.

Campos AC, Guimarães FS (2009). Evidence for a potential role for TRPV1 receptors in the dorsolateral periaqueductal gray in the attenuation of the anxiolytic effects of cannabinoids. Prog Neuropsychopharmacol Biol Psychiatry 33: 1517–1521.

Campos AC, Guimarães FS (2008). Involvement of 5HT1A receptors in the anxiolytic-like effects of cannabidiol injected into the dorsolateral periaqueductal gray of rats. Psychopharmacology (Berl) 199: 223–230.

Campos AC, Moreira FA, Gomes FV, Del Bel EA, Guimarães FS (2012b). Multiple mechanisms involved in the large-spectrum therapeutic potential of cannabidiol in psychiatric disorders. Philos Trans R Soc Lond B Biol Sci 367: 3364–3378.

Campos AC, Ortega Z, Palazuelos J, Fogaça MV, Aguiar DC, Díaz-Alonso J *et al.* (2013b). The anxiolytic effect of cannabidiol on chronically stressed mice depends on hippocampal neurogenesis: involvement of the endocannabinoid system. Int J Neuropsychopharmacol 16: 1407–1419.

Canteras NS, Resstel LB, Bertoglio LJ, Carobrez Ade P, Guimarães FS (2010). Neuroanatomy of anxiety. Curr Top Behav Neurosci 2: 77–96.

Carobrez AP, Bertoglio LJ (2005). Ethological and temporal analyses of anxiety-like behavior: the elevated plus-maze model 20 years on. Neurosci Biobehav Rev 29: 1193–1205.

Casarotto PC, Gomes FV, Resstel LB, Guimarães FS (2010). Cannabidiol inhibitory effect on marble-burying behaviour: involvement of CB_1 receptors. Behav Pharmacol 21: 353–358.

Chemel BR, Roth BL, Armbruster B, Watts VJ, Nichols DE (2006). WAY-100635 is a potent dopamine D4 receptor agonist. Psychopharmacology (Berl) 188: 244–251.

Cheng D, Low JK, Logge W, Garner B, Karl T (2014). Chronic cannabidiol treatment improves social and object recognition in double transgenic APPswe/PS1ΔE9 mice. Psychopharmacology (Berl) 231: 3009–3017.

Crippa JA, Zuardi AW, Garrido GE, Wichert-Ana L, Guarnieri R, Ferrari L *et al.* (2004). Effects of cannabidiol (CBD) on regional cerebral blood flow. Neuropsychopharmacology 29: 417–426.

Crippa JA, Derenusson GN, Ferrari TB, Wichert-Ana L, Duran FL, Martin-Santos R *et al.* (2011). Neural basis of anxiolytic effects of cannabidiol (CBD) in generalized social anxiety disorder: a preliminary report. J Psychopharmacol 25: 121–130.

Das RK, Kamboj SK, Ramadas M, Yogan K, Gupta V, Redman E *et al.* (2013). Cannabidiol enhances consolidation of explicit fear extinction in humans. Psychopharmacology (Berl) 226: 781–792.

Deiana S, Watanabe A, Yamasaki Y, Amada N, Arthur M, Fleming S *et al.* (2012). Plasma and brain pharmacokinetic profile of cannabidiol (CBD), cannabidivarine (CBDV), Δ^9-tetrahydrocannabivarin (THCV) and cannabigerol (CBG) in rats and mice following oral and intraperitoneal administration and CBD action on obsessive–compulsive behaviour. Psychopharmacology (Berl) 219: 859–873.

de Carvalho CR, Takahashi RN (2016). Cannabidiol disrupts the reconsolidation of contextual drug-associated memories in Wistar rats. Addict Biol. doi:10.1111/adb.12366.

Di Luca M, Baker M, Corradetti R, Kettenmann H, Mendlewicz J, Olesen J *et al.* (2011). Consensus document on European brain research. Eur J Neurosci 33: 768–818.

Do Monte FH, Souza RR, Bitencourt RM, Kroon JA, Takahashi RN (2013). Infusion of cannabidiol into infralimbic cortex facilitates fear extinction via CB_1 receptors. Behav Brain Res 250: 23–27.

ElBatsh MM, Assareh N, Marsden CA, Kendall DA (2012). Anxiogenic-like effects of chronic cannabidiol administration in rats. Psychopharmacology (Berl) 221: 239–247.

Elmes MW, Kaczocha M, Berger WT, Leung K, Ralph BP, Wang L *et al.* (2015). Fatty acid-binding proteins (FABPs) are intracellular carriers for Δ9-tetrahydrocannabinol (THC) and cannabidiol (CBD). J Biol Chem 290: 8711–8721.

Everitt BJ (2014). Neural and psychological mechanisms underlying compulsive drug seeking habits and drug memories – indications for novel treatments of addiction. Eur J Neurosci 40: 2163–2182.

Fagherazzi EV, Garcia VA, Maurmann N, Bervanger T, Halmenschlager LH, Busato SB *et al.* (2012). Memory-rescuing effects of cannabidiol in an animal model of cognitive impairment relevant to neurodegenerative disorders. Psychopharmacology (Berl) 219: 1133–1140.

Fang Q, Li FQ, Li YQ, Xue YX, He YY, Liu JF *et al.* (2011). Cannabinoid CB_1 receptor antagonist rimonabant disrupts nicotine reward-associated memory in rats. Pharmacol Biochem Behav 99: 738–742.

Fenton GE, Pollard AK, Halliday DM, Mason R, Bredy TW, Stevenson CW (2014). Persistent prelimbic cortex activity contributes to enhanced learned fear expression in females. Learn Mem 21: 55–60.

Flavell CR, Lee JLC (2013). Reconsolidation and extinction of an appetitive pavlovian memory. Neurobiol Learn Mem 104: 25–31.

Fogaça MV, Reis FM, Campos AC, Guimarães FS (2014). Effects of intra-prelimbic prefrontal cortex injection of cannabidiol on anxiety-like behavior: involvement of 5HT1A receptors and previous stressful experience. Eur Neuropsychopharmacol 24: 410–419.

Fusar-Poli P, Allen P, Bhattacharyya S, Crippa JA, Mechelli A, Borgwardt S *et al.* (2010). Modulation of effective connectivity during emotional processing by delta 9-tetrahydrocannabinol and cannabidiol. Int J Neuropsychopharmacol 13: 421–432.

Fusar-Poli P, Crippa JA, Bhattacharyya S, Borgwardt SJ, Allen P, Martin-Santos R *et al.* (2009). Distinct effects of {delta}9-tetrahydrocannabinol and cannabidiol on neural activation during emotional processing. Arch Gen Psychiatry 66: 95–105.

Gaoni Y, Mechoulam R (1964). Isolation, structure and partial synthesis of an active constituent of hashish. J Am Chem Soc 86: 1646.

Gazarini L, Stern CA, Piornedo RR, Takahashi RN, Bertoglio LJ (2015). PTSD-like memory generated through enhanced noradrenergic activity is mitigated by a dual step pharmacological intervention targeting its reconsolidation. Int J Neuropsychopharmacol 18. doi:10.1093/ijnp/pyu026.

Giustino TF, Maren S (2015). The role of the medial prefrontal cortex in the conditioning and extinction of fear. Front Behav Neurosci 9: 298.

Gofshteyn JS, Wilfong A, Devinsky O, Bluvstein J, Charuta J, Ciliberto MA *et al.* (2016). Cannabidiol as a potential treatment for febrile infection-related epilepsy syndrome (FIRES) in the acute and chronic phases. J Child Neurol 32: 35–40.

Gomes FV, Reis DG, Alves FH, Corrêa FM, Guimarães FS, Resstel LB (2012). Cannabidiol injected into the bed nucleus of the stria terminalis reduces the expression of contextual fear conditioning via 5-HT1A receptors. J Psychopharmacol 26: 104–113.

Gomes FV, Resstel LB, Guimarães FS (2011). The anxiolytic-like effects of cannabidiol injected into the bed nucleus of the stria terminalis are mediated by 5-HT1A receptors. Psychopharmacology (Berl) 213: 465–473.

Gould J (2015). The Cannabis crop. Nature 525: S2–S3.

Graeff FG (2002). On serotonin and experimental anxiety. Psychopharmacology (Berl) 163: 467–476.

Granjeiro EM, Gomes FV, Guimarães FS, Corrêa FM, Resstel LB (2011). Effects of intracisternal administration of cannabidiol on the cardiovascular and behavioral responses to acute restraint stress. Pharmacol Biochem Behav 99: 743–748.

Gross CT, Canteras NS (2012). The many paths to fear. Nat Rev Neurosci 13: 651–658.

Guimarães FS, Chiaretti TM, Graeff FG, Zuardi AW (1990). Antianxiety effect of cannabidiol in the elevated plus-maze. Psychopharmacology (Berl) 100: 558–559.

Guimarães FS, de Aguiar JC, Mechoulam R, Breuer A (1994). Anxiolytic effect of cannabidiol derivatives in the elevated plus-maze. Gen Pharmacol 25: 161–164.

Handley SL, Mithani S (1984). Effects of alpha2-adrenoceptor agonists and antagonists in a maze-exploration model of fear-motivated behavior. Naunyn Schmiedebergs Arch Pharmacol 327: 1–5.

Hanuš LO, Tchilibon S, Ponde DE, Breuer A, Fride E, Mechoulam R (2005). Enantiomeric cannabidiol derivatives: synthesis and binding to cannabinoid receptors. Org Biomol Chem 3: 1116–1123.

Hsiao YT, Yi PL, Li CL, Chang FC (2012). Effect of cannabidiol on sleep disruption induced by the repeated combination tests consisting of open field and elevated plus-maze in rats. Neuropharmacology 62: 373–384.

Hurd YL, Yoon M, Manini AF, Hernandez S, Olmedo R, Ostman M *et al.* (2015). Early phase in the development of cannabidiol as a treatment for addiction: opioid relapse takes initial center stage. Neurotherapeutics 12: 807–815.

Ibeas Bih C, Chen T, Nunn AV, Bazelot M, Dallas M, Whalley BJ (2015). Molecular targets of cannabidiol in neurological disorders. Neurotherapeutics 12: 699–730.

Izzo AA, Borrelli F, Capasso R, Di Marzo V, Mechoulam R (2009). Non-psychotropic plant cannabinoids: new therapeutic opportunities from an ancient herb. Trends Pharmacol Sci 30: 515–527.

Jurkus R, Day HL, Guimarães FS, Lee JL, Bertoglio LJ, Stevenson CW (2016). Cannabidiol regulation of learned fear: implications for treating anxiety-related disorders. Front Pharmacol 7: 454.

Karniol IG, Carlini EA (1973). Pharmacological interaction between cannabidiol and delta-9-tetrahydrocannabinol. Psychopharmacologia 33: 53–70.

Katsidoni V, Anagnostou I, Panagis G (2013). Cannabidiol inhibits the reward-facilitating effect of morphine: involvement of 5-HT1A receptors in the dorsal raphe nucleus. Addict Biol 18: 286–296.

Kindt M (2014). A behavioural neuroscience perspective on the aetiology and treatment of anxiety disorders. Behav Res Ther 62: 24–36.

Lee JL (2009). Reconsolidation: maintaining memory relevance. Trends Neurosci 32: 413–420.

Lemos JI, Resstel LB, Guimarães FS (2010). Involvement of the prelimbic prefrontal cortex on cannabidiol-induced attenuation of contextual conditioned fear in rats. Behav Brain Res 207: 105–111.

Levin R, Almeida V, Peres FF, Calzavara MB, da Silva ND, Suiama MA *et al.* (2012). Antipsychotic profile of cannabidiol and rimonabant in an animal model of emotional context processing in schizophrenia. Curr Pharm Des 18: 4960–4965.

Leweke FM, Piomelli D, Pahlisch F, Muhl D, Gerth CW, Hoyer C *et al.* (2012). Cannabidiol enhances anandamide signaling and alleviates psychotic symptoms of schizophrenia. Transl Psychiatry 2: e94.

Long LE, Chesworth R, Huang XF, McGregor IS, Arnold JC, Karl T (2010). A behavioural comparison of acute and chronic delta9-tetrahydrocannabinol and cannabidiol in C57BL/6JArc mice. Int J Neuropsychopharmacol 13: 861–876.

Long LE, Chesworth R, Huang XF, Wong A, Spiro A, McGregor IS *et al.* (2012). Distinct neurobehavioural effects of cannabidiol in transmembrane domain neuregulin 1 mutant mice. PLoS One 7: e34129.

Mahmud A, Gallant S, Sedki F, D'Cunha T, Shalev U (2016). Effects of an acute cannabidiol treatment on cocaine self-administration and cue-induced cocaine seeking in male rats. J Psychopharmacol. doi:10.1177/0269881116667706.

Malone DT, Jongejan D, Taylor DA (2009). Cannabidiol reverses the reduction in social interaction produced by low dose delta(9)-tetrahydrocannabinol in rats. Pharmacol Biochem Behav 93: 91–96.

Marinho AL, Vila-Verde C, Fogaça MV, Guimarães FS (2015). Effects of intra-infralimbic prefrontal cortex injections of cannabidiol in the modulation of emotional behaviors in rats: contribution of 5HT A receptors and stressful experiences. Behav Brain Res 286: 49–56.

McNaughton N, Corr PJ (2004). A two-dimensional neuropsychology of defense: fear/anxiety and defensive distance. Neurosci Biobehav Rev 28: 285–305.

McPartland JM, Duncan M, DI Marzo V, Pertwee RG (2015). Are cannabidiol and Δ(9) -tetrahydrocannabivarin negative modulators of the endocannabinoid system? A systematic review. Br J Pharmacol 172: 737–753.

Mechoulam R, Shvo Y (1963). 1. Structure of cannabidiol. Tetrahedron 19: 2073–2078.

Moreira FA, Aguiar DC, Guimarães FS (2006). Anxiolytic-like effect of cannabidiol in the rat Vogel conflict test. Prog Neuropsychopharmacol Biol Psychiatry 30: 1466–1471.

Morgan CJ, Das RK, Joye A, Curran HV, Kamboj SK (2013). Cannabidiol reduces cigarette consumption in tobacco smokers: preliminary findings. Addict Behav 38: 2433–2436.

Musty RE, Conti LH, Mechoulam R (1985). Anxiolytic properties of cannabidiol. In: Harvey D (ed). Marihuana '84. IRL Press: Oxford, pp. 713–719.

Nardo M, Casarotto PC, Gomes FV, Guimarães FS (2014). Cannabidiol reverses the mCPP-induced increase in marble-burying behavior. Fundam Clin Pharmacol 28: 544–550.

Norris C, Loureiro M, Kramar C, Zunder J, Renard J, Rushlow W *et al.* (2016). Cannabidiol modulates fear memory formation

through interactions with serotonergic transmission in the mesolimbic system. Neuropsychopharmacology 41: 2839–2850.

O'Brien LD, Wills KL, Segsworth B, Dashney B, Rock EM, Limebeer CL *et al.* (2013). Effect of chronic exposure to rimonabant and phytocannabinoids on anxiety-like behavior and saccharin palatability. Pharmacol Biochem Behav 103: 597–602.

Onaivi ES, Green MR, Martin BR (1990). Pharmacological characterization of cannabinoids in the elevated plus maze. J Pharmacol Exp Ther 253: 1002–1009.

Parker LA, Burton P, Sorge RE, Yakiwchuk C, Mechoulam R (2004). Effect of low doses of delta9-tetrahydrocannabinol and cannabidiol on the extinction of cocaine-induced and amphetamine-induced conditioned place preference learning in rats. Psychopharmacology (Berl) 175: 360–366.

Pellow S, Chopin P, File SE, Briley M (1985). Validation of open: closed arm entries in an elevated plus-maze as a measure of anxiety in the rat. J Neurosci Methods 14: 149–167.

Peters J, Kalivas PW, Quirk GJ (2009). Extinction circuits for fear and addiction overlap in prefrontal cortex. Learn Mem 16: 279–288.

Prud'homme M, Cata R, Jutras-Aswad D (2015). Cannabidiol as an intervention for addictive behaviors: a systematic review of the evidence. Subst Abuse 9: 33–38.

Ren Y, Whittard J, Higuera-Matas A, Morris CV, Hurd YL (2009). Cannabidiol, a nonpsychotropic component of cannabis, inhibits cue-induced heroin seeking and normalizes discrete mesolimbic neuronal disturbances. J Neurosci 29: 14764–14769.

Renard J, Loureiro M, Rosen LG, Zunder J, de Oliveira C, Schmid S *et al.* (2016). Cannabidiol counteracts amphetamine-induced neuronal and behavioral sensitization of the mesolimbic dopamine pathway through a novel mTOR/p70S6 kinase signaling pathway. J Neurosci 36: 5160–5169.

Resstel LB, Joca SR, Moreira FA, Corrêa FM, Guimarães FS (2006). Effects of cannabidiol and diazepam on behavioral and cardiovascular responses induced by contextual conditioned fear in rats. Behav Brain Res 172: 294–298.

Resstel LB, Tavares RF, Lisboa SF, Joca SR, Corrêa FM, Guimarães FS (2009). 5-HT1A receptors are involved in the cannabidiol-induced attenuation of behavioural and cardiovascular responses to acute restraint stress in rats. Br J Pharmacol 156: 181–188.

Russo E, Guy GW (2006). A tale of two cannabinoids: the therapeutic rationale for combining tetrahydrocannabinol and cannabidiol. Med Hypotheses 66: 234–246.

Sakurai S, Yu L, Tan SE (2007). Roles of hippocampal N-methyl-D-aspartate receptors and calcium/calmodulin-dependent protein kinase II in amphetamine-produced conditioned place preference in rats. Behav Pharmacol 18: 497–506.

Schiavon AP, Bonato JM, Milani H, Guimarães FS, Weffort de Oliveira RM (2016). Influence of single and repeated cannabidiol administration on emotional behavior and markers of cell proliferation and neurogenesis in non-stressed mice. Prog Neuropsychopharmacol Biol Psychiatry 64: 27–34.

Shannon S, Opila-Lehman J (2016). Effectiveness of cannabidiol oil for pediatric anxiety and insomnia as part of posttraumatic stress disorder: a case report. Perm J 20: 108–111.

Silveira Filho NG, Tufik S (1981). Comparative effects between cannabidiol and diazepam on neophobia, food intake and conflict behavior. Res Comm Psychol Psychiatr Behav 6: 25–66.

Singewald N, Schmuckermair C, Whittle N, Holmes A, Ressler KJ (2015). Pharmacology of cognitive enhancers for exposure-based therapy of fear, anxiety and trauma-related disorders. Pharmacol Ther 149: 150–190.

Soares Vde P, Campos AC, Bortoli VC, Zangrossi H Jr, Guimarães FS, Zuardi AW (2010). Intra-dorsal periaqueductal gray administration of cannabidiol blocks panic-like response by activating 5-HT1A receptors. Behav Brain Res 213: 225–229.

Song C, Stevenson CW, Guimarães FS, Lee JL (2016). Bidirectional effects of cannabidiol on contextual fear memory extinction. Front Pharmacol 7: 493.

Southan C, Sharman JL, Benson HE, Faccenda E, Pawson AJ, Alexander SP *et al.* (2016). The IUPHAR/BPS Guide to PHARMACOLOGY in 2016: towards curated quantitative interactions between 1300 protein targets and 6000 ligands. Nucl Acids Res 44: D1054–D1068.

Steketee JD, Kalivas PW (2011). Drug wanting: behavioral sensitization and relapse to drug-seeking behavior. Pharmacol Rev 63: 348–365.

Stern CA, Gazarini L, Takahashi RN, Guimarães FS, Bertoglio LJ (2012). On disruption of fear memory by reconsolidation blockade: evidence from cannabidiol treatment. Neuropsychopharmacology 37: 2132–2142.

Stern CA, Gazarini L, Vanvossen AC, Zuardi AW, Guimaraes FS, Takahashi RN *et al.* (2014). Involvement of the prelimbic cortex in the disruptive effect of cannabidiol on fear memory reconsolidation. Eur Neuropsychopharmacol 24: S322.

Stern CA, Gazarini L, Vanvossen AC, Zuardi AW, Galve-Roperh I, Guimaraes FS *et al.* (2015). Δ9-Tetrahydrocannabinol alone and combined with cannabidiol mitigate fear memory through reconsolidation disruption. Eur Neuropsychopharmacol 25: 958–965.

Tipps ME, Raybuck JD, Lattal KM (2014). Substance abuse, memory, and post-traumatic stress disorder. Neurobiol Learn Mem 112: 87–100.

Todd SM, Arnold JC (2016). Neural correlates of interactions between cannabidiol and Δ(9)-tetrahydrocannabinol in mice: implications for medical cannabis. Br J Pharmacol 173: 53–65.

Tovote P, Fadok JP, Lüthi A (2015). Neuronal circuits for fear and anxiety. Nat Rev Neurosci 16: 317–331.

Treit D, Menard J, Royan C (1993). Anxiogenic stimuli in the elevated plus-maze. Pharmacol Biochem Behav 44: 463–469.

Tronson NC, Taylor JR (2013). Addiction: a drug-induced disorder of memory reconsolidation. Curr Opin Neurobiol 23: 573–580.

Twardowschy A, Castiblanco-Urbina MA, Uribe-Mariño A, Biagioni AF, Salgado-Rohner CJ, Crippa JA *et al.* (2013). The role of 5-HT1A receptors in the anti-aversive effects of cannabidiol on panic attack-like behaviors evoked in the presence of the wild snake *Epicrates cenchria crassus* (Reptilia, Boidae). J Psychopharmacol 27: 1149–1159.

Uribe-Mariño A, Francisco A, Castiblanco-Urbina MA, Twardowschy A, Salgado-Rohner CJ, Crippa JA *et al.* (2012). Anti-aversive effects of cannabidiol on innate fear-induced behaviors evoked by an ethological model of panic attacks based on a prey vs the wild snake *Epicrates cenchria crassus* confrontation paradigm. Neuropsychopharmacology 37: 412–421.

Valjent E, Corbille AG, Bertran-Gonzalez J, Herve D, Girault JA (2006). Inhibition of ERK pathway or protein synthesis during reexposure to drugs of abuse erases previously learned place preference. Proc Natl Acad Sci U S A 103: 2932–2937.

Vann RE, Gamage TF, Warner JA, Marshall EM, Taylor NL, Martin BR *et al.* (2008). Divergent effects of cannabidiol on the discriminative stimulus and place conditioning effects of delta(9)-tetrahydrocannabinol. Drug Alcohol Depend 94: 191–198.

Wang XY, Zhao M, Ghitza UE, Li YQ, Lu L (2008). Stress impairs reconsolidation of drug memory via glucocorticoid receptors in the basolateral amygdala. J Neurosci 28: 5602–5610.

Weber M, Hart J, Richardson R (2007). Effects of D-cycloserine on extinction of learned fear to an olfactory cue. Neurobiol Learn Mem 87: 476–482.

Zuardi AW, Cosme RA, Graeff FG, Guimarães FS (1993). Effects of ipsapirone and cannabidiol on human experimental anxiety. J Psychopharmacol 7 (1 Suppl): 82–88.

Zuardi AW, Karniol IG (1983). Changes in the conditioned emotional response of rats induced by 9-THC, CBD and mixture of the two cannabinoids. Arq Biol Tecnol 26: 391–397.

Zuardi AW, Shirakawa I, Finkelfarb E, Karniol IG (1982). Action of cannabidiol on the anxiety and other effects produced by delta 9-THC in normal subjects. Psychopharmacology (Berl) 76: 245–250.

is inability of the mutant chain to participate in trimer assembly, leading to a 50% reduction in collagen X. We suggest that the mechanism of growth plate abnormalities in Schmid MCD is similar to that in the mice. The transgenic mice described here will, therefore, not only provide insights into collagen X regulation and function during EO, but can also serve as models for chondrodysplasias with spondylometaphyseal involvement. □

Received 15 April; accepted 17 June 1993.

1. Ham, A. W. *Histology* 5th edn 384–457 (Lippincott, Philadelphia, 1965).
2. Caplan, A. I. & Pechak, D. G. *Bone Min. Res.* **5,** 117–183 (1987).
3. Jacenko, O., Olsen, B. R. & LuValle, P. *Crit. Rev. Eukaryotic Gene Exp.* **1,** 327–353 (1991).
4. McKusick, V. A., Francomano, C. A. & Antonarakis, S. E. (eds) *Mendelian Inheritance in Man. Catalogs of Autosomal Dominant, Autosomal Recessive, and X-linked Phenotypes* For examples, see Vol. 1, entry numbers 156500, 156400, 184250, 184253, and Vol. 2, entry numbers 250250, 260400, 271660 (The Johns Hopkins University Press, Baltimore, London, 1992).
5. Schmid, T. M., Popp, R. G. & Linsenmayer, T. F. *Ann. N.Y. Acad. Sci.* **580,** 64–73 (1990).
6. Gibson, G. J. & Flint, M. H. *J. Cell Biol.* **101,** 277–284 (1985).
7. Brass, A., Kadler, K., Thomas, J. T., Grant, M. E. & Boot-Handford, R. P. *FEBS Lett.* **303,** 126–128 (1992).
8. Apte, S. S., Seldin, M. F., Hayashi, M. & Olsen, B. R. *Eur. J. Biochem.* **206,** 217–224 (1992).
9. LuValle, P., Ninomiya, Y., Rosenblum, N. D. & Olsen, B. R. *J. biol. Chem.* **263,** 18378–18385 (1988).
10. LuValle, P., Iwamoto, M., Fanning, P., Pacifici, M. & Olsen, B. R. *J. Cell Biol.* **121,** 1173–1179.
11. Grigoriadis, A., Heersche, J. M. & Aubin, J. E. *Devl Biol.* **142,** 313–318 (1990).
12. Summers, T. A., Irwin, M. H., Mayne, R. & Balian, G. *J. biol. Chem.* **263,** 581–587 (1988).
13. Iyama, K.-I. *et al. Anat. Rec.* **229,** 462–472 (1991).
14. Kwan, A. P. L., Cummings, C. E., Chapman, J. A. & Grant, M. E. *J. Cell Biol.* **114,** 597–604 (1991).
15. Sawada, H., Konomi, H. & Hirosawa, K. *Eur. J. Cell Biol.* **110,** 219–227 (1990).
16. Warman, M. L. *et al. Nature Genet.* (in the press).
17. Ninomiya, Y. *et al.* in *Extracellular Matrix Genes* (eds Sandell, L. J. & Boyd, C. D.) 79–113 (Academic, New York, 1990).
18. Luckow, B. & Schütz, G. *Nucleic Acids Res.* **15,** 5490 (1987).
19. Lair, P. W. *et al. Nucleic Acids Res.* **19,** 4293 (1991).

ACKNOWLEDGEMENTS. We thank G. Balian (University of Virginia, School of Medicine) for the 6F6 and 1A6 monoclonal antibodies and advice, B. Burke (Harvard Medical School) for the peroxidase-conjugated anti-mouse IgG, K. Solum for technical assistance including preparation of DNA from tail biopsies and M. Jakoulov for secretarial assistance. This research was supported by grants from the NIH to B.R., O.J. and P.A.L. and from the Arthritis Foundation to O.J. and P.A.L. The microinjection was by DNX, Inc. under a contract from the NIH.

Molecular characterization of a peripheral receptor for cannabinoids

Sean Munro, Kerrie L. Thomas & Muna Abu-Shaar

MRC Laboratory of Molecular Biology, Hills Road, Cambridge CB2 2QH, UK

THE major active ingredient of marijuana, Δ^9-tetrahydrocannabinol (Δ^9-THC), has been used as a psychoactive agent for thousands of years. Marijuana, and Δ^9-THC, also exert a wide range of other effects including analgesia, anti-inflammation, immunosuppression, anticonvulsion, alleviation of intraocular pressure in glaucoma, and attenuation of vomiting[1]. The clinical application of cannabinoids has, however, been limited by their psychoactive effects, and this has led to interest in the biochemical bases of their action. Progress stemmed initially from the synthesis of potent derivatives of Δ^9-THC[4,5], and more recently from the cloning of a gene encoding a G-protein-coupled receptor for cannabinoids[6]. This receptor is expressed in the brain but not in the periphery, except for a low level in testes. It has been proposed that the non-psychoactive effects of cannabinoids are either mediated centrally or through direct interaction with other, non-receptor proteins[1,7,8]. Here we report the cloning of a receptor for cannabinoids that is not expressed in the brain but rather in macrophages in the marginal zone of spleen.

To identify novel G-protein-coupled receptors expressed in myeloid cells, polymerase chain reaction (PCR) using degenerate primers was done on complementary DNA prepared from the human promyelocytic leukaemic line HL60. Treatment of HL60 cells with dimethylformamide (DMF) induces granulocyte differentiation, whereas tetradecanoylphorbol acetate (TPA) induces macrophage differentiation[9]. Amplification products from DMF-treated cells were cloned and sequenced, and six classes of clone showed homology to the G-protein-coupled receptor family. Two of these classes corresponded to previously identified receptors; the interleukin-8 receptor-B (ref. 10) and the adenosine A3 receptor[11] (S.M., manuscript in preparation). Of the remaining four sequences, only one showed particular homology to a published receptor. This clone, CX5, was related to a cannabinoid receptor cloned originally from rat brain[6]. To investigate the functional significance of this homology, the CX5 insert was used to screen an HL60 cDNA library. Two cDNA clones were obtained, hCX5.1 and hCX5.36, the latter extending the furthest 5′ and the complete nucleotide sequence of this clone is shown in Fig. 1*a*. The protein encoded by hCX5.36 shows 44% identity with the human cannabinoid receptor and the degree of identity rises to 68% for those transmembrane residues proposed to confer ligand specificity[12].

To determine if the CX5 receptor binds cannabinoids, the hCX5.36 cDNA was inserted into an expression vector and transfected into tissue culture cells. Figure 2*a* shows a binding curve of the cannabinoid receptor ligand Win 55212-2 (ref. 13) to membranes prepared from the transfected cells. The control cells do not express receptors for cannabinoids, but expression of hCX5.36 causes the appearance of a saturable number of high-affinity binding sites for WIN 5512-2 and also for a second high-affinity cannabinoid CP55,940 (ref. 5; Fig. 2*b*, and data not shown). The affinities of the receptor for these structurally unrelated ligands (Win 55212-2: dissociation constant K_d 3.7 nM (+/−0.4 nM); CP55,940: K_d 1.6 nM (+/−0.5 nM)), are comparable to the analogous figures (24 nM and 2–15 nM) reported for the brain receptor[13–15]. Furthermore, competition binding analysis showed that the CX5 receptor can distinguish between closely related derivatives of the archetypal cannabinoid Δ^9-THC, showing a lower affinity for the relatively inactive cannabidiol, than for the biologically active Δ^9-THC, cannabinol and 11-OH-Δ^9-THC (Fig. 2*b*). Thus it appears that hCX5.36 encodes a selective, high-affinity receptor for cannabinoids. Note that although cannabinol is only weakly cannabimimetic and binds the brain receptor with an affinity about 10-fold less than that of Δ^9-THC[5,14], this ligand binds to the CX5 receptor with an affinity comparable to that of Δ^9-THC (250 nM versus 320 nM, Fig. 2*b*). This suggests that cannabinol may have a preference for the CX5 receptor over the brain receptor. Recently, a novel compound isolated from brain, arachidonylethanolamide (anandamide), has been identified as a candidate ligand for the brain receptor[16] and Fig. 2*b* shows that this compound can also bind to the CX5 receptor. The binding affinity (K_i 1.6 μM (+/−0.4)) is lower than that reported for brain membranes (K_i 52 nM), but it should be noted that the apparent receptor affinities of cannabinoids can vary depending on the assay system used[5,14,15]. In the following text we shall refer to the original receptor as CB-R and this new receptor as CX5.

When CX5 was used to probe northern blots of RNA from HL60 cells it hybridized to two transcripts of about 2.5 and 5.0 kilobases (kb) (Fig. 3*a*). The two transcripts probably arise from the use of alternative poly(A)$^+$ addition sites. Clone hCX5.1 does not have a poly(A)$^+$ tail at the position of that in hCX5.36, but instead extends further in the 3′ direction (Fig. 1*a*). The putative polyadenylation sequence of hCX5.36 (GAUAAA) is a variant of the AAUAAA consensus that is found in a small fraction of messages and which can be used, albeit inefficiently, *in vitro*[17]. CX5 is expressed in uninduced HL60 cells, but transcript levels are elevated further on myeloid, or granulocyte, differentiation, although the gene does not appear to be expressed in mature neutrophils isolated from blood (data not shown).

To investigate the tissue distribution of CX5, a portion of a rat homologue was isolated by PCR. This rat probe (rCX5) detects an mRNA of about 2.5 kb in spleen, but not in a variety

FIG. 1 Nucleotide and protein sequences of the cDNAs hCX5.36 and hCX5.1. *a*, Nucleotide sequence of the hCX5.36 cDNA and the protein sequence encoded by the longest open ready frame, the in-frame stop codon upstream of the most 5′ ATG is underlined. Also shown is the nucleotide sequence of hCX5.1 where it diverges from that of hCX5.36 after the putative poly(A) addition site (underlined). *b*, Comparison of the protein encoded by hCX5.36 with the previously reported human cannabinoid receptor[28]. Identities are boxed and the seven putative transmembrane segments are underlined.

METHODS. Oligo-dT primed cDNA was synthesized from poly(A)$^+$ RNA prepared from HL60 cells induced with 0.5% DMF for 3 days. cDNA (5 ng in 20 μl) was amplified with *Taq* polymerase using degenerate primers encoding regions conserved between many G-protein-coupled receptors. Those that produced CX5 were GAGGGCCCATYISNNTNGAYMGNTA and TGAAGCTTSHRTANANSANNGGRTT (encoded regions in bold in sequence alignment). 40 cycles of 94 °C, 1 min, 50 °C, 2 min and 72 °C 2 min, in 10 mM Tris–HC1 pH 8.3, 3 mM $MgCl_2$, 100 mM tetramethylammonium chloride, 0.05% Tween 20, 0.05% NP–40, 250 μM dNTPs, 20 μM each primer. Gel-purified amplification products were digested with *Apa*I and *Hind*III and cloned into Bluescript. After classification of the products by sequencing, the insert from clone CX5 was used to screen 2×10^5 colonies of a cDNA library from TPA-treated HL60 cells[29] (from D. Simmons). Both hCX5.1 and hCX5.36 were isolated several times and after restriction mapping and partial sequencing of both clones, the complete nucleotide sequence of hCX5.36 was determined by primer walking using double-stranded dideoxy-sequencing. The GenBank accession number for hCX5.36 (CB2) is X74328.

a

HCX5.36

```
CAGGTCCTGGGAGAGGACAGAAAACAACTGGACTCCTCAGCCCCCGGCAGCTCCCAGTGCCCAGCCACCCACAACACAACCCAAAGCCTT   90

                                                    MetGluGluCysTrpValThrGluIleAlaAsnGlySerLysAspGlyLeuAsp
CTAGACAAGCTCAGTGGAATCTGAAGGGCCCACCCCATGGAGGAATGCTGGGTGACAGAGATAGCCAATGGCTCCAAGGATGGCTTGGAT  180

SerAsnProMetLysAspTyrMetIleLeuSerGlyProGlnLysThrAlaValAlaValLeuCysThrLeuLeuGlyLeuLeuSerAla
TCCAACCCTATGAAGGATTACATGATCCTGAGTGGTCCCCAGAAGACAGCTGTTGCTGTGTTGTGCACTCTTCTGGGCCTGCTAAGTGCC  270

LeuGluAsnValAlaValLeuTyrLeuIleLeuSerSerHisGlnLeuArgArgLysProSerTyrLeuPheIleGlySerLeuAlaGly
CTGGAGAACGTGGCTGTGCTCTATCTGATCCTGTCCTCCCACCAACTCCGCCGGAAGCCCTCATACCTGTTCATTGGCAGCTTGGCTGGG  360

AlaAspPheLeuAlaSerValValPheAlaCysSerPheValAsnPheHisValPheHisGlyValAspSerLysAlaValPheLeuLeu
GCTGACTTCCTGGCCAGTGTGGTCTTTGCATGCAGCTTTGTGAATTTCCATGTTTTCCATGGTGTGGATTCCAAGGCTGTCTTCCTGCTG  450

LysIleGlySerValThrMetThrPheThrAlaSerValGlySerLeuLeuLeuThrAlaIleAspArgTyrLeuCysLeuArgTyrPro
AAGATTGGCAGCGTGACTATGACCTTCACAGCCTCTGTGGGTAGCCTCCTGCTGACCGCCATTGACCGATACCTCTGCCTGCGCTATCCA  540

ProSerTyrLysAlaLeuLeuThrArgGlyArgGlyLeuValThrLeuGlyIleMetTrpValLeuSerAlaLeuValSerTyrLeuPro
CCTTCCTACAAAGCTCTGCTCACCCGTGGAAGGGGACTGGTGACCCTGGGCATCATGTGGGTCCTCTCAGCACTAGTCTCCTACCTGCCC  630

LeuMetGlyTrpThrCysCysProArgProCysSerGluLeuProLeuIleProAsnAspTyrLeuLeuSerTrpLeuLeuPheIle
CTCATGGGATGGACTTGCTGTCCCAGGCCCTGCTCTGAGCTTTTCCCACTGATCCCCAATGACTACCTGCTGAGCTGGCTCCTGTTCATC  720

AlaPheLeuPheSerGlyIleIleTyrThrTyrGlyHisValLeuTrpLysAlaHisGlnHisValAlaSerLeuSerGlyHisGlnAsp
GCCTTCCTCTTTTCCGGAATCATCTACACCTATGGGCATGTTCTCTGGAAGGCCCATCAGCATGTGGCCAGCTTGTCTGGCCACCAGGAC  810

ArgGlnValProGlyMetAlaArgMetArgLeuAspValArgLeuAlaLysThrLeuGlyLeuValLeuAlaValLeuLeuIleCysTrp
AGGCAGGTGCCAGGAATGGCCCGAATGAGGCTGGATGTGAGGTTGGCCAAGACCCTAGGGCTAGTGTTGGCTGTGCTCCTCATCTGTTGG  900

ProProValLeuAlaLeuMetAlaHisSerLeuAlaThrThrLeuSerAspGlnValLysLysAlaPheAlaPheCysSerMetLeuCys
TTCCCAGTGCTGGCCCTCATGGCCCACAGCCTGGCCACTACGCTCAGTGACCAGGTCAAGAAGGCCTTTGCTTTCTGCTCCATGCTGTGC  990

LeuIleAsnSerMetValAsnProValIleTyrAlaLeuArgSerGlyGluIleArgSerSerAlaHisHisCysLeuAlaHisTrpLys
CTCATCAACTCCATGGTCAACCCTGTCATCTATGCTCTACGGAGTGGAGAGATCCGCTCCTCTGCCCATCACTGCCTGGCTCACTGGAAG 1080

LysCysValArgGlyLeuGlySerGluAlaLysGluGluAlaProArgSerSerValThrGluThrGluAlaAspGlyLysIleThrPro
AAGTGTGTGAGGGGCCTTGGGTCAGAGGCAAAAGAAGAAGCCCCGAGATCCTCAGTCACCGAGACAGAGGCTGATGGGAAAATCACTCCG 1170

TrpProAspSerArgAspLeuAspLeuSerAspCys***
TGGCCAGATTCCAGAGATCTAGACCTCTCTGATTGCTGATGAGGCCTCTTCCCAATTTAAACAACTCAAGTCAGAAATCAGTTCACTCCC 1260
TGGAAGAGAGAGAGGGGTCTTGGCACTCTCTTCTTACTTAAACCAGTCCCAGACACCTAGACACGGACCCCTTTTTGCTGATGAGTGTTG 1350
GGACTGACTCCTGGAAGACAGCCTGGCCTTGCCCACCTGCACACAGTCTGTTGGATAGGTAGGGCCACGAGGAGTAGCCAGGTAGGCGAG 1440
ACACAAAAAGGCCTGGGACAGGGTCAGTACAAGTCAGGACAGGCTTCATGCCTGCATCCTCCAGAGACCACCAGGAGCCAAAGCGAGCCT 1530
CCAGGCCCAGCAATGAGGGACTTGGGAGAAATCTGAGAAGAATGGGTTGTTCTCTTGGGAAGTCAGGGTATCAGATGGGATGGACATCCA 1620
GGTCTTCTCTCTGCCTAATTGTCAAGGCCTCCTTGGCTCTGGAGCTATGAAAGGCCCCACTTTCAAGTCACCCTTGCCACTGAGGACCGA 1710
GGACTATGCTATGATGAGGATTAAGGTGTTGACTTGCCTCTTTCAGAGATAAATGACAAGCCTTCAAAAAAAAAAAAAAA            1790
```

HCX5.1:

```
....TATGCTATGATGAGGATTAAGGTGTTGACTTGCCTCTTTCAGAGATAAATGACAAGCCTTCAGTTTGGGGCATCCTGTTGTTTG.
```

b

of other tissues (Fig. 3*b*). In particular, the rCX5 transcript is not detected in brain, even though the 6 kb mRNA encoding the rat CB-R can be readily detected in the same sample. The expression pattern of the CB-R gene corresponds well to the distribution of binding sites for cannabinoids in the brain[6,18]. But it is possible that CX5 is expressed in a subset of these sites and its expression level is too low to be detected in total brain RNA. To investigate this possibility horizontal sections of rat brain were probed by *in situ* hybridization with labelled oligonucleotides corresponding to rat CB-R and to rCX5 (Fig. 4). As previously reported, the brain receptor has a widespread distribution with high levels of expression in the cortex, hippocampus, striatum and cerebellum. When adjacent sections were probed for rCX5, no expression could be detected in these, or any other, regions. The rCX5 oligonucleotide does, however, hybridize to localized regions of the spleen (Fig. 4*b*, *c*). The expression appears concentrated in the marginal zones found around the periarteriolar lymphoid sheaths. The expression of hCX5 in HL60 cells differentiated along the myeloid lineage implies that this expression is likely to be in macrophages. To confirm this, splenic macrophages/monocytes were purified using cell sorting

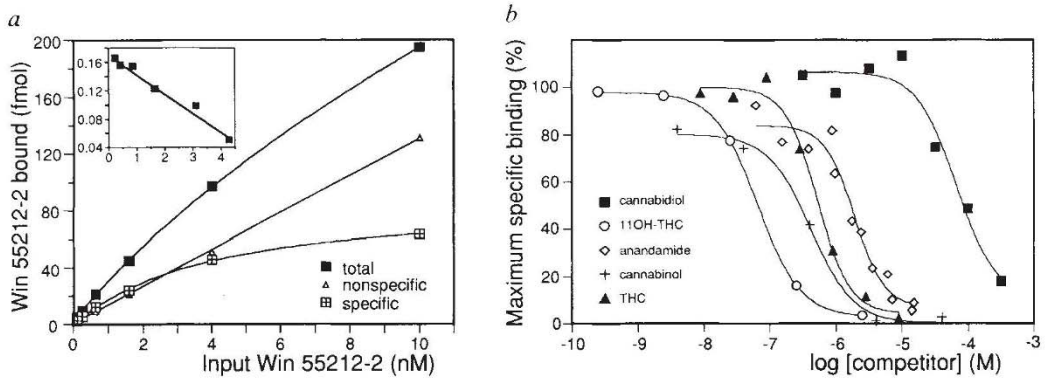

FIG. 2 Binding of cannabinoids to the receptor encoded by hCX5.36. *a*, Binding of [^{3}H]Win 55212-2 to membranes from COS cells transfected with an expression plasmid SC36, that contains the hCX5.36 cDNA. The inset plot show the specific binding presented as bound/free against [bound] ($Mx10^{-10}$). *b*, Displacement by cold cannabinoids of [^{3}H]CP55,940, or of [^{3}H]Win 55212-2, bound to membranes from COS cells transfected with SC36.

METHODS. Plasmid SC36 is hCX5.36 inserted into the vector CDM8[30]. 72 h after transfection, cells were Dounce homogenized and the membranes pelleted from the post-nuclear supernatant at 90,000g for 20 min, washed and then resuspended in 50 mM Tris–HC1 pH 7.4, 3 mM $MgCl_2$, 1 mM EDTA and stored in liquid N_2. Binding of [^{3}H]Win 55212-2 (49.6 Ci $mmol^{-1}$; New England Nuclear) to membranes (40 μg membrane protein per 150 μl reaction), was determined essentially as described, except that siliconized 1.5 ml polypropylene tubes were used for the binding reactions and 5% ethanol, 5% Triton X-100 was used to solubilize the membrane pellets[5]. Nonspecific binding was measured in the presence of 10 μM Δ^9-THC, and data points shown are means of duplicates (average duplicate's difference 4.3%). Displacement by cold cannabinoids (Sigma) was determined using 1.0 nM [^{3}H]CP55,940 (107 Ci mol^{-1}; New England Nuclear), or for anandamide (provided by R. Mechoulam) and cannabidiol, 1.0 nM [^{3}H]Win55212-2, although similar results were obtained for all competitors with both hot ligands (not shown). The anandamide displacement curve comprises data from two separate experiments. All data points are means of duplicates and all experiments were repeated at least twice. Inhibition constants (K_i) in nM: 11-OH-Δ^9-THC, 40 +/− 1.5; Δ^9-THC, 320 +/− 80; cannabinol, 250 +/− 80; cannabidol, 38,000 +/−18,000.

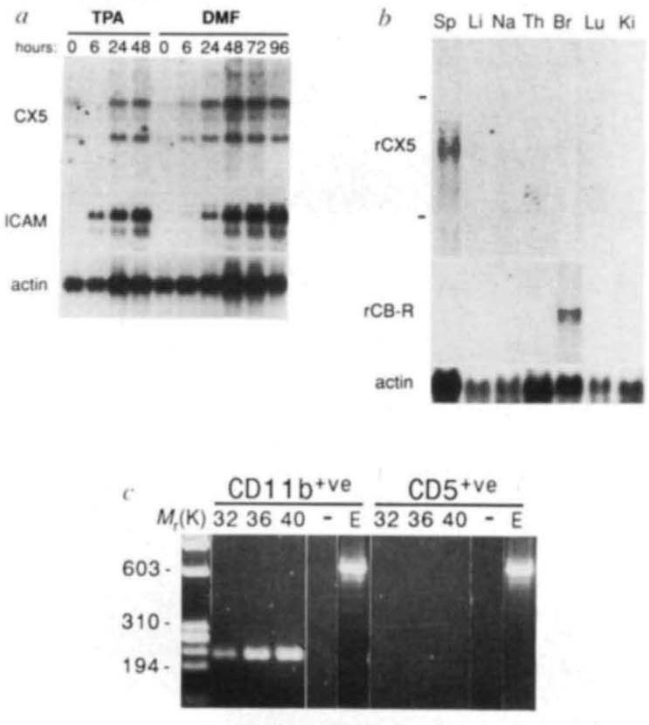

FIG. 3 Expression of CX5 transcripts in HL60 cells and in rat tissues. *a*, Northern blots of RNA from HL60 cells induced with either 20 ng ml^{-1} TPA or with 0.7% DMF, probed with either hCX5, or with ICAM-1 to follow induction. The hCX5 blot was then reprobed for γ-actin. *b*, Northern blot of RNA from various rat tissues probed with a rat homologue of CX5 (SP, spleen; Li, liver; Na, nasal epithelium; Th, thymus; Br, brain; Lu, lung; Ki, kidney). The blot was then reprobed with the rat cannabinoid receptor (rCB-R) and then with actin. *c*, PCR analysis of rCX5 expression in sorted rat spleenocytes. cDNA from rat spleenocytes sorted using antibodies against CD11b for macrophages/monocytes, or CD5 for T-cells, was amplified with primers specific for rCX5, with products being removed after the indicated number of cycles (32,36,40). To demonstrate that the rCX5 signal derives from mRNA, cDNA reactions without added reverse transcriptase were amplified for 40 cycles (−) and, as a positive control, cDNAs were amplified with primers specific for elongation factor 1α (E).

METHODS. Total RNA was isolated from HL60 cells by lysis in guanidinium/LiCl, and 7.5 μg per sample was separated on a 1.2% agarose/4% formaldeyhde gel, transferred to nylon (Hybond-N, Amersham) and ultraviolet cross-linked. Parallel blots were probed at 42 °C in 5 × SSPE/50% formamide/100 μg/ml salmon sperm DNA/5x Denhards/0.1% SDS with either CX5 or ICAM-1[29] labelled with ^{32}P by random-priming (Pharmacia). After washing with 1 × SSC at 42 °C, the blot was exposed to Kodak XAR with an intensifying screen, ICAM, 8 days; hCX5, 10 days). The blots were then stripped according to the manufacturer's instructions and reprobed with human γ-actin, exposure 6 h. The fall in expression at the 6 h time point in TPA was reproducible. A rat homologue of CX5 was cloned from genomic DNA by PCR using primers. GGGCTCGAGGTNRAYTTYCAYGTNTT and GAGGGATCCATNSWRCARAANGCRAA that encode sequences in hCX5 which are also found in the cannabinoid receptor but not in other G-proten-coupled receptors (VNFHVF (91–96) and FAFCSM (279–284)). Cloning of PCR products of 600–650 bp produced primarily the rat cannabinoid receptor or a sequence with 88% homology to hCX5, which was termed rCX5 (S.M. unpublished observations). Total RNA extracted by guanidinium lysis from various rat tissues (5–10 μg per lane) was blotted and probed as before with rCX5, rat cannabinoid receptor and γ-actin and then exposed using a phospho-imager (Molecular Dynamics) for rCX5 (9 h), CB-R (4 h) or XAR film (12 h) for actin. For PCR analysis, rat spleenocytes were separated by FACS using MRC OX-42 (CD11b)[31] or MRC OX-19 (CD5)[32] (Serotec). Cytoplasmic RNA prepared from 3×10^5 cells by detergent lysis, (20 μg glycogen added as carrier) was treated with ribonuclease-free DNase (0.5 unit for 10 min; RQ1, Promega), phenol extracted, ethanol precipitated, resuspended in reverse transcriptase buffer with random primers, divided in two and MMLV reverse transcriptase was added to one set (GIBCO). After 60 min at 37 °C, PCR amplification was done with the primers TTTCACGGTGTGGACTCC and TAGGTAGGAGATCAAGCG (rCX5, 214 bp product) or GAAATGCACCATGAAGCT and TTACGATGCATTGTTATC (EF-1α, 645 bp product from spliced transcript[33]) using 94 °C, 1 min 54 °C, 1 min, 72°C 1 min with the manufacturer's buffer (Promega).

and the expression of CX5 examined using PCR. Expression was detected in the macrophage/monocyte population but not in the CD5-positive population used as a control.

The marginal zone is the site through which blood-borne cells and antigens enter the spleen, and the marginal zone macrophages comprise a distinct population of highly phagocytic cells thought to play a role in both digesting and processing bacterial antigens and in directing lymphocyte recirculation[19,21]. We are currently preparing antibodies specific for CX5 to investigate its cellular distribution in more detail, but the *in situ* distribution suggests that its expression is concentrated in these marginal zone macrophages. The *in vivo* function of CX5 is presumably to transduce a signal through a G-protein in response to an endogenous ligand, although we do not yet have direct evidence

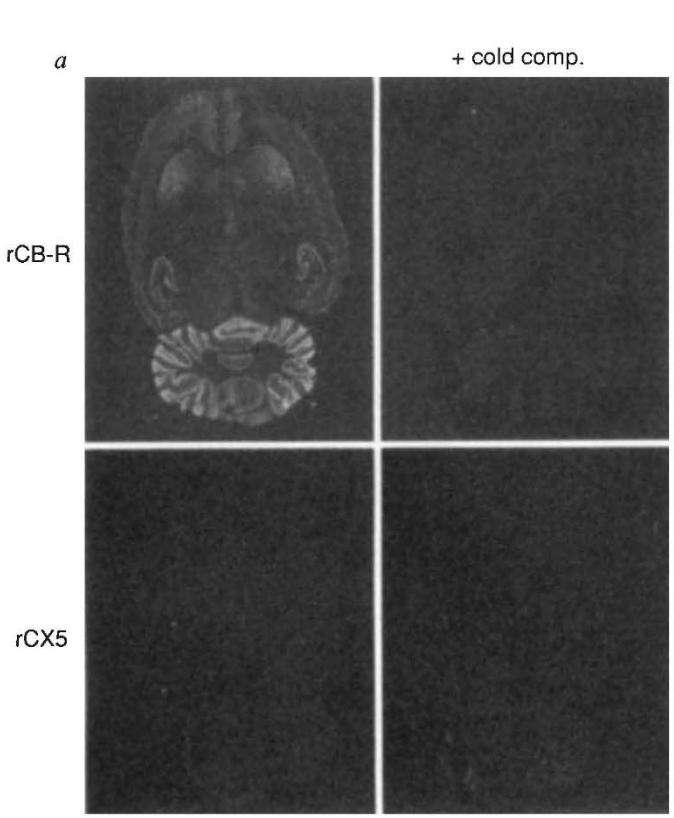

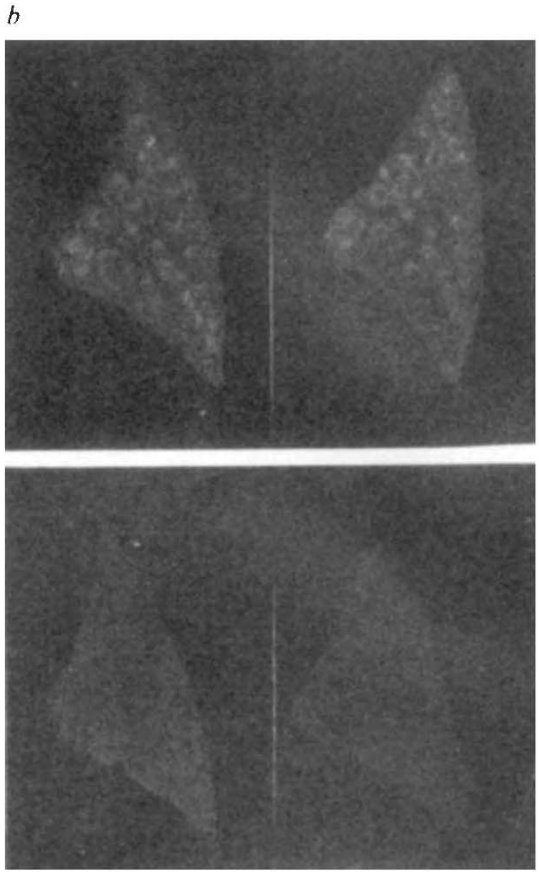

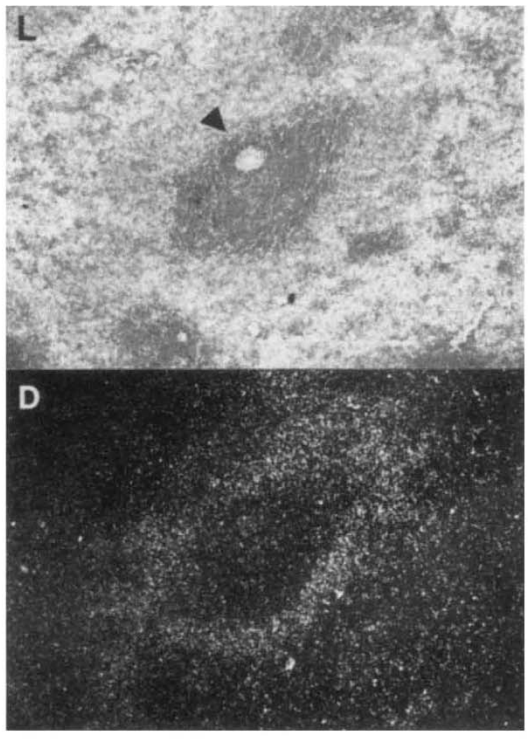

FIG. 4 *In situ* analysis of expression of CX5 in brain and spleen. *a*, Autoradiographs of *in situ* hybridizations with labelled oligonucleotides for rat CX5 and for the rat cannabinoid receptor (rCB-R) to horizontal sections of rat brain. Hybridizations were done on parallel sections in the absence or presence (+ cold comp.) of a excess of unlabelled oligonucleotide. *b*, Autoradiographs of *in situ* hybridization of CX5 to pairs of transverse sections of the spleen without cold competitor (top) or with (bottom). *c*, Hybridization of CX5 to the periphery of the white pulp in spleen, an arrow head marks the central arteriole. Darkfield (D) and haematoxylin/eosin staining in bright field (L).

METHODS. Oligonucleotides (45 bp long) were chosen from the antisense of the second cytoplasmic loop of CX5 (residues 132–147) or the equivalent region of the rat cannabinoid receptor, as this region is highly divergent between the two genes and between other G-protein-coupled receptors: GGTGACGAGAGCTTTGTAGGTAGGTGGGTAGCACAGACATAGGTA and GGTGACGATCCTCTTATAGGCCAGAGGCCTTGTAATGGATATGTA. The oligonucleotides were tailed with ^{35}S-dATP and used at 0.5 ng ml^{-1} to probe 15 μm sections as described previously[34]. If present, cold competitor was at 100-fold excess. Sections were exposed to Kodak XAR film for 7 days, and then to Ilford K5 emulsion for one month at 4 °C. The CB-R oligonucleotide gave no specific staining to spleen (not shown).

for such coupling. Analysis of other seven spanning receptors has suggested that basic, amphipathic helixes at either end of the third cytoplasmic loop are involved in G-protein coupling and appropriate residues are found in these positions both in the CX5 sequence and in the brain receptor, which has been shown to be G-protein coupled[6,22].

There are many reports of cannabinoids exerting suppressive effects on various cells of the immune system, including macrophages[23–25], although the significance of some of these observations has been questioned because of the high doses of drug used[26]. But the location of the CX5 receptor, and its distinct structure from the brain receptor, strongly suggest that the endogenous ligand for these receptors will have an immuno-modulatory role in addition to its neuronal function. Anandamide has been recently identified as a candidate ligand for the cannabinoid receptor[16] and this compound also binds to the CX5 receptor, although with an apparent affinity 30-fold less than that reported for the brain receptor. Anandamide is able to cross the blood brain barrier rapidly[27] but worthwhile speculation as to its function, and possible interactions between the neural and immunological systems, will require the identification of all the sources of this intriguing molecule. Furthermore, the question of further potential ligands from brain remains to the resolved[16]. Even so the existence of the CX5 receptor does have further implications. G-protein-coupled receptors are highly conserved throughout evolution[12], and yet the sequence of CX5 is considerably divergent from that of CB-R. Of the 162 residues in transmembrane sections of the human CB-R, three are different in rat CB-R, but 68 are different in human CX5. This suggests that the two receptors did not diverge recently and furthermore it suggests that it should be possible to identify receptor-specific cannabinoids. The fact that cannabinol appears to have a higher relative affinity for the CX5 receptor than for the brain receptor, may provide the basis for identifying such a ligand for the CX5 receptor. We suggest that in future the two receptors be distinguished by calling the brain receptor CB1 and the CX5 receptor CB2. It has been proposed that the peripheral effects of cannabinoids are either indirect effects of central actions, or reflect interactions with non-receptor proteins such as lipoxygenases[1,8]. It is clearly possible that some of these peripheral effects are in fact mediated through the CB2 receptor and it will be interesting to determine the activities of any cannabinoids specific for this receptor. □

Received 11 June; accepted 14 July 1993.

1. Dewey, W. L. *Pharmac. Rev.* **38,** 151–178 (1986).
2. Howlett, A. C. *et al. Trends Neurosci.* **13,** 420–432 (1990).
3. Hollister, L. E. *Pharmac. Rev.* **38,** 1–20 (1986).
4. Razdan, R. K. *Pharmac. Rev.* **38,** 75–149 (1986).
5. Devane, W. A., Dysarz, F. A., Johnson, M. R., Melvin, L. S. & Howlett, A. C. *Molec. Pharmacol.* **34,** 605–613 (1988).
6. Matsuda, L. A., Lolait, S. J., Brownstein, B. J., Young, A. C. & Bonner, T. I. *Nature* **356,** 561–564 (1990).
7. Martin, B. R. *Pharmac. Rev.* **38,** 45–74 (1986).
8. Reichman, M., Nen, W. & Hokin, L. E. *Molec. Pharmac.* **40,** 547–555 (1991).
9. Collins, S. J. *Blood* **70,** 1233–1244 (1987).
10. Lee, J. *et al. J. biol. Chem.* **267,** 16283–16287 (1992).
11. Zhou, Q. Y. *et al. Proc. natn. Acad. Sci. U.S.A.* **89,** 7432–7436 (1992).
12. Baldwin, J. M. *EMBO J.* **12,** 1693–1703 (1993).
13. Jansen, E. M., Haycock, D. A., Ward, S. J. & Seybold V. S. *Brain Res.* **575,** 93–102 (1992).
14. Devane, W. A. *et al. J. med. Chem.* **35,** 2065–2069 (1992).
15. Herkenham, M. *et al. Proc. natn. Acad. Sci. U.S.A.* **87,** 1932–1936 (1990).
16. Devane, W. A. *et al. Science* **258,** 1946–1949 (1992).
17. Sheets, M. D., Ogg, S. C. & Wickens, M. P. *Nucleic. Acids Res.* **18,** 5799–5805 (1990).
18. Mailleux, P. & Vanderhaeghen, J.-J. *Neuroscience* **48,** 655–668 (1992).
19. Kraal, G. *Int. Rev. Cytol.* **132,** 31–74 (1992).
20. Humphrey, J. H. & Grennan, D. *Eur. J. Immun.* **11,** 221–228 (1981).
21. Keshav, S., Chung, P., Milon, G. & Gordon, S. *J. exp. Med.* **174,** 1049–1058 (1991).
22. Conklin, B. R. & Bourne, H. R. *Cell* **73,** 631–641 (1993).
23. Munson, A. E. & Fehr, K. O. in *Adverse Health and Behavioral Consequences of Cannabis Use* (eds Fehr, K. O. & Kalant, H.) 257–353 (Addiction Research Foundation, Toronto, 1983).
24. Schatz, A. R., Kessler, F. K. & Kaminski, N. E. *Life Sci.* **51,** 25–30 (1992).
25. Lopez-Cepero, M., Friedman, M., Klein, T. & Friedman, H. *J. Leukocyte Biol.* **39,** 679–686 (1986).
26. Hollister, L. E. *J. Psychoactive Drugs* **24,** 159–164 (1992).
27. Fride, E. & Mechoulam, R. *Eur. J. Pharmac.* **231,** 313–314 (1993).
28. Gerard, C. M., Mollereau, C., Vassart, G. & Parmentier, M. *Biochem. J.* **279,** 129–134 (1991).
29. Simmons, D., Makgoba, M. W. & Seed, B. *Nature* **331,** 624–627 (1988).
30. Seed, B. *Nature* **329,** 840–842 (1987).
31. Robinson, A. P., White, T. M. & Mason, D. W. *Immunology* **57,** 239–247 (1986).
32. Dallman, M. J., Thomas, M. L. & Green, J. R. *Eur. J. Immun.* **12,** 511–518 (1982).
33. Shirasawa, T., Sakamoto, K., Akashi, T., Takahashi, H. & Kawashima, A. *Nucleic Acids Res.* **20,** 909 (1992).
34. Wisden, W., Morris, B. J. & Hunt, S. P. in *Molecular Neurobiology: a Practical Approach* (eds Chad, J. & Wheal, H.) 205–225 (IRL at Oxford Univ. Press, Oxford, 1991).

ACKNOWLEDGEMENTS. We thank J. Baldwin and T. Jackson for advice on receptors, D. Simmons for libraries and clones, N. Dear and A. Venkitaraman for RNA samples, R. Mechoulam and R. Pertwee for generously providing a sample of anandamide, D. Gilmore for cell sorting, J. Fogg and T. Smith for oligonucleotides, M. Bretscher, R. Chapman, H. Pelham and D. Zarkower for criticism of the manuscript and D. Cunningham and colleagues at the MRC Laboratory of Molecular Biology for help, guidance and support. K.L.T is funded by the Human Frontiers of Science Program.

Cloning and gene defects in microsomal triglyceride transfer protein associated with abetalipoproteinaemia

Daru Sharp*, Laura Blinderman*, Kelly A. Combs†, Bernadette Kienzle*, Beverly Ricci*, Karen Wager-Smith*, Cleris M. Gil†, Christoph W. Turck‡, Marie-Elizabeth Bouma§, Daniel J. Rader‖, Lawrence P. Aggerbeck¶, Richard E. Gregg*, David A. Gordon* & John R. Wetterau*#

* Department of Metabolic Diseases, Bristol-Myers Squibb, Princeton, New Jersey 08543-4000, USA
† Department of Pharmacology and Cell Biophysics, University of Cincinnati, Cincinnati, Ohio 45267, USA
‡ Howard Hughes Medical Institute, Department of Medicine, University of California, San Francisco, California 94143, USA
§ U327 Institut National de la Sante et de la Recherche Médicale, Faculté de Médicine Xavier Bichat, 75018 Paris, France
‖ Molecular Disease Branch, National Heart, Lung, and Blood Institute, National Institutes of Health, Bethesda, Maryland 20892, USA
¶ Centre de Génétique Moléculaire, Centre National de la Recherche Scientifique, 91198 Gif-sur-Yvette, France

THE microsomal triglyceride transfer protein (MTP), which catalyses the transport of triglyceride, cholesteryl ester and phospholipid between phospholipid surfaces, is a heterodimer composed of the multifunctional protein, protein disulphide isomerase, and a unique large subunit with an apparent M_r of 88K (refs 1–3). It is isolated as a soluble protein from the lumen of the microsomal fraction of liver and intestine[4]. The large subunit of MTP was not detectable in four unrelated subjects with abetalipoproteinaemia[5], a rare autosomal recessive disease characterized by a defect in the assembly or secretion of plasma lipoproteins that contain apolipoprotein B (ref. 6). We report here the isolation and sequencing of complementary DNA encoding the large subunit of MTP. A comparison of this sequence to corresponding genomic sequences from two abetalipoproteinaemic subjects revealed a homozygous frameshift mutation in one subject and a homozygous nonsense mutation in the other. The results indicate that a defect in the gene for the large subunit of MTP is the proximal cause of abetalipoproteinaemia in these two subjects, and that MTP is required for the secretion of plasma lipoproteins that contain apolipoprotein B.

Based on the sequence of 1 of 10 peptides isolated from the large subunit of MTP (Fig. 1), a 20-base, 32-fold degenerate oligonucleotide probe was designed and used to screen a λgt10, bovine small intestine cDNA library. Overlapping bovine clones

To whom correspondence should be addressed.

Tetrahedron, 1963, Vol. 19, pp. 2073 to 2078. Pergamon Press Ltd. Printed in Northern Ireland

HASHISH—I

THE STRUCTURE OF CANNABIDIOL[1]

R. MECHOULAM and Y. SHVO
Daniel Sieff Research Institute, The Weizmann Institute of Science,
Rehovoth, Israel

(*Received* 2 *May* 1963)

Abstract—Cannabidiol, one of the major components of hashish, has been shown to possess structure IIIa.

HASHISH (marihuana), the psychotomimetically active resin of the female flowering tops of *Cannabis sativa L.*, is one of the most widely used drugs in the illicit market of narcotics in many parts of the world. The chemistry of the constituents of hashish has been the subject of numerous publications since the beginning of this century.[2] Due mainly to the masterly investigations[2] of Cahn, Adams and Todd, substantial progress has been made in this field. However up till now the structure of only one compound of the cannabis group,namely the physiologically inactive cannabinol (I), has been fully elucidated.

We have initiated a program aimed at clarifying some of the remaining problems connected with the chemistry of the constituents of hashish. This paper deals with the structure and stereochemistry of cannabidiol, one of the major components of hashish. Cannabidiol was isolated by Adams[3] and Todd[4] from marihuana and Indian hemp resin, respectively. Structure II (without stereochemical assignments) was suggested for cannabidiol.[5a,d] The carbon skeleton and the position of the hydroxyl groups are undoubtly correctly represented by II, for cannabidiol has been converted[5b] into cannabinol (I), whose structure has been proved by synthesis,[6] The terminal position of the double bond has been adequately proved by chemical means.[5c] The position of the double bond in the alicyclic ring,[5c] however, seemed to require additional corroboration. We now present evidence that cannabidiol in fact possesses structure IIIa.

The UV spectral analysis of cannabidiol reported by Adams[5a,c,d] unequivocally shows that the double bond in the terpene ring is conjugated neither to the terminal

[1] A portion of this study has been reported at a Meeting of the Israeli Chemical Society, Jerusalem, April 1963 [R. Mechoulam, *Bull. Research Council Israel* **12A**, 57 (1963)].

[2] For reviews on the subject see D. F. Downing, *Quart. Rev.* **16**, 133 (1962); A. R. Todd, *Experientia* **2**, 55 (1946); R. Adams, *Harvey Lectures* **37**, 168 (1942); see also the series of papers by R. Adams, the latest one of which is R. Adams, M. Harfenist and S. Loewe, *J. Amer. Chem. Soc.* **71**, 1624 (1949).

[3] R. Adams, M. Hunt and J. H. Clark, *J. Amer. Chem. Soc.* **62**, 196 (1940).

[4] A. Jacob and A. R. Todd, *J. Chem. Soc.* 649 (1940).

[5] R. Adams and co-workers, *J. Amer. Chem. Soc.* [a] **62**, 2566 (1940); [b] **62**, 2402 (1940); [c] **62**, 2215 (1940); [d] **63**, 2209 (1941); [e] **62**, 2194 (1940).

[6] R. Adams, B. R. Baker and R. B. Wearn, *J. Amer. Chem. Soc.* **62**, 2204 (1940); R. Ghosh, A. R. Todd and S. Wilkinson, *J. Chem. Soc.* 1121, 1393 (1940).

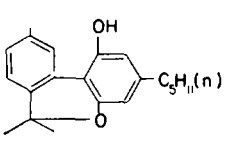

I

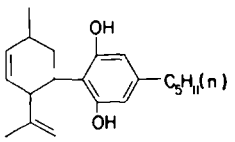

II

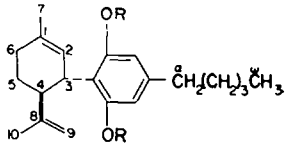

III

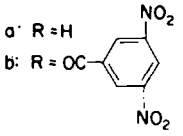

a: R = H
b: R = OC

methylene group nor to the aromatic nucleus. Therefore the only three possible positions are Δ^1, $\Delta^{1(6)}$ and Δ^5.

The NMR spectra of cannabidiol (IIIa) and of its dinitrobenzoate (IIIb) (see Table) show the presence of three olefinic protons only. Two of these are the terminal methylene group protons, while the third one is on the alicyclic ring double bond. The presence of just one proton on this double bond excludes its formerly accepted position (Δ^5) in the proposed structure (II). This is further supported by the presence of two vinylic methyl groups, and only one methyl on a saturated carbon (ω-methyl), as shown by the NMR spectra. It is necessary now to decide between positions 1 and 1(6) for the location of the nuclear double bond.

Of special interest in the NMR spectra is the signal at 3·85 ppm in cannabidiol (IIIa) and at 3·58 ppm in its ester (IIIb). In both compounds the area of this signal corresponds to one proton and we assign it to the hydrogen attached to C_3. Such a chemical shift is rather low for a proton α to a phenyl ring only, and it is therefore postulated that the additional deshielding contribution must arise from an adjacent olefinic center.[7] Placing the double bond at $\triangle^1$ and not at the alternative $\triangle^{1(6)}$ position will satisfy this requirement. The C_3 proton couples its spin with the C_4 proton, and the former appears as a doublet (J = 11 cps) with only minimal splitting from the adjacent C_2 vinylic proton with which it forms an angle of $\phi = 85° (\pm 5)$,[8] taking into account the stereochemistry of the molecule (*vide infra*). The doublet is somewhat broad, which is probably due to a long range interreaction with the 7 methyl protons.

Further support for these assignments is obtained from the NMR spectrum of tetrahydrocannabidiol[9] (IV) in which the two olefinic double bonds are reduced. The signal originally found at 3·85 ppm in the spectrum of IIIa, moves upfield to the

[7] In *p*-cymene (A) the proton on the tertiary carbon α to the phenyl ring has a signal at 2·87 ppm, while in saffrol (B) the corresponding signal is at 3·30 ppm (N.S. Bhacca, L. F. Johnson and J. N. Shoolery, *NMR Spectra Catalog*, Varian Associates, 1962).

A

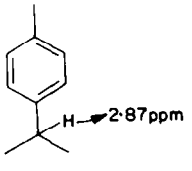

B

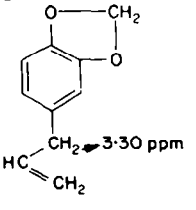

[8] ϕ values were measured from Dreiding models.

[9] R. Adams, M. Hunt and J. H. Clark, *J. Amer. Chem. Soc.* **62**, 735 (1940).

2·60 ppm region, and is masked by the signals arising from the two additional protons α to the phenyl ring on the side chain (Cα protons). Such a shift of this signal is consistent with its assignment to the C_3 proton in IIIa provided the double bond is situated at Δ^1. If the C_3 proton in IIIa were not allylic, hydrogenation of the double bond would not have appreciably effected its chemical shift.

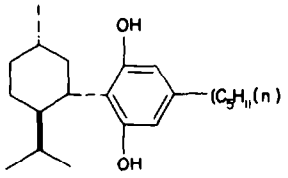

IV

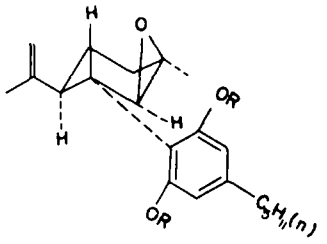

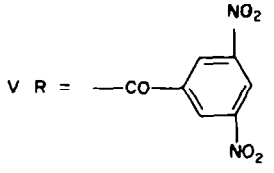

In order to confirm the position of the alicyclic double bond it seemed desirable to convert this double bond into another chemical function and study the NMR properties of the adjacent protons. Epoxidation, being an electrophilic reaction, seemed to offer a facile route for a selective attack on the ring double bond without a reaction on the terminal olefinic group, as the electron density on the latter is lower than in the former.[10] Indeed epoxidation of cannabidiol bisdinitrobenzoate (IIIb) with one mole of perbenzoic acid yielded the monoepoxide V, m.p. 120–122°. The NMR spectrum of the epoxide was instructive. It retained the signals due to the two terminal olefinic protons at C_9 but lacked the signal for the proton on the alicyclic ring double bond, indicating therefore that only the latter double bond had undergone epoxidation. Furthermore a sharp new singlet appeared at 3·01 ppm due to a proton α to an epoxide oxygen atom.[11] It has been demonstrated that the coupling constant between two protons on adjacent carbon atoms is a function of the dihedral angle (ϕ).[12] One of the implications of this relationship is that for $\phi = 70$–$110°$ the coupling constant (J) is quite small.[11–13] In the case of epoxides fused to rigid cyclohexane systems, the dihedral angles between the proton α to the epoxide oxygen and the two adjacent methylene protons are of such an order as to give rise to observable splitting with one of the latter protons only.[11] As an unsplit signal was observed in the NMR spectrum of V for the proton α to the epoxide oxygen

[10] For some recent examples of selective epoxidations see J. S. Showell, J. R. Russell and D. Swern, *J. Org. Chem.* **27**, 2853 (1962); F. C. Frostick, B. Phillips and P. S. Starcher, *J. Amer. Chem. Soc.* **81**, 3350 (1959); L. S. Silbert, Z. B. Jacobs, W. E. Palm, L. P. Witnauer, W. S. Port and D. Swern, *J. Polymer Sci.* **21**, 161 (1956).

[11] A. D. Cross, *J. Amer. Chem. Soc.* **84**, 3206 (1962).

[12] M. Karplus, *J. Chem. Phys.* **30**, 11 (1959).

[13] K. L. Williamson and W. S. Johnson, *J. Amer. Chem. Soc.* **83**, 4623 (1961).

atom (C_2 proton), it must be concluded that this proton is flanked by only one adjacent proton. This can be realized only if the epoxide occupies the 1,2 and not the alternative 1,6 position. Indeed the dihedral angle (H—C_2—C_3—H) in epoxide V was found to be 105° (±10°) and should not give rise to an observable splitting. The C_3 proton in the NMR spectrum of V appears as a sharp doublet at 3·24 ppm (J = 11 cps) which is consistent with structure V for the epoxide. The C_3 proton couples its spin only with the single proton at C_4; no splitting could be observed due to the C_2 proton which is in accordance with the above interpretation. If the epoxide oxygen atom were on C_1–C_6 then the signal of the C_3 proton should not have changed from that of the starting material and its splitting pattern should have been much more complex.

On the ground of the above experimental results we propose the modified structure IIIa for cannabidiol.

It is noteworthy that neither basic nor acidic treatment of cannabidiol induces isomerization of the Δ^1 double bond *into conjugation* with the aromatic system.[4,5a,d,e] The reason for this rather surprising observation might be due to hyperconjugation.[14] Conformational factors also must be taken into account. Due to the numerous substituents in the vinicity of the carbon–carbon bond between the phenyl and the alicyclic rings, a double bond in the alicyclic ring conjugated to the phenyl ring will not be in the same plane as the phenyl ring. Hence, the driving force for an isomerization leading to conjugation with the phenyl ring may be considerably diminished.

Adams[9] has shown that oxidation of tetrahydrocannabidiol (IV) with potassium permanganate in acetone gives a menthane carboxylic acid (VIa), which is identical with the acid obtained from menthyl chloride (VII) through a Grignard reaction with carbon dioxide. Grignard reactions of this type have been shown to give the thermodynamically more stable acid. Thus Shoppee[15] has reported that carbonation

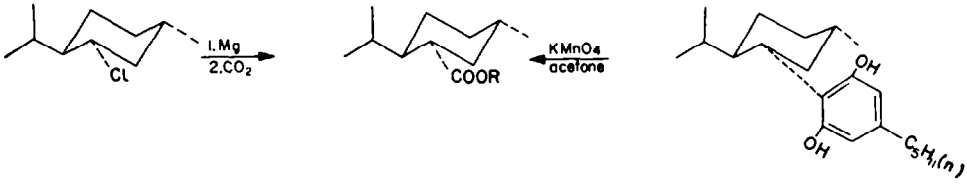

VII VI a, R = H b, R = CH_3 IV

of a Grignard reagent prepared from either 3α-bromo-cholestane or 3β-bromo-cholestane gives the same cholestane-3β-carboxylic acid in which the carboxyl group is equatorial. By equilibration experiments we have now shown that the carboxylic group in (VIa) is also equatorial. Methyl menthane carboxylate (VIb) when boiled with sodium methoxide in benzene or in absolute methanol gave back unchanged starting

[14] It has been observed that the unconjugated 1,1 dimethyl-3-phenyl propene (C) is more stable than the isomeric styrene (above 150°, at which temp the experiments were performed). (H. Pines and J. Shabtai, unpublished data communicated to us by Dr. J. Shabtai).

C H_2C—CH=$C(CH_3)_2$

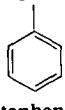

[15] G. Roberts, C. W. Shoppee and R. J. Stephenson, *J. Chem. Soc.* 2705 (1954).

material. Gastambide[16] has also assigned structure VIa to menthane carboxylic acid by comparing the rotations of different menthyl and neomenthyl derivatives.

If it is assumed that during the relatively mild oxidation of tetrahydrocannabidiol no inversions have taken place, then the stereochemistry of cannabidiol is correctly represented by IIIa. Further support for this stereochemistry assignment can be found in the NMR spectra. The large coupling constant (J = 11 cps) between the C_3 and C_4 protons in both III and V indicates that the dihedral angle between them is that of two trans diaxial hydrogens.[11–13]

The stereochemistry of the epoxide ring in V can also be deduced from the NMR spectrum. It was shown already that the C_3 proton, which appears as a doublet in the NMR spectrum of the epoxide V, forms an angle of 105 (±10°) with the C_2 proton. These two hydrogens are therefore in a trans relationship, and it follows that the epoxide ring and the phenyl ring are also trans oriented, as depicted in V.

Some insight into the conformation of the bisdinitrobenzoate ester of cannabidiol (IIIb) could be gained by inspection of its NMR spectrum. It can be seen from the Table that the dinitrobenzoylation of the two phenolic groups induces a significant upfield shift of all protons associated with the cyclohexene ring structure. Such shifts can be accounted for in terms of diamagnetic currents arising from the aromatic nuclei. However the cyclohexene ring must be at least partially disposed above (or below) the plane of one of the 3,5 dinitrobenzene rings to account for its shielding. Since the phenolic ring carries two bulky ortho substituents it is probably forced out of planarity with the cyclohexene ring and a situation where the 3,5-dinitrobenzene rings fold over and below the cyclohexene ring can be readily attained.*

TABLE—NMR SPECTRA OF CANNABIDIOL AND ITS DERIVATIVES[a]

	C_2—H	C_9—H	C_3—H	10 & 7-methyls		ω-methyl
Cannabidiol (IIIa)	5·59(s) (1)	4·66, 4·58(s) (2)	3·85(br)(d) (1)	1·80, 1·68(s) (6)		0·88(t) (3)
Cannabidiol-bisdinitrobenzoate (IIIb)	5·33(s) (1)	4·73, 4·55(s) (2)	3·58(br)(d) (J = 11 cps) (1)	1·59, 1·22(s) (6)		0·92(t) (3)
Tetrahydro cannabidiol (IV)				0·91	0·81 (12)	(br)
Epoxy-cannabidiol bis dinitrobenzoate (V)	3·01(s) (1)	4·75, 4·55(s) (2)	3·24(d) (J = 11 cps) (1)	1·56 (9)	0·90	

[a] Spectra were determined on a Varian A-60 spectrometer in deuteriochloroform. Values given in p.p.m. relative to tetramethylsilane as internal standard. Numbers in parentheses denote number of protons, determined by integration of areas. Letters in parentheses denote singlet (s); doublet (d); triplet (t); and broad (br).

* *Note added in proof*

Prof. F. Šantavy of Palacký University, Olomouc, Czechoslovakia has kindly informed us that, mainly on the basis of optical rotation data, he has reached the same conclusions as reported in this paper regarding the structure of cannabidiol and that his manuscript is in preparation.

A. J. Bose[16a] has found, by a method different than ours, that methane carboxylic acid has structure VIa.

[16] B. Gastambide, *Ann. Chim.*, (*Paris*) **9**, 257 (1954).

[16a] A. K. Bose, S. Harrison and L. Farber, *J. Org. Chem.* **28**, 1223 (1963).

EXPERIMENTAL[17]

Monoepoxycannabidiol bisdinitrobenzoate (V). To a cooled solution of perbenzoic acid (207 mg, by titration) in 20 cc chloroform was added 1·05 g cannabidiol bis 3,5-dinitrobenzoate. The solution was left in the dark at 20° for 16 hr, washed with cold 5% sodium hydroxide solution, then several times with water and was dried (sodium sulphate). After evaporation a solid residue was recrystallized from acetone–pentane, giving 900 mg monoepoxy cannabidiol bis 3,5-dinitrobenzoate, m.p. 116–120°. The analytical sample showed m.p. 120–122°, $(\alpha)_D$-54° ($CHCl_3$). Purity was determined by chromatoplate. (Found: C, 58·68; H, 4·78; N, 7·84. $C_{35}H_{34}O_{13}N_4$ requires: C, 58·49; H, 4·77; N, 7·80%).

Equilibration experiments of methyl menthane carboxylate (VIb). (-)Menthane carboxylic acid[18] (m.p. 65–66°; 200 mg) $(\alpha)_D$-44° ($CHCl_3$) was reacted with freshly distilled diazomethane. The resulting methyl ester was dissolved in benzene, sodium methoxide (1 g) was added and the reaction mixture was boiled for 16 hr. After acidification with 5% hydrochloric acid, the benzene solution was washed with water, dried (sodium sulphate) and evaporated. The resulting oil was identical with the starting ester by its IR spectrum, by chromatoplate, and by vapour phase chromatography (on 7% silicon oil, temp 110°, gas flow 430 cc/min, on a Perkin Elmer vapour fractometer model 154 as well as on 10% Apiezon L, APL, temp 146°, gas flow 70 cc/min on a Pye Argon Chromatograph). In another run the methyl menthyl carboxylate was not isolated, but after the equilibration water was added to the reaction mixture which was boiled for another 1 hr. After cooling the aqueous phase was washed with ether, acidified with 5% hydrochloric acid and extracted with ether. Evaporation of the ether solution gave pure (−) menthane carboxylic acid, m.p. 65–66°, $(\alpha)_D$-44°, identical with the starting material (IR, mixture m.p., NMR spectra). Identical results were obtained when the experiments were performed with sodium methoxide in absolute methanol rather than in benzene.

Acknowledgements—The authors wish to thank Prof. F. Sondheimer for his interest and encouragement, Dr. A. Melera of Varian AG, Zurich for his help in some of the NMR work, Dr. J. Shabtai for use of a VPC instrument, and especially the Israeli Police for supplying the crude hashish.

[17] Microanalyses were carried out by our microanalytical laboratory under the supervision of Mr. R. Heller.

[18] N. I. Kursanov, *J. Russ. Phys. Chem. Soc.* **46**, 815 (1914); *Chem. Abstr.* **9**, 1751 (1915); J. G. Smith and G. F. Wright, *J. Org. Chem.* **17**, 1116 (1952).

Identification and Functional Characterization of Brainstem Cannabinoid CB_2 Receptors

Marja D. Van Sickle,[1]* Marnie Duncan,[1]* Philip J. Kingsley,[2] Abdeslam Mouihate,[1] Paolo Urbani,[3] Ken Mackie,[4] Nephi Stella,[5] Alexandros Makriyannis,[6] Daniele Piomelli,[7] Joseph S. Davison,[1] Lawrence J. Marnett,[2] Vincenzo Di Marzo,[3] Quentin J. Pittman,[1] Kamala D. Patel,[1] Keith A. Sharkey[1]†

The presence and function of CB_2 receptors in central nervous system (CNS) neurons are controversial. We report the expression of CB_2 receptor messenger RNA and protein localization on brainstem neurons. These functional CB_2 receptors in the brainstem were activated by a CB_2 receptor agonist, 2-arachidonoylglycerol, and by elevated endogenous levels of endocannabinoids, which also act at CB_1 receptors. CB_2 receptors represent an alternative site of action of endocannabinoids that opens the possibility of nonpsychotropic therapeutic interventions using enhanced endocannabinoid levels in localized brain areas.

Endocannabinoids, anandamide, and 2-arachidonoylglycerol (2-AG) are lipid mediators that act at CB_1 and CB_2 receptors (*1*, *2*). Their actions are terminated through cellular uptake facilitated by a putative endocannabinoid transporter, followed by intracellular enzymatic hydrolysis. Two degradative enzymes for endocannabinoid metabolism are known; fatty acid amide hydrolase (FAAH) preferentially degrades anandamide, and monoacylglycerol lipase preferentially degrades 2-AG (*1*, *3*, *4*). The CB_1 receptor is highly expressed in the CNS, where cannabinoids act at presynaptic CB_1 receptors to elicit changes in the synaptic efficacy of neuronal circuits (*5*). The CB_2 receptor has been found outside the CNS and is particularly associated with immune tissues, such as the spleen and thymus, as well as in various circulating immune cell populations (*6*). In the CNS, CB_2 receptor mRNA has been reported in cerebellar granule cells (*7*), and CB_2 receptors have been described on perivascular microglial cells and in cultured cerebrovascular endothelium (*8*, *9*). CB_2 receptor expression is enhanced on glia in neuritic plaques and on immune cells in simian immunodeficiency virus encephalitis (*10*, *11*). To date, however, the CB_2 receptor protein has not been localized on central neurons, and the effects of endocannabinoids in the brain have always been attributed to an action at CB_1 receptors.

We found CB_2 receptor mRNA expression in the brain (cerebellum, cortex, and brainstem) and spleen of the rat using reverse transcription polymerase chain reaction (RT-PCR) (Fig. 1). Sequencing of the 472–base pair PCR product showed that the products amplified from the spleen, cortex, and brainstem were identical to the rat CB_2 receptor sequence (*12*, *13*). Using quantitative real-time RT-PCR, we determined that the brainstem contained $1.5 \pm 0.9\%$ of the CB_2 receptor mRNA found in the spleen (fig. S1) (*14*). Amplification of CB_2 receptor from the brainstem was not due to genomic contamination of our sample, because amplification of RNA that was not reverse-transcribed did not lead to the generation of a product. Furthermore, our real-time PCR primers spanned intron-exon borders, which ensured that the only product that could be amplified was the spliced mRNA.

We next investigated whether CB_2 receptor protein could be detected by Western blotting and/or immunohistochemistry (*14*). Western blotting for the CB_2 receptor in the brainstem and cerebellum revealed three bands at about 45, 55, and 60 kD (Fig. 1), similar to previous reports in spleen (*15*). In the brainstem, CB_2 receptor immunoreactivity was found in neurons within the dorsal motor nucleus of the vagus (DMNX), the nucleus ambiguous, and the spinal trigeminal nucleus; glial cells and blood vessels did not express detectable CB_2 receptor immunoreactivity (*16*). Preincubation with the cognate peptide of the CB_2 receptor antibody completely abolished cellular staining. These results are in contrast to the conclusions drawn by Derbenev *et al.* (*17*), who reported no CB_2 mRNA or receptor protein in similar regions of the rat brainstem. However, evaluation of their figures reveals a faint band of immunoreactivity in Western blots, consistent with our observations, and their RT-PCR primers were directed against different regions of the CB_2 receptor mRNA. The differences in the conclusions drawn likely reflect the low abundance of CB_2 receptor in the brain relative to the spleen and the choice of RT-PCR primers.

We next pursued the functional significance of this observation. The major psychoactive cannabinoid, Δ^9-tetrahydrocannabinol (THC), is effective in the treatment of nausea and vomiting (emesis) (*18*). THC acts on neurons in the dorsal vagal complex of the brainstem, the site of integration of emetic reflexes that includes the nucleus of the solitary tract (NTS), the area postrema, and DMNX (*18*, *19*), where we found CB_2 receptor expression. These well-characterized actions of CBs have been demonstrated in the ferret. Because of the inability of rodents to vomit, we verified our observations of the receptor distribution in this species (Fig. 1). Indeed, as in the rat, we observed major bands of immunoreactivity in Western blots at about the same relative molecular weights and a similar distribution of CB_2 receptor expression in neurons of the DMNX.

These results led us to investigate whether endocannabinoids could act at the CB_2 receptor in the brainstem to inhibit emesis. Using morphine-6-glucuronide (M6G) as an emetic stimulus, we found that both anandamide and 2-AG dose-dependently reduced emesis in the ferret (Fig. 2) (*14*). Using selective CB receptor antagonists, we attempted to reverse the actions of these endocannabinoids. The antiemetic effect of anandamide was almost completely reversed by the selective CB_1 receptor antagonist AM251 but was not significantly altered by the CB_2 antagonist AM630, which is consistent with the fact that the anandamide is not very efficacious at CB_2 receptors (*2*) and indicates that the dose of AM630 used does not antagonize CB_1 receptors. In contrast, the antiemetic effects of 2-AG were reversed by both AM251 and AM630 (Fig. 2). Thus, the CB_2 receptor may be functionally expressed in the ferret brainstem and could be targeted by an endocannabinoid. As we observed the ferrets during our studies, we noted that 2-AG administration was far less sedating than anandamide (Fig. 2). This action is consistent with a preferential effect at a CB_2 receptor, because CB_1 receptor activation *in vivo* is associated with sedation (*2*).

[1]Institute of Infection, Immunity, and Inflammation and Hotchkiss Brain Institute, Department of Physiology and Biophysics, University of Calgary, Calgary, AB, Canada T2N 4N1. [2]Department of Biochemistry, Vanderbilt Institute of Chemical Biology, Center in Molecular Toxicology, Vanderbilt-Ingram Cancer Center, Vanderbilt University School of Medicine, Nashville, TN 37232–0146, USA. [3]Endocannabinoid Research Group, Institute of Biomolecular Chemistry, Consiglio Nazionale delle Ricerche, Pozzuoli, Naples, Italy. [4]Department of Anesthesiology and Department of Physiology and Biophysics, University of Washington, Seattle, WA 98195–6540, USA. [5]Department of Pharmacology, Psychiatry, and Behavioral Sciences, University of Washington, Seattle, WA 98195–7280, USA. [6]Center for Drug Discovery, Department of Pharmaceutical Sciences, Northeastern University, Boston, MA 02115, USA. [7]Department of Pharmacology, Gillespie Neuroscience Facility, University of California, Irvine, CA 92697–6180, USA.

*These authors contributed equally to this work.
†To whom correspondence should be addressed. E-mail: ksharkey@ucalgary.ca

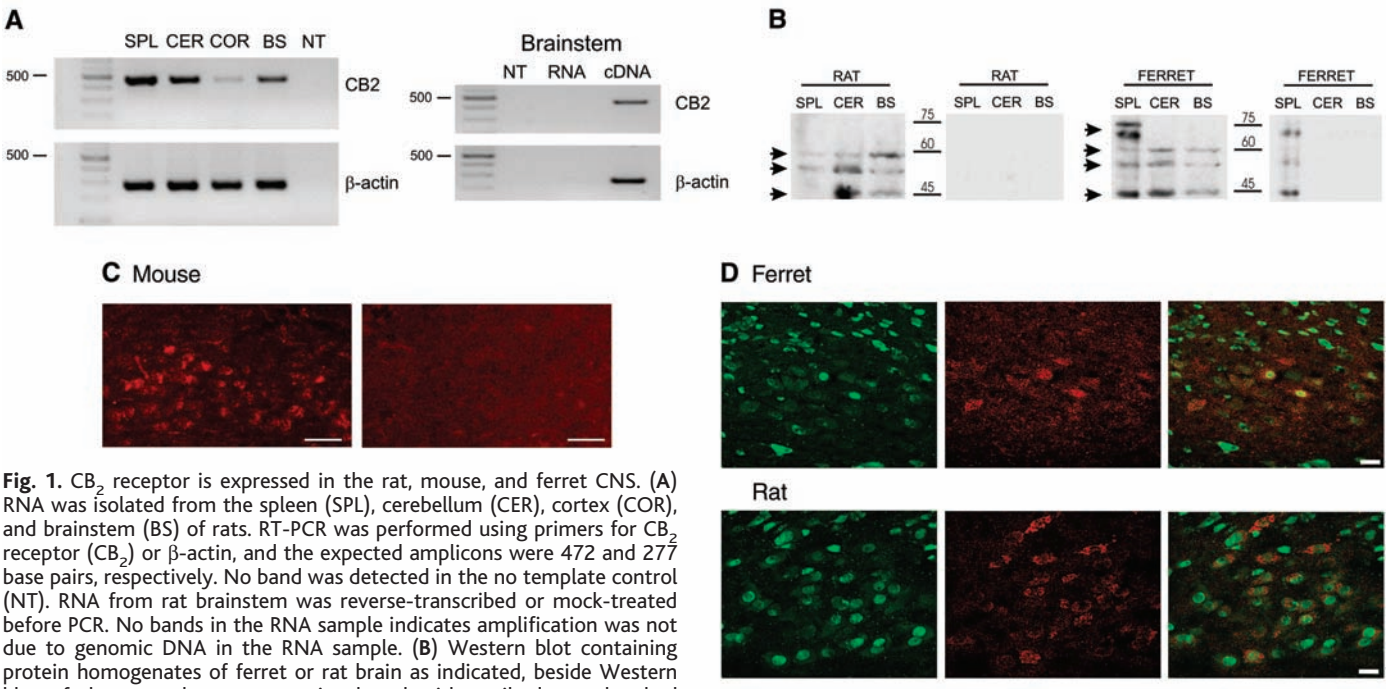

Fig. 1. CB_2 receptor is expressed in the rat, mouse, and ferret CNS. (**A**) RNA was isolated from the spleen (SPL), cerebellum (CER), cortex (COR), and brainstem (BS) of rats. RT-PCR was performed using primers for CB_2 receptor (CB_2) or β-actin, and the expected amplicons were 472 and 277 base pairs, respectively. No band was detected in the no template control (NT). RNA from rat brainstem was reverse-transcribed or mock-treated before PCR. No bands in the RNA sample indicates amplification was not due to genomic DNA in the RNA sample. (**B**) Western blot containing protein homogenates of ferret or rat brain as indicated, beside Western blot of the same homogenates incubated with antibody preabsorbed with control peptide. Major bands were observed at about 45, 55, and 60 kD in rat and ferret brainstem (arrows; $n = 6$). In the ferret spleen, higher molecular weight bands were also observed (arrow). In the rat brain and spleen and ferret brain, we completely preabsorbed all the immunoreactive bands. However, in the ferret spleen, bands were substantially reduced, but not completely preabsorbed, with the concentration of peptide used. (**C**) CB_2 receptor immunoreactivity in the dorsal motor nucleus of the vagus of wild-type (left) and $CB_2^{-/-}$ (right) mice (*30*). Note the lack of immunoreactive cell bodies in the knockout mouse ($n = 3$ per group). Scale bar, 50 μm. (**D**) Immunoreactivity for the neuronal nuclear marker NeuN (left, green) and CB_2 receptor immunoreactivity (center, red) in neurons of the dorsal motor nucleus of the vagus of the ferret and rat, as indicated. Overlay (right) of NeuN and CB_2 receptor illustrates that CB_2 receptor immunoreactivity is present in neurons of both the ferret and rat ($n = 4$), where it is localized on the cell membrane and in the cytoplasm of the neurons. Scale bars, 20 μm.

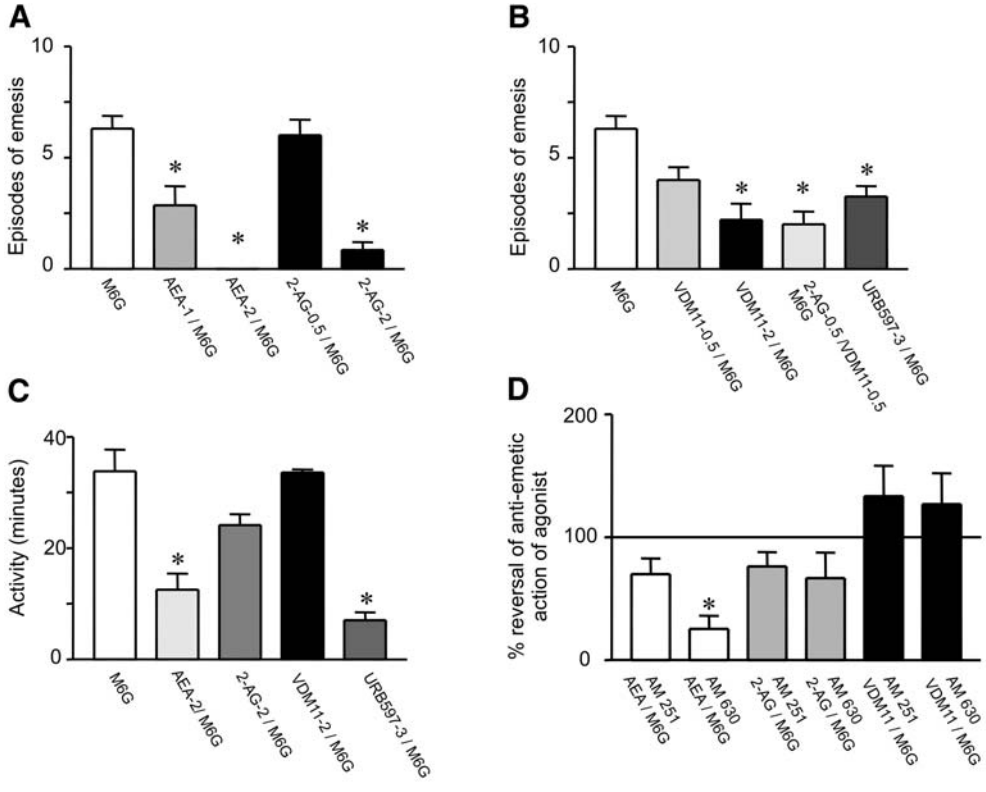

Fig. 2. Endocannabinoids reduce emesis induced by M6G. (**A**) Episodes of emesis after treatments of emetic agent alone, M6G (0.05 mg/kg, subcutaneously; $n = 10$) or the following treatments ($n = 3$ to 7) preceding M6G; anandamide (AEA-1, 1 mg/kg; and AEA-2, 2 mg/kg); and 2-arachidonoyl glycerol (2-AG-0.5, 0.5 mg/kg; and 2-AG-2, 2 mg/kg). AEA and 2-AG had no emetic actions when given alone. (**B**) Episodes of emesis after M6G alone; or with the transport inhibitor (VDM11-0.5, 0.5 mg/kg; and VDM11-2, 2 mg/kg); paired ineffective doses of VDM11 and 2-AG (0.5 mg/kg); an FAAH inhibitor URB 597 (3 mg/kg). (**C**) Activity during the 60-min observation after the treatments indicated. (**D**) CB_1 antagonist AM251 (5 mg/kg) reversed the effects of anandamide (AEA, 2 mg/kg), 2-AG (2 mg/kg), and VDM11 (2 mg/kg). In contrast, the CB_2 antagonist AM630 (5 mg/kg) did not reverse the effect of AEA (2 mg/kg), but effectively reversed the action of 2-AG (2 mg/kg) and VDM11 (2 mg/kg). In the presence of AM630 (5 mg/kg), there were 3.4 ± 0.7 emetic episodes ($n = 5$) in animals given a lower dose of AEA (1 mg/kg), which is not significantly different from the 2.8 ± 1.3 emetic episodes ($n = 5$) in the absence of AM630. AM251 and AM630 had no emetic actions when given alone. AM630 did not potentiate the effects of M6G, whereas AM251 enhanced emesis as previously described (*17*). Results are expressed as percentage of number of episodes of emesis induced by M6G. *Significant differences compared with M6G alone, $P < 0.05$. Bars represent mean ± SEM.

Although these data were strongly indicative of the actions of 2-AG at CB_2 receptors, it was important to evaluate whether endogenously released endocannabinoids reduce emesis through an action at CB_2 receptors. We used two approaches that would raise endocannabinoid levels in the brain. First, we tested whether the selective endocannabinoid reuptake inhibitor VDM11 (*20*) inhibited emesis. Second, we tested whether an FAAH inhibitor (URB 597) (*21*) reduced emesis. In both cases, we blocked or reduced the extent of emesis induced by M6G (Fig. 2). We extended these studies to find whether VDM11 would potentiate the effects of 2-AG. We used doses of VDM11 and 2-AG that alone did not significantly reduce emesis. When VDM11 was given together with 2-AG, we found a significant attenuation in the number of emetic episodes (Fig. 2). URB 597 strongly sedated animals, which suggested that this compound may selectively enhance anandamide levels. Conversely, VDM11 had no sedative effects, and the antiemetic effects were reversed by both AM251 and AM630, which suggested that VDM11 may preferentially affect 2-AG levels.

If the arguments made above were correct and if endocannabinoids undergo increased turnover in response to an emetic stimulus, treatment with VDM11 or URB 597 would be expected to increase the levels of endocannabinoids in the brainstem. We investigated this using a model of emesis under anesthetized conditions, so that the brains could be rapidly removed and frozen in order to limit the inherent instability of endocannabinoids in tissue samples (*14*). Ferrets were given hypertonic saline as an emetic stimulus because M6G is an inconsistent emetic in anesthetized animals. Levels of anandamide and total arachidonoyl glycerol [which reflect tissue 2-AG levels (*14*)] were measured in the brainstem and, for comparison, the cerebellum. Levels of endocannabinoids in the ferret under basal conditions or after emesis were comparable to levels previously found in rodents (Fig. 3). As expected from the pharmacological experiments described above, VDM11 specifically increased levels of total arachidonoyl glycerol in the brainstem and cerebellum, whereas pretreatment with URB 597 only increased the levels of anandamide in the brainstem.

These results led us to investigate whether selective CB_2 receptor agonists reduced emesis. We observed no statistically significant reductions in emesis in animals given the CB_2 receptor agonists AM1241 (1 or 2 mg/kg) or JWH 133 (1 or 5 mg/kg) before M6G (*22*). This finding was not completely surprising, as inhibitors of endocannabinoid inactivation can be more efficacious than "direct" agonists (*23*–*25*). Furthermore, these data suggest that CB_2 receptor activation alone is not sufficient to inhibit emesis and that, under appropriate conditions, for example, those produced by inhibiting endocannabinoid inactivation, the CB_2 receptor can be activated in local brain regions together with CB_1 receptors and can inhibit emesis. This hypothesis was supported by a significant reduction in episodes of emesis (7.1 ± 0.5 to 5.0 ± 0.7; $n = 6$ to 10; $P < 0.05$) when anandamide (0.5 mg/kg) and AM1241 (1 mg/kg) were administrated together at doses that were not antiemetic when either compound was given alone with M6G.

The behavioral evidence cited above is not a direct measure of neuronal activation and does not directly show functionally active CB_2 receptors in the brainstem. To determine whether CB_2 receptor agonists can activate neurons of the DMNX, we investigated the expression of phosphorylated extracellular signal–regulated kinase 1/2 (pERK) in rat DMNX neurons by immunohistochemistry (*14*), because phosphorylation of this enzyme is enhanced by cannabinoid agonists in other regions of the brain and in cell lines (*26*, *27*). Administration of the CB_2 receptor agonist AM1241 increased pERK in DMNX neurons when compared with vehicle-treated controls (Fig. 4).

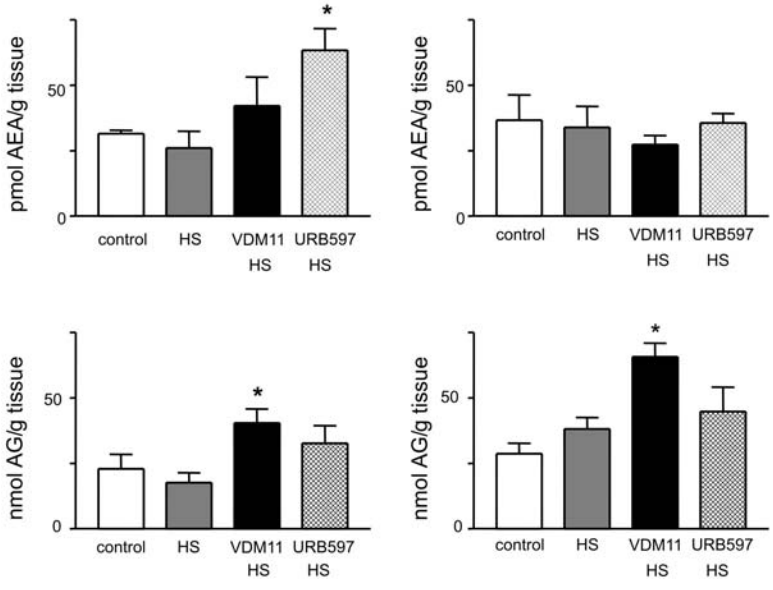

Fig. 3. Endocannabinoid levels in the ferret brainstem (**left**) and cerebellum (**right**). Control ferrets received intragastric normal saline ($n = 4$ to 7). After the emetic stimulus intragastric hypertonic saline (HS), levels were not significantly increased. URB597 (5 mg/kg) increased anandamide (AEA) levels in the brainstem but not in the cerebellum. VDM11 (3 mg/kg) increased total arachidonoyl glycerol (1-AG and 2-AG, 1AG accounts for about 20% and 2-AG about 80% of total) in both the brainstem and cerebellum when compared with the HS group ($P < 0.05$).

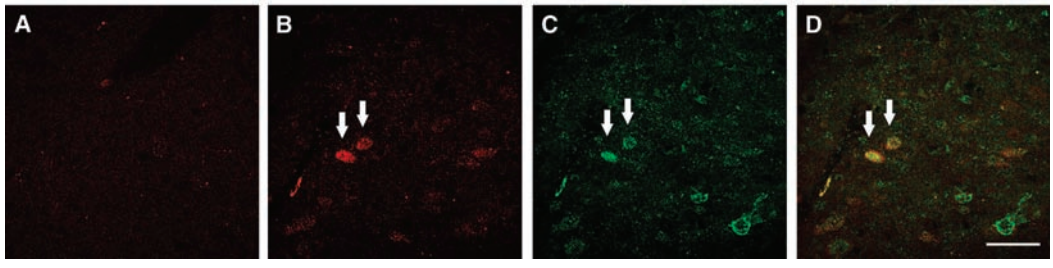

Fig. 4. A CB_2 receptor agonist activates neurons in the dorsal motor nucleus of the vagus (DMNX) of the rat. Immunoreactivity for pERK in rats treated with vehicle (**A**) ($n = 3$) and (**B**) the selective CB_2 receptor agonist, AM1241 (1 mg/kg; $n = 7$). AM1241 stimulated the expression of 5.6 ± 1.2 pERK immunoreactive cells per section in the DMNX compared with 1.2 ± 0.2 pERK immunoreactive cells in vehicle-treated animals. pERK immunoreactive cells were also observed in the nucleus of the solitary tract (not shown on figure). pERK immunoreactivity (red) was observed in nuclei and cytoplasm of activated cells. (**C**) CB_2 receptor immunoreactivity (green) was observed on the cell membrane and in the cytoplasm of DMNX neurons. (**D**) Overlay of pERK and CB_2 receptor illustrate the presence of pERK in neurons that express the CB_2 receptor (arrows). pERK immunoreactivity was observed in about 15 to 20% of the CB_2 immunoreactive neurons. Scale bar, 50 μm.

We have shown that CB_2 receptors are present in the brainstem and also in the cortex and cerebellum. As inferred by the use of a selective CB_2 antagonist, the brainstem receptors are functionally coupled to inhibition of emesis when costimulated with CB_1 receptors by an endogenous cannabinoid capable of activating both receptors. The extent of participation of CB_2 receptors in this effect is sufficient to reduce the widespread behavioral actions associated with the administration of CB_1 agonists. However, generalized activation of CB_2 receptors leads to immunosuppression (*28*) and is potentially deleterious if used as a therapy. Others have suggested that modulating the endocannabinoid system in the CNS represents a promising strategy for therapies for CNS disorders (*29*). Our observations suggest that targeting specific local populations of cannabinoid receptors (both CB_1 and CB_2) by enhancing endocannabinoid levels where they are released represents a therapeutic strategy that may be useful in disorders where either CB_1 or CB_2 receptor activation alone would not be desirable. This approach would circumvent the psychotropic and immunosuppressive side effects of exogenously administered cannabinoids and would provide an alternative approach for the therapeutic utilization of this unique neuroregulatory system.

References and Notes

1. V. Di Marzo, M. Bifulco, L. De Petrocellis, *Nat. Rev. Drug Discov.* **3**, 771 (2004).
2. A. C. Howlett *et al.*, *Pharmacol. Rev.* **54**, 161 (2002).
3. L. De Petrocellis, M. G. Cascio, V. Di Marzo, *Br. J. Pharmacol.* **141**, 765 (2004).
4. T. P. Dinh *et al.*, *Proc. Natl. Acad. Sci. U.S.A.* **99**, 10819 (2002).
5. T. F. Freund, I. Katona, D. Piomelli, *Physiol. Rev.* **83**, 1017 (2003).
6. T. W. Klein *et al.*, *J. Leukoc. Biol.* **74**, 486 (2003).
7. S. D. Skaper *et al.*, *Proc. Natl. Acad. Sci. U.S.A.* **93**, 3984 (1996).
8. E. Nunez *et al.*, *Synapse* **53**, 208 (2004).
9. S. A. Golech *et al.*, *Brain Res. Mol. Brain Res.* **132**, 87 (2004).
10. C. Benito *et al.*, *J. Neurosci.* **25**, 2530 (2005).
11. C. Benito *et al.*, *J. Neurosci.* **23**, 11136 (2003).
12. G. Griffin, Q. Tao, M. E. Abood, *J. Pharmacol. Exp. Ther.* **292**, 886 (2000).
13. S. M. Brown, J. Wager-Miller, K. Mackie, *Biochim. Biophys. Acta* **1576**, 255 (2002).
14. Materials and methods are available as supporting material on *Science* Online.
15. I. Matias *et al.*, *Eur. J. Biochem.* **269**, 3771 (2002).
16. M. D. Van Sickle, Q. J. Pittman, K. A. Sharkey, unpublished observations.
17. A. V. Derbenev, T. C. Stuart, B. N. Smith, *J. Physiol.* **559**, 923 (2004).
18. M. D. Van Sickle *et al.*, *Gastroenterology* **121**, 767 (2001).
19. P. J. Hornby, *Am. J. Med.* **111** (suppl. 8A), 106S (2001).
20. L. De Petrocellis, T. Bisogno, J. B. Davis, R. G. Pertwee, V. Di Marzo, *FEBS Lett.* **483**, 52 (2000).
21. D. Fegley *et al.*, *J. Pharmacol. Exp. Ther.* **313**, 352 (2005).
22. M. D. Van Sickle, J. S. Davison, K. A. Sharkey, unpublished observations.
23. G. Marsicano *et al.*, *Science* **302**, 84 (2003).
24. S. Gaetani, V. Cuomo, D. Piomelli, *Trends Mol. Med.* **9**, 474 (2003).
25. J. P. Chhatwal, M. Davis, K. A. Maguschak, K. J. Ressler, *Neuropsychopharmacology* **30**, 516 (2005).
26. E. Valjent *et al.*, *Proc. Natl. Acad. Sci. U.S.A.* **102**, 491 (2005).
27. M. Bouaboula *et al.*, *Eur. J. Biochem.* **237**, 704 (1996).
28. T. W. Klein *et al.*, *J. Leukoc. Biol.* **74**, 486 (2003).
29. B. F. Cravatt, A. H. Lichtman, *Curr. Opin. Chem. Biol.* **7**, 469 (2003).
30. N. E. Buckley *et al.*, *Eur. J. Pharmacol.* **396**, 141 (2000).

31. We thank L. Oland, W. Ho, and N. Shariat for excellent technical support and animal care. Q.J.P., J.S.D., and K.A.S. were supported by the Canadian Institutes of Health Research (CIHR); K.D.P. by a CIHR group grant in leukocyte trafficking; L.J.M. by GM15431; and K.M., N.S., A.M., and D.P. by U.S. National Institutes of Health. M.D.V.S. is an Alberta Heritage Foundation for Medical Research (AHFMR) graduate student; M.D. is an AHFMR and Canadian Association of Gastroenterology/CIHR/Janssen-Ortho postdoctoral fellow; K.D.P. holds a Canada research chair and is an AHFMR senior scholar; and Q.J.P. and K.A.S. are AHFMR medical scientists.

Supporting Online Material
www.sciencemag.org/cgi/content/full/310/5746/329/DC1
Materials and Methods
Fig. S1
References

6 June 2005; accepted 9 September 2005
10.1126/science.1115740

Observing Others: Multiple Action Representation in the Frontal Lobe

Koen Nelissen,[1] Giuseppe Luppino,[2] Wim Vanduffel,[1,3] Giacomo Rizzolatti,[2] Guy A Orban[1]*

Observation of actions performed by others activates monkey ventral premotor cortex, where action meaning, but not object identity, is coded. In a functional MRI (fMRI) study, we investigated whether other monkey frontal areas respond to actions performed by others. Observation of a hand grasping objects activated four frontal areas: rostral F5 and areas 45B, 45A, and 46. Observation of an individual grasping an object also activated caudal F5, which indicates different degrees of action abstraction in F5. Observation of shapes activated area 45, but not premotor F5. Convergence of object and action information in area 45 may be important for full comprehension of actions.

Understanding actions performed by others is a fundamental social ability. There is now wide consensus that the activation of the motor system is a necessary requisite for this ability. A mere visual representation, without involvement of the motor system, provides a description of the visible aspects of the movements of the agent, but does not give information critical for understanding action semantics, i.e., what the action is about, what its goal is, and how it is related to other actions (*1*, *2*). Action information, however, without knowledge about the identity of the object acted upon, is not sufficient to provide a full understanding of the observed action. Only when information about the object identity is added to the semantic information about the action can the actions of other individuals be completely understood (*3*).

The functional properties of a set of neurons in monkey ventral premotor cortex (area F5) provide evidence for the involvement of the motor system in action understanding. These "mirror" neurons discharge both when the individual performs an action and when the individual observes another person performing the same action (*4*, *5*). They therefore match the observed action with its internal motor representation. F5 neurons responding to the observation of grasping respond equally well when a piece of food or a solid object of similar size and shape is being grasped. The object's identity appears to be ignored in F5 (*4*, *5*).

We used fMRI in five awake monkeys (M1, M3 to M6) (*6*–*9*) to test how actions performed by others are represented in the monkey frontal lobe. In experiment 1, we intended to localize the frontal lobe regions involved in action observation. Monkeys saw video clips showing a full view of a person grasping an object ("acting person"), or an isolated hand grasping objects ("hand action") and static single frames or scrambled videos as controls. The acting person movies approximate the visual stimulation used in F5 single-cell studies (*4*, *5*) and provide context information that is lacking in the hand action movies, which has been used in most human

[1]Laboratorium voor Neuro-en Psychofysiologie, Katholieke Universiteit Leuven Medical School, Leuven, Belgium. [2]Dipartimento di Neuroscienze, Università di Parma, via Volturno 39, 43100 Parma, Italy. [3]Massachusetts General Hospital, Massachusetts Institute of Technology, Harvard Medical School, Athinoula A. Martino's Center for Biomedical Imaging, Charlestown, MA 02129, USA.

*To whom correspondence should be addressed. E-mail: guy.orban@med.kuleuven.ac.be

Identification and Functional Characterization of Brainstem Cannabinoid CB_2 Receptors

Marja D. Van Sickle, Marnie Duncan, Philip J. Kingsley, Abdeslam Mouihate, Paolo Urbani, Ken Mackie, Nephi Stella, Alexandros Makriyannis, Daniele Piomelli, Joseph S. Davison, Lawrence J. Marnett, Vincenzo Di Marzo, Quentin J. Pittman, Kamala D. Patel and Keith A. Sharkey

Science **310** (5746), 329-332.
DOI: 10.1126/science.1115740

Send Orders for Reprints to reprints@benthamscience.ae

206 *Current Drug Metabolism*, 2016, *17*, 206-226

Cannabinoids and Cytochrome P450 Interactions

Ondřej Zendulka[a,b,*], Gabriela Dovrtělová[a], Kristýna Nosková[a], Miroslav Turjap[a,c], Alexandra Šulcová[b], Lumír Hanuš[d] and Jan Juřica[a,b]

[a]*Department of Pharmacology, Faculty of Medicine, Masaryk University, Brno, Czech Republic;* [b]*Experimental and Applied Neuropsychopharmacology Research Group, Central European Institute of Technology, Brno, Czech Republic;* [c]*Department of Clinical Pharmacy, University Hospital Ostrava, Ostrava, Czech Republic;* [d]*School of Pharmacy, Faculty of Medicine, The Hebrew University of Jerusalem, Jerusalem, Israel*

Ondrej Zendulka

Abstract: ***Objective:*** This review consists of three parts, representing three different possibilities of interactions between cannabinoid receptor ligands of both exogenous and endogenous origin and cytochrome P450 enzymes (CYPs). The first part deals with cannabinoids as CYP substrates, the second summarizes current knowledge on the influence of various cannabinoids on the metabolic activity of CYP, and the third outline a possible involvement of the endocannabinoid system and cannabinoid ligands in the regulation of CYP liver activity.

Methods: We performed a structured search of bibliographic and drug databases for peer-reviewed literature using focused review questions.

Results: Biotransformation via a hydrolytic pathway is the major route of endocannabinoid metabolism and the deactivation of substrates is characteristic, in contrast to the minor oxidative pathway via CYP involved in the bioactivation reactions. Phytocannabinoids are extensively metabolized by CYPs. The enzymes CYP2C9, CYP2C19, and CYP3A4 catalyze most of their hydroxylations. Similarly, CYP represents a major metabolic pathway for both synthetic cannabinoids used therapeutically and drugs that are abused. In vitro experiments document the mostly CYP inhibitory activity of the major phytocannabinoids, with cannabidiol as the most potent inhibitor of many CYPs. The drug-drug interactions between cannabinoids and various drugs at the CYP level are reported, but their clinical relevance remains unclear. The direct activation/inhibition of nuclear receptors in the liver cells by cannabinoids may result in a change of CYP expression and activity. Finally, we hypothesize the interplay of central cannabinoid receptors with numerous nervous systems, resulting in a hormone-mediated signal towards nuclear receptors in hepatocytes.

Keywords: Cannabinoids, cytochrome P450, endocannabinoid system, interaction, metabolism, regulation.

1. INTRODUCTION

Cytochrome P450 (CYP) enzymes are haem-containing monooxygenases (EC 1.14.14.1) bound to the membranes of the endoplasmic reticulum or mitochondria in the liver, intestine, kidney, lung, brain, skin, and heart, with the highest level of expression in the liver and intestine [1, 2]. CYPs are functionally coupled with cytochrome P450 reductase, which enables the transfer of electrons from NADPH, the reduced form of NADP (nicotinamide adenine dinucleotide phosphate), to CYP. Microsomal enzymes from subfamilies CYP3A, CYP2C, CYP2D, CYP1A, and CYP2B play a pivotal role in the metabolism of xenobiotics [2]. Variability in the drug plasma levels may diverge depending on different factors, and according to some authors may reach up to 40-fold differences [3]. The most important factors influencing drug plasma levels include the activities of the CYPs with their genetic polymorphisms, epigenetic changes such as DNA methylation and histone deacetylation, together with exogenous factors. These factors substantially influencing CYP metabolic activity are the major source of variability in the pharmacokinetics of drugs and thus in drug responses [3]. CYPs are therefore of particular relevance in clinical pharmacokinetics. On the other hand, the importance of CYP in the metabolism of endogenous substances is also crucial. CYPs are involved in the metabolism of steroid hormones, cholesterol, vitamin D, bile acids and eicosanoids [1], and also most endocannabinoids [4].

Cannabinoids are a group of substances originally isolated from the cannabis plant (*Cannabis sativa*). Today over 100 different molecules with similar structure, most of them with a C21 terpenophenolic moiety, have been isolated and described [5, 6]. They are known to have a wide range of pharmacologic effects [7, 8], for which the hemp plant has been used for over 6000 years in herbal medicine and as a recreational drug.

The first cannabinoid isolated from the cannabis oil was cannabinol (CBN) in 1898 [9, 10], followed by cannabidiol (CBD) in 1940 [11]. Nevertheless, the major psychoactive compound of cannabis remained unknown until 1964, when Δ^9-tetrahydrocannabinol (Δ^9-THC) was isolated in its pure form [12, 13] and its structure was described [14]. The second breakthrough in cannabinoid research was the finding that Δ^9-THC elicits its activity by binding to specific receptors. The first two G-protein coupled receptors (GPCRs) to be discovered, which when activated inhibit adenylyl cyclase, were called the CB1 and CB2 receptors. The CB1 receptor was identified in the brain in 1988 [15], and the CB2 receptor in immune cells in 1993 [16]. These were the first pieces of direct evidence for the possible existence of the endocannabinoid system [17]. The cloning of both of these receptors [16, 18] opened the door to the identification of their endogenous ligands (endocannabinoids), and to the description of their distribution and transduction signal pathways. Anandamide (N-arachidonoylethanolamine) [19] and 2-arachidonoylglycerol (2-AG) [20, 21] are among the first detected and most studied endocannabinoids so far. More recent studies indicate that endocannabinoids, besides the cannabinoid receptor, can also activate multiple receptor targets, including nuclear peroxisome proliferator-activated receptors (PPARs) [22, 23], the transient receptor potential vanilloid type 1 receptor (TRPV1) [24, 25], and orphan G protein-coupled receptors, such as GPR55, GPR119, and GPR18 [26-29]. Other works indicate that cannabinoids have the ability to modulate the activity of additional receptors and their signal transduction pathways, for example

*Address correspondence to this author at the Department of Pharmacology, Faculty of Medicine, Masaryk University, 625 00, Brno, Czech Republic; Tel: +420-549-493-971; Fax: +420-542-213-996;
E-mail: zendulka@med.muni.cz

1875-5453/16 $58.00+.00

opioid, serotonin, NMDA, and nicotinic acetylcholine receptors [29, 30].

Nowadays, the terminology concerning cannabinoids is not unified. Some authors describe cannabinoids as ligands of cannabinoid CB1 or CB2 receptors of herbal (phytocannabinoids), endogenous (endocannabinoids) or xenogenic origin (synthetic cannabinoids). Some others differentiate between a) true cannabinoids with the structure derived from endogenous arachidonic acid or natural herbal cannabis-derived compounds, b) synthetic cannabinoid-like compounds of different structures with either direct or indirect cannabimimetic effects, or compounds inhibiting the cannabinoid receptor activities. Moreover, some authors consider endogenous molecules with a similar structure, but without the ability to bind to CB receptors to also be cannabinoids. These endocannabinoid-like compounds can interfere with the activity of true endocannabinoids, as they are in several cases synthetized and biotransformed via the same pathways [31]. For the above reasons and to maintain the clarity the authors of this review decided to use the name cannabinoids for all of the substances described. An overview of endocannabinoids and endocannabinoid-like substances as well as the most common phytocannabinoids, synthetic ligands of cannabinoid receptors used in preclinical studies, and cannabinoid derived drugs is shown in Table **1**.

The aim of this work is to provide a comprehensive review of the interactions between CYPs and the endocannabinoid system and its ligands. Here, we describe the role of CYP in the metabolism of cannabinoids and vice versa the role of cannabinoids in the regulation of CYP activity.

2. CANNABINOIDS AS SUBSTRATES OF CYTOCHROME P450 MONOOXYGENASES

The endogenous and exogenous cannabinoids are substrates of various CYPs. Due to the possibility of interaction between endocannabinoids, phytocannabinoids, or synthetic cannabinoids and other drugs at the CYP site, there is a risk of treatment failure or drug toxicity. It is therefore important to identify possible sites of such interactions for the successful prevention of pharmacokinetic drug-drug interactions.

2.1. Endocannabinoids and Endocannabinoid-Like Compounds

Numerous amides of fatty acids, notably amides of arachidonic acid, its derivatives, and their metabolites, are potent ligands of cannabinoid receptors. To date, anandamide (AEA), 2-AG and its isomer 1-arachidonoylglycerol, oleamide (oleic acid amide), virodhamine (O-arachidonoylethanolamine), di-homo-γ-linolenoyl-ethanolamide, N-arachidonoyldopamine, noladin ether (2-arachidonylglyceryl ether), and N-arachidonoylserine were identified and proved to be endogenous ligands of at least some cannabinoid receptors. Other endogenous N-acylethanolamines, N-acylethanolamides, and N-acyl-aminoacids such as palmitoylethanolamide, N-arachidonoyltaurine, N-arachidonoylglycine [32-35], N-docosatetraenoyl-ethanolamine, N-docosahexaenoylethanolamine, or N-eico-sapentaenoylethanolamine were found in mammalian tissues over the last decade and exhibit varying affinity to cannabinoid receptors CB1 and CB2. It is also possible that they potentiate the effects of „classical" endocannabinoids such as anandamide and 2-AG independently of binding to CB receptors. Therefore, they are sometimes called „endocannabinoid-like compounds" [4, 35-37].

The metabolism of AEA and 2-AG, being the first investigated and most studied endocannabinoids, was recently reviewed by Snider *et al*. [38] and Zelasko *et al*. [4].

The biological effects of most endocannabinoids are terminated by transport to the cells and enzymatic inactivation. It was hypothesized that the transport of endocannabinoids to the cells may also regulate their biological effects. Mechanisms such as simple diffusion, facilitated diffusion or endocytosis are thought to uptake AEA to the cells [38]. A major degradation pathway is catalyzed by fatty acid amide hydrolase (FAAH) and monoacylglycerol lipase (MAGL) [4, 38]. The oxidative degradation of endocannabinoids is only a minor pathway and involves the enzymes cyclooxygenase-2 (COX-2), 12- and 15-lipoxygenase (12-LOX, 15-LOX, respectively), and CYPs [38-41]. Since some of the metabolites of endocannabinoids originating via CYP enzymes are active ligands of CB receptors, the role of this oxidative pathway remains unclear [4, 35, 37, 38]. Due to the focus of this review, CYP-mediated pathways are described in detail.

Table 1. Overview of cannabinoids.

Endocannabinoids	Endocannabinoid-like compounds	Phytocannabinoids	Synthetic cannabinoids
anandamide	palmitoylethanolamide	Δ^9-tetrahydrocannabinol	dronabinol[a]
2-arachidonoylglycerol	N-docosatetraenoylethanolamine	Δ^8-tetrahydrocannabinol	nabilone[a]
noladin ether	di-homo-γ-linolenoyl-ethanolamide	cannabidiol	rimonabant
virodhamine	2-oleoylglycerol	cannabinol	methanandamide
arachidonoyldopamine	N-oleoylethanolamine	cannabigerol	JWH-0133
N-arachidonoylserine	N-eicosapentaenoylethanolamine	cannabichromen	AM-251
homo-γ-linolenoylethanolamide	N-docosahexaenoylethanolamine	cannabivarin	ACEA
			ACPA
7,10,13,16-docosatetraenoylethanolamide	oleamide	cannabielsoin	WIN 55,212-2
	N-arachidonoylglycine	cannabitriol	CP 55,940
	1- arachidonoylglycerol		HU-210
	N-arachidonoyltaurine		

[a] synthetic analogues of Δ^9-THC

2.1.1. Arachidonic Acid

Since the CYP-mediated metabolic pathways of endocannabinoids are closely similar to the metabolism of arachidonic acid (AA), this CYP-mediated metabolism of AA is reviewed briefly so as to elucidate theoretical possibilities of the oxidations at the "fatty acid" site of endocannabinoid molecules.

CYPs are known to metabolize arachidonic acid by epoxidation, ω/ω-1 hydroxylation, bis allylic oxidations, and hydroxylation to conjugated dienols (Fig. **1**) [42-44]. As a result, a wide variety of metabolites with biological activities are produced.

Arachidonic acid has four double bonds and epoxidation may occur on any of them. The products of epoxidation, epoxyeicosatrienoic acids (EET), may be further hydrolyzed to dihydroxyeicosatrienoic acids (diHETE). EET are produced by several hepatic and extrahepatic CYPs - CYP2C8, CYP2C9, CYP1A2, and CYP2B6, with the latter playing only a minor role (Table **2**). The ω/ω-1 hydroxylations of arachidonic acid to hydroxyeicosatrienoic acid (HETE) are catalyzed by the CYP4A, CYP2E1, and CYP4F families (Table **3**). Finally, bis-allylic oxidations and hydroxylations with double bond migration are catalyzed by CYP families 1A, 3A, 2C, and 4F (Table **4**).

2.1.2. Anandamide

Anandamide, the first known endocannabinoid, was isolated from the porcine brain by L. O. Hanuš and W. A. Devane from the team of prof. R. Mechoulam at Hebrew University, Jerusalem in 1992 [19]. AEA is hydrolyzed by the membrane-bound enzyme FAAH, with the highest level of expression in the liver. This degradative pathway is the most important in the regulation of AEA cellular and tissue concentrations. FAAH hydrolyses AEA towards arachidonic acid and ethanolamine. Thus the inhibition of FAAH may become a useful alternative in cannabinergic treatment options [38]. COX-2, an enzyme expressed in an inducible manner in inflammation, converts anandamide to several prostaglandin ethanolamides [46, 47]. Oxidation of the aliphatic chain by 12-LOX and 15-LOX yields 12- and 15-hydroxyanandamide. 12-hydroxyanandamide in particular may play a significant role in the modulation of neuronal functions via its influence on neurotransmitter levels [48].

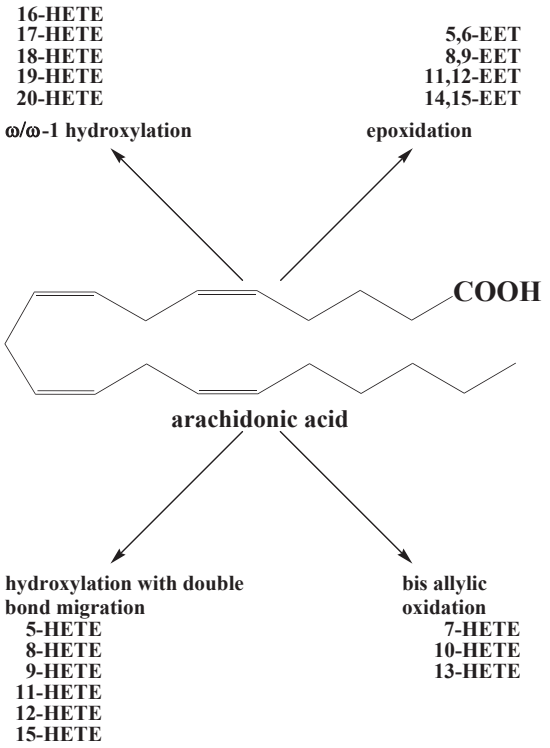

Fig. (1). CYP-mediated metabolism of AA [42-44].

CYPs involved in the degradation of AEA belong to the CYP3A and CYP4F families. The biodegradation of anandamide by CYPs was reported for the first time by Bornheim *et al*. in 1995 [49], who described its conversion by mouse liver microsomal fraction to approximately 20 products, whose structures were not identified. Furthermore, pretreatment with common CYP inducers such

Table 2. Epoxidation of AA catalyzed by cytochrome P450 enzymes [42-44].

CYP	Product	Tissue
2B6	14,15-EET, 11,12-EET	liver
2C8	14,15-EET, 11,12- EET, 8,9-EET	liver, lung, vascular endothelium
2C9	14,15- EET, 11,12- EET, 8,9-EET	liver, lung, vascular endothelium
2C19	14,15- EET, 8,9-EET	liver
2J2	5,6- EET, 8,9- EET, 11,12- EET, 14,15-EET	kidney, GIT, pancreas
1A2	8,9- EET, 11,12-EET	liver, lung

Table 3. ω/ω-1 hydroxylations of AA catalyzed by cytochrome P450 enzymes [44, 45].

CYP	Product	Tissue
4A11	19-, 20-HETE	liver, kidney
4F2	20-HETE	liver, kidney
4F3	hydroxy-LTB_4	polymorphonuclears
4F11	?	liver, kidney
4F12	18-HETE	liver, kidney
2E1	19(*S*)-HETE, 19(*R*)-HETE, 18(*R*)- HETE	

Table 4. Bis-allylic oxidations and hydroxylations of AA with double bond migration which are catalyzed by cytochrome P450 enzymes [42].

CYP	Product	Tissue
1A2	7-, 10-, 13-HETE	liver
3A4	7-, 10-, 13-HETE	liver
2C8	11-, 13-, 15-HETE	liver
2C9	12-, 13-HETE	liver
2C19	13-, 19-HETE	liver
4F8	13-HETE	liver, ovary/testes
4F12	18-HETE	liver, kidney, GIT

as dexamethasone increased the formation of metabolites 5-15 fold, and pre-treatment with a CYP3A antibody diminished the production of anandamide metabolites. Bornheim *et al*. also suggested that the CYP3A, CYP2B, and CYP1A subfamilies are involved in the metabolism of AEA in mouse liver microsomes. Similarly, Costa *et al*. suggested that CYP3A and CYP2B subfamilies are involved in the metabolism of anandamide in rat liver microsomes [50].

To the best of our knowledge, Snider *et al*. was the first to investigate the biotransformation sites of AEA by human liver and kidney microsomal CYPs, and identified the metabolites [51]. The biotransformation routes are fundamentally similar to those of AA. Anandamide may be epoxygenated by several CYPs at positions 5-6, 8-9, 11-12, and 14-15 to form four epoxyeicosatrienoic acid ethanolamides (EET-EAs). At least in some of them, this oxidative pathway is more bioactivation than degradation, since 5,6-EET-EA seems to be a more stable CB ligand than AEA itself [38]. Nevertheless, all EET-EAs may be further hydroxylated in the ω positions (again, similarly to AA metabolism) predominantly by CYP2D6 and thus 20-hydroxy-epoxyeicosatrienyl ethanolamides (HEET-EAs) are produced [51]. With 5,6-EET-EA and 14,15-EET-EA, hydroxylations at positions 16, 17, 18, and 19 were also described. EET-EA may be hydrolyzed by epoxyhydrolase to form dihydroxylated EET-EA [52].

Besides these reactions, ω- and ω-1-hydroxylations of AEA were also described [4, 38, 51, 53]. Details on the oxidative metabolism of AEA are shown in Figure **2**.

2.1.3. 2-arachidonoylglycerol

The main metabolic degradation of 2-AG is catalyzed by MAGL, FAAH, and α,β-hydrolase domains (ABHD) 6 and 12 [4, 38, 54]. The structure of 2-AG suggests that they are subject to the same oxidative metabolism as AA and AEA, which would lead to four regioisomeric 2-epoxyeicosatrienylglycerol derivatives (EET-G) (Fig. **3**). In contrast to this assumption, only 2 EET-G were identified to date – 2-(11,12-epoxyeicosatrienyl)-glycerol and 2-(14, 15-epoxyeicosatrienyl) glycerol, which are produced by CYP2J2 in rat kidney and spleen [55] and in bovine and porcine myocardium [56, 57]. These metabolites demonstrate regulatory effects on blood pressure, as was shown in the study of Awumey *et al*. [58].

As well as in EET-EA, the CYP-mediated epoxygenation of 2-AG to EET-G seems to be a kind of bioactivation, since these metabolites exhibit a tighter binding to CB receptors than 2-AG [56]. EET-G may be oxidatively decomposed by CYP2J2 to AA and glycerol.

2.1.4. N-arachidonoyldopamine

N-arachidonoyldopamine (NADA) is another endocannabinoid known to exert significant biological activity, e.g. in the immune system and pain perception [59, 60]. Besides hydrolysis to AA and dopamine by FAAH [35], NADA may be hydroxylated by rat microsomal protein in the presence of NADPH in the ω and ω-1 positions to form 19- and 20-hydroxyeicosatetraenyl dopamine (19-HETE-DA and 20-HETE-DA) [60] (Fig. **4**).

The question of epoxygenase reactions analogous to the CYP-mediated metabolism of AA and anandamide remains to be further elucidated.

2.1.5. Other Endocannabinoids and Cannabinoid-Like Compounds

The metabolic fate of the other endocannabinoids and cannabinoid-like compounds, such as virodhamine, oleamide, N-arachidonoylglycine, N-arachidonoylserine, or N-arachidonoyltaurine is not well understood, but hydrolysis with esterases or amide hydrolases is likely. On the other hand, hydrolysis of the ether group (e.g. noladin ether) by these enzymes is not likely, in contrast to oxidative metabolism, which may be an alternative degradative pathway for ethers, but there is still no direct evidence for this.

2.1.6. Concluding Remarks Concerning Endocannabinoid Metabolism

The metabolism of endocannabinoids via the hydrolytic pathway (namely FAAH) usually produces inactive metabolites, in terms of their affinity to bind to CB receptors. On the other hand, the products of the oxidative pathway may be both metabolites with a lower affinity to CB receptors (20-HETE-EA and 14,15-EET-EA) and products with a higher affinity to the CB (or PPAR) receptor than the parent compound, as shown with some 2-11,12-EET-Gs and 2-14,15-EET-Gs [38]. Moreover, a molecule with higher stability (5,6-EET-EA) can be produced. From this point of view, the inhibition of endocannabinoid degradation may be a valuable pharmacological target, and has been shown to produce anxiolytic-like and antidepressant-like effects in animal models [62]. Despite promising results from animal studies, there are no reliable data on efficacy from clinical studies. The clinical trials were focused mostly on safety; in general, the inhibitors were well tolerated and lacked typical "cannabinoid-like effects" [62]. There has also been a reported lack of efficacy in a clinical trial of an FAAH inhibitor in the treatment of osteoarthritic pain [63]. Modulation of the oxidative metabolic pathway was not studied in terms of a possible therapeutic approach; modulating the oxidative pathway would be problematic due to the involvement of CYPs (CYP2D6, CYP2C8, CYP3A) in the metabolism of other endogenous substances and possibly also co-administered drugs.

2.2. The Metabolism of Phytocannabinoids *via* Cytochrome P450 Monooxygenases

The term phytocannabinoids covers naturally occurring phytochemicals from *Cannabis sativa*, *Cannabis indica,* or *Cannabis*

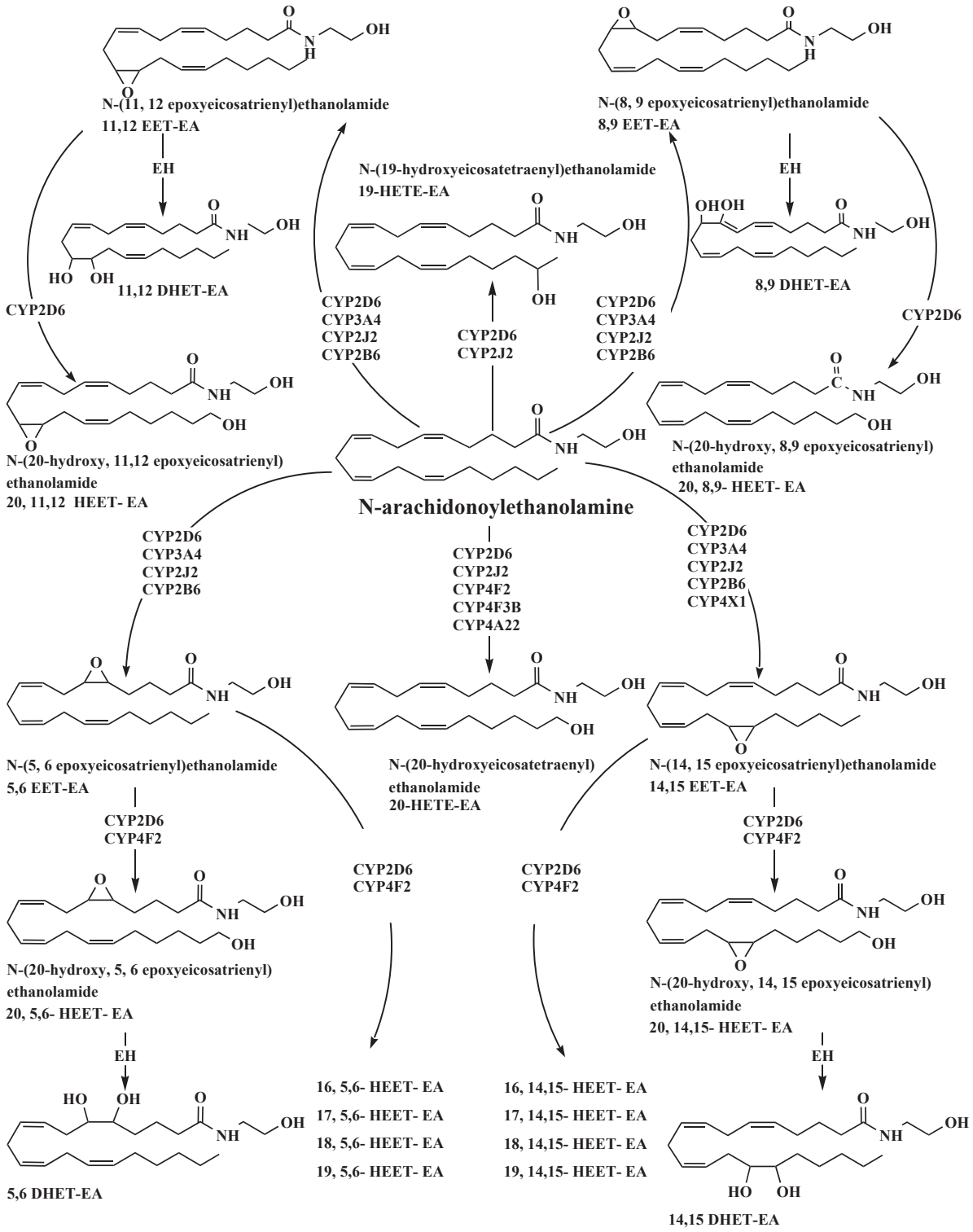

Fig. (2). CYP-mediated metabolism of anandamide [4, 38, 61].

ruderalis which are able to interact with cannabinoid receptors [64, 65]. Nearly 500 chemical entities were identified in *Cannabis* herbage, of which about 70 are phytocannabinoids. These compounds are present in the highest amounts in the viscous resin produced by the glandules of female cannabis inflorescence [64, 66]. As a result, several chemical classes of phytocannabinoids were defined by ElSohly *et al*. [66]: 1) cannabigerol type, 2) cannabichromene type, 3) cannabidiol type, 4) (-)-Δ^9-trans-tetrahydrocannabinol type, 5) (-)-Δ^8-trans-tetrahydrocanna-binol type, 6) cannabicyclol type, 7) cannabielsoin type, 8) cannabinol type, 9) cannabinodiol type, 10) cannabitriol type, and 11) miscellaneous type. In terms of this classification, the (-)-Δ^9-trans-tetrahydrocannabinol type, cannabinol type, and cannabidiol type are the most abundant and best known and studied. Out of 70 known phytocannabinoids, only Δ^9-THC, CBN, and CBD are reviewed in terms of oxidative metabolism by CYPs. No data were found for the other phytocannabinoids.

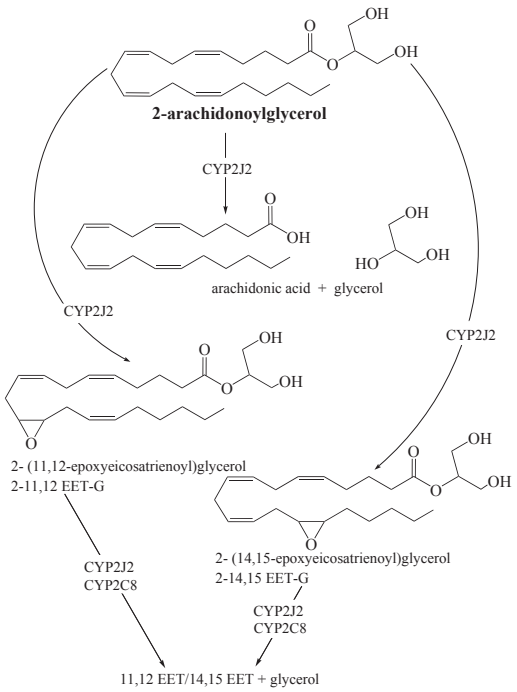

Fig. (3). CYP-mediated metabolism of 2-arachidonoylglycerol [4, 38].

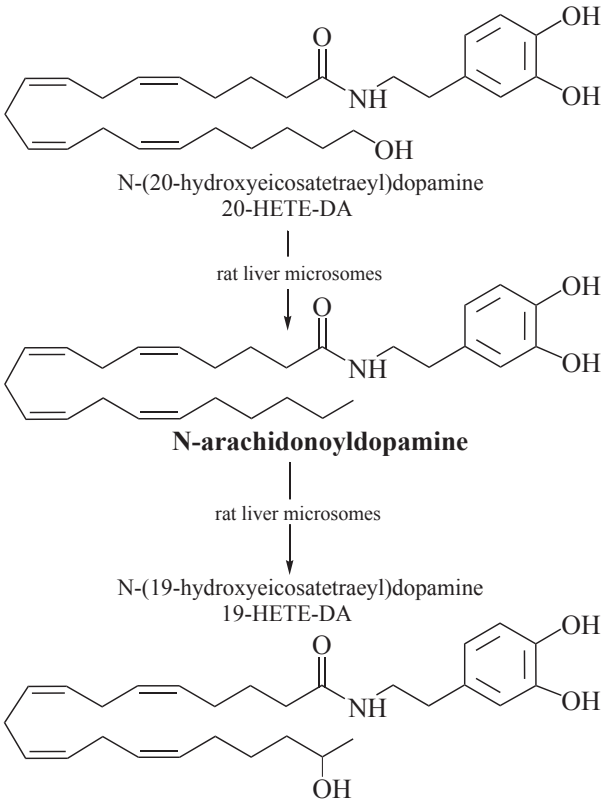

Fig. (4). CYP-mediated metabolism of N-arachidonoyldopamine [60].

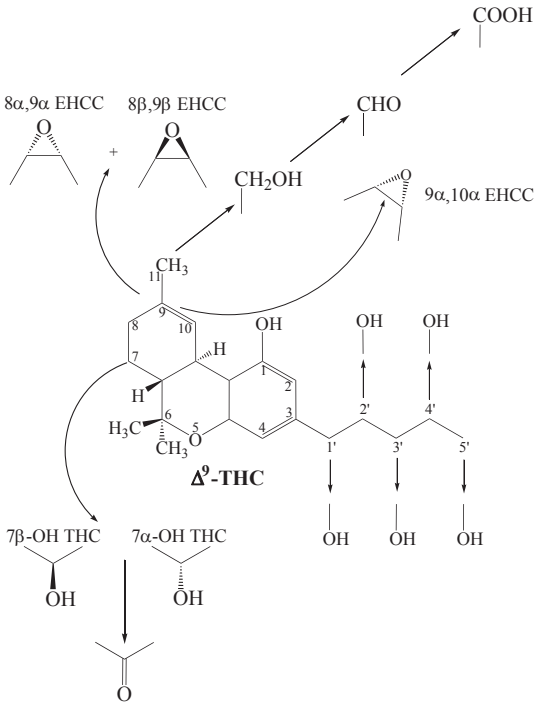

Fig. (5). Structure and CYP-mediated oxidative metabolism of Δ^9-THC [69].

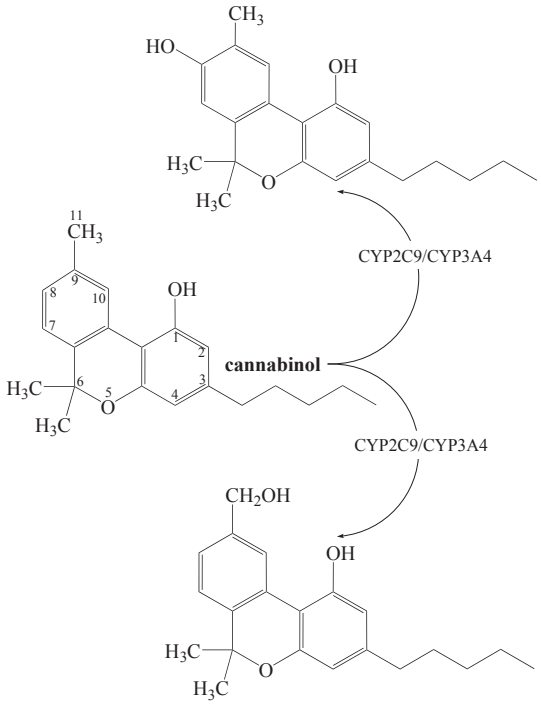

Fig. (6). Hydroxylation of CBN by CYP enzymes [69, 71].

2.2.1. Δ^9-tetrahydrocannabinol

The oxidative biotransformation of Δ^9-THC is quite complicated – approximately 80 metabolites were identified in humans [67]. The majority of the biotransformation processes of Δ^9-THC are catalyzed by CYPs (Fig. **5**). The first metabolite of Δ^9-THC was described back in 1970 by Nilsson *et al*., who used NMR to identify 11-hydroxy-Δ^9- THC in an extract from the incubation of a crude

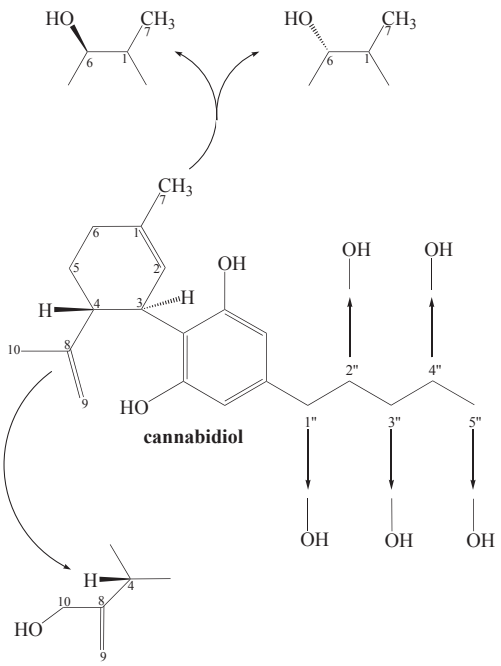

Fig. (7). Hydroxylation of CBD by CYP enzymes [72].

microsomal fraction of rabbit liver with Δ^9-THC [68]. This metabolite was formerly named 7-hydroxy-Δ^1-THC, because of the different numbering of the terpenophenolic ring in the past. The second most abundant hydroxy-derivative of Δ^9-THC is 8β-hydroxy-Δ^9-THC [69]. Later on, many other metabolites were identified, mostly in experiments with liver microsomes of different species, including humans, and the relative importance of CYPs was also examined, containing epoxygenated metabolites of THC [70]. The authors suggest that CYP2C9 and CYP3A4 probably play the most important roles in the oxidative metabolism of Δ^9-THC. Recently, Stout *et al*. [65] published a unique systematic review on the metabolism of cannabinoids.

Some of the metabolites of Δ^9-THC seem to be active (e.g. 11-hydroxy-Δ^9-THC) and therefore some authors think that the oxidative metabolism of Δ^9-THC may be necessary for the effects of cannabis [69].

2.2.2. Cannabinol

Cannabinol metabolism was studied by Kuzuoka *et al*. [71] and Watanabe *et al*. [69]. The chemical structure of CBN, being similar to Δ^9-THC, leads us to expect similar metabolic pathways mediated by microsomal monooxygenases. The hydroxylations occur at positions 8 and 11, and CYP2C9 and CYP3A4 are involved in their formation as reported in [65, 69, 71] (Fig. **6**).

2.2.3. Cannabidiol

The metabolism of cannabidiol was investigated both *in vivo* and *in vitro*. 33 different metabolites were found in human urine from a patient treated with CBD, 600 mg/day [72].

CBD is metabolized primarily by the enzymes CYP2C19 and CYP3A4 [65, 73]. The hydroxylation reactions occur at positions 6, 7, and positions 1″- 5″ of the aliphatic pentyl- and position 10 on the propenyl- substituent (Fig. **7**). Moreover, these metabolites may be further oxidized to form dihydroxylated metabolites and CBD-oic acid derivatives [72]. In an experiment with recombinant human liver microsomes, Jiang *et al*. proved that 7 out of 14 recombinant human CYP enzymes may be involved in CBD metabolism [73]. These include CYP1A1, CYP1A2, CYP2C9, CYP2C19, CYP2D6, CYP3A4, and CYP3A5.

Among monohydroxylated metabolites, the most abundant were 6α-OH-, 6β-OH-, 7-OH-, 1″-OH-, 2″-OH-, 3″-OH-, 4″-OH-, and 5″-OH-CBD [73]. The authors also confirmed the importance of CYP3A4 and CYP2C19 in the overall metabolism of CBD, namely in the 6α-, 6β-, 7-, and 4″-hydroxylations of CBD with the use of selective isoform-specific inhibitors and anti-CYP3A4 antibodies.

2.2.4. Other Phytocannabinoids

The metabolism of other phytocannabinoids has not been studied in humans, but the hydroxylation of several cannabinoids, including THC, CBD, CBN, cannabichromene (CBC), and cannabigerol (CBG) was studied *in vitro* in the liver microsomal fraction in several animal species [74]. In general, similar hydroxylation reactions are catalyzed by microsomal fractions, but particular CYPs responsible for the reactions were not identified. Hydroxylation occurs most abundantly at the allylic part of the molecule at positions C5' and C6'. Apart from C5' and C6' hydroxylations, hydroxylation also occurs at positions C2' and C1'' to C5'', and epoxidation at the double bond of the methylpentenyl group [74] (Fig. **8**).

Cannabigerol metabolism appeared to be similar to the metabolism of CBC. Hydroxylations at the terminal allylic group of the side chain were the most abundant reactions in the liver microsomes of all species except for mouse, where C6' or C7' epoxide was the most abundant [74] (Fig. **8**).

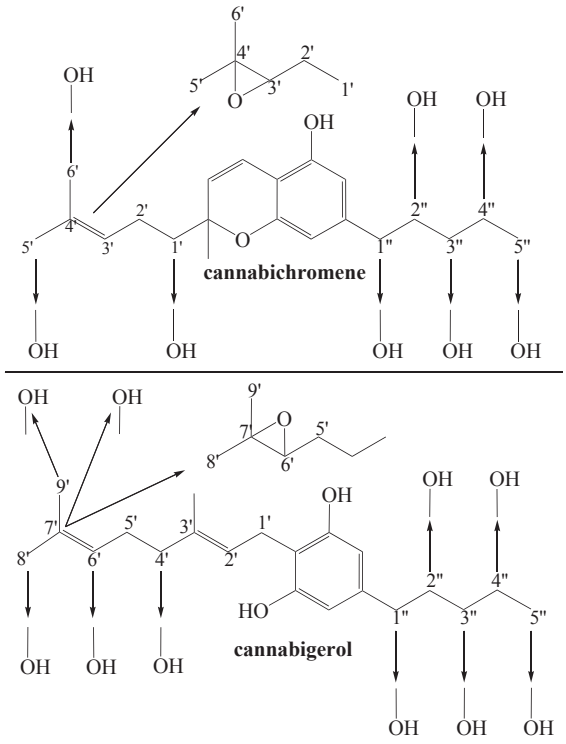

Fig. (8). Structure of CBC (**A**) and CBG (**B**) and positions of oxidative metabolism mediated by microsomal enzymes in mouse, rat, guinea pig, rabbit, hamster, gerbil, cat [74].

In summary, phytocannabinoids are extensively metabolized by CYP enzymes. For the most studied THC, CBN, and CBD, the enzymes CYP2C9, CYP2C19, and CYP3A4 catalyze the majority of hydroxylations. Most cannabinoids exhibit a similar pattern of oxidative metabolism [74]. At first, tricyclic cannabinoids (THC, CBD, and CBN) are the most effectively hydroxylated at the C-11 position and to a lesser extent also at the C-8 position. Various degrees of hydroxylation and epoxidation also occur at the carbons of the side chain in all cannabinoids, with the exception of CBN.

2.3. Synthetic Cannabinoids

Besides the substances isolated from natural materials, many other ligands of CB receptors were synthetized *in vitro*. Synthetic cannabinoids cover the whole spectrum of receptor ligand types from full agonists to inverse agonists, and their biological effects are therefore miscellaneous [75]. For the purposes of this review, synthetic cannabinoids are classified into groups of drugs for therapeutic purposes, molecules used as research tools, and abused drugs.

2.3.1. Synthetic Cannabinoids as Medicinal Products

Dronabinol (Marinol®) is a synthetic Δ^9-THC for oral use. It is approved for medical use in the United States and several other countries. Dronabinol is indicated for the treatment of anorexia associated with weight loss in patients suffering from AIDS and for the treatment of nausea and vomiting associated with cancer chemotherapy in patients who have failed to respond adequately to conventional antiemetic therapy [76]. It undergoes extensive first-pass hepatic metabolism, primarily by microsomal hydroxylation via multiple CYPs, yielding both active and inactive metabolites. Its principal active metabolite is 11-OH-Δ^9-THC [76].

Nabilone (Cesamet®) is a synthetic THC analogue for oral administration. It is registered in Canada, the USA, and several other countries for the treatment of nausea and vomiting associated with cancer chemotherapy in patients who have failed to respond adequately to conventional antiemetic treatments [77]. It has been suggested that the antiemetic effect of nabilone is mediated by its interaction with the cannabinoid CB1 receptor within the central nervous system. The metabolism of nabilone is extensive, and several metabolites have been identified. According to the data from Cesamet® SPC [77], there are at least two metabolic pathways involved in the biotransformation of nabilone. A minor pathway is initiated by the stereospecific enzymatic reduction of the 9-keto moiety of nabilone to produce the isomeric carbinol metabolite. Secondly, a metabolite of nabilone in faeces has been identified as a diol formed by reduction of the 9-keto group plus oxidation at the penultimate carbon of the dimethylheptyl side chain. In addition, there is evidence of extensive metabolism of nabilone by multiple CYPs. *In vitro* CYP inhibition studies using human liver microsomes showed that nabilone did not significantly inhibit the metabolic activity of CYP1A2, 2A6, 2C19, 2D6, and 3A4. In clinical use, nabilone is unlikely to alter the CYP-mediated metabolism of co-administered drugs [77].

Rimonabant (Acomplia®) was the first CB1 antagonist/inverse agonist to be approved for therapeutic use in metabolic syndrome and obesity [78]. Because of the significant risk of serious psychiatric adverse effects, it was withdrawn from the market [79]. *In vitro* experiments revealed CYP3A4 and amidohydrolase to be the major metabolic pathways involved in the biotransformation of rimonabant into inactive metabolites [80].

A buccal spray preparation containing *Cannabis* extracts, whose main active ingredients are Δ^9-THC and CBD (Sativex®), is now available in many countries including the UK, Spain, Italy, and Germany (not available in the US). It is used for the symptomatic relief of spasticity or neuropathic pain in multiple sclerosis and in cancer pain [81]. The active substances have the same structures as natural Δ^9-THC and CBD, therefore they undergo the same metabolic pathways.

2.3.2. Synthetic Cannabinoids as Experimental Tools

Compounds that are known to activate CB1 and CB2 receptors with approximately equal potency and that are most commonly used in the laboratory as CB1/CB2 receptor agonists fall essentially into one of four chemical groups: classical cannabinoids, nonclassical cannabinoids, amino-alkylindoles, and eicosanoids [29].

The classical group consists of dibenzopyran derivatives. The prototypic synthetic member of this group is HU-210, a synthetic analogue of (-)-Δ^8-THC. HU-210 displays a high affinity for CB1 and CB2 receptors, and also a high potency and relative intrinsic activity as a cannabinoid receptor agonist [29]. In the study of Kim *et al*. [82], the *in vitro* metabolism of HU-210 was investigated using human liver microsomes to characterize associated phase I metabolites. HU-210 was metabolized to yield a total of 24 metabolites, characterized as mono-oxygenated, mono-hydroxylated, di-oxygenated, or di-hydroxylated metabolites. The specific enzymes involved in the formation of the metabolites were not investigated.

The nonclassical group contains bicyclic and tricyclic analogues of Δ^9-THC that lack the pyran ring. The most widely used member of this group is CP 55,940. The oxidative metabolism of CP 55,940 was studied in mouse liver microsomes by Thomas *et al*. [83]. The mass spectral data indicated that five monohydroxylated metabolites had been formed differing in their position of hydroxylation. Two additional compounds were detected whose mass spectral data suggested that these metabolites were hydroxylated at two positions on the side chain. Side chain hydroxylation is consistent with the metabolic profile of Δ^9-THC [83].

The prototype of the aminoalkylindole group widely used in cannabinoid research is WIN 55,212-2. WIN 55,212-2 exhibits a relatively high efficacy at the CB1 and CB2 receptors and possesses CB1 and CB2 affinities in the low nanomolar range. The structure of WIN 55,212-2 bears no structural similarity to classical, nonclassical, or eicosanoid cannabinoids [84]. The metabolism of WIN 55,212-2 in rat liver microsomes was investigated in the study of Zhang *et al*. [85]. The HPLC chromatogram revealed two major and at least six minor metabolites derived from the parent compound. The two major metabolites (representing 60 to 75 % of the total metabolites) were each identified as dihydrodiol metabolites resulting from the arene oxide pathway. Three of the minor metabolites corresponded to structural isomers of the trihydroxylated parent compound, the other two represent monohydroxylated isomers and another was determined to be a dehydrogenation product. Specific enzymes involved in the formation of metabolites were not investigated.

Members of the eicosanoid group of cannabinoid CB1/CB2 receptor agonists have structures quite unlike those of classical, nonclassical, or aminoalkylindole cannabinoids. Two prominent members of this group are the endocannabinoids AEA and 2-AG.

The starting point for the development of the first CB1 selective agonists was the AEA molecule [29]. A number of agonists with significant selectivity for CB1 or CB2 receptors have been developed. Important CB1 selective agonists include the AEA analogues R-(+)-methanandamide, arachidonyl-2´-chloroethylamide (ACEA), and arachidonyl-cyclopropylamide (ACPA). Of these, both ACEA and ACPA share the susceptibility of AEA to enzymatic hydrolysis by FAAH [29, 86]. In contrast, methanandamide is less susceptible to enzymatic hydrolysis, probably because it is protected from this by the presence of a methyl substituent at the 1´ carbon [87].

The CB2 selective agonists most widely used as experimental tools have been the classical cannabinoid JWH-133, and the less selective aminoalkylindole JWH-015 [29]. The *in vitro* phase I metabolism of JWH-015 using human liver microsomes was studied by Mazarino *et al*. [88]. A total of 18 metabolites were formed. The biotransformation pathways detected consist of mono-hydroxylation, di-hydroxylation, tri-hydroxylation, carboxylation, N-dealkylation, dehydratation, and combinations of them, confirming data from the study with rat liver microsomes [89]. Specific enzymes involved in the oxidative metabolism were not studied.

2.3.3. Synthetic Cannabinoids as Abused Drugs

Synthetic cannabinoids recently became the largest group of compounds to be monitored in Europe by the EU Early Warning System on new psychoactive substances [90]. “Legal high” products containing synthetic cannabinoids (SCs) have probably been sold as herbal smoking mixtures since 2006. In 2008, a synthetic

cannabinoid JWH-018 was detected for the first time in a herbal mixture. In 2014, a further 30 new synthetic cannabinoids were reported for the first time, bringing the total number reported by the EU Early Warning System to 137 in February 2015 [91]. New drugs are synthesized by slight modifications of the known psychoactive "parent" compound, to obtain similar - or even stronger - psychoactive effects and to circumvent the law, being not yet included in the lists of controlled substances [92]. The common property of all SCs is that they interact with the CB1 and CB2 cannabinoid receptors and elicit cannabimimetic effects similar to Δ^9-THC. They are synthesized in clandestine laboratories and illegally added to commercial products such as herbal blends (these are sold under brand names such as "Spice" and "K2"), which are claimed to be air fresheners or herbal incenses. The most common way of administration is smoking.

The majority of compounds are chemically unrelated to Δ^9-THC. To date hundreds of SCs were categorized into the following structural groups: adamantoylindoles, aminoalkylindoles, benzoylindoles, cyclohexylphenols, dibenzopyrans, naphthoylindoles, naphthylmethylindoles, naphthylmethylindenes, naphthoylpyrroles, phenylacetyl-indoles, tetramethylcyclopropylketone indoles, quinolinyl ester indoles, and indazole carboxamide compounds [93].

Only limited data are available on the metabolism of the huge variety of synthetic cannabinoids. Due to the insufficient toxicity data, controlled human drug administration studies are not feasible. Therefore, *in vitro* experiments are alternative approaches for metabolite profiling and structure elucidation. Most of the recent *in vitro* metabolite-profiling studies utilize human liver microsomes or human hepatocytes. So far, we have identified such studies for the following synthetic cannabinoids: AB-CHIMINACA [94], AB-FUBINACA [95-97], AB-PINACA [95, 96, 98], 5F-AB-PINACA [98], ADB-FUBINACA [95], AKB-48 [99, 100], 5F-AKB-48 [100], AM-2201 [101, 102], APICA [103], CP 47,497 [104], HU-210 [82], JWH-015 [88], JWH-018 [105-108], JWH-073 [108], JWH-073 4-methylnaphthoyl analogue [108], JWH-122 [108-110], JWH-200 [109], JWH-210 [88], MAM-2201 [110], PB-22 [95, 111], 5F-PB-22 [95, 111], RCS-4 [112], RCS-8 [113], STS-135 (5F-APICA) [103, 114], UR-144 [102], and XLR-11 [115].

In vitro metabolite-profiling studies with subsequent confirmation in authentic specimens provide critically important information for the identification of suitable *in vivo* biomarkers to document the intake of SCs in clinical and forensic settings.

Two of the above-cited investigations also focused on the identification of specific CYP enzymes involved in oxidative metabolism. Chimalakonda *et al*. [101] studied the oxidative metabolism of [1-naphthalenyl-(1-pentyl-1H-indol-3-yl]-methanone (JWH-018) and its fluorinated counterpart AM-2201 [1-(5-fluoropentyl)-1H-indol-3-yl]-1-naphthalenyl-methanone. Kinetic analysis using human liver microsomes and six human recombinant CYPs (CYP1A2, 2C9, 2C19, 2D6, 2E1, and 3A4) identified CYP2C9 and CYP1A2 as the major CYPs responsible for the generation of hydroxylated and carboxylated metabolites of JWH-018 and AM-2201. The contribution of CYP2C19, 2D6, 2E1, and 3A4 in the hepatic metabolic clearance of these synthetic cannabinoids was minimal. These findings are further supported by the results of another investigation that observed a concentration-dependent inhibition of JWH-018 and AM-2201 oxidation in human liver microsomes by the CYP2C9- and 1A2-selective chemical inhibitors sulfaphenazole and α-naphthoflavone, respectively [116]. The study of Holm *et al*. [100] was focused on the elucidation of CYP enzymes involved in the oxidative metabolism of N-(1-adamantyl)-1-pentyl-1H-indazole-3-carboxamide (AKB-48, also known as APINACA). Metabolite formation was screened using a panel of nine recombinant CYPs (CYP1A2, 2B6, 2C8, 2C9, 2C18, 2C19, 2D6, 2E1, 3A4) and compared the metabolites formed to human liver microsomal incubations with specific inhibitors against CYP2D6, 2C19, and 3A4, respectively. The results demonstrate that CYP3A4 is the major CYP responsible for the oxidative metabolism of AKB-48, preferentially performing the oxidation on the adamantyl moiety of the compound. Such detailed data are not available for other SCs. However, SCs are structurally diverse and the involvement of other CYPs and non-CYP enzymes in phase I biotransformations is likely. This was recently demonstrated for the quinolineindole synthetic cannabinoids PB-22, 5F-PB-22, and BB-22, where carboxylesterase 1 hydrolyzes an ester bond [96]. In addition, carboxylesterase 1 also hydrolyzes the primary amide group of two other synthetic cannabinoids, AB-PINACA and AB-FUBINACA [96].

Based on the recent evidence, synthetic cannabinoids are extensively metabolized in phase I and phase II biotransformation reactions. CYPs are involved in phase I metabolism. Oxidative metabolism forms preferably mono-, di-, and tri- hydroxylated, carboxylated, and N-dealkylated metabolites. Unlike Δ^9-THC metabolism, several SC metabolites retain a high affinity for the CB1 and CB2 receptors and exhibit a range of intrinsic activities. The majority of phase II SC metabolites are glucuronides.

3. CANNABINOIDS AS REGULATORS OF CYP METABOLIC ACTIVITY

The therapeutic use of cannabis, its extracts and synthetic cannabinoids together with the pleiotropic regulatory activity of the endocannabinoid system and the role of CYP in the metabolism of cannabinoids raises the question of drug-drug interaction with co-administered medicines. The decrease in the metabolic activity of individual CYPs can increase the plasma levels of their substrates, and symptoms of toxicity could appear. In the opposite direction, increased CYP activity will decrease the efficacy of its substrates, and can lead to the failure of a therapy.

The interactions between cannabinoids and CYPs could be simply caused by the competition of two substrates at the same CYP protein. Nevertheless, the huge metabolic capacity of CYP and involvement of alternative metabolic pathways decreases the clinical importance of such drug-drug interplay. The second possibility involves the direct interaction of cannabinoids with the CYP protein in a non-competitive (allosteric) manner, which usually leads to enzyme inactivation or a slowdown of the metabolic reaction. On the other hand, the possibility of allosteric induction for some substances was also described [117]. The final possibility for how cannabinoids can influence the CYP-mediated metabolism of co-administered drugs is by targeting the expression of CYP genes. This possibility is likely, due to the involvement of the endocannabinoid system in many physiological functions, including some metabolic pathways [118, 119], and its interaction with many other neuronal systems and circuits which might also be involved. Therefore, the results of research focused on the direct interaction of cannabinoids with CYP enzymes and the influence of cannabinoids on the metabolic activity assessed after systemic administration or in models using living cells with intact signal pathways could give different results and are described separately.

3.1. Direct Interactions of Cannabinoids and CYP Proteins

Rimonabant was tested for the ability to bind to CYPs in the model of human liver microsomes (HLM). Approximately 19 % of the metabolites produced were covalently bound to CYPs [120]. Therefore it is not surprising that a mechanism-based inhibition of CYP3A4 and decrease in the metabolic activity over 70 % was described. A search for other CB1 antagonists for possible therapeutic use led to the synthesis of aminopyrazine CB1 inverse agonists. The chlorine in the para position of the 5-phenyl ring was found to be responsible for the inhibition of CYP3A4 and its substitution with a trifluoromethyl moiety did not change the potency at the CB1 receptor, increased aqueous solubility, and decreased potential for CYP3A4 inhibition [121]. The negative psychotropic effects of rimonabant could be eliminated with analogues not crossing the blood-brain barrier but with the effect on peripheral CB

receptors. LH-21, a CB1 antagonist with poor brain penetration, is similar to rimonabant in both its anorectic affect and also CYP inhibiting activity [122]. It inhibits the metabolic activity of CYP3A4, 2C9, and 2D6 with the IC_{50} of 1.62, 8.14, and >105 μM, respectively. The inhibition was weaker in comparison to the control inhibitors ketoconazole, sulfaphenazole, and quinidine. LH-21 is reported to be a moderate inhibitor of CYP3A4 and CYP2C9 and weak inhibitor of CYP2D6.

Ashino *et al*. described the inhibition of the CYP1A2 metabolic activity of different synthetic cannabinoids with the indole structure moiety in the model of mouse liver microsomes [123]. MAM-2201 and JWH-019 with the naphtoylindole structure were the most potent inhibitors, and decreased the activity to 47.7 % and 64.3 % of the control values at a concentration of 100 μM. Most of the adamantoylindole derivatives inhibited the activity weakly (up to a 10 % decrease) except for STS-135, which exhibited an inhibition comparable to naphtoylindole ligands. The last molecule tested with the tetramethylcyclopropylindole core exhibited moderate inhibitory activity with a decrease to 73.4 % of the control values at a 100 μM concentration.

Δ^9-THC, CBN, and CBD are the most studied substances of the phytocannabinoids group in terms of CYP interactions. All of them competitively inhibit the CYP1A enzyme family, but with different strengths [124]. The most potent inhibitor of CYP1A1 is CBD followed by CBN, while the inhibition of CYP1A2 and CYP1B1 was stronger after CBN treatment. All the enzymes were inhibited by Δ^9-THC less potently, with a low selectivity for individual CYP1 enzymes. The subsequent studies revealed the pentylresorcinol [125] or methylresorcinol [126] structures to be important for the direct inhibition of CYP1A1. The same moiety is probably involved in the potent CYP2B6 inhibition by CBD [127], while Δ^9-THC and CBN have a weaker effect. All of the substances decreased the activity in a mixed fashion in comparison to the inhibition of CYP2A6, which is non-competitive, and the inhibition potency of all three phytocannabinoids was weaker than the inhibition of CYP2B6. Similar results were obtained with CYP2C9, which was also inhibited by all three substances [128]. The strongest inhibition was reported for CBN, followed by Δ^9-THC and CBD. The same substances were incubated with rat liver microsomes, and the 16α- and 2α–hydroxylation of testosterone was assessed [129]. The reaction is mediated by CYP2C11, which is considered to be the counterpart of human CYP2C9 [130]. However, the results are different from those obtained in the human studies. The inhibition was only detected in CBD-treated samples, while Δ^9-THC and CBN did not influenced the enzyme activity. Both CBN and Δ^9-THC decreased the omeprazole 5-hydroxylase activity, indicating their inhibitory effect on CYP2C19 [131], and at least one of the free phenolic groups and pentyl side chain are the structural determinants of this effect. The activity of CYP2D6 is again most sensitive to the effect of CBD [132]. Its IC_{50} values were 2-4 times lower than those of Δ^9-THC and CBN. The CYP2D6 inhibition potency of these two is similar. Similarly to the influence on the enzymes of the CYP1A family, CYP3A enzymes are differentially sensitive to the effect of the major phytocannabinoids. CBD inhibited the activity of CYP3A4 and CYP3A5 most potently, while the influence of all three substances on the activity of CYP3A7 was comparable [133]. The inhibition of 3A4 can also be indirectly evidenced by the suppression of cyclosporine A metabolism in both mouse and human liver microsomes preincubated with CBD [134]. The effect of phytocannabinoids on the activity of 17α-hydroxylase (CYP17) was tested in the model of rat testis microsomes. However, CBD was the most potent inhibitor of CYP enzymes in most of the documented experiments, its inhibitory effect on the CYP17 activity was the weakest, and required IC_{50} concentrations over 290 μM [135]. On the other hand, Δ^9-THC and CBN inhibited the enzyme's activity with EC_{50} values of 42.8 μM and 32.9 μM, respectively. The inhibition of individual CYPs by phytocannabinoids is in accordance with the older data obtained with less selective CYP substrates [136-138].

The clinical relevance of the presented data is questionable, due to the high concentrations of the tested drugs used in *in vitro* studies and their correspondence to plasma levels reached when phytocannabinoids are used therapeutically or abused. When a marijuana cigarette (15.8 mg Δ^9-THC) is smoked, the peak plasma concentrations of Δ^9-THC is reported to be only 268 nM [139]. Similarly after CBD and CBN (20 mg) administration by smoking a cigarette, the levels reached 363 nM and 406 nM, respectively [140, 141]. Moreover, the plasma levels of synthetic Δ^9-THC dronabinol reached a nanomolar concentration when administered in the recommended therapeutic doses [124]. The review of inhibition constants (Ki) values are presented in Table **5**. It is obvious that clinically relevant inhibition of CYP by phytocannabinoids is likely for enzymes of the CYP1 family with CBN and for the CYP1A1, 2B6, 2C19, and 3A5 enzymes with CBD. The inhibition of CYP enzymes by THC is probably too weak to cause a clinically significant interaction with the co-administered drugs.

3.2. The Influence of Cannabinoids on CYP Metabolic Activity – *In vivo* and Cell Culture Models

The possible discrepancy in the results of direct interaction experiments and the systemic administration of drugs can be demonstrated in the work of Bornheim *et al*. [142]. Different analogues of THC were tested for both direct interaction with naïve mouse liver microsomes, and microsomes sampled 2 hours after the systemic administration of THC analogues to mice. While in the direct interaction part of the study, some of the tested substances inhibited the activities of CYP3A and CYP2C, the same molecules produced no effect after systemic drug administration.

An important factor influencing the result of the study is the duration of drug pre-treatment before the activity is assessed. The results after a single dose of a drug and after the repeated administration can be different. After the repeated administration of a drug, higher values of plasma/tissue concentrations can be reached than with a single dose. Moreover, there is probably interplay between cannabinoids and endocannabinoid CB receptors, which can lead to changes in signal pathways including CYP liver regulation mechanisms. The subsequent change could therefore be time-dependent, such as for instance the induction of the enzyme activity by the mechanism of increased gene transcription, and *de novo* protein synthesis usually takes at least several hours from the drug administration. An example can be found in the study concerning the effect of the synthetic cannabinoid receptor agonist CP 55,940 on CYP activity in rats [143]. The only parameter that changed after a single intraperitoneal dose of the drug (0.4 mg/kg) was an increase in the oxygen consumption by the brain and liver. However after 11 days of treatment with the same dose of the substance the increased brain and hepatic mitochondrial respiration disappeared, and the P-450 reductase, benzo(A)pyrene hydroxylase, and ethoxycoumarin deethylase activities as well as the protein content of the liver microsomes were increased.

The results of the *in vivo* experiment undoubtedly also depend on the experimental model used. When CP 55,940 was administered to mice (intraperitoneally, 0.5 mg/kg/day) for 5 or 24 days, the microsomal protein content was decreased after the latter type of administration [144], in contrast to the previous results with the same substance in rats. Nevertheless, the activity of CYP2E1, measured as p-nitrophenol oxidation, was unaffected. These data correspond with the results of Yang *et al*. from HepG2 cells incubated with a natural CB receptor agonist CBD [145]. Other researchers reported an increase in the expression of CYP2E1 and CYP2C6, together with an increased amount of total CYP hepatic content in mice after a single dose or repeated administration of hashish [146].

Table 5. Inhibition of CYP metabolic activity *in vitro* [124, 125, 127-129, 131-133, 135].

	1A1	1A2	1B1	2A6	2B6	2C9[1]	2C11[2]	2C19	2D6[1]	3A4	3A5	3A7	17[3]
CBD	0.16[C]	2.69[C]	3.63[C]	55.0[N]	0.69[M]	5.6[C]	19.9 - 21.6[C]	0.793[M]	2.42	1.0[C]	0.195	12.3[C]	124.4[M]
Δ^9-THC	4.78[C]	7.54[C]	2.47[C]	28.9[N]	2.81[M]	1.5[M]	none	1.93[M]	17.1[A]	>50[A]	35.6[A]	30.3[A]	15.9[M]
CBN	0.54[C]	0.08[C]	0.15[C]	39.8[N]	2.55[M]	0.93[C]	none	no data	12.3[A]	>50[A]	>50[A]	23.8[A]	4.5[M]

[A]Half maximal inhibitory concentration (IC_{50}) in μM. Other reported values are inhibition constants (Ki) in μM; [M]Mixed type of inhibition; [C]Competitive type of inhibition; [N]Non-competitive type of inhibition; Enzymes are recombinant human proteins, if not indicated different; [1] Human liver microsomes.; [2] Rat liver microsomes; [3] Rat testis microsomes.

The variability in the experimental design thus leads to a high variation in the results obtained. However, if the data from the experiments with the same designs are compared, the variability disappears. The first data regarding the influence of phytocannabinoids on the activity of CYP in the animal models were homologous. An extract from cannabis prolonged the sleeping time of mice treated with the CYP substrate pentobarbitone, documenting the inhibition of its metabolism [147]. Similar results were obtained with CBD [148], the most studied cannabinoid in terms of CYP interactions. Moreover, CBD inhibited the enzyme activities of various more or less selective CYP substrates including p-nitroanisole O-demethylase [137], aniline hydroxylase [137], hexobarbital hydroxylase [149], erythromycin N-demethylase [149], 6β-testosterone hydroxylase [149], and aminopyrine N-demethylase [150].

The influence of CBD on single CYPs was evaluated in a number of studies. CBD administered to mice at a dose of 120 mg/kg inactivated CYP2C and CYP3A proteins by covalent binding after a single dose [151]. Whereas after repeated administration of the same dose, the expression of the mRNA of these two enzymes increased as well as the protein content, while the activity remained unchanged [152], probably because of the inactivation reported previously. Similarly, in rats CBD decreased the total CYP hepatic content after repeated administration [153]. Further research revealed decreased activities of CYP17 and CYP2C [154]. The influence of CBD on CYP2C activity is probably also sex-dependent [155].

The most recent results from human cell cultures described the induction of CYP1A enzymes by marijuana smoke [156, 157], Δ^9-THC [157-159], and CBD [159], probably mediated by the aryl hydrocarbon receptor (AhR) [157, 159].

One of the great advantages of animal models is the possibility of studying the effects of prenatal exposure to drugs. Maternal exposure to Δ^9-THC, CBD, and CBN increased the levels of hepatic CYP content, whereas postnatal exposure had the opposite effect in male rat offspring [160].

3.3. Drug-Drug CYP-Mediated Interactions of Cannabinoids

The interspecies differences in the CYP system [161] creates a great barrier to the clinical approximation of data obtained from animals. Nevertheless, in most preclinical studies either with Δ^9-THC or CBD, the results correspond to *in vitro* experiments, and generally these cannabinoids are reported to be CYP inhibitors. CBD significantly decreased the metabolism of CYP substrates, e.g. cocaine [162], anandamide [163], cyclosporine A [134], or THC [162, 164, 165]. However, the dose of CBD necessary to evoke the effect was 30 mg/kg in mice, which is higher than any dose of CBD used in clinical practice.

Although there is enough evidence of the influence of cannabinoids on the total hepatic amounts of CYPs and their activities from preclinical studies, the clinical data on the topic are scarce. The risk of interaction is significantly dependent on the dose administered. Rimonabant (40 mg/day for 8 days) did not affect the steady-state concentration of co-administered digoxin, midazolam, warfarin, nicotine or oral contraceptives [166]. The effect of medicinal cannabis (Bedrocan®), containing 18 % Δ^9-THC and 0.8 % CBD administered for 15 days, on the levels of irinotecan and docetaxel were tested in oncologic patients [167]. Similarly, no significant change in the clearance or exposure to the monitored drugs was observed. Finally, the summary of medicinal product characteristics of the synthetic Δ^9-THC and CBD mixture (Sativex®) declares that no interactions with CYP3 substrates are expected [168]. It has to be stressed, that these results describe the risk of interaction of low doses of CBD. Nadulski *et al*. tested the effect of 5.4 mg of CBD on the pharmacokinetics of 10 mg of Δ^9-THC [169] and concluded that the inhibitory effect of CBD on CYP in this dose is small compared to the variability of CYP activity caused by other factors. This conclusion could be generalized for the clinical use of CBD at doses of up to 5 mg per day. On the other hand, higher doses of CBD in the range 8-25 mg/kg/day were described to markedly inhibit the metabolism of hexobarbital [170] or clobazam [171], both CYP3A4 substrates. The interaction potential of the higher doses of CBD with CYP3A4 substrates is therefore clinically relevant.

4. POSSIBLE INVOLVEMENT OF ENDOCANNABINOID SYSTEM IN THE REGULATION OF CYP EXPRESSION AND CYP METABOLIC ACTIVITY IN THE LIVER

The regulation of CYP metabolic activity is complex in nature, including many endogenous and exogenous factors determining the actual amounts of enzymes and their catalytic activities. Besides the exogenous ones, genetic polymorphisms, and the role of hormones are known to be endogenous factors regulating the expression and activity of CYPs. Recently, the involvement of some neuronal systems was reported [172-174]. The regulatory role of the endocannabinoid system raises the question of its participation in this process, too. Here, we hypothesize that the central and peripheral pathways of the endocannabinoid system and interplay between cannabinoid ligands and various receptors are probably involved in CYP regulation.

4.1. The Role of Central Endocannabinoid System in the CYP Regulation

It is known that genes coding for various CYPs are regulated by endogenous hormones, which are under the control of the central nervous system. It has been also shown that changes in the brain dopaminergic, noradrenergic, and serotonergic systems can affect hepatic CYP expression [175]. The central endocannabinoid system modulates neurotransmission at inhibitory and excitatory synapses, and therefore could be also involved in the regulation of CYP activity. Thus the endocannabinoid system and possible interactions with other neuronal systems, its impact on the hypothalamic-pituitary axis (HPA) and on the levels of circulating hormones are reviewed.

4.1.1. The Brain and Endocannabinoid System

Most central cannabinoid effects are mediated by the CB1 receptors widely expressed throughout the brain, where they are the most abundant in regions controlling a number of key functions [30, 176]. Therefore, CB1 receptors are present at a high density in the basal ganglia, frontal cortex, hippocampus, and cerebellum, and at a

moderate/low density in the nucleus accumbens, hypothalamus, and amygdala [177].

The predominant localization of CB1 receptors at the presynaptic terminals of neurons plays an important regulatory role, because they can influence the release of a number of different neurotransmitters [178, 179]. The postsynaptic localization of CB1 receptors has been also observed, but only rarely [177]. The endocannabinoids are synthesized and released by postsynaptic neurons, and they act as retrograde neuronal messengers at presynaptic CB1 receptors. The activation of CB1 receptors by endocannabinoids suppresses the presynaptic release of γ-aminobutyric acid (GABA), glutamate, acetylcholine, serotonin, and noradrenaline [179].

Another reason for the increased complexity of endocannabinoid signaling is the evidence that CB1 receptors form heteromers with a variety of other GPCRs [180]. CB1 receptors can form functional heterodimers with μ-opioid receptors [181], orexin-1 receptors [182, 183], adenosine A_{2A} receptors [184, 185], serotonergic (mainly 5-HT_3) receptors [186, 187], or dopaminergic D_2 receptors [188]. Another possible interaction between the dopaminergic and endocannabinoid system is indirectly via the GABAergic [189, 190] and glutamatergic system [191, 192].

Endocannabinoid signaling in the brain may influence liver CYP activity, but the signal has to be somehow mediated from the CNS to the periphery. It is known that such signal transduction could be found in hormones released from HPA and leading to subsequent changes in the hormonal levels released from peripheral organs. Hormones influence not only hepatic glucose or lipid metabolism, but also the expression of genes coding for different CYP liver enzymes [193-196].

Dopaminergic pathways which could possibly contribute to the release of hormones are the mesolimbic and the tuberoinfundibular pathways. It was reported that stimulation of the dopaminergic system increases growth hormone (GH) [197, 198], adrenocorticotropic hormone (ACTH), and corticosterone levels [199, 200]. In contrast, the levels of thyroid-stimulating hormone (TSH) after activation of the dopaminergic system were decreased [198, 201]. The ability of the brain dopaminergic system to affect liver CYP expression by altering the levels of pituitary hormones was first reported in the studies of Wójcikowski *et al*. [174, 202]. Dopaminergic D_2 receptors were identified to be involved in the regulation of hormones and liver CYP enzymes in the mesolimbic pathway [174].

Noradrenaline is one of the main neurotransmitters controlling the release of GH [172, 203]. It also controls the production and release of corticotropin-releasing hormone (CRH) and thyrotropin-releasing hormone (TRH) [204]. The release of somatostatin is regulated by noradrenaline, among other neurotransmitters and neuropeptides. It was reported that a damage of the noradrenergic innervation in the arcuate nucleus (ARC) or periventricular hypothalamic nucleus (PVN) proved an opposite effect on the regulation of CYP expression [172]. This can be explained by the fact that destruction of the noradrenergic innervation in the ARC leads to a decrease of the noradrenaline level and also to a decrease of the level of GH. While destruction of the noradrenergic innervation in the PVN causes a decrease of the level of noradrenaline, but the plasma concertation of GH are increased probably due to the decreased secretion of somatostatin. The involvement of the noradrenergic system in CYP regulation was confirmed by Kot *et al*. [205]. Again the hormones were identified to be the mediators of the effect from the brain to the liver. The same author reported the serotonergic system to also take part in CYP neurohumoral regulation [173, 206, 207].

The influence of exogenous cannabinoids on the secretion of pituitary hormones has been known for a long time, but the role of endocannabinoids in the neuroendocrine system is not fully understood yet [208, 209]. Based on available studies, two options for how endocannabinoids influence HPA are suggested: (i) a direct effect mediated by endocannabinoids receptors and/or (ii) an indirect effect when cannabinoids change the activity of the endocannabinoid system and this modulates the activity of other neuronal systems controlling HPA. CB1 receptors are expressed in various regions of the brain, and were also detected in the hypothalamus and pituitary gland [210, 211]. Many studies describe the influence of cannabinoids or endocannabinoids on the levels of CRH, GH, TSH, prolactin (PRL), and luteinizing hormone (LH), but their findings are often contradictory [208, 212-216]. It seems that the main structure of endocannabinoid influence on neuroendocrine functions is the hypothalamus, where they act as retrograde messengers activating the CB1 receptors. Importantly, it was revealed that endocannabinoids are involved in the rapid negative feedback actions of glucocorticoids (GCs) in parvocellular neurons of the hypothalamic paraventricular nuclei (PVN) containing CRH. GCs, after binding to glucocorticoid (GR) receptors localized in the PVN, activate the postsynaptic GPCRs. This leads to the synthesis and release of endocannabinoids. These endocannabinoids act as retrograde messengers to the CB1 receptors located at presynaptic glutamate terminals and inhibit glutamate release [217]. These findings thus provide a possible mechanism for the rapid feedback inhibition of the hypothalamic pituitary adrenal axis by GCs. Moreover, the CB1 receptors and endocannabinoids are found throughout all of the extrahypothalamic sites that regulate PVN neuronal activation, such as the hippocampus, prefrontal cortex, amygdala, bed nucleus of the stria terminalis, and midbrain monoaminergic nuclei, such as the locus coeruleus and dorsal raphe [218]. These brain regions are the most likely sites of interaction between the endocannabinoid system and other nervous systems [190, 219-221].

Once the CB ligands directly change the activity of the endocannabinoid system or indirectly the activity of other neurotransmitters and the HPA is changed, hormones start the signal transduction towards the liver (Fig. **9**). The regulation of liver CYP enzymes by hormones involves binding the hormone to the nuclear receptor and translocation of the ligand-receptor complex into the cell nucleus. The expression of specific genes including CYP enzymes is activated or inhibited. GH, GCs, and TSH are ligands of nuclear receptors able to change the expression of CYP genes [222-224]. The influence of hormones on the transcription activity of CYP genes is described at a glance in Table **6**.

4.2. The Involvement of Peripheral Cannabinoid Receptors in the CYP Regulation

When administered systemically, cannabinoids are able to target both the regulation centers in the brain and the receptors in peripheral tissues including the liver. Except for the direct interaction with CYPs (see chapter 3.1.) there is a possibility of the influence of cannabinoids on the receptors of target cells. The receptor specificity of cannabinoids is broad due to their high structure variability, therefore there are many receptors which might be activated or inhibited with regard to the properties of the ligand. Here we describe the evidence of interaction between cannabinoids and peripheral receptors involved in the signal pathways of CYP regulation and the role of these receptors in CYP regulation.

The key ligand-activated transcriptional regulators of CYPs are the pregnane X receptor (PXR), constitutive androstane receptor (CAR), retinoid X receptors (RXRs), peroxisome proliferator-activated receptors (PPARs), glucocorticoid receptors (GRs), and aryl hydrocarbon receptor (AhR) [222].

Briefly, PXR plays a key role in the regulation of the CYP2B6, CYP2C, CYP2A6, CYP3A, and CYP4F12 genes [238-245]. Agonists of PXR induce these CYP enzymes. In addition to the induction of CYP enzymes, PXR activation also represses CYP7A1 expression as a protective feedback in response to the accumulation of bile acids in the liver [224, 246].

Table 6. Hormonal regulation of CYP genetic transcription [175, 193-195, 225-237].

GC	T3	GH	PRL
↑2A6[b]	↓1A1/2[a]	↑1A2[b]	↓2C11[a]
↑2B6[b]	↓2A1/2[a]	↑2A1[a]	↓2D1[a]
↑2B8[b]	↓3A1/2[a]	↑2C7[a]	↓3A4[a]
↑2C8[b]	↓3A4[b]	↑2C12[a]	
↑2C9[b]	↑7A1[b]	↑2C11[a]	
↑2C19[b]		↓2C19[b]	
↑3A4[b]		↑2D1[a]	
↑3A5[b]		↓2E1[a]	
		↑3A1[a]	

[a]Data from preclinical experiments on rats. [b]Data obtained from human cell lines.

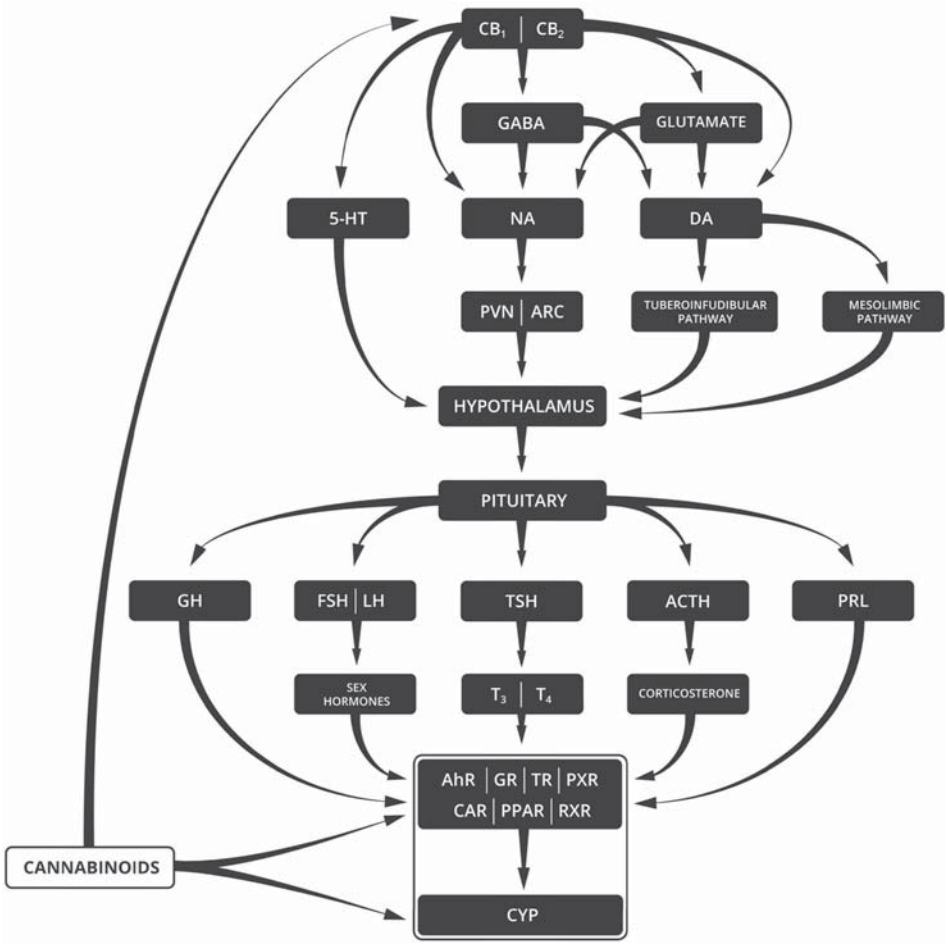

Fig. (9). Endocannabinoid system and cannabinoids in the regulation of CYP activity.

The activation of CAR is linked to the induction of CYP2B [247]. There is signaling cross-talk between PXR and CAR. These receptors control the expression of human CYP2A6 [238], CYP2B6 [248], CYP2C8/9 [230, 249], CYP2C19 [232], CYP3A4 [250], CYP3A5 [251], and CYP3A7 [252].

AhR is not a true nuclear receptor; it belongs to a family of transcription factors that contain the basic-helix-loop-helix and Per-ARNT-Sim domains. AhR requires the AhR nuclear translocator as its heterodimerization partner to be translocated into the nucleus and turn on the CYP gene transcription. AhR triggers the expression of CYP1A and CYP1B [222, 223].

The PPAR family currently has four members - PPARα, PPARβ, PPARγ, and PPARδ - which differ in their localization [253]. After activation by appropriate ligands, PPARs bind as heterodimers with RXR (PPAR/RXR) to peroxisome proliferator response elements. It has been shown that CYP2B, CYP3A, and

Table 7. Cannabinoid ligands of nuclear receptors [157, 159, 257, 258].

PPARα	PPARγ	PPARδ	AhR
N-oleoylethanolamine	AEA, 2-AG	N-oleoylethanolamine	Δ^9-THC
palmitoylethanolamide	NADA, Δ9-THC		CBD
virodhamine	ajulemic acid		
noladin ether	CP 55,940, HU-210		
	WIN 55,212-2		

CYP4A are activated by PPAR, and CYP2C11 is suppressed by the PPAR agonist [254, 255].

CYP3A and CYP2B proteins are distinctly regulated by GRs [256]. GRs may induce the expression of a gene that does not contain GRE in its promoter. This is exerted by indirect "trans-regulation". Moreover, GRs contribute to functional cross-talk between the PXR, CAR, AhR, and RXR signaling pathways [222, 226].

RXR is directly or indirectly involved in the regulation of many enzymes and can be considered to be a limiting factor in the overall regulation of hepatic gene expression patterns [253].

Some endocannabinoids, phytocannabinoids, and synthetic cannabinoids are ligands of different PPARs and the AhR. An overview of the selectivity of drugs to individual receptors is given in Table **7**.

5. CONCLUSION

Cannabinoids are a structurally and pharmacodynamically heterogeneous group of drugs with great potential for therapeutic use in the near future. The involvement of CYP in their metabolism is clear and indisputable, whereas the clinical significance of their drug-drug interactions has yet to be evaluated in detail. These interplays may have various mechanisms from the direct interaction of two substrates at the same enzyme, through different types of antagonism with the CYP protein to the activation of various receptors and changes in hormonal levels leading to an alteration in the expression of CYP genes. The latter describes the suggested involvement of the endocannabinoid system in the central regulation of hepatic CYP activity. This hypothesis is based on indirect evidence, and could be proved or refuted by further studies. Moreover, we suggest that changes in liver CYP metabolic activity could be time-dependent. Our idea is based on the signal transduction from the brain to the liver via hormones which are under HPA control, and a negative feedback mechanism plays a significant role here. Therefore, the hormonal changes induced by drug administration can be short-lived as well as the changes in CYP activity. To the best of our knowledge, the factor of time was not studied in any of the previous works focusing on the role of the central nervous system in the regulation of liver CYP activity.

LIST OF ABBREVIATIONS

Δ^9-THC	=	(-)-trans-Δ^9-tetrahydrocannabinol
2-AG	=	2-arachidonoylglycerol
5-HT	=	5-hydroxytryptamine, serotonin
AA	=	Arachidonic acid
ABHD	=	α,β-hydrolase domain
ACEA	=	Arachidonyl-2′-chloroethylamid
ACPA	=	Arachidonyl-cyclopropylamide
ACTH	=	Adrenocorticotropic hormone
AhR	=	Aryl hydrocarbon receptor
ARC	=	Arcuate nucleus
CAR	=	Constitutive androstane receptor
CBC	=	Cannabichromene
CBD	=	Cannabidiol
CBG	=	Cannabigerol
CBN	=	Cannabinol
CYP	=	Cytochrome P450
DA	=	Dopamine
diHETE	=	Dihydroxyeicosatrienoic acids
EET	=	Epoxyeicosatrienoic acids
EET-EA	=	Epoxyeicosatrienoic acid ethanolamide
EET-G	=	Epoxyeicosatrienylglycerol derivatives
FAAH	=	Fatty acid amide hydrolase
GABA	=	γ-aminobutiric acid
GCs	=	Glucocorticoids
GH	=	Growth hormone
GPCRs	=	G-protein coupled receptors
GRs	=	Glucocorticoid receptors
HEET-EA	=	20-hydroxy-epoxyeicosatrienyl ethanolamide
HETE	=	Hydroxyeicosatrienoic acid
HETE-DA	=	Hydroxyeicosatetraenyl dopamine
HPA	=	Hypothalamic-pituitary axis
LH	=	Luteinizing hormone
NA	=	Noradrenaline
NADA	=	N-arachidonoyldopamine
PPARs	=	Peroxisome proliferator-activated receptors
PRL	=	Prolactin
PVN	=	Paraventricular nucleus
RXRs	=	Retinoid X receptors
SC	=	Synthetic cannabinoid
T3	=	Triiodothyronine
T4	=	Thyroxine
TSH	=	Thyroid-stimulating hormone

CONFLICT OF INTEREST

The authors confirm that this article content has no conflict of interest.

ACKNOWLEDGEMENTS

Authors thanks for grant support from the projects CZ.1.05/1.1.00/02.0068 and MUNI/A/1116/2014.

REFERENCES

[1] Hasler, J.A.; Estabrook, R.M.M.; Pikuleva, I.; Waterman, M.; Capdevila, J.; Holla, V.; Helvig, C.; Falck, J.R.; Farrell, G.; Kaminsky, L.S.; Spivack, S.D.; Boitier, E.; Beaune, P. Human cytochromes P450. *Mol. Aspects Med.*, **1999**, *20*(1-2), 1-137.

[2] Anzenbacher, P.; Anzenbacherová, E. Cytochromes P450 and metabolism of xenobiotics. *Cell. Mol. Life Sci.*, **2001**, *58*(5-6), 737-747.

[3] Zanger, U.M.; Schwab, M. Cytochrome P450 enzymes in drug metabolism: regulation of gene expression, enzyme activities, and impact of genetic variation. *Pharmacol. Ther.*, **2013**, *138*(1), 103-141.

[4] Zelasko, S.; Arnold, W.R.; Das, A. Endocannabinoid metabolism by cytochrome P450 monooxygenases. *Prostaglandins Other Lipid Mediat.*, **2015**, *116-117*, 112-123.

[5] Ahmed, S.A.; Ross, S.A.; Slade, D.; Radwan, M.M.; Khan, I.A.; ElSohly, M.A. Minor oxygenated cannabinoids from high potency Cannabis sativa L. *Phytochemistry*, **2015**, *117*, 194-199.

[6] Pertwee, R.G. *Handbook of cannabis*, 1st ed.; Oxford University Press: New York, **2014**.

[7] Grotenhermen, F.; Müller-Vahl, K. The therapeutic potential of cannabis and cannabinoids. *Dtsch. Arztebl. Int.*, **2012**, *109*(29-30), 495-501.

[8] Alexander, S.P. Therapeutic potential of cannabis-related drugs. *Prog. Neuropsychopharmacol. Biol. Psychiatry*, **2015**, in press available from: http://www.sciencedirect.com/science/article/pii/S0278584615300105 (Accessed August 27, **2015**).

[9] Dunstan, W.R.; Henry, T.A. On oxycannabin from Indian hemp. *Proc. Chem. Soc.*, **1898**, *14*, 44-45.

[10] Wood, T.B. Cannabinol, part I. *J. Chem. Soc.*, **1899**, 75, 20-36.

[11] Adams, R.; Hunt, M.; Clark, J. Structure of cannabidiol, a product Isolated from the Marihuana Extract of Minnesota Wild Hemp. I. *J. Am. Chem. Soc.*, **1940**, *62*(1), 196-200.

[12] Gaoni, Y.; Mechoulam R. Isolation, structure, and partial synthesis of an active constituent of hashish. *J. Am. Chem. Soc.*, **1964**, *86*(8), 1646-1647.

[13] Šantavý, F. Notes on the structure of cannabidiol compounds. *Acta Univ. Palacki. Olomuc. Fac. Med.*, **1964**, *35*, 5-9.

[14] Mechoulam, R.; Gaoni, Y. The absolute configuration of delta-1-tetrahydrocannabinol, the major active constituent of hashish. *Tetrahedron Lett*., **1967**, *12*, 1109-1111.

[15] Devane, W.A.; Dysarz, F.A.; Johnson, M.R.; Melvin, L.S.; Howlett, A.C. Determination and characterization of a cannabinoid receptor in rat brain. *Mol. Pharmacol.*, **1988**, *34*(5), 605-613.

[16] Munro, S.; Thomas, K.L.; Abu-Shaar, M. Molecular characterization of a peripheral receptor for cannabinoids. *Nature,* **1993**, *365*, 61-65.

[17] Di Marzo, V.; Stella, N.; Zimmer, A.; Endocannabinoid signalling and the deteriorating brain. *Nat. Rev. Neurosci.*, **2015**, *16*(1), 30-42.

[18] Matsuda, L.A.; Lolait, S.J.; Brownstein, M.J.; Young, A.C.; Bonner, T.I. Structure of a cannabinoid receptor and functional expression of the cloned cDNA. *Nature*, **1990**, *346*(6284), 561-564.

[19] Devane, W.A.; Hanus, L.; Breuer, A.; Pertwee, R.G.; Stevenson, L.A.; Griffin, G.; Gibson, D.; Mandelbaum, A.; Etinger, A.; Mechoulam, R. Isolation and structure of a brain constituent that binds to the cannabinoid receptor. *Science*, **1992**, *258*(5090), 1946-1949.

[20] Mechoulam, R.; Ben-Shabat, S.; Hanus, L.; Ligumsky, M.; Kaminski, N.E.; Schatz, A.R.; Gopher, A.; Almog, S.; Martin, B.R.; Compton, D.R. Identification of an endogenous 2-monoglyceride, present in canine gut, that binds to cannabinoid receptors. *Biochem. Pharmacol.*, **1995**, *50*(1), 83-90.

[21] Sugiura, T.; Kondo, S.; Sukagawa, A.; Nakane, S.; Shinoda, A.; Itoh, K.; Yamashita, A.; Waku, K. 2-Arachidonoylglycerol: a possible endogenous cannabinoid receptor ligand in brain. *Biochem. Biophys. Res. Commun.*, **1995**, *215*(1), 89-97.

[22] Bouaboula, M.; Hilairet, S.; Marchand, J.; Fajas, L.; Le Fur, G.; Casellas, P. Anandamide induced PPARgamma transcriptional activation and 3T3-L1 preadipocyte differentiation. *Eur. J. Pharmacol.*, **2005**, *517*(3), 174-181.

[23] O'Sullivan, S.E.; Kendall, D.A. Cannabinoid activation of peroxisome proliferator-activated receptors: potential for modulation of inflammatory disease. *Immunobiology*, **2010**, *215*(8), 611-616.

[24] Zygmunt, P.M.; Petersson, J.; Andersson, D.A; Chuang, H.; Sørgård, M.; Di Marzo, V.; Julius, D.; Högestätt, E.D. Vanilloid receptors on sensory nerves mediate the vasodilator action of anandamide. *Nature*, **1999**, *400*(6743), 452-457.

[25] Pacher, P.; Bátkai, S.; Kunos, G. Haemodynamic profile and responsiveness to anandamide of TRPV1 receptor knock-out mice. *J. Physiol.*, **2004**, *558*(Pt2), 647-657.

[26] Overton, H.A.; Babbs, A.J.; Doel, S.M.; Fyfe, M.C.; Gardner, L.S.; Griffin, G.; Jackson, H.C.; Procter, M.J.; Rasamison, C.M.; Tang-Christensen, M.; Widdowson, P.S.; Williams, G.M.; Reynet, C. Deorphanization of a G protein-coupled receptor for oleoylethanolamide and its use in the discovery of small-molecule hypophagic agents. *Cell. Metab.*, **2006**, *3*(3), 167-175.

[27] Ryberg, E.; Larsson, N.; Sjögren, S.; Hjorth, S.; Hermansson, N.O.; Leonova, J.; Elebring, T.; Nilsson, K.; Drmota, T.; Greasley, P.J. The orphan receptor GPR55 is a novel cannabinoid receptor. *Br. J. Pharmacol.*, **2007**, *152*(7), 1092-1101.

[28] De Petrocellis, L.; Di Marzo, V. Non-CB1, non-CB2 receptors for endocannabinoids, plant cannabinoids, and synthetic cannabimimetics: focus on G-protein-coupled receptors and transient receptor potential channels. *J. Neuroimmune Pharmacol.*, **2010**, *5*(1), 103-121.

[29] Pertwee, R.G.; Howlett, A.C.; Abood, M.E.; Alexander, S.P.; Di Marzo, V.; Elphick, M.R.; Greasley, P.J.; Hansen, H.S.; Kunos, G.; Mackie, K.; Mechoulam, R.; Ross, R.A. International Union of Basic and Clinical Pharmacology. LXXIX. Cannabinoid receptors and their ligands: beyond CB_1 and CB_2. *Pharmacol. Rev.*, **2010**, *62*(4), 588-631.

[30] Demuth, D.G.; Molleman, A. Cannabinoid signalling. *Life Sci.*, **2006**, *78*(6), 549-563.

[31] Kleberg, K.; Hassing, H.A.; Hansen, H.S. Classical endocannabinoid-like compounds and their regulation by nutrients. *Biofactors*, **2014**, *40*(4), 363-372.

[32] Zhang, X.; Maor, Y.; Wang, J.F.; Kunos, G.; Groopman, J.E. Endocannabinoid-like N-arachidonoyl serine is a novel pro-angiogenic mediator. *Br. J. Pharmacol.*, **2010**, *160*(7), 1583-1594.

[33] Giuffrida, A.; McMahon, L.R. *In vivo* pharmacology of endocannabinoids and their metabolic inhibitors: therapeutic implications in Parkinson's disease and abuse liability. *Prostaglandins Other Lipid Mediat.*, **2010**, *91*(3-4), 90-103.

[34] Di Marzo, V.; Deutsch, D.G. Biochemistry of the endogenous ligands of cannabinoid receptors. *Neurobiol. Dis.*, **1998**, *5*(6PtB), 386-404.

[35] Fonseca, B.M.; Costa, M.A.; Almada, M.; Correia-da-Silva, G.; Teixeira, N.A. Endogenous cannabinoids revisited: a biochemistry perspective. *Prostaglandins Other Lipid Mediat.*, **2013**, *102-103*, 13-30.

[36] Tan, B.; Bradshaw, H.B.; Rimmerman, N.; Srinivasan, H.; Yu, Y.W.; Krey, J.F.; Monn, M.F.; Chen, J.S.; Hu, S.S.; Pickens, S.R.; Walker, J.M. Targeted lipidomics: discovery of new fatty acyl amides. *AAPS J.*, **2006**, *8*(3), E461-E465.

[37] Fezza, F.; Bari, M.; Florio, R.; Talamonti, E.; Feole, M.; Maccarrone, M. Endocannabinoids, related compounds and their metabolic routes. *Molecules*, **2014**, *19*(11), 17078-17106.

[38] Snider, N.T.; Walker, V.J.; Hollenberg, P.F. Oxidation of the endogenous cannabinoid arachidonoyl ethanolamide by the cytochrome P450 monooxygenases: physiological and pharmacological implications. *Pharmacol. Rev.*, **2010**, *62*(1), 136-154.

[39] Hillard, C.J.; Wilkison, D.M.; Edgemond, W.S.; Campbell, W.B. Characterization of the kinetics and distribution of N-arachidonylethanolamine (anandamide) hydrolysis by rat brain. *Biochim. Biophys. Acta*, **1995**, *1257*(3), 249-256.

[40] Sugiura, T.; Kobayashi, Y.; Oka, S.; Waku, K. Biosynthesis and degradation of anandamide and 2-arachidonoylglycerol and their possible physiological significance. *Prostaglandins Leukot. Essent. Fatty Acids*, **2002**, *66*(2-3), 173-192.

[41] Ueda, N.; Tsuboi, K. Enzymes involved in the biosynthesis and degradation of anandamide. *Seikagaku*, **2005**, *77*(12), 1505-1509.

[42] Roman R.J. P-450 metabolites of arachidonic acid in the control of cardiovascular function. *Physiol. Rev.*, **2002**, *82*(1), 131-185.

[43] Bylund, J.; Ericsson, J.; Oliw, E.H. Analysis of cytochrome P450 metabolites of arachidonic and linoleic acids by liquid chromatography-mass spectrometry with ion trap MS. *Anal. Biochem.*, **1998**, *265*(1), 55-68.

[44] Rifkind, A.B.; Lee, C.; Chang, T.K.; Waxman, D.J. Arachidonic acid metabolism by human cytochrome P450s 2C8, 2C9, 2E1, and

1A2: regioselective oxygenation and evidence for a role for CYP2C enzymes in arachidonic acid epoxygenation in human liver microsomes. *Arch. Biochem. Biophys.*, **1995**, *320*(2), 380-389.

[45] Laethem, R.M.; Balazy, M.; Falck, J.R.; Laethem, C.L.; Koop, D.R. Formation of 19(S)-, 19(R)-, and 18(R)-hydroxyeicosatetraenoic acids by alcohol-inducible cytochrome P450 2E1. *J. Biol. Chem.*, **1993**, *268*(17), 12912-12918.

[46] Yu, M.; Ives, D.; Ramesha, C.S. Synthesis of prostaglandin E2 ethanolamide from anandamide by cyclooxygenase-2. *J. Biol. Chem.*, **1997**, *272*(34), 21181-21186.

[47] Kozak, K.R.; Crews, B.C.; Morrow, J.D.; Wang, L.H.; Ma, Y.H.; Weinander, R.; Jakobsson, P.J.; Marnett, L.J. Metabolism of the endocannabinoids, 2-arachidonylglycerol and anandamide, into prostaglandin, thromboxane, and prostacyclin glycerol esters and ethanolamides. *J. Biol. Chem.*, **2002**, *277*(47), 44877-44885.

[48] Hampson, A.J.; Hill, W.A.; Zan-Phillips, M.; Makriyannis, A.; Leung, E.; Eglen, R.M.; Bornheim, L.M. Anandamide hydroxylation by brain lipoxygenase:metabolite structures and potencies at the cannabinoid receptor. *Biochim. Biophys. Acta*, **1995**, *1259*(2), 173-179.

[49] Bornheim, L.M.; Kim, K.Y.; Chen, B.; Correia, M.A. Microsomal cytochrome P450-mediated liver and brain anandamide metabolism. *Biochem. Pharmacol.*, **1995**, *50*(5), 677-686.

[50] Costa, B.; Parolaro, D.; Colleoni, M. Chronic treatment with the endocannabinoid anandamide increases cytochrome P450 metabolizing system in the rat. *Eur. J. Pharmacol.*, **2002**, *449*(1-2), 61-69.

[51] Snider, N.T.; Kornilov, A.M.; Kent, U.M.; Hollenberg, P.F. Anandamide metabolism by human liver and kidney microsomal cytochrome p450 enzymes to form hydroxyeicosatetraenoic and epoxyeicosatrienoic acid ethanolamides. *J. Pharmacol. Exp. Ther.*, **2007**, *321*(2), 590-597.

[52] Yu, Z.; Xu, F.; Huse, L.M.; Morisseau, C.; Draper, A.J.; Newman, J.W.; Parker, C.; Graham, L.; Engler, M.M.; Hammock, B.D.; Zeldin, D.C.; Kroetz, D.L. Soluble epoxide hydrolase regulates hydrolysis of vasoactive epoxyeicosatrienoic acids. *Circ. Res.*, **2000**, *87*(11), 992-998.

[53] Snider, N.T.; Sikora, M.J.; Sridar, C.; Feuerstein, T.J.; Rae, J.M.; Hollenberg, P.F. The endocannabinoid anandamide is a substrate for the human polymorphic cytochrome P450 2D6. *J. Pharmacol. Exp. Ther.*, **2008**, *327*(2), 538-545.

[54] Stark, K.; Dostalek, M.; Guengerich, F.P. Expression and purification of orphan cytochrome P450 4X1 and oxidation of anandamide. *FEBS J.*, **2008**, *275*(14), 3706-3717.

[55] Navia-Paldanius, D.; Savinainen, J.R.; Laitinen, J.T. Biochemical and pharmacological characterization of human α/β-hydrolase domain containing 6 (ABHD6) and 12 (ABHD12). *J. Lipid. Res.*, **2012**, *53*(11), 2413-2424.

[56] Chen, J.; Chen, J.K.; Falck, J.R.; Guthi, J.S.; Anjaiah, S.; Capdevila, J.H.; Harris R.C. Mitogenic activity and signaling mechanism of 2-(14,15- epoxyeicosatrienoyl)glycerol, a novel cytochrome p450 arachidonate metabolite. *Mol. Cell. Biol.*, **2007**, *27*(8), 3023-3034.

[57] Chen, J.K.; Chen, J.; Imig, J.D.; Wei, S.; Hachey, D.L.; Guthi, J.S.; Falck, J.R.; Capdevila, J.H.; Harris, R.C. Identification of novel endogenous cytochrome p450 arachidonate metabolites with high affinity for cannabinoid receptors. *J. Biol. Chem.*, **2008**, *283*(36), 24514-24524.

[58] McDougle, D.R.; Kambalyal, A.; Meling, D.D.; Das, A. Endocannabinoids anandamide and 2-arachidonoylglycerol are substrates for human CYP2J2 epoxygenase. *J. Pharmacol. Exp. Ther.*, **2014**, *351*(3), 616-627.

[59] Awumey, E.M.; Hill, S.K.; Diz, D.I.; Bukoski, R.D. Cytochrome P-450 metabolites of 2-arachidonoylglycerol play a role in Ca2+-induced relaxation of rat mesenteric arteries. *Am. J. Physiol. Heart Circ. Physiol.*, **2008**, *294*(5), H2363-H2370.

[60] Manzanares, J.; Julian, M.; Carrascosa, A. Role of the cannabinoid system in pain control and therapeutic implications for the management of acute and chronic pain episodes. *Curr. Neuropharmacol.*, **2006**, *4*(3), 239-257.

[61] Rimmerman, N.; Bradshaw, H.B.; Basnet, A.; Tan, B.; Widlanski, T.S.; Walker, J.M. Microsomal omega-hydroxylated metabolites of N-arachidonoyl dopamine are active at recombinant human TRPV1 receptors. *Prostaglandins Other Lipid Mediat.*, **2009**, *88*(1-2), 10-17.

[62] Fowler, C.J. The potential of inhibitors of endocannabinoid metabolism as anxiolytic and antidepressive drugs--A practical view. *Eur. Neuropsychopharmacol.*, **2015**, *25*(6), 749-762.

[63] Huggins, J.P.; Smart, T.S.; Langman, S.; Taylor, L.; Young, T. An efficient randomised, placebo-controlled clinical trial with the irreversible fatty acid amide hydrolase-1 inhibitor PF-04457845, which modulates endocannabinoids but fails to induce effective analgesia in patients with pain due to osteoarthritis of the knee. *Pain*, **2012**, *153*(9), 1837-1846.

[64] Fisar, Z. Phytocannabinoids and endocannabinoids. *Curr. Drug Abuse Rev.*, **2009**, *2*(1), 51-75.

[65] Stout, S.M.; Cimino, N.M. Exogenous cannabinoids as substrates, inhibitors, and inducers of human drug metabolizing enzymes: a systematic review. *Drug Metab. Rev.*, **2014**, *46*(1), 86-95.

[66] ElSohly, M.A.; Slade, D. Chemical constituents of marijuana: the complex mixture of natural cannabinoids. *Life Sci.*, **2005**, *78*(5), 539-548.

[67] Agurell, S.; Halldin, M.; Lindgren, J.E.; Ohlsson, A.; Widman, M.; Gillespie, H.; Hollister, L. Pharmacokinetics and metabolism of delta 1-tetrahydrocannabinol and other cannabinoids with emphasis on man. *Pharmacol. Rev.*, **1986**, *38*(1), 21-43.

[68] Nilsson, I.M.; Agurell, S.; Nilsson, J.L.; Ohlsson, A.; Sandberg, F.; Wahlqvist, M. Delta-1-tetrahydrocannabinol: structure of a major metabolite. *Science*, **1970**, *168*(3936), 1228-1229.

[69] Watanabe, K.; Yamaori, S.; Funahashi, T.; Kimura, T.; Yamamoto, I. Cytochrome P450 enzymes involved in the metabolism of tetrahydrocannabinols and cannabinol by human hepatic microsomes. *Life Sci.*, **2007**, *80*(15), 1415-1419.

[70] Yamamoto, I.; Watanabe, K.; Matsunaga, T.; Kimura, T.; Funahashi, T.; Yoshimura, H. Pharmacology and toxicology of major constituents of marijuana - on the metabolic activation of cannabinoids and its mechanism. *J. Toxicol. Toxin. Rev.*, **2003**, *22*(4), 577-589.

[71] Kuzuoka, K.; Watanabe, K.; Matsunaga, T.; Yamamoto, I.; Yoshimura, H. Characterisation of mouse hepatic microsomal enzyme that catalyzes oxidation of cannabinol at the 11-position. *Jpn. J. Toxicol. Env. Health*, **1992**, *38*(4), 349-354.

[72] Harvey, D.J.; Samara, E.; Mechoulam, R. Urinary metabolites of cannabidiol in dog, rat and man and their identification by gas chromatography-mass spectrometry. *J. Chromatogr.*, **1991**, *562*(1-2), 299-322.

[73] Jiang, R.; Yamaori, S.; Takeda, S.; Yamamoto, I.; Watanabe, K. Identification of cytochrome P450 enzymes responsible for metabolism of cannabidiol by human liver microsomes. *Life Sci.*, **2011**, *89*(5-6), 165-170.

[74] Harvey, D.J.; Brown, N.K. Comparative *in vitro* metabolism of the cannabinoids. *Pharmacol. Biochem. Behav.*, **1991**, *40*(3), 533-540.

[75] Gunderson, E.W.; Haughey, H.M.; Ait-Daoud, N.; Joshi, A.S.; Hart, C.L. "Spice" and "K2" herbal highs: a case series and systematic review of the clinical effects and biopsychosocial implications of synthetic cannabinoid use in humans. *Am. J. Addict.*, **2012**, *21*(4), 320-326.

[76] Marinol®, AbbVie Inc., Prescribing information. Available from: http://www.rxabbvie.com/pdf/marinol_PI.pdf (Accessed August 15, **2015**).

[77] Van Gaal, L.F.; Rissanen, A.M.; Scheen, A.J.; Ziegler, O.; Rössner, S.; Group R-ES. Effects of the cannabinoid-1 receptor blocker rimonabant on weight reduction and cardiovascular risk factors in overweight patients: 1-year experience from the RIO-Europe study. *Lancet*, **2005**, *365*(9468), 1389-1397.

[78] Christensen, R.; Kristensen, P.K.; Bartels, E.M.; Bliddal, H.; Astrup, A. Efficacy and safety of the weight-loss drug rimonabant: a meta-analysis of randomised trials. *Lancet*, **2007**, *370*(9600), 1706-1713.

[79] Acomplia®, Sanofi-Aventis. Summary of Product Characteristics. Available from: http://www.sanofi-aventis.co.uk/products/Acomplia_SPC.pdf (Accessed August 15, **2015**).

[80] Lexicomp Online®. Lexi-Drugs®: Hudson, Ohio: Lexi-Comp, Inc. Available from: http://online.lexi.com/ (Accessed August 15, **2015**).

[82] Kim, U.; Jin, M.J.; Lee, J.; Han, S.B.; In, M.K.; Yoo, H.H. Tentative identification of phase I metabolites of HU-210, a classical synthetic cannabinoid, by LC-MS/MS. *J. Pharm. Biomed. Anal.*, **2012**, *64-65*, 26-34.

[83] Thomas, B.F.; Martin, B.R. *In vitro* metabolism of (-)-cis-3-[2-hydroxy-4-(1,1-dimethylheptyl) phenyl]-trans-4-(3-hydroxypropyl)

cyclohexanol, a synthetic bicyclic cannabinoid analog. *Drug Metab. Dispos.*, **1990**, *18*(6), 1046-1054.

[84] Pertwee, R. Cannabinoid Receptor Ligands, Tocris Bioscience Scientific Review Series No. 27. Available from: http://www. tocris.com/pdfs/pdf_downloads/Cannabinoid_Receptor_Ligands_Review.pdf (Accessed August 15, **2015**).

[85] Zhang, Q.; Ma, P.; Iszard, M.; Cole, R.B.; Wang, W.; Wang, G. *In vitro* metabolism of R(+)-[2,3-dihydro-5-methyl-3-[(morpholinyl)methyl]pyrrolo [1,2,3-de]1,4-benzoxazinyl]-(1-naphthalenyl) methanone mesylate, a cannabinoid receptor agonist. *Drug Metab. Dispos.*, **2002**, *30*(10), 1077-1086.

[86] Hillard, C.J.; Manna, S.; Greenberg, M.J.; DiCamelli, R.; Ross, R.A.; Stevenson, L.A.; Murphy, V.; Pertwee, R.G.; Campbell, W.B. Synthesis and characterization of potent and selective agonists of the neuronal cannabinoid receptor (CB1). *J. Pharmacol. Exp. Ther.*, **1999**, *289*(3), 1427-1433.

[87] Pertwee, R.G. The pharmacology of cannabinoid receptors and their ligands: an overview. *Int. J. Obes. (Lond)*, **2006**, *30*, Suppl 1, S13-18.

[88] Mazzarino, M.; de la Torre, X.; Botrè, F. A liquid chromatography-mass spectrometry method based on class characteristic fragmentation pathways to detect the class of indole-derivative synthetic cannabinoids in biological samples. *Anal. Chim. Acta*, **2014**, *837*, 70-82.

[89] Zhang, Q.; Ma, P.; Cole, R.B.; Wang, G. Identification of *in vitro* metabolites of JWH-015, an aminoalkylindole agonist for the peripheral cannabinoid receptor (CB2) by HPLC-MS/MS. *Anal. Bioanal. Chem.*, **2006**, *386*(5), 1345-1355.

[90] European Monitoring Centre for Drugs and Drug Addiction (EMCDDA). *New psychoactive substances in Europe - An update from the EU Early Warning System (March 2015)*, Publications Office of the European Union: Luxembourg, **2015**.

[91] European Monitoring Centre for Drugs and Drug Addiction (EMCDDA). *Synthetic cannabinoids in Europe*, Publications Office of the European Union: Luxembourg, **2015**.

[92] Strano-Rossi, S.; Anzillotti, L.; Dragoni, S.; Pellegrino, R.M.; Goracci, L.; Pascali, V.L.; Cruciani, G. Metabolism of JWH-015, JWH-098, JWH-251, and JWH-307 in silico and *in vitro*: a pilot study for the detection of unknown synthetic cannabinoids metabolites. *Anal. Bioanal. Chem.*, **2014**, *406*(15), 3621-3636.

[93] Castaneto, M.S.; Gorelick, D.A.; Desrosiers, N.A.; Hartman, R.L.; Pirard, S.; Huestis, M.A. Synthetic cannabinoids: epidemiology, pharmacodynamics, and clinical implications. *Drug Alcohol Depend.*, **2014**, *144*, 12-41.

[94] Erratico, C.; Negreira, N.; Norouzizadeh, H.; Covaci, A.; Neels, H.; Maudens, K.; van Nuijs, A.L. *In vitro* and *in vivo* human metabolism of the synthetic cannabinoid AB-CHMINACA. *Drug Test. Anal.*, **2015**, in press. Available from: http://onlinelibrary.wiley.com/doi/10.1002/dta.1796/abstract;jsessionid=7D79BC8B2D2E563E8A96F95046AE07DE.f01t02 (Accessed August 27, **2015**).

[95] Takayama, T.; Suzuki, M.; Todoroki, K.; Inoue, K.; Min, J.Z.; Kikura-Hanajiri, R.; Goda, Y.; Toyo'oka, T. UPLC/ESI-MS/MS-based determination of metabolism of several new illicit drugs, ADB-FUBINACA, AB-FUBINACA, AB-PINACA, QUPIC, 5F-QUPIC and α-PVT, by human liver microsome. *Biomed. Chromatogr.*, **2014**, *28*(6), 831-838.

[96] Thomsen, R.; Nielsen, L.M.; Holm, N.B.; Rasmussen, H.B.; Linnet, K.; Consortium, I. Synthetic cannabimimetic agents metabolized by carboxylesterases. *Drug Test. Anal.*, **2015**, *7*(7), 565-576.

[97] Castaneto, M.; Wohlfarth, A.; Pang, S.; Zhu, M.; Scheidweiler, K.; Kronstrand, R.; Huestis, M. Identification of AB-FUBINACA metabolites in human hepatocytes and urine using high-resolution mass spectrometry. *Forensic Toxicol.*, **2015**, *33*(2), 295-310.

[98] Wohlfarth, A.; Castaneto, M.S.; Zhu, M.; Pang, S.; Scheidweiler, K.B.; Kronstrand, R.; Huestis, M.A. Pentylindole/Pentylindazole Synthetic Cannabinoids and Their 5-Fluoro Analogs Produce Different Primary Metabolites: Metabolite Profiling for AB-PINACA and 5F-AB-PINACA. *AAPS J.*, **2015**, *17*(3), 660-677.

[99] Gandhi, A.S.; Zhu, M.; Pang, S.; Wohlfarth, A.; Scheidweiler, K.B.; Liu, H.F.; Huestis, M.A. First characterization of AKB-48 metabolism, a novel synthetic cannabinoid, using human hepatocytes and high-resolution mass spectrometry. *AAPS J.,* **2013**, *15*(4), 1091-1098.

[100] Holm, N.B.; Nielsen, L.M.; Linnet, K. CYP3A4 Mediates Oxidative Metabolism of the Synthetic Cannabinoid AKB-48. *AAPS J.*, **2015**, *17*(5), 1237-1245.

[101] Chimalakonda, K.C.; Seely, K.A.; Bratton, S.M.; Brents, L.K.; Moran, C.L.; Endres, G.W.; James, L.P.; Hollenberg, P.F.; Prather, P.L.; Radomiska-Pandya, A.; Moran, J.H. Cytochrome P450-mediated oxidative metabolism of abused synthetic cannabinoids found in K2/Spice: identification of novel cannabinoid receptor ligands. *Drug Metab. Dispos.*, **2012**, *40*(11), 2174-2184.

[102] Sobolevsky, T.; Prasolov, I.; Rodchenkov, G. Detection of urinary metabolites of AM-2201 and UR-144, two novel synthetic cannabinoids. *Drug Test. Anal.*, **2012**, *4*(10), 745-753.

[103] Sobolevsky, T.; Prasolov, I.; Rodchenkov, G. Study on the phase I metabolism of novel synthetic cannabinoids, APICA and its fluorinated analogue. *Drug Test. Anal.*, **2015**, *7*(4), 131-142.

[104] Jin, M.J.; Lee, J.; In, M.K.; Yoo, H.H. Characterization of *in vitro* metabolites of CP 47,497, a synthetic cannabinoid, in human liver microsomes by LC-MS/MS. *J. Forensic Sci.*, **2013**, *58*(1), 195-199.

[105] Wintermeyer, A.; Möller, I.; Thevis, M.; Jübner, M.; Beike, J.; Rothschild, M.A.; Bender, K. *In vitro* phase I metabolism of the synthetic cannabimimetic JWH-018. *Anal. Bioanal. Chem.*, **2010**, *398*(5), 2141-2153.

[106] ElSohly, M.A.; Gul, W.; ElSohly, K.M.; Murphy, T.P.; Madgula, V.L.; Khan, S.I. Liquid chromatography-tandem mass spectrometry analysis of urine specimens for K2 (JWH-018) metabolites. *J. Anal. Toxicol.*, **2011**, *35*(7), 487-495.

[107] Chimalakonda, K.C.; Bratton, S.M.; Le, V.H.; Yiew, K.H.; Dineva, A.; Moran, C.L.; James, L.P.; Moran, J.H.; Radominska-Pandya, A. Conjugation of synthetic cannabinoids JWH-018 and JWH-073, metabolites by human UDP-glucuronosyltransferases. *Drug Metab. Dispos.*, **2011**, *39*(10), 1967-1976.

[108] Gambaro, V.; Arnoldi, S.; Bellucci, S.; Casagni, E.; Dell'Acqua, L.; Fumagalli, L.; Pallavicini, M.; Roda, G.; Rusconi, C.; Valoti, E. Characterization of *in vitro* metabolites of JWH-018, JWH-073 and their 4-methyl derivatives, markers of the abuse of these synthetic cannabinoids. *J. Chromatogr. B Analyt. Technol. Biomed. Life Sci.*, **2014**, *957*, 68-76.

[109] De Brabanter, N.; Esposito, S.; Tudela, E.; Lootens, L.; Meuleman, P.; Leroux-Roels, G.; Deventer, K.; Van Eenoo, P. *In vivo* and *in vitro* metabolism of the synthetic cannabinoid JWH-200. *Rapid Commun. Mass. Spectrom.*, **2013**, *27*(18), 2115-2126.

[110] Jang, M.; Shin, I.; Yang, W.; Chang, H.; Yoo, H.H.; Lee, J.; Kim, E. Determination of major metabolites of MAM-2201 and JWH-122 in *in vitro* and *in vivo* studies to distinguish their intake. *Forensic Sci. Int.*, **2014**, *244*, 85-91.

[111] Wohlfarth, A.; Gandhi, A.S.; Pang, S.; Zhu, M.; Scheidweiler, K.B.; Huestis, M.A. Metabolism of synthetic cannabinoids PB-22 and its 5-fluoro analog, 5F-PB-22, by human hepatocyte incubation and high-resolution mass spectrometry. *Anal. Bioanal. Chem.*, **2014**, *406*(6), 1763-1780.

[112] Gandhi, A.S.; Zhu, M.; Pang, S.; Wohlfarth, A.; Scheidweiler, K.B.; Huestis, M.A. Metabolite profiling of RCS-4, a novel synthetic cannabinoid designer drug, using human hepatocyte metabolism and TOF-MS. *Bioanalysis*, **2014**, *6*(11), 1471-1485.

[113] Wohlfarth, A.; Pang, S.; Zhu, M.; Gandhi, A.S.; Scheidweiler, K.B.; Huestis, M.A. Metabolism of RCS-8, a synthetic cannabinoid with cyclohexyl structure, in human hepatocytes by high-resolution MS. *Bioanalysis*, **2014**, *6*(9), 1187-1200.

[114] Gandhi, A.S.; Wohlfarth, A.; Zhu, M.; Pang, S.; Castaneto, M.; Scheidweiler, K.B.; Huestis, M.A. High-resolution mass spectrometric metabolite profiling of a novel synthetic designer drug, N-(adamantan-1-yl)-1-(5-fluoropentyl)-1H-indole-3-carboxamide (STS-135), using cryopreserved human hepatocytes and assessment of metabolic stability with human liver microsomes. *Drug Test. Anal.*, **2015**, *7*(3), 187-198.

[115] Wohlfarth, A.; Pang, S.; Zhu, M.; Gandhi, A.S.; Scheidweiler, K.B.; Liu, H.F.; Huestis, M.A. First metabolic profile of XLR-11, a novel synthetic cannabinoid, obtained by using human hepatocytes and high-resolution mass spectrometry. *Clin. Chem.*, **2013**, *59*(11), 1638-1648.

[116] Chimalakonda, K.C.; James, L.P.; Radominska-Pandya, A.; Moran, J.H. Sulfaphenazole and α-naphthoflavone attenuate the metabolism of the synthetic cannabinoids JWH-018 and AM2201 found in K2/spice. *Drug Metab. Lett.*, **2013**, *7*(1), 34-38.

[117] Liu, J.; Tawa, G.J.; Wallqvist, A. Identifying cytochrome p450 functional networks and their allosteric regulatory elements. *PLoS One*, **2013**, *8*(12), e81980.

[118] Sun, L.J.; Yu, J.W.; Wan, L.; Zhang, X.Y.; Shi, Y.G.; Chen, M.Y. Endocannabinoid system activation contributes to glucose metabolism disorders of hepatocytes and promotes hepatitis C virus replication. *Int. J. Infect. Dis.*, **2014**, *23*, 75-81.

[119] Masoodi, M.; Kuda, O.; Rossmeisl, M.; Flachs, P.; Kopecky, J. Lipid signaling in adipose tissue: Connecting inflammation & metabolism. *Biochim. Biophy.s Acta*, **2015**, *1851*(4) 503-518.

[120] Bergström, M.A.; Isin, E.M.; Castagnoli, N.; Milne, C.E. Bioactivation pathways of the cannabinoid receptor 1 antagonist rimonabant. *Drug Metab. Dispos.*, **2011**, *39*(10), 1823-1832.

[121] Wustrow, D.J.; Maynard, G.D.; Yuan, J.; Zhao, H.; Mao, J.; Guo, Q.; Kershaw, M.; Hammer, J.; Brodbeck, R.M.; Near, K.E.; Zhou, D.; Beers, D.S.; Chenard, B.L.; Krause, J.E; Hutchinson, A.J. Aminopyrazine CB1 receptor inverse agonists. *Bioorg. Med. Chem. Lett.*, **2008**, *18*(11), 3376-3381.

[122] Alonso, M.; Serrano, A.; Vida, M.; Crespillo, A.; Hernandez-Folgado, L.; Jagerovic, N.; Goya, P.; Reyes-Cabello, C.; Peres-Valero, V.; Decara, J.; Macías-González, M.; Bermúndez-Silva, F.J.; Suárez, J.; Rodríguey se Fonseca, F.; Pavón, F.J. Anti-obesity efficacy of LH-21, a cannabinoid CB(1) receptor antagonist with poor brain penetration, in diet-induced obese rats. *Br. J. Pharmacol.*, **2012**, *165*(7), 2274-2291.

[123] Ashino, T.; Hakukawa, K.; Itoh, Y.; Numazawa, S. Inhibitory effect of synthetic cannabinoids on CYP1A activity in mouse liver microsomes. *J. Toxicol. Sci.*, **2014**, *39*(6), 815-820.

[124] Yamaori, S.; Kushihara, M.; Yamamoto, I.; Watanabe, K. Characterization of major phytocannabinoids, cannabidiol and cannabinol, as isoform-selective and potent inhibitors of human CYP1 enzymes. *Biochem. Pharmacol.*, **2010**, *79*(11), 1691-1698.

[125] Yamaori, S.; Okushima, Y.; Masuda, K.; Kushihara, M.; Katsu, T.; Narimatsu, S.; Yamamoto, I.; Watanabe, K. Structural requirements for potent direct inhibition of human cytochrome P450 1A1 by cannabidiol: role of pentylresorcinol moiety. *Biol. Pharm. Bull.*, **2013**, *36*(7), 1197-1203.

[126] Yamaori, S.; Okushima, Y.; Yamamoto, I.; Watanabe, K. Characterization of the structural determinants required for potent mechanism-based inhibition of human cytochrome P450 1A1 by cannabidiol. *Chem. Biol. Interact.*, **2014**, 2*15*, 62-68.

[127] Yamaori, S.; Maeda, C.; Yamamoto, I.; Watanabe, K. Differential inhibition of human cytochrome P450 2A6 and 2B6 by major phytocannabinoids. *Forensic Toxicol.*, **2011**, *29*(2), 117-124.

[128] Yamaori, S.; Koeda, K.; Kushihara, M.; Hada, Y.; Yamamoto, I.; Watanabe, K. Comparison in the *in vitro* inhibitory effects of major phytocannabinoids and polycyclic aromatic hydrocarbons contained in marijuana smoke on cytochrome P450 2C9 activity. *Drug Metab. Pharmacokinet.*, **2012**, *27*(3), 294-300.

[129] Narimatsu, S.; Watanabe, K.; Yamamoto, I.; Yoshimura, H. Mechanism for inhibitory effect of cannabidiol on microsomal testosterone oxidation in male rat liver. *Drug Metab. Dispos.*, **1988**, *16*(6), 880-889.

[130] Yan, J.; He, X.; Feng, S.; Zhai, Y.; Ma, Y.; Liang, S.; Jin, C. Up-regulation on cytochromes P450 in rat mediated by total alkaloid extract from Corydalis yanhusuo. *BMC Complement Altern. Med.*, **2014**, *14*, 306.

[131] Jiang, R.; Yamaori, S.; Okamoto, Y.; Yamamoto, I.; Watanabe, K. Cannabidiol is a potent inhibitor of the catalytic activity of cytochrome P450 2C19. *Drug Metab. Pharmacokinet.*, **2013**, *28*(4), 332-338.

[132] Yamaori, S.; Okamoto, Y.; Yamamoto, I.; Watanabe, K. Cannabidiol, a major phytocannabinoid, as a potent atypical inhibitor for CYP2D6. *Drug Metab. Dispos.*, **2011**, *39*(11), 2049-2056.

[133] Yamaori, S.; Ebisawa, J.; Okushima, Y.; Yamamoto, I.; Watanabe, K. Potent inhibition of human cytochrome P450 3A isoforms by cannabidiol: role of phenolic hydroxyl groups in the resorcinol moiety. *Life Sci.*, **2011**, *88*(15-16), 730-736.

[134] Jaeger, W.; Benet, L.Z.; Bornheim, L.M. Inhibition of cyclosporine and tetrahydrocannabinol metabolism by cannabidiol in mouse and human microsomes. *Xenobiotica*, **1996**, *26*(3), 275-284.

[135] Funahashi, T.; Ikeuchi, H.; Yamaori, S.; Kimura, T.; Yamamoto, I.; Watanabe, K. *In vitro* Inhibitory Effects of Cannabinoids on Progesterone 17α-Hydroxylase Activity in Rat Testis Microsomes. *J. Health Sci.*, **2005**, *51*(3), 369-375.

[136] Fernandes, M.; Warning, N.; Christ, W.; Hill, R. Interactions of several cannabinoids with the hepatic drug metabolizing system. *Biochem. Pharmacol.*, **1973**, *22*(23), 2981-2987.

[137] Watanabe, K.; Yamamoto, I.; Oguri, K.; Yoshimura, H. *In vitro* and *in vivo* interactions of delta 8-tetra-hydrocannabinol and its metabolites with hepatic microsomal drug metabolizing enzyme systems of mice. *J. Pharmacobiodyn.*, **1981**, *4*(8), 604-611.

[138] Watanabe, K.; Arai, M.; Narimatsu, S.; Yamamoto, I.; Yoshimura, H. Self-catalyzed inactivation of cytochrome P-450 during microsomal metabolism of cannabidiol. *Biochem. Pharmacol.*, **1987**, *36*(20), 3371-3377.

[139] Huestis, M.A.; Henningfield, J.E.; Cone, E.J. Blood cannabinoids. I. Absorption of THC and formation of 11-OH-THC and THCCOOH during and after smoking marijuana. *J. Anal. Toxicol.*, **1992**, *16*(5), 276-282.

[140] Ohlsson, A.; Lindgren, J.E.; Andersson, S.; Agurell, S.; Gillespie, H.; Hollister, L.E. Single-dose kinetics of deuterium-labelled cannabidiol in man after smoking and intravenous administration. *Biomed. Environ. Mass Spectrom.*, **1986**, *13*(2), 77-83.

[141] Johansson, E., Ohlsson, A., Lindgren, J.E., Agurell, S., Gillespie, H., Hollister, L.E. Single-dose kinetics of deuterium-labelled cannabinol in man after intravenous administration and smoking. *Biomed. Environ. Mass Spectrom.*, **1987**, *14*(9), 495-499.

[142] Bornheim, L.M. Effects of unsaturated side-chain analogs of tetrahydrocannabinol on cytochromes P450. *Biochem. Pharmacol.*, **2000**, *60*(7), 955-961.

[143] Costa, B.; Parolaro, D.; Colleoni, M. Chronic cannabinoid, CP-55,940, administration alters biotransformation in the rat. *Eur. J. Pharmacol.*, **1996**, *313*(1-2), 17-24.

[144] Fontanellas, A.; Manzanares, J.; García-Bravo, M.; Buzaleh, A.M.; Méndez, M.; Oliva, J.M.; Batlle, A.; Paloma, T.; Enríquez de Salamance, R. Effects of repeated administration with CP-55,940, a cannabinoid CB1 receptor agonist on the metabolism of the hepatic heme. *Int. J. Biochem. Cell Biol.*, **2005**, *37*(8), 1620-1625.

[145] Yang, L.; Rozenfeld, R.; Wu, D.; Devi, L.A.; Zhang, Z.; Cederbaum, A. Cannabidiol protects liver from binge alcohol-induced steatosis by mechanisms including inhibition of oxidative stress and increase in autophagy. *Free Radic. Biol. Med.*, **2014**, *68*, 260-267.

[146] Sheweita, S.A. Narcotic drugs change the expression of cytochrome P450 2E1 and 2C6 and other activities of carcinogen-metabolizing enzymes in the liver of male mice. *Toxicology*, **2003**, *191*(2-3), 133-142.

[147] Paton, W.D.; Pertwee, R.G. Effect of cannabis and certain of its constituents on pentobarbitone sleeping time and phenazone metabolism. *Br. J. Pharmacol.*, **1972**, *44*(2), 250-261.

[148] Borys, H.K.; Ingall, G.B.; Karler, R. Development of tolerance to the prolongation of hexobarbitone sleeping time caused by cannabidiol. *Br. J. Pharmacol.*, **1979**, *67*(1), 93-101.

[149] Bornheim, L.M.; Correia, M.A. Effect of cannabidiol on cytochrome P-450 isozymes. *Biochem. Pharmacol.*, **1989**, *38*(17), 2789-2794.

[150] Bornheim, L.M.; Borys, H.K.; Karler, R. Effect of cannabidiol on cytochrome P-450 and hexobarbital sleep time. *Biochem. Pharmacol.*, **1981**, *30*(5), 503-507.

[151] Bornheim, L.M.; Everhart, E.T.; Li, J.; Correia, M.A. Characterization of cannabidiol-mediated cytochrome P450 inactivation. *Biochem. Pharmacol.*, **1993**, *45*(6), 1323-1331.

[152] Bornheim, L.M.; Everhart, E.T.; Li, J.; Correia, M.A. Induction and genetic regulation of mouse hepatic cytochrome P450 by cannabidiol. *Biochem. Pharmacol.*, **1994**, *48*(1), 161-171.

[153] List, A.; Nazar, B.; Nyquist, S.; Harclerode, J. The effects of delta9-tetrahydrocannabinol and cannabidiol on the metabolism of gonadal steroids in the rat. *Drug Metab. Dispos.*, **1977**, *5*(3), 268-272.

[154] Narimatsu, S.; Watanabe, K.; Matsunaga, T.; Yamamoto, I.; Imaoka, S.; Funae, Y.; Yoshimura, H. Inhibition of hepatic microsomal cytochrome P450 by cannabidiol in adult male rats. *Chem. Pharm. Bull. (Tokyo)*, **1990**, *38*(5), 1365-1368.

[155] Narimatsu, S.; Watanabe, K.; Matsunaga, T.; Yamamoto, I.; Imaoka, S.; Funae, Y.; Yoshimura, H. Suppression of liver microsomal drug-metabolizing enzyme activities in adult female rats pretreated with cannabidiol. *Biol. Pharm. Bull.*, **1993**, *16*(4), 428-430.

[156] Lee, S.Y.; Oh, S.M.; Lee, S.K.; Chung, K.H. Antiestrogenic effects of marijuana smoke condensate and cannabinoid compounds. *Arch. Pharm. Res.*, **2005**, *28*(12), 1365-1375.

[157] Roth, M.D.; Marques-Magallanes, J.A.; Yuan, M.; Sun, W.; Tashkin, D.P.; Hankinson, O. Induction and regulation of the carcinogen-metabolizing enzyme CYP1A1 by marijuana smoke and delta (9)-tetrahydrocannabinol. *Am. J. Respir. Cell. Mol. Biol.*, **2001**, *24*(3), 339-344.

[158] Sarafian, T.; Habib, N.; Mao, J.T.; Tsu, I.H.; Yamamoto, M.L.; Hsu, E.; Tashkin, D.P.; Roth, M.D. Gene expression changes in human small airway epithelial cells exposed to Delta9-tetrahydrocannabinol. *Toxicol. Lett.*, **2005**, *158*(2), 95-107.

[159] Yamaori S.; Kinugasa Y.; Jiang, R.; Takeda, S.; Yamamoto, I.; Watanabe, K. Cannabidiol induces expression of human cytochrome P450 1A1 that is possibly mediated through aryl hydrocarbon receptor signaling in HepG2 cells. *Life Sci.*, **2015**, *136*, 87-93.

[160] Dalterio, S.; Thomford, P.J.; Michael, S.D.; DeAngelo, L.; Mayfield, D. Perinatal cannabinoid exposure: effects on hepatic cytochrome P-450 and plasma protein levels in male mice. *Teratology*, **1986**, *33*(2), 195-201.

[161] Martignoni, M.; Groothuis, G.M.; de Kanter, R. Species differences between mouse, rat, dog, monkey and human CYP-mediated drug metabolism, inhibition and induction. *Expert Opin. Drug. Metab. Toxicol.*, **2006**, *2*(6), 875-894.

[162] Reid, M.J.; Bornheim, L.M. Cannabinoid-induced alterations in brain disposition of drugs of abuse. *Biochem. Pharmacol.*, **2001**, *61*(11), 1357-1367.

[163] Bornheim, L.M.; Kim, K.Y.; Chen, B.; Correia, M.A. The effect of cannabidiol on mouse hepatic microsomal cytochrome P450-dependent anandamide metabolism. *Biochem. Biophys. Res. Commun.*, **1993**, *197*(2), 740-746.

[164] Klein, C.; Karanges, E.; Spiro, A.; Wong, A.; Spencer, J.; Huynh, T.; Gunasekaran, N.; Karl, T.; Long, L.E.; Huang, X.F.; Liu, K.; Arnold, J.C.; McGregor, I.S. Cannabidiol potentiates Δ^9-tetrahydrocannabinol (THC) behavioural effects and alters THC pharmacokinetics during acute and chronic treatment in adolescent rats. *Psychopharmacology (Berl)*, **2011**, *218*(2), 443-457.

[165] Varvel, S.A.; Wiley, J.L.; Yang, R.; Bridgen, D.T.; Long, K.; Lichtman, A.H.; Martin, B.R. Interactions between THC and cannabidiol in mouse models of cannabinoid activity. *Psychopharmacology (Berl)*, **2006**, *186*(2), 226-234.

[166] European Medicines Agency. Scientific disscussion about rimonabant. Publications Office of the European Union: Luxembourg, **2006**.

[167] Engels, F.K.; de Jong, F.A.; Sparreboom, A.; Mathot, R.A.; Loos, W.J.; Kitzen, J.J.; de Bruijn, P.; Verweij, J.; Mathijssen, R.H. Medicinal cannabis does not influence the clinical pharmacokinetics of irinotecan and docetaxel. *Oncologist*, **2007**, *12*(3), 291-300.

[168] Sativex®, GW Pharma Ltd, Summary of Product Characteristics. Available from: http://www.medicines.org.uk/emc/medicine/23262 (Accessed August 23, **2015**).

[169] Nadulski, T; Pragst, F.; Weinberg, G.; Roser, P.; Schnelle, M.; Fronk, E.M.; Stadelmann, A.M. Randomized, double-blind, placebo-controlled study about the effects of cannabidiol (CBD) on the pharmacokinetics of Delta9-tetrahydrocannabinol (THC) after oral application of THC verses standardized cannabis extract. *Ther. Drug Monit.*, **2005**, *27*(6), 799-810.

[170] Benowitz, N.L.; Nguyen, T.L.; Jones, R.T.; Herning, R.I.; Bachman, J. Metabolic and psychophysiologic studies of cannabidiol-hexobarbital interaction. *Clin. Pharmacol. Ther.*, **1980**, *28*(1), 115-120.

[171] Geffrey, A.L.; Pollack, S.F.; Bruno, P.L.; Thiele, E.A. Drug-drug interaction between clobazam and cannabidiol in children with refractory epilepsy. *Epilepsia*, **2015**, *56*(8), 1246-1251.

[172] Bromek, E.; Wójcikowski, J.; Daniel, W.A. Involvement of the paraventricular (PVN) and arcuate (ARC) nuclei of the hypothalamus in the central noradrenergic regulation of liver cytochrome P450. *Biochem. Pharmacol.*, **2013**, *86*(11), 1614-1620.

[173] Kot, M.; Daniel, W.A. Cytochrome P450 is regulated by noradrenergic and serotonergic systems. *Pharmacol. Res.*, **2011**, *64*(4), 371-380.

[174] Wójcikowski, J.; Gołembiowska, K.; Daniel, W.A. Regulation of liver cytochrome P450 by activation of brain dopaminergic system: physiological and pharmacological implications. *Biochem. Pharmacol.*, **2008**, *76*(2), 258-267.

[175] Wójcikowski, J.; Daniel, W.A. The role of the nervous system in the regulation of liver cytochrome p450. *Curr. Drug Metab.*, **2011**, *12*(2), 124-138.

[176] Svíženská, I.; Dubový, P.; Šulcová, A. Cannabinoid receptors 1 and 2 (CB1 and CB2), their distribution, ligands and functional involvement in nervous system structures--a short review. *Pharmacol. Biochem. Behav.*, **2008**, *90*(4), 501-511.

[177] Mackie, K. Distribution of cannabinoid receptors in the central and peripheral nervous system. *Handb. Exp. Pharmacol.*, **2005**, *168*, 299-325.

[178] Marsicano, G.; Lutz, B. Expression of the cannabinoid receptor CB1 in distinct neuronal subpopulations in the adult mouse forebrain. *Eur. J. Neurosci.*, **1999**, *11*(12), 4213-4225.

[179] Schlicker, E.; Kathmann, M. Modulation of transmitter release *via* presynaptic cannabinoid receptors. *Trends Pharmacol. Sci.*, **2001**, *22*(11), 565-572.

[180] Wager-Miller, J.; Westenbroek, R.; Mackie, K. Dimerization of G protein-coupled receptors: CB1 cannabinoid receptors as an example. *Chem. Phys. Lipids*, **2002**, *121*(1-2), 83-89.

[181] Canals, M.; Milligan, G. Constitutive activity of the cannabinoid CB1 receptor regulates the function of co-expressed Mu opioid receptors. *J. Biol. Chem.*, **2008**, *283*(17), 11424-11434.

[182] Ellis, J.; Pediani, J.D.; Canals, M.; Milasta, S.; Milligan, G. Orexin-1 receptor-cannabinoid CB1 receptor heterodimerization results in both ligand-dependent and -independent coordinated alterations of receptor localization and function. *J. Biol. Chem.*, **2006**, *281*(50), 38812-38824.

[183] Hilairet, S.; Bouaboula, M.; Carrière, D.; Le Fur, G.; Casellas, P. Hypersensitization of the Orexin 1 receptor by the CB1 receptor: evidence for cross-talk blocked by the specific CB1 antagonist, SR141716. *J. Biol. Chem.*, **2003**, *278*(26), 23731-23737.

[184] Carriba, P.; Ortiz, O.; Patkar, K.; Justinova, Z.; Stroik, J.; Themann, A.; Müller, C.; Woods, A.S.; Hope, B.T.; Ciruela, F.; Casadó, V.; Canela, E.I.; Lluis, C.; Goldberg, S.; Morattala, R.; Franco, R.; Ferré, S. Striatal adenosine A2A and cannabinoid CB1 receptors form functional heteromeric complexes that mediate the motor effects of cannabinoids. *Neuropsychopharmacology*, **2007**, *32*(11), 2249-2259.

[185] Ferreira, S.G.; Gonçalves, F.Q.; Marques, J.M.; Tomé, Â.; Rodrigues, R.J.; Nunes-Correia, I.; Ledent, C.; Harkany, T.; Venance, L.; Cunha, R.A.; Köfalvi, A. Presynaptic adenosine A2A receptors dampen cannabinoid CB1 receptor-mediated inhibition of corticostriatal glutamatergic transmission. *Br. J. Pharmacol.*, **2015**, *172*(4), 1074-1086.

[186] Hermann, H.; Marsicano, G.; Lutz, B. Coexpression of the cannabinoid receptor type 1 with dopamine and serotonin receptors in distinct neuronal subpopulations of the adult mouse forebrain. *Neuroscience*, **2002**, *109*(3), 451-460.

[187] Morales, M.; Wang, S.D.; Diaz-Ruiz, O.; Jho, D.H. Cannabinoid CB1 receptor and serotonin 3 receptor subunit A (5-HT3A) are co-expressed in GABA neurons in the rat telencephalon. *J. Comp. Neurol.*, **2004**, *468*(2), 205-216.

[188] Pickel, V.M.; Chan, J.; Kearn, C.S.; Mackie, K. Targeting dopamine D2 and cannabinoid-1 (CB1) receptors in rat nucleus accumbens. *J. Comp. Neurol.*, **2006**, *495*(3), 299-313.

[189] Szabo, B.; Siemes, S.; Wallmichrath, I. Inhibition of GABAergic neurotransmission in the ventral tegmental area by cannabinoids. *Eur. J. Neurosci.*, **2002**, *15*(12), 2057-2061.

[190] Sperlágh, B.; Windisch, K.; Andó, R.D.; Sylvester Vizi, E. Neurochemical evidence that stimulation of CB1 cannabinoid receptors on GABAergic nerve terminals activates the dopaminergic reward system by increasing dopamine release in the rat nucleus accumbens. *Neurochem. Int.*, **2009**, *54*(7), 452-457.

[191] Melis, M.; Pistis, M.; Perra, S.; Muntoni, A.L.; Pillolla, G.; Gessa, G.L. Endocannabinoids mediate presynaptic inhibition of glutamatergic transmission in rat ventral tegmental area dopamine neurons through activation of CB1 receptors. *J. Neurosci.*, **2004**, *24*(1), 53-62.

[192] Robbe, D.; Alonso, G.; Duchamp, F.; Bockaert, J.; Manzoni, O.J. Localization and mechanisms of action of cannabinoid receptors at the glutamatergic synapses of the mouse nucleus accumbens. *J. Neurosci.*, **2001**, *21*(1), 109-116.

[193] Pascussi, J.M.; Drocourt, L.; Gerbal-Chaloin, S.; Fabre, J.M.; Maurel, P.; Vilarem, M.J. Dual effect of dexamethasone on CYP3A4 gene expression in human hepatocytes. Sequential role of glucocorticoid receptor and pregnane X receptor. *Eur. J. Biochem.*, **2001**, *268*, 6346-6358.

[194] Daskalopoulos, E.P.; Lang, M.A.; Marselos, M.; Malliou, F.; Konstandi, M. D_2-dopaminergic receptor-linked pathways: critical

regulators of CYP3A, CYP2C, and CYP2D. *Mol. Pharmacol.*, **2012**, *82*(4), 668-678.

[195] Jürgens, G.; Lange, K.H.; Reuther, L.; Rasmussen, B.B.; Brøsen, K.; Christensen, H.R. Effect of growth hormone on hepatic cytochrome P450 activity in healthy elderly men. *Clin. Pharmacol. Ther.*, **2002**, *71*(3), 162-168.

[196] Lammel Lindemann, J.A.; Angajala, A.; Engler, D.A.; Webb, P.; Ayers, S.D. Thyroid hormone induction of human cholesterol 7 alpha-hydroxylase (Cyp7a1) *in vitro*. *Mol. Cell. Endocrinol.*, **2014**, *388*(1-2), 32-40.

[197] Lal, S.; Tolis, G.; Martin, S.B.; Brown, G.M.; Guyda, H. Effect of clonidine on growth hormone, prolactin, luteinizing hormone, follicle-stimulating hormone, and thyroid-stimulating hormone in the serum of normal men. *J. Clin. Endocrinol. Metab.*, **1975**, *41*(5), 827-832.

[198] Mueller, G.P.; Simpkins, J.; Meites, J.; Moore, K.E. Differential effects of dopamine agonists and haloperidol on release of prolactin, thyroid stimulating hormone, growth hormone and luteinizing hormone in rats. *Neuroendocrinology*, **1976**, *20*(2), 121-135.

[199] Fuller, R.W.; Snoddy, H.D. Elevation of serum corticosterone concentrations in rats by pergolide and other dopamine agonists. *Endocrinology*, **1981**, *109*(4), 1026-1032.

[200] Ježová, D.; Jurčovičová, J.; Vigas, M.; Murgas, K.; Labrie, F. Increase in plasma ACTH after dopaminergic stimulation in rats. *Psychopharmacology (Berl)*, **1985**, *85*(2), 201-203.

[201] Morley, J.E.; Brammer, G.L.; Sharp, B.; Yamada, T.; Yuwiler, A.; Hershman, J.M. Neurotransmitter control of hypothalamic-pituitary-thyroid function in rats. *Eur. J. Pharmacol.*, **1981**, *70*(3), 263-271.

[202] Wójcikowski, J.; Gołembiowska, K.; Daniel, W.A. The regulation of liver cytochrome p450 by the brain dopaminergic system. *Curr. Drug Metab.*, **2007**, *8*(6), 631-638.

[203] Iqbal, J.; Manley, T.R.; Yue, Q.; Namavar, M.R.; Clarke, I.J. Noradrenergic regulation of hypothalamic cells that produce growth hormone-releasing hormone and somatostatin and the effect of altered adiposity in sheep. *J. Neuroendocrinol.*, **2005**, *17*(6), 341-352.

[204] Wittmann, G. Regulation of hypophysiotrophic corticotrophin-releasing hormone- and thyrotrophin-releasing hormone-synthesising neurones by brainstem catecholaminergic neurones. *J. Neuroendocrinol.*, **2008**, *20*(7), 952-960.

[205] Kot, M.; Sadakierska-Chudy, A.; Haduch, A.; Rysz, M.; Bromek, E.; Gołembiowska, K.; Daniel, W.A. The role of the dorsal noradrenergic pathway of the brain (locus coeruleus) in the regulation of liver cytochrome P450 activity. *Eur. J. Pharmacol.*, **2015**, *751*, 34-41.

[206] Kot, M.; Pilc, A.; Daniel, W.A. Simultaneous alterations of brain and plasma serotonin concentrations and liver cytochrome P450 in rats fed on a tryptophan-free diet. *Pharmacol. Res.*, **2012**, *66*(4), 292-299

[207] Haduch, A.; Wójcikowski, J.; Daniel, W.A. The effect of tricyclic antidepressants, selective serotonin reuptake inhibitors (SSRIs) and newer antidepressant drugs on the activity and level of rat CYP3A. *Eur. Neuropsychopharmacol.*, **2006**, *16*(3), 178-186.

[208] Pagotto, U.; Marsicano, G.; Cota, D.; Lutz, B.; Pasquali, R. The emerging role of the endocannabinoid system in endocrine regulation and energy balance. *Endocr. Rev.*, **2006**, *27*(1), 73-100.

[209] Brown, T.T.; Dobs, A.S. Endocrine effects of marijuana. *J. Clin. Pharmacol.*, **2002**, *42*, 11 Suppl, 90S-96S.

[210] Herkenham, M.; Lynn, A.B.; de Costa, B.R.; Richfield, E.K. Neuronal localization of cannabinoid receptors in the basal ganglia of the rat. *Brain Res.*, **1991**, *547*(2), 267-274.

[211] Pagotto, U.; Marsicano, G.; Fezza, F.; Theodoropoulou, M.; Grübler, Y.; Stalla, J.; Arzberger, T.; Milone, A.; Losa, M.; Di MArzo, V.; Lutz, V.; Stalla, G.K. Normal human pituitary gland and pituitary adenomas express cannabinoid receptor type 1 and synthesize endogenous cannabinoids: first evidence for a direct role of cannabinoids on hormone modulation at the human pituitary level. *J. Clin. Endocrinol. Metab.*, **2001**, *86*(6), 2687-2696.

[212] Steiner, M.A.; Wotjak, C.T. Role of the endocannabinoid system in regulation of the hypothalamic-pituitary-adrenocortical axis. Prog. *Brain Res.*, **2008**, *170*, 397-432.

[213] da Veiga, M.A.; Fonseca Bloise, F.; Costa-E-Sousa, R.H.; Souza, L.L.; Almeida, N.A.; Oliveira, K.J.; Pazos-Moura, C.C. Acute effects of endocannabinoid anandamide and CB1 receptor antagonist, AM251 in the regulation of thyrotropin secretion. *J. Endocrinol.*, **2008**, *199*(2), 235-242.

[214] Deli, L.; Wittmann, G.; Kalló, I.; Lechan, R.M.; Watanabe, M.; Liposits, Z.; Fekete, C. Type 1 cannabinoid receptor-containing axons innervate hypophysiotropic thyrotropin-releasing hormone-synthesizing neurons. *Endocrinology*, **2009**, *150*(1), 98-103.

[215] de Miguel, R.; Romero, J.; Muñoz, R.M.; García-Gil, L.; González, S.; Villanua, M.A.; Makriyannis, A.; Ramos, J.A.; Fernández-Ruiz, J.J. Effects of cannabinoids on prolactin and gonadotrophin secretion: involvement of changes in hypothalamic gamma-aminobutyric acid (GABA) inputs. *Biochem. Pharmacol.*, **1998**, *56*(10), 1331-1338

[216] Hill, M.N.; Tasker, J.G. Endocannabinoid signaling, glucocorticoid-mediated negative feedback, and regulation of the hypothalamic-pituitary-adrenal axis. *Neuroscience*, **2012**, 204, 5-16.

[217] Di, S.; Malcher-Lopes, R.; Halmos, K.C.; Tasker, J.G. Nongenomic glucocorticoid inhibition via endocannabinoid release in the hypothalamus: a fast feedback mechanism. *J. Neurosci.*, **2003**, *23*(12), 4850-4857.

[218] Gorzalka, B.B.; Hill, M.N. Integration of endocannabinoid signaling into the neural network regulating stress-induced activation of the hypothalamic-pituitary-adrenal axis. *Curr. Top. Behav. Neurosci.*, **2009**, *1*, 289-306.

[219] Kirilly, E.; Hunyady, L.; Bagdy, G. Opposing local effects of endocannabinoids on the activity of noradrenergic neurons and release of noradrenaline: relevance for their role in depression and in the actions of CB(1) receptor antagonists. *J. Neural. Transm.*, **2013**, *120*(1), 177-186.

[220] Nakazi, M.; Bauer, U.; Nickel, T.; Kathmann, M.; Schlicker, E. Inhibition of serotonin release in the mouse brain via presynaptic cannabinoid CB1 receptors. *Naunyn Schmiedebergs Arch. Pharmacol.*, **2000**, *361*(1), 19-24.

[221] Häring, M.; Marsicano, G.; Lutz, B.; Monory, K. Identification of the cannabinoid receptor type 1 in serotonergic cells of raphe nuclei in mice. *Neuroscience*, **2007**, *146*(3), 1212-1219.

[222] Dvořák, Z.; Pávek, P. Regulation of drug-metabolizing cytochrome P450 enzymes by glucocorticoids. *Drug Metab. Rev.*, **2010**, *42*(4), 621-635.

[223] Honkakoski, P.; Negishi, M. Regulation of cytochrome P450 (CYP) genes by nuclear receptors. *Biochem. J.*, **2000**, *347*(Pt 2), 321-337.

[224] Tolson, A.H.; Wang, H. Regulation of drug-metabolizing enzymes by xenobiotic receptors: PXR and CAR. *Adv. Drug. Deliv. Rev.*, **2010**, *62*(13), 1238-1249.

[225] Onica, T.; Nichols, K.; Larin, M.; Ng, L.; Maslen, A.; Dvorak, Z.; Pascussi, J.M.; Vilarem, M.J.; Maurel, P.; Kirby, G.M. Dexamethasone-mediated up-regulation of human CYP2A6 involves the glucocorticoid receptor and increased binding of hepatic nuclear factor 4 alpha to the proximal promoter. *Mol. Pharmacol.*, **2008**, *73*(2), 451-460.

[226] Pávek, P.; Červený, L.; Švecová, L.; Brysch, M.; Libra, A.; Vrzal, R.; Nachtigal, P.; Staud, F.; Ulrichová, J.; Fendrich, Z.; Dvořák, Z. Examination of Glucocorticoid receptor alpha-mediated transcriptional regulation of P-glycoprotein, CYP3A4, and CYP2C9 genes in placental trophoblast cell lines. *Placenta*, **2007**, *28*(10), 1004-1011.

[227] Wang, H.; Faucette, S.R.; Gilbert, D.; Jolley, S.L.; Sueyoshi, T.; Negishi, M.; LeCluyse, E.L. Glucocorticoid receptor enhancement of pregnane X receptor-mediated CYP2B6 regulation in primary human hepatocytes. *Drug Metab. Dispos.*, **2003**, *31*(5), 620-630.

[228] Pascussi, J.M.; Gerbal-Chaloin, S.; Drocourt, L.; Maurel, P.; Vilarem, M.J. The expression of CYP2B6, CYP2C9 and CYP3A4 genes: a tangle of networks of nuclear and steroid receptors. *Biochim. Biophys. Acta*, **2003**, *1619*(3), 243-253.

[229] Pascussi, J.M.; Gerbal-Chaloin, S.; Fabre, J.M.; Maurel, P;. Vilarem, M.J. Dexamethasone enhances constitutive androstane receptor expression in human hepatocytes: consequences on cytochrome P450 gene regulation. *Mol. Pharmacol.*, **2000**, *58*(6), 1441-1450.

[230] Ferguson, S.S.; Chen, Y.; LeCluyse, E.L.; Negishi, M.; Goldstein, J.A. Human CYP2C8 is transcriptionally regulated by the nuclear receptors constitutive androstane receptor, pregnane X receptor, glucocorticoid receptor, and hepatic nuclear factor 4alpha. *Mol. Pharmacol.*, **2005**, *68*(3), 747-757.

[231] Schuetz, J.D.; Schuetz, E.G.; Thottassery, J.V.; Guzelian, P.S.; Strom, S.; Sun, D. Identification of a novel dexamethasone respon-

sive enhancer in the human CYP3A5 gene and its activation in human and rat liver cells. *Mol. Pharmacol.*, **1996**, *49*(1), 63-72.

[232] Chen, Y.; Ferguson, S.S.; Negishi, M.; Goldstein, J.A. Identification of constitutive androstane receptor and glucocorticoid receptor binding sites in the CYP2C19 promoter. *Mol. Pharmacol.*, **2003**, *64*(2), 316-324.

[233] Liddle, C.; Goodwin, B.J.; George, J.; Tapner, M.; Farrell, G.C. Separate and interactive regulation of cytochrome P450 3A4 by triiodothyronine, dexamethasone, and growth hormone in cultured hepatocytes. *J. Clin. Endocrinol. Metab.*, **1998**, *83*(7), 2411-2416.

[234] Waxman, D.J.; Morrissey, J.J.; LeBlanc, G.A. Female-predominant rat hepatic P-450 forms j (IIE1) and 3 (IIA1) are under hormonal regulatory controls distinct from those of the sex-specific P-450 forms. *Endocrinology*, **1989**, *124*(6), 2954-2966.

[235] Chen, G.F.; Ronis, M.J.; Ingelman-Sundberg, M.; Badger, T.M. Hormonal regulation of microsomal cytochrome P4502E1 and P450 reductase in rat liver and kidney. *Xenobiotica*, **1999**, *29*(5), 437-451.

[236] Waxman, D.J.; O'Connor, C. Growth hormone regulation of sex-dependent liver gene expression. *Mol. Endocrinol.*, **2006**, *20*(11), 2613-2629.

[237] Ortiz de Montellano P. *Cytochrome P450: Structure, Mechanism, and Biochemistry*, 3rd ed.; Kluwer academic/Plenum Publishers: New York, **2005**.

[238] Itoh, M.; Nakajima, M.; Higashi, E.; Yoshida, R.; Nagata, K.; Yamazoe, Y.; Yokoi, T. Induction of human CYP2A6 is mediated by the pregnane X receptor with peroxisome proliferator-activated receptor-gamma coactivator 1alpha. *J. Pharmacol. Exp. Ther.*, **2006**, *319*(2), 693-702.

[239] Hariparsad, N.; Chu, X.; Yabut, J.; Labhart, P.; Hartley, D.P.; Dai, X.; Evers R. Identification of pregnane-X receptor target genes and coactivator and corepressor binding to promoter elements in human hepatocytes. *Nucleic Acids Res.*, **2009**, *37*(4), 1160-1173.

[240] Goodwin, B.; Moore, L.B.; Stoltz, C.M.; McKee, D.D.; Kliewer, S.A. Regulation of the human CYP2B6 gene by the nuclear pregnane X receptor. *Mol. Pharmacol.*, **2001**, *60*(3), 427-431.

[241] Faucette, S.R.; Wang, H.; Hamilton, G.A.; Jolley, S.L.; Gilbert, D.; Lindley, C.; Yan, B.; Negishi, M.; LeCluyse, E.L. Regulation of CYP2B6 in primary human hepatocytes by prototypical inducers. *Drug Metab. Dispos.*, **2004**, *32*(3), 348-358.

[242] Rana R.; Chen Y.; Ferguson S.S.; Kissling G.E.; Surapureddi S.; Goldstein J.A. Hepatocyte nuclear factor 4{alpha} regulates rifampicin-mediated induction of CYP2C genes in primary cultures of human hepatocytes. *Drug Metab. Dispos.*, **2010**, *38*(4), 591-599

[243] Blumberg B.; Sabbagh W.; Juguilon H.; Bolado J.; van Meter C.M.; Ong E.S.; Evans R.M. SXR, a novel steroid and xenobiotic-sensing nuclear receptor. *Genes Dev.*, **1998**, *12*(20), 3195-3205

[244] Bertilsson G.; Heidrich J.; Svensson K.; Asman M.; Jendeberg L.; Sydow-Bäckman M.; Ohlsson R.; Postlind H.; Blomquist P.; Berkenstam A. Identification of a human nuclear receptor defines a new signaling pathway for CYP3A induction. *Proc. Natl. Acad. Sci. USA*, **1998**, *95*(21), 12208-12213.

[245] Kliewer, S.A.; Moore, J.T.; Wade, L.; Staudinger, J.L.; Watson, M.A.; Jones, S.A.; McKee, D.D.; Oliver, B.B.; Willson, T.M.; Zetterström, R.H.; Perlmann, T.; Lehman, J.M. An orphan nuclear receptor activated by pregnanes defines a novel steroid signaling pathway. *Cell*, **1998**, *92*(1), 73-82.

[246] Staudinger, J.L.; Goodwin, B.; Jones, S.A.; Hawkins-Brown, D.; MacKenzie, K.I.; LaTour, A.; Liu, Y.; Klaasen, C.D.; Brown, K.K.; Reinhard, J.; Willson, T.M.; Koller, B.H.; Kliewer, S.A. The nuclear receptor PXR is a lithocholic acid sensor that protects against liver toxicity. *Proc. Natl. Acad. Sci. USA*, **2001**, *98*(6), 3369-3374.

[247] Kawamoto, T.; Sueyoshi, T.; Zelko, I.; Moore, R.; Washburn, K.; Negishi, M. Phenobarbital-responsive nuclear translocation of the receptor CAR in induction of the CYP2B gene. *Mol. Cell. Biol.*, **1999**, *19*(9), 6318-6322.

[248] Kohalmy, K.; Tamási, V.; Kóbori, L.; Sárváry, E.; Pascussi, J.M.; Porrogi, P.; Rozman, D.; Prough, R.A.; Meyer, U.A.; Monostory, K. Dehydroepiandrosterone induces human CYP2B6 through the constitutive androstane receptor. *Drug Metab. Dispos.*, **2007**, *35*(9), 1495-1501.

[249] Ferguson, S.S.; LeCluyse, E.L.; Negishi, M.; Goldstein, J.A. Regulation of human CYP2C9 by the constitutive androstane receptor: discovery of a new distal binding site. *Mol. Pharmacol.*, **2002**, *62*(3), 737-746.

[250] Martínez-Jiménez, C.P.; Jover, R.; Donato, M.T.; Castell, J.V.; Gómez-Lechón, M.J. Transcriptional regulation and expression of CYP3A4 in hepatocytes. *Curr. Drug. Metab.*, **2007**, *8*(2), 185-194.

[251] Burk, O.; Koch, I.; Raucy, J;. Hustert, E.; Eichelbaum, M.; Brockmöller, J.; Zanger, U.M.; Wojniwski, L. The induction of cytochrome P450 3A5 (CYP3A5) in the human liver and intestine is mediated by the xenobiotic sensors pregnane X receptor (PXR) and constitutively activated receptor (CAR). *J. Biol. Chem.*, **2004**, *279*(37), 38379-38385.

[252] Pascussi, J.M.; Jounaidi, Y.; Drocourt, L.; Domergue, J.; Balabaud, C.; Maurel, P.; Vilarem, M.J. Evidence for the presence of a functional pregnane X receptor response element in the CYP3A7 promoter gene. *Biochem. Biophys. Res. Commun.*, **1999**, *260*(2), 377-381.

[253] Wang, H.; LeCluyse, E.L. Role of orphan nuclear receptors in the regulation of drug-metabolising enzymes. *Clin. Pharmacokinet.*, **2003**, *42*(15), 1331-1357.

[254] Johnson, E.F.; Palmer, C.N.; Griffin, K.J.; Hsu, M.H. Role of the peroxisome proliferator-activated receptor in cytochrome P450 4A gene regulation. *FASEB J.*, **1996**, *10*(11), 1241-1248.

[255] Shaban, Z.; Soliman, M.; El-Shazly, S.; El-Bohi, K; Abdelazeez, A.; Kehelo, K.; Kim, H.S.; Muzandu, K.; Ishizuka, M.; Kazusaka, A.; Fujita, S. AhR and PPARalpha: antagonistic effects on CYP2B and CYP3A, and additive inhibitory effects on CYP2C11. *Xenobiotica*, **2005**, *35*(1), 51-68.

[256] Schuetz, E.G.; Schmid, W.; Schutz, G.; Brimer, C.; Yasuda, K.; Kamataki, T.; Bornheim, L.; Myles, K.; Cole, T.J. The glucocorticoid receptor is essential for induction of cytochrome P-4502B by steroids but not for drug or steroid induction of CYP3A or P-450 reductase in mouse liver. *Drug Metab. Dispos.*, **2000**, *28*(3), 268-278.

[257] O'Sullivan, S.E. Cannabinoids go nuclear: evidence for activation of peroxisome proliferator-activated receptors. *Br. J. Pharmacol.*, **2007**, *152*(5), 576-582.

[258] Liu, J.; Li, H.; Burstein, S.H.; Zurier, R.B.; Chen, J.D. Activation and binding of peroxisome proliferator-activated receptor gamma by synthetic cannabinoid ajulemic acid. *Mol. Pharmacol.*, **2003**, *63*(5), 983-992.

Received: August 31, 2015 **Revised: December 10, 2015** **Accepted: December 14, 2015**